

IAEA-TECDOC-1618

***Application of Isotopes to the  
Assessment of Pollutant Behaviour in  
the Unsaturated Zone  
for Groundwater Protection***

*Final report of a coordinated research project  
2004–2005*



**IAEA**

International Atomic Energy Agency

May 2009

IAEA-TECDOC-1618

***Application of Isotopes to the  
Assessment of Pollutant Behaviour in  
the Unsaturated Zone  
for Groundwater Protection***

*Final report of a coordinated research project  
2004–2005*



**IAEA**

International Atomic Energy Agency

May 2009

The originating Section of this publication in the IAEA was:

Isotope Hydrology Section  
International Atomic Energy Agency  
Wagramer Strasse 5  
P.O. Box 100  
A-1400 Vienna, Austria

APPLICATION OF ISOTOPES TO THE ASSESSMENT OF POLLUTANT BEHAVIOUR  
IN THE UNSATURATED ZONE FOR GROUNDWATER PROTECTION

IAEA, VIENNA, 2009  
ISBN 978-92-0-105509-5  
ISSN 1011-4289  
© IAEA, 2009

Printed by the IAEA in Austria  
May 2009

## FOREWORD

A coordinated research project (CRP) was conducted by the IAEA with the purpose of studying what isotopic and other ancillary data are required to help understand migration of potential contaminants through the unsaturated zone (UZ) into the underlying groundwater. To this end, research projects were conducted in ten countries to study recharge and infiltration processes, as well as contaminant migration in a wide variety of UZ environments.

This publication contains the reports of these ten projects and a summary of the accomplishments of the individual projects. The IAEA-TECDOC reviews the usefulness and current status of application of the combined use of isotope and other hydrogeochemical tools for the assessment of flow and transport processes in the UZ. A number of isotope and hydrochemical tools have been used to simultaneously study groundwater recharge and transport of pollutants in the UZ. This information is relevant for assessing the vulnerability of groundwater to contamination.

The ten projects covered climates ranging from humid to arid, and water table depths from the near surface to over 600 m. The studies included measuring movement of water, solutes, and gases through the UZ using an assortment of isotope and geochemical tracers and approaches. Contaminant issues have been studied at most of the ten sites and the UZ was found to be very effective in protecting groundwater from most heavy metal contaminants. The publication is expected to be of interest to hydrologists, hydrogeologists and soil scientists dealing with pollution aspects and protection of groundwater resources, as well as counterparts of TC projects in Member States.

The IAEA officers in charge of designing and coordinating all of the related work in this CRP were P.K. Aggarwal and K.M. Kulkarni of the Division of Physical and Chemical Sciences. J.A. Izbicki, R.L. Michel and B.D. Newman assisted in technical editing of the contributions. The IAEA officers responsible for this publication were P.K. Aggarwal and K.M. Kulkarni of the Division of Physical and Chemical Sciences.

## *EDITORIAL NOTE*

*The papers in these proceedings are reproduced as submitted by the authors and have not undergone rigorous editorial review by the IAEA.*

*The views expressed do not necessarily reflect those of the IAEA, the governments of the nominating Member States or the nominating organizations.*

*The use of particular designations of countries or territories does not imply any judgement by the publisher, the IAEA, as to the legal status of such countries or territories, of their authorities and institutions or of the delimitation of their boundaries.*

*The mention of names of specific companies or products (whether or not indicated as registered) does not imply any intention to infringe proprietary rights, nor should it be construed as an endorsement or recommendation on the part of the IAEA.*

*The authors are responsible for having obtained the necessary permission for the IAEA to reproduce, translate or use material from sources already protected by copyrights.*

## CONTENTS

Summary .....	1
Chemical, isotopic, and microbiological evidence for nitrification below the plant root zone from intensive fertilized agricultural area in Austria: Insights from lysimeter studies and soil cores .....	15
<i>A. Leis</i>	
Nitrate in groundwater and the unsaturated zone, Shijiazhuang City, China .....	31
<i>Guo Yonghai , Xu Guoqing , Gao Zhenyu , Liu Shufen , Jiang Guilin</i>	
Regulation function of the unsaturated zone on discharge and the export of inorganic agrochemicals from arable lands in south Germany.....	67
<i>K.-P. Seiler, W. Stichler</i>	
Multi-tracer technique and hydro-geochemical approach to assess pollutants dynamics in the unsaturated zone at the IARI farm site, New Delhi, India.....	81
<i>U.P. Kulkarni, U.K. Sinha, S.V. Navada, U. Saravana Kumar Y.K. Sud, P.S. Datta</i>	
Salinity and metal transport through the unsaturated zone, Kasur, Pakistan .....	109
<i>M. A. Tasneem, M. Ali, Z. Latif, M. Ahmad, T. Javed, A. Mashiatullah, W. Akram</i>	
Water dynamics in the unsaturated zone of fractured rock: Test site Sinji Vrh.....	133
<i>B. Čenčur Curk</i>	
Behaviour of nitrogen in the unsaturated zone in southern Africa .....	149
<i>A.S. Talma, G. Tredoux, J.F.P. Engelbrecht</i>	
Chemical and isotopic study of pollutant transport through unsaturated zone in Damascus Oasis (Syrian Arab Republic).....	169
<i>B. Abou Zakhem, R. Hafez</i>	
Contaminant attenuation through glacial drift overlying the chalk aquifer in southern East Anglia, UK.....	195
<i>D.C. Gooddy, W.G. Darling</i>	
Use of isotopes for the study of pollutant behaviour in the unsaturated zone at three semi-arid sites in the USA .....	205
<i>R.L. Michel, J.A. Izbicki, P.B. McMahon, D.A. Stonestrom</i>	
List of participants.....	219



## SUMMARY

### 1. INTRODUCTION

Recharge to the most of the world's aquifers occurs through the unsaturated zone (UZ) in many places. For proper management of resources, it is important to know the location and rate of recharge. One of the purposes of this coordinated research project (CRP) was to determine the best strategies for determining the location of recharge and outline methods of determining the recharge rate through the UZ. Another purpose of the CRP was to determine the transport processes that are important for movement of pollutants in the UZ. Its focus included determining potential reactions in the depths between the root zone and the water table that might alter the concentrations of solutes, particularly the concentrations of potential contaminants such as nitrate, heavy metals and organic pesticides/herbicides.

Of particular interest was whether reactions in the UZ can only occur in the root zone and the saturated/unsaturated interface region (SUIR) that lies at the top of the water table. In the SUIR, conditions exist that allow reactions to modify the UZ chemistry [1]. This effect may be heightened by falling or fluctuating water tables in many of the world's aquifers that can result in areas of enhanced biogeochemical reactivity. However, the question was whether the SUIR is the only active region for chemical reactions in the UZ.

A third focus of the CRP was the movement of gas through the UZ. Contaminants can move as gases through the UZ, although this is probably not a common method of aquifer contamination. A more important issue is that many gases are used for age dating of groundwaters underneath the UZ. One of the major issues that have caused problems for hydrologists is the initial value problem. This is particularly true for carbon-14 but is also an issue for CFCs and other transient age dating techniques [2]. Also, when using  $^3\text{H}/^3\text{He}$  dating and other age dating tracers it is important to know the timescale for water transfer through the UZ as this is crucial in determining what groundwater dates mean in terms of real years since water infiltrated. Another issue for gas movement is the release of certain gases (e.g.  $\text{N}_2\text{O}$ ,  $\text{CO}_2$ ) which are formed in the UZ [3]. It is important to know what the rates of formation are for these gases in the UZ and how rapidly they can exit the UZ to the atmosphere.

The ten projects in this CRP cover a wide range of approaches and sites typically encountered in UZ research. One project was in a karst setting in Slovenia, where transport can be relatively rapid through channels/large fractures. At the same site, slower movement occurs through small fractures where chemicals can be retained in the UZ for some years after they have been introduced. The site in Germany can have relatively rapid movement through the UZ and investigations showed the differences in contributions between overland flow, subsurface flow and groundwater input in total runoff. The Austrian site was at a research station in an intensive agricultural area. The project made use of isotopic data from lysimeters and soil cores to elucidate microbial processes in the UZ. The contribution from the United Kingdom investigated UZ processes in the Chalk aquifer system, beneath an extensive impermeable drift cover. Determination of nitrogen species combined with groundwater age indicators and data from gas samplers were used to develop a conceptual regional model of contaminant transport for the study site. The project in Pakistan studied an area where extensive industrial pollution occurred. Gas samples and soil cores were used to study the movement and reactions of pollutants in the UZ. The site in India, which was selected for extensive study, was in an agricultural research site where agrochemical use has occurred. Radiotracers were applied to the surface and their movement through the UZ was monitored by analysis of soil cores and in situ measurements. The project in China, located near Shijiazhuang City, was in an area which has suffered extensive degradation of its groundwater quality due to leaching of nitrate and other contaminants through the UZ. The site was investigated using tritium and stable isotopes from soil cores and groundwater. The project in the USA collected data from sites in arid and semi-arid climates with deep (~100-200 m) UZ. One of the locations, the High Plains Aquifer, is a region where irrigation has increased movement of pollutants through the UZ. The Syrian study, in the region of the Damascus Oasis, investigated migration of heavy metals into the UZ. Nitrogen isotopes were also used

to determine the source of increasing nitrate concentrations in groundwater. The South African study looked at cases of extreme nitrate pollution in agricultural areas due to intense rainfall events. Particular emphasis was placed on pollution caused by livestock mismanagement.

## **2. ISOTOPIC APPROACHES**

### **2.1. Applied Tracers**

One of the most common approaches used for tracing movement through the UZ is the direct application of tracers to the surface of the study sites [4,5]. These tracers can be inorganic ions (e.g. Li, Br), dyes, or isotopes (tritium, deuterium,  $^{60}\text{Co}$ , etc). Deuterium and tritium have the advantage of being part of the water molecule, and do not undergo any chemical reactions.  $^{60}\text{Co}$  has a low absorption capacity and so can be an effective tracer for water studies. These tracers are best used in systems where timescales for flow through the UZ range from days to about one year. They work best for relatively compact study areas and experimental sites where it is easy to apply the tracer to the site. This approach has been successfully applied in several projects of the CRP.

### **2.2. Stable Isotopes of Water**

Probably the most useful isotopes for studying hydrologic processes are the natural variations of stable isotopes of water (deuterium and  $^{18}\text{O}$ ). Since their discovery, they have been applied to scientific studies in a wide variety of hydrologic disciplines, including UZ studies. They are frequently used to study events with very short timescales such as hydrograph studies of individual storm events. In the UZ, they can be used to determine in what season precipitation is most likely to result in recharge. In deeper UZs these isotopes also offer useful information on sources of recharge and possible climatic changes occurring on the order of a few years or greater.

### **2.3. Tritium**

Tritium, being a part of the water molecule [6], has been recognized as one of the most useful tracers used in hydrology. It was released in large quantities during the nuclear testing of the 1950s and 1960s [7], with the burden on the earth increasing from about 3.5 kg to 600–800 kg. As the peak concentration of tritium occurred over 40 years ago and concentrations in precipitation have not shown significant change in recent years, this approach is best used at the present time in areas where recharge is slow, thick UZs are present, and water movement through the UZ is on the order of decades. In this CRP, tritium has shown itself to be very useful in the sites where the UZs are greater than 100 meters deep. Tritium can be used to identify areas of preferential recharge in arid and semi-arid areas that must be considered when modelling recharge.

### **2.4. Isotopes of Nitrate**

Nitrate is one of the most important pollutants on a worldwide basis and nitrate isotopes have been used widely to study pollutant transfer. Isotopes of nitrate can be used to distinguish sources of nitrate, and identify biogeochemical processes occurring in the UZ. The use of only  $^{15}\text{N}$  will frequently result in equivocal interpretations, but used together with  $^{18}\text{O}$  in the nitrate molecule can be extremely valuable [8]. Both  $^{15}\text{N}$  and the dual isotope approach have been used in this CRP to study nitrate behaviour in the UZ.

### **2.5. Gas Tracers**

The main gas tracers used in the UZ are chlorofluorocarbons (CFCs), sulphur hexafluoride ( $\text{SF}_6$ ), and  $^{14}\text{C}$ . CFCs and  $\text{SF}_6$  are conservative in almost all UZ sites and are valuable in providing bulk properties of gas penetration through the UZ [9]. Frequently, calculations of bulk properties for gas diffusion in the UZ are based on the physical properties measured in a core [10]. However, these measurements are limited in that they represent only one point in the system which may or may not be

representative of the whole system. Some projects in this CRP made extensive use of CFC measurements to determine the rate of movement of gases through the UZ. This CRP found that the movement of gases in the UZ can vary substantially from site to site even though the physical properties of the core seem to be very similar.

### **3. STUDY DESIGN ELEMENTS AND ANCILLARY DATA COLLECTION**

It has long been recognized that the application of isotopic data to study of groundwater source movement and age and to the understanding of chemical processes that occur within the saturated zone can lead to misinterpretations if the isotopic data are not constrained by a basic understanding of the system derived from geology, hydrology, and chemistry. The same need for interpretation of isotopic data within the constraints of basic geologic, hydrologic, and chemical data exists within the UZ. However, the study approaches and data required to assess the physical movement of water in the UZ, although well-known and understood within the discipline of soil physics, are less commonly known and understood by isotope hydrologists. Furthermore, much of the work on water and solute transport in the UZ has been done at shallow depths within the root zone underlying agricultural sites to help understand water and nutrient availability to plants. Approaches and techniques used within the upper meter of the unsaturated zone often require modifications to “upscale” them to UZs that may be ten’s or hundred’s of meters thick and highly heterogeneous. Much of the discussion that follows is applicable to unsaturated studies in porous media such as alluvium. Unsaturated transport of water and contaminants through fractures such as encountered in the Slovenian study is often highly complex and difficult to study requiring special instrumentation and techniques.

#### **3.1. Drilling Techniques**

The first and most obvious requirement for data collection within thick UZs is the ability to penetrate to the desired depths (without contamination or undue disturbance to the UZ), collect samples from those depths, and install instrumentation at selected depths within the UZ.

Hand augers suitable for work within the soil zone and upper part of the unsaturated zone were used successfully as part of this CRP at the South African, Syrian, and Pakistani study sites. However, hand augers can only reach maximum depths of 5 to 8 meters into the UZ depending on site conditions. Although hand-augered cuttings and core material are generally of high-quality and suitable for most applications; instrument installation in hand-augered boreholes is limited by both the depth and diameter of the hole.

A drill rig with the ability to collect high-quality cuttings and cores is required to go to deeper depths. The first and foremost requirement is that the rig does not contaminate the UZ with water used as a drilling fluid. Secondary concerns relevant to the design of some UZ studies are contamination of the UZ with (1) atmospheric air, (2) compressed air used to lift cuttings from the borehole, and (3) volatile industrial compounds used to lubricate drill bits, augers, and drill steel. The drilling process also should not excessively disturb the surrounding UZ.

Auger drilling used in the Chinese, Indian, and United Kingdom studies are suitable for many applications, relatively inexpensive, and commonly commercially available. Auger drilling can reach depths as great as 50m in some settings [11]. Lithology data from cuttings collected during auger drilling is often poor unless supplemented with frequent coring. Cores collected during auger drilling are of high-quality, easily preserved and protected from physical changes such as drying and chemical changes such as oxidation after collection. Standard hollow-stem augers, commonly having internal diameters of about 10 cm, provide little room for equipment installation. Larger diameter augers, such as those used on the Indian site, provide more room within the borehole to install equipment for measurement of physical properties and water quality at different depths within the borehole.

ODEX (Overburden Drilling EXploration) [11, 12] used in the US study has the greatest range in depth (reaching as deep as 200 m in the western Mojave Desert study) and is possibly the most

suitable drilling technique for studies in thick UZs. In ODEX drilling, air rather than water, is used as the drilling fluid and remove cuttings from the borehole. An air-hammer on an off-centre cam cuts a hole slightly larger in diameter than the drill bit. The hole is stabilized by steel pipe the diameter of the borehole which is emplaced in the hole behind the air-hammer as drilling progresses. The ODEX technique provides for high-quality cuttings suitable for detailed lithologic description, particle-size, and chemical analysis at intervals as frequent as 0.3 m. Frequent coring is required to obtain material for water content, water potential, hydraulic properties, and most isotopic analysis. Sample preservation techniques are described in [12]. The steel pipe is removed from the borehole as instruments, appropriate backfill, and low-permeability sealing material are placed in the borehole during construction [12]. Steel pipes used to stabilize ODEX borehole in the US studies had diameters as large as 25 cm and were large enough to allow placement of instruments, appropriate backfill, and low-permeability sealing material at different depths in the UZ. There is substantially less disturbance of the surrounding unsaturated material in ODEX drilling than in auger drilling. Because the surrounding material is only minimally disturbed, geophysical logs, such as gamma logs and neutron logs, can be run through the steel pipe before instrument installation. These logs used with field lithologic data and the field specific conductance of water extracts from drill cuttings are useful to guide borehole design and instrument installation.

### **3.2. Physical Measures of Unsaturated Zone Properties**

Lithology is the most basic physical property of interest within the UZ. Simple measures of lithology such as field or laboratory descriptions of texture (either based on soil or geologic nomenclature) and particle-size analysis are often highly useful because they are inexpensive and consequently can be measured on a large number of samples. Most of the studies in the CRP utilized texture and/or particle-size data to describe lithology in the UZ and were able to relate changes in lithology to chemical and physical processes occurring at their sites.

Texture can be done in the field in great detail in deep boreholes where samples are collected at a high frequency. Texture data, and geophysical logs if available, aid in borehole design ensuring instrument placement above, within, or below layers critical to the movement of water or contaminants. Texture data collected during drilling at 0.3 m intervals were invaluable in the design and instrument placement within boreholes greater than 200 m deep in thick UZs in the USA [12]. These same data were used later to assess the movement of water, water vapour, and solutes [13,14], and to statistically describe heterogeneity within the unsaturated flow as part of flow-modelling studies [14].

Particle-size data provide a more quantitative assessment of UZ lithology than texture data. Although inexpensive, costs can be prohibitive for deep boreholes sampled at frequent intervals. Particle-size data were used extensively in the CRP to describe changing lithology and associated changes in water content, chemistry and isotopic composition. Particle-size data can more easily and accurately be related to soil hydraulic properties that control water and contaminant flux through the UZ using available computer models, such as Rosetta [15,16].

Water content and matric potential provide the basic measures of water availability and potential for water drainage within the UZ [17]. Water content (either gravimetric measured as mass of water per unit mass of material, or volumetric measured as volume of water per unit volume of material) are measures of what is commonly described as how wet is the material. Water content data are necessary to convert rates of downward movement estimated from tritium data or from some other method to recharge rates. Matric potential is a measure of how tightly water is held within a material [17, 18]. Matric potential may be the single most important physical measure of water status within the UZ, ultimately controlling water availability to plant, drainage, and vapour transport.

Volumetric water content can be calculated by multiplying the gravimetric water content by the bulk density of the sample (neglecting the density of water) [17, 18]. Bulk density is the dry mass of the sample divided by the volume of the sample [17, 18]. The saturation of different layers within the UZ, and hence the potential for oxidizing or reducing reactions to occur, the potential for gas diffusion, or water vapour transport in very dry materials can be assessed from these data. The Chinese study

demonstrated that saturated conditions within fined-grained layers were associated with denitrification in the UZ. Work in the USA demonstrated that saturated lenses on regional geologic contacts provided a barrier to the diffusion of CFC's to deeper depths within the UZ [19]. The effect of vapour movement on the isotopic composition of the remaining water was evident in the dry UZs in both China and the USA.

Matric potential can be measured using different methods including tensiometers, filter paper, and chilled mirror hygrometers depending on the range of matric potentials in a given set of samples [12]. Each of these measurement techniques can incorporate artefacts from other forces, such as osmotic, barometric, or overburden pressures, that may partly control the movement of water within the UZ [17, 18]. Matric potential data can normalize the effect of lithology on water content data described in the Chinese study, and are most useful when converted to total potential. In most studies this will be the matric potential, expressed in units of head or length (neglecting the influence of other forced described above) plus the height above the water table, know as gravitational potential. The resulting value is known as total potential. Total potential in a column of unsaturated material determines the direction of water flow and is analogous to measurements of head or the water table contour map in a saturated flow system (Fig. 1). Total potential values near 1 indicate gravity driven drainage through a comparatively wet UZ. Values greater than 1 indicate saturated or perched conditions within the UZ. Values near zero indicate no potential for movement or drainage within the UZ. Negative values indicate the potential for vapour movement upward against the pull of gravity. In the absence of total potential data water in comparatively wet UZs is assumed to be moved downward as a unit gradient, or the rate of change in the gravitational potential, in drier UZs this may not always be true. Total potential may vary widely on a seasonal basis in UZs near land surface where changing recharge, evaporation, transpiration, and drainage remove or add water to unsaturated material. In many cases, total potentials damp to a constant value at some depth. Large recharge pulses associated with wet years, streamflow, or climatic changes may be preserved at depth within the UZ. Total potential values at depth may be perturbed by contrasting coarse- fine-grained materials or salt accumulations within thick UZs.

Water content and matric potential in unsaturated deposits are related through water retention curves (or water characteristic curves). Data describing these curves are commonly fit to models described by [20, 21], or others and may be used to estimate other hydraulic properties. The relation between water content and hydraulic conductivity is not unique for a given material but rather differs for drying and wetting conditions. Information on water retention along with residual water content (the driest water content that the unsaturated material will drain to) are required inputs for most computer models that simulate unsaturated flow.

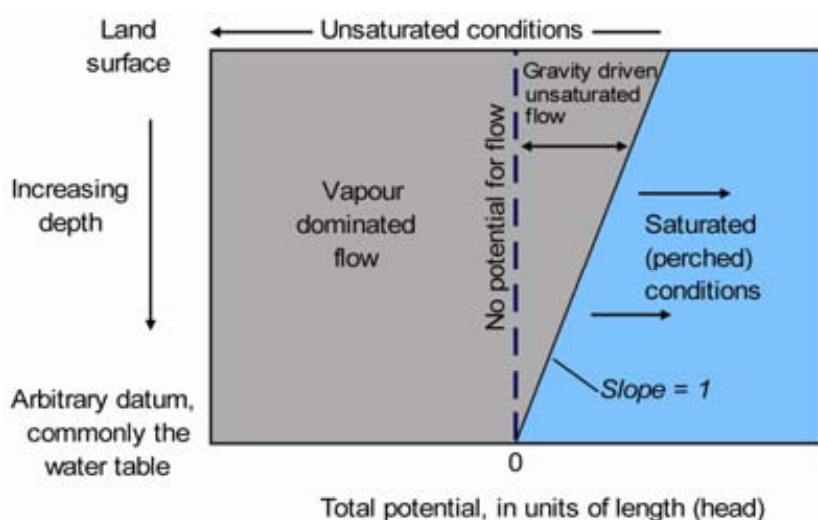


FIG. 1. Total potential and water flow as a function of depth in the UZ.

### **3.3. Hydraulic Measures of Unsaturated Zone Properties**

Total potential (the gradient) and unsaturated hydraulic conductivity determine or movement of water within the UZ according to Richard's equation [18] in the same manner as the gradient and saturated hydraulic conductivity determine the movement of water in the saturated zone according to Darcy's Law. Unlike saturated hydraulic conductivity, unsaturated hydraulic conductivity changes in a highly nonlinear manner water content (and matric potential). The unsaturated hydraulic conductivity of a dry material is likely to be several orders of magnitude less than that of a wet soil. If the unsaturated hydraulic conductivity of unsaturated material is known or can be estimated as a function of water content or water potential and these values are known, then the downward flux of water can be estimated [22]. If recharge is areal, and the data are collected deep enough in the UZ to damp seasonal variations in the recharge rate (and the UZ is sufficiently homogeneous that matric potential effects associated with layering can be ignored) a spatially representative recharge rate can be inferred. If focused recharge processes from a point source or from a line source such as a pond or a stream predominate recharge fluxes will decrease as water moves downward through the UZ and spreads laterally away from the recharge source [13, 22]. Computer models are generally required to obtain accurate estimates of recharge from these sources.

Unsaturated hydraulic conductivity, expressed either as a function of water content or total potential, is very difficult and expensive to measure directly. Typically only a few direct measurements of unsaturated hydraulic conductivity can be made in even the most thorough and well-funded study of the UZ. Unsaturated hydraulic conductivity is commonly estimated from other data including texture, particle-size, water-retention, saturated hydraulic conductivity using computer models, such as Rosetta [15, 16].

### **3.4. Chemical Data from Cuttings and Core Material**

A wide range of information on recharge, water movement, chemical reactions, and storage of contaminants within the UZ can be derived from chemical data used with unsaturated physical property data—especially water content. Chemical data can be obtained from cuttings and core material by leaching of cutting and core material for water soluble anions, pressure squeezing water from cores, and extraction of sorbed metals using acids or other extractants of varying strengths.

Cuttings from hand augers and ODEX drilling methods may have dried or been physically disturbed during the drilling and collection process and are not suitable for many physical analysis, such as water content or matric potential. However, these cuttings represent material from specific depths within the UZ and are suitable for many of the extraction techniques described above. The mass of chloride, nitrate and other water soluble ions in a given mass of unsaturated material are easily measured using this approach and were used in the Syrian, South African, Chinese, and US CRP studies.

Chloride accumulation in the UZ can be used to determine if recharge is occurring or if soluble salts are accumulating in the UZ [12, 13, 23, 24]. If certain assumptions about chloride deposition are made recharge rates, or in very arid settings time since recharge has last occurred, can be estimated. Chloride was used for the purpose in studies in the western Mojave Desert of the USA.

The total mass of a constituent, such as chloride or nitrate, stored within the UZ can be estimated to provide an upper bound on the potential contamination yet to reach the UZ. This was done in the China CRP for the Shijiazhuang City CRP. Porewater concentrations can be estimated from water extract and water content data to normalize the distribution of soluble constituents, such as chloride and nitrate, to changes in water content in fine-grained and coarse-grained layers within the UZ. Porewater concentrations also provide an estimate of the maximum concentration of a constituent reaching the water table. Ratios of reactive constituents such as nitrate to conservative constituents such as chloride can be used with nitrogen isotope data to evaluate denitrification processes in the UZ. The extent and location of denitrification in the UZ underlying Shijiazhuang City, China became apparent when chemical data from water extracts were compared to water content data in fine-grained

layers in the UZ. The behaviour of nitrate in the unsaturated study site in the South African CRP also was evaluated in this manner.

Extractions using acids or solvents other than water provide information on the total mass of constituents such as metals in the UZ. The distribution of these constituents provides a measure of their relative mobility and can be used to determine if these constituents are reaching the saturated zone — potentially contaminating water from wells. Acid extraction data cannot readily be converted into porewater concentrations in the same manner as water extractions of soluble salts. As a consequence these data are best used for comparison with environmental guidelines for protection of public health or in the absence of such guidelines for comparison with average elemental abundances. Because the concentrations of strongly sorbed, the contaminant concentration is related to surface area or organic carbon content in the UZ at the sample depth and it is often necessary to normalize these extraction data for changing lithology. This is commonly done on the basis of particle-size analysis or through the measurement of the solid phase sorbent such as organic carbon or extracted iron and manganese data. Metal extraction data were used in contamination studies in the Kasur area of Pakistan and in the Damascus Oasis, Syria.

### **3.5. Unsaturated Zone Instrumentation**

Considerable information can be developed on water and pollutant transport through the UZ from physical and chemical measurements made on cuttings and core material collected at the time of drilling. Once drilled, instruments can be installed in the boreholes for routine monitoring and the collection of time-series data from the UZ.

The most common instruments installed in borehole are wells. Water-level and water-quality data from water-table wells, where wells screens intersect the water table, are the most valuable for studies of the UZ since they provide information on the quantity and quality of water at the water table surface. Obviously, such wells may have a limited useful life in areas where the water table is declining. Wells cased with PVC provide access for repeated borehole geophysical measurements such as neutron logs, electro-magnetic logs, and temperature logs. Changes in these logs through time may indicate changes in the water content, and water movement through the UZ.

Instruments placed within UZs in the USA and India to monitor changes in water potential as part of this series of studies included heat-dissipation probes (HDPs), and advanced tensiometers (ATs). Other instruments to monitor changes in matric potential having various underlying physical principals and designs also are commercially available. Heat-dissipation probes consist of a heating element and a sensor embedded in a ceramic material. The rate of heat movement from the heating element to the sensor is individually calibrated the water potential of the ceramic. An equilibration period of several months is required after installation, before the water potential of the ceramic is in equilibrium with the water potential of the surrounding material. HDPs function best in comparatively dry settings having water potentials more negative than about  $-700$  cm. HDPs are connected to the surface by a wire and monitored from a data logger in a vault at land surface. Their small size and relatively inexpensive cost allows many HDPs to be installed in a single borehole. Advanced tensiometers operate on the same physical principals as regular tensiometer but their design allows a physical connection between the porous tensiometer cup and the surface through a 2.5 centimeter diameter PVC pipe. This connection allows for removal of the pressure transducer and for routine servicing of the equipment. ATs work in a relatively wet range from about  $-800$  cm to  $+800$  cm (saturated condition). As a consequence AT are usually installed above clay layers or at other depths where saturated conditions may develop. The 1 inch diameter PVC pipe physically limits the number of ATs that can be installed in a single borehole. The ATs are monitored from a data logger at land surface.

Suction-cup lysimeters installed in boreholes are used to collect water samples from the UZ. Samples are collected by first applying a vacuum to the lysimeter usually with a hand pump. After a period of time, water that has accumulated in the body of the lysimeter is forced to the surface using compressed gas, usually nitrogen. Lysimeters are connected to the surface by two tubes about 50 mm in diameter, one for application of vacuum and pressure the other for sample delivery to the surface. Tubes are

commonly colour coded for depth and pressure/vacuum and sample collection. Commercially available suction-cup lysimeters are designed to lift from depths as great as 100 m in material having matric potential less negative than about  $-600$  cm. The small diameter of the tubes does not limit the number of lysimeters that can be installed in a single borehole.

Air-samplers installed in boreholes commonly consist of a small diameter tube. In the UZ the tube has a screen of some type to prevent blockage by sand grains. On the surface the tube is equipped with a cap of some type to exclude atmospheric air. The air samplers require purging to remove air entrained during drilling and purging prior to sample collection. Excessive purging may move air within the UZ mixing air from different depths within the UZ (or even from land surface) in the sample.

Instrumented boreholes drilled to depths exceeding 100 m and instrumented using the equipment described above have functioned at environmental sites in the western Mojave Desert, USA for more than 8 years (since 1998) without difficulty or signs of failure. Instrumented boreholes having a more simple design containing only wells for sample collection and access tubes, suction-cup lysimeters, and air samplers have been operated without difficulty for more than 12 years (since 1994). Several instrumented borehole based on these designs has been constructed at the Indian Agricultural Research Institute in New Delhi, India.

Permanent experimental lysimeter stations were used to monitor changes in UZ chemistry in the UZ beneath agricultural land in both Germany and Austria. These stations consist of large-diameter caissons installed to depths of several meters. Suction-cup lysimeters and other instruments extend laterally into the UZ from the caisson. The caissons are sufficiently large to permit access by a person to service the instruments and support equipment, and to collect samples from lysimeters. The German and Austrian sites are located at agricultural research stations that are permanently manned and serviced. Caissons of this design are physically limited by the depth they can be extended into thick UZs and by the cost of installation.

### **3.6. Temperature Data**

In many settings, especially near intermittent streams, temperature is an easily measured parameter containing important information on infiltration of streamflow and ultimately groundwater recharge. In areas, where precipitation and resultant streamflow is seasonally dominated (either the colder winter season, or warmer summer season), the streambed will be cooled or warmed in proportion to the quantity of streamflow infiltrated. In the western Mojave Desert of the USA precipitation and streamflow occur largely in the winter months. Measured temperature differences between the streambed and the surrounding alluvial material were as large as  $1.5^{\circ}\text{C}$  and extended into the ground to depths as great as 10 m. Infiltration rates estimated at these sites exceeded 50 cm/yr along some stream reaches.

Temperature is extremely attractive in these types of studies because large numbers of measurements can be made inexpensively. Thermal properties of materials (such as thermal conductivity, heat capacity, and heat diffusivity) are easily measured or readily estimated from physical measurements such as bulk density or water content. Temperature data can be used to quantify estimates of infiltration using either analytical approaches or numerical models. Numerical models easily account for focused recharge processes that may be more difficult to address with isotopic data alone. Analytical solutions and numerical model results are highly sensitive to advective infiltration rates and less sensitive to estimated or measured thermal property data used as model input.

## **4. APPROACHES USED IN THE CRP STUDIES**

No single protocol was established for UZ data collection for the studies done as part of this CRP because of the differing objectives and scope of the studies, and the wide range of environmental conditions from arid to humid. However, research done at each CRP site recognized the need for basic care in study design, sample collection, sample preservation, and data limitations described in the

previous section. Each CRP site utilized data from different disciplines including groundwater hydrology, soil physics, and isotope hydrology to constrain estimates of recharge rates, environmental processes and contamination within reasonable ranges. Below is a synopsis of the programs carried out under this CRP and the parameters involved in each study. Factors such as climate, depth, tracers used, method of sampling, land use type and pollutants of concern at each site are included in Table 1. It can be seen that the programs of this CRP cover a wide range of conditions in almost all parameters including climate and UZ depth. The primary pollutants of concern for this CRP have been nitrate, agrochemicals, and heavy metals. For short timescales (days to a few years), applied tracers are capable of offering useful information on transport. Applied tracers and stable isotopes of water can furnish important information on details of water (and chemical) movement through the UZ, helping to differentiate between the importance of preferential flows and matrix flows. For longer times and deeper UZs, tritium is still the best tracer for determining recharge rates. Nitrogen isotopes offer clear indications of sources of nitrate pollution in a wide variety of settings and make it possible to distinguish between natural and various anthropogenic sources. Isotopes of nitrate can also help determine potential reactions in the UZ. Gases have been used extensively in this program to obtain information on physical factors affecting gas transport.

## **5. ACHIEVEMENTS OF THE PROJECT**

The CRP has demonstrated the use of isotopic methodologies for understanding the migration of potential contaminants through the unsaturated zone (UZ) into the underlying groundwater. Contamination of aquifers usually occurs via transport (as recharge) through the unsaturated zone (UZ). The ten projects in this CRP covered a wide range of approaches and sites typically encountered in unsaturated zone research. A demonstration site was set up at an agricultural experimental farm near New Delhi, India with instrumentation to conduct controlled studies in the UZ. The studies included measuring movement of water, solutes, and gasses through the UZ using an assortment of isotope and geochemical tracers and approaches.

One project was in a karst terrain in Slovenia, where transport can be relatively rapid through channels/large fractures. At the same site, slower movement occurs through small fractures where chemicals can be retained in the UZ for some years after they have been introduced. The site in Germany had relatively rapid movement through the UZ and investigations showed the differences in contributions between overland flow, subsurface flow and groundwater input in total runoff. The Austrian site was at a research station in an intensive agricultural area. The project made use of isotopic data from lysimeters and soil cores to elucidate microbial processes in the UZ. The contribution from the United Kingdom investigated UZ processes in the Chalk aquifer system, beneath an extensive impermeable drift cover. Determination of nitrogen species combined with groundwater age indicators and data from gas samplers were used to develop a conceptual regional model of contaminant transport for the study site. The project in Pakistan studied an area where extensive industrial pollution occurred. Gas samples and soil cores were used to study the movement and reactions of pollutants in the UZ. The site in India, which was selected for extensive study, was in an agricultural research site where agro-chemical use has occurred. Radiotracers were applied to the surface and their movement through the UZ was monitored by analysis of soil cores and in-situ measurements. The project in China, which was located near Shijiazhuang City, was in an area which has suffered extensive degradation of its groundwater quality due to leaching of nitrate and other contaminants through the UZ. The site was investigated using tritium and stable isotopes from soil cores and groundwater. The project in the United States of America collected data from sites in arid and semi-arid climates with deep (~100-200m) UZ's. One of the locations, the High Plains Aquifer, is a region where irrigation has increased movement of pollutants through the UZ. The Syrian study, in the region of the Damascus Oasis, investigated migration of heavy metals into the UZ. Nitrogen isotopes were also used to determine the source of increasing nitrate concentrations in groundwater. The South African study looked at cases of extreme nitrate pollution in agricultural areas due to intense rainfall events. Particular emphasis was placed on identifying the fate of pollutants caused by livestock.

TABLE 1. PARAMETERS OF STUDIES CARRIED OUT UNDER THE CRP

Sites	Climate	Depth (m)	Timescale	Tracer <sup>1</sup>	Method <sup>2</sup>	Land Use <sup>3</sup>	Pollutants <sup>4</sup>
USA	Arid /semi-arid	10–250	40y –18000y	S, T, N, G	A, L	A, N	N, P, C
S. Africa	Arid /semi-arid	5	2y – 20y	S, N	H	A, L	N, S
UK	Humid	20–25	20y –25y	N, T, G	G	A	N
China	Semi-arid	0–30	30y–40y	S, T, N,	T, G	A, U, S	N, S, B
Germany	Humid	0–10	Hours – 10y	N, S, A	L, C	A, E	N, S
India	Semi-arid	14	2y–5y	S, A, G	L, G	A, E	N, S
Slovenia	Humid	600	Days – 2y	S, A	L	A, H, E	N, B
Austria	Humid	0–3.5	10y	S, A, N	L, T, C, M	A, E	N, B
Pakistan	Semi-arid	5–9	20y	S, N, G	H,	I, U, S	H, S, B
Syrian Arab Republic	Arid	25–30	10y	S, N, C	H	A, I, S, U	N, H, S, B

<sup>1</sup> S = stable isotopes of water, T = tritium, N= nitrogen compound isotopes, A = applied tracer, G = gases, C = carbon isotopes.

<sup>2</sup> H = hand auger, L = lysimeter, A = air hammer, C = suction cups, M = microbiology, T =trench, G = auger.

<sup>3</sup> A = agriculture, N = native/natural, L = livestock, E = experimental, U = urban, S = sewage, I = industrial, H = hard rock

<sup>4</sup> N = nitrogen compounds, H = heavy metals, P = pesticides and herbicides, S = salts, B = bacteria.

The UZ was found to be effective in protecting groundwater from most heavy metal contaminants. Other contaminants like nitrate and chloride generally move conservatively through the UZ. Very limited information was collected on interactions at the Saturated/Unsaturated Interface Region (SUIR), but it appears that there may be some mitigation of contaminants in this zone. There was also evidence presented that, with proper conditions, reactions involving both nitrate and ammonia can occur in the UZ above the SUIR. When determining sources of nitrate in the UZ, isotopes are crucial in identifying the difference between natural and anthropogenic loads.

Many studies made use of sampling of UZ gases in this CRP. CFCs, being generally conservative in oxygenated soil zones, have been found to be important in determining basic physical parameters controlling gas transport in the UZ. Frequently, gas diffusion rates are calculated from measurements of physical properties from soil cores (porosities, water content etc.) which represent only a one dimensional sample. Using gases like CFCs, it is possible to obtain bulk diffusion rate for the UZ as a whole, which can then be used to study other gases. This CRP has shown that this is the best approach for obtaining information on potential gas movement in the UZ.

The best method to measure recharge rates is dependent on the timescale of the study area. For relatively short timescales, applied tracers are the most appropriate with deuterium, as part of the water molecule, probably being the best choice. For longer timescales (decadal), the use of tritium, either by identification of the 1963 peak or the tritium interface method, represents the best approach. For extremely long timescales, chloride is still the only reliable tracer. It is also evident that at all timescales, soil texture, topography, vegetation type, rainfall amount are dominant factors in determining where recharge occurs and how rapidly it occurs. Advances have been made in identifying locations where preferential recharge is likely to occur, and this type of information has major implications for mitigating contaminant movement to the water table. It should also be taken into account when UZ studies are set up.

## 6. CONCLUSIONS AND RECOMMENDATIONS

The present CRP was undertaken to develop recommendations and standard methodology for sampling and monitoring in the UZ. It also aimed to provide a methodology to determine best management practices for studying the movement of water and pollutants from the surface through the UZ into groundwater systems. A goal was to learn which tracers work best in UZ studies and how different situations dictate which approaches should be applied. To this end, a demonstration site was established in India that offered an opportunity to test the various approaches available for UZ studies.

This CRP differed from previous CRPs by including focuses on gas movement through the UZ, and on the complex interactions involving gases at the SUIR. These interactions may have implications for initial concentrations for age dating gas tracers, especially  $^{14}\text{C}$ . There was also a desire to look at the transport of potentially non-conservative contaminant tracers (e.g.,  $\text{NO}_3^-$  and agrochemicals) thru the UZ in relation to transport of conservative tracers such as tritium and applied tracers. It was hoped to determine what reactions occurred to change concentrations of contaminants in the UZ, and whether these reactions occurred throughout the UZ or only at the SUIR.

Many, although not all, of the objectives have been achieved by this CRP. An experimental site was set up to study processes in the UZ at the Indian Agricultural Research Institute (IARI), an experimental site near New Delhi, and it is now operational. Soil cores have been analyzed and tracer tests have been conducted at an irrigated and an unirrigated site during the CRP. Borehole instrumentation was installed including lysimeters and water potential probes that continue to collect data. Tracer tests were conducted to determine the mobility of water and ionic species in the UZ. Gas sampling systems were installed at multiple depths to study gas movement and interactions in the UZ. It is hoped that this site will serve as an example of how to set up UZ studies in similar locations.

The other sites studied in this CRP covered a wide variety of different systems, as demonstrated in Table 1. The results from the other sites will be of value to potential researchers in a large variety of environments. The hydrologic settings studied include fractured rock systems, small experimental agricultural systems, large regional systems covering many different sources of potential contamination, and deep UZs in arid and semi-arid regions. The diversity of these sites resulted in a wide range of approaches being needed in this CRP to resolve movement of water and solutes through the UZ. Other researchers can study these sites and determine which study most closely resembles their system. They will then have information on which available isotopic techniques are likely to yield the most useful results for their investigations.

One of the major outcomes of this CRP is the confirmation of the importance of landscape factors and physical factors in the soil column in allowing or limiting recharge and the movement of chemicals through the UZ. It has become apparent that in many areas, recharge is preferentially focused in certain locations. Recent studies, including those in this CRP, have indicated that the locations of preferential recharge can be predicted in many cases. Future studies by researchers should make use of this information in determining where to locate UZ sites and where to collect UZ cores and data.

Sampling difficulties that have yet to be resolved have limited the ability to study chemical reactions occurring within the SUIR. However, some indication of the impact of chemical reactions in this region can be discerned from measurements of gas and isotopic tracers within the UZ above the SUIR and in groundwater. Results from some of these studies can help in resolving this question. The presence of  $\text{N}_2\text{O}$  and occasional excess nitrogen near the SUIR does indicate that nitrate reduction reactions can occur in this region. It is likely that other contaminants like agrochemicals may also undergo transformations in this zone. However, in most cases, where the movement of contaminants is assumed to come directly through the UZ, isotopic ratios of chemicals in the UZ seem to closely match those found in the water column. Thus, if there are reactions in the SUIR, either they are not large enough in extent to shift isotopic values of contaminants going into the groundwater, or the reactions are so complete where they do occur that no nitrate is left, and no change in isotopic values is imparted to the remaining contaminant. These two possibilities cannot be distinguished with the

present data sets. However, looking at passive data such as  $N_2O$  production and the lack of shifts of nitrate isotopic values as UZ nitrate moves into the water column, it is likely that the SUIR does not impact the nitrate concentrations greatly at the sites studied in this CRP. Further work needs to be carried out to determine if this is true in controlled settings. A site such as the IARI experimental station could be used for further study of this issue.

In most cases, it seems that chemicals move through the UZ without major transformations. Nitrate isotopic values in the UZ usually seem to be conservative, indicating little reaction. However, the existence of an  $N_2O$  peak in the UZ at a site in Nebraska, USA, indicates that under proper conditions, some reactions do occur in areas of the UZ other than the SUIR. Work at the Austrian site also indicated microbial transformations can take place in the UZ beneath the root zone and above the SUIR. The wide range of nitrate isotopic values found at the Syrian sites are not likely to result from input processes, and thus may result from reactions within the UZ. The conditions that are required to produce reactions at these locations are not known at this time.

Many studies made use of sampling of UZ gases in this CRP. CFCs, being generally conservative in oxygenated soil zones, have been found to be important in determining basic physical parameters controlling gas transport in the UZ. Frequently, gas diffusion rates are calculated from measurements of physical properties from soil cores (porosities, water content etc.) which represent only a one dimensional sample. Using gases like CFCs, it is possible to obtain bulk diffusion rate for the UZ as a whole, which can then be used to study other gases. This CRP has shown that this is the best approach for obtaining information on potential gas movement in the UZ.

The major shortfall of this CRP in terms of meeting its objectives is obtaining an understanding of the movement of gases across the SUIR. In the UZ above the SUIR, the research conducted during this CRP has produced significant findings. But very little sampling was carried out in the SUIR itself to determine if gases in the groundwater were at equilibrium with UZ gases above. This is a zone that can fluctuate and it is not easy to install proper equipment for studying these problems. The equilibria and interactions are also important for the movement of gases produced in the SUIR (such as  $N_2O$ ) into the UZ and ultimately to the atmosphere. It was hoped that the research site in India would be able to address these issues, but installation of proper equipment was not finished in time for sampling prior to the end of the program. Gas samplers are now in place and might be able to address some of these issues in the future.

Any future CRP should probably focus on the three issues that have proved most problematic to resolve in this CRP: 1. Use of isotopes to understand chemical reactions at the SUIR. 2. Gas equilibrium at the groundwater/UZ interface. 3. Movement and reactions of pesticides and herbicides through the UZ. Resolving all these issues will require the development of new approaches and sampling techniques. As the SUIR is relatively small, it may be difficult to obtain adequate samples for some isotopic measurements. It may be best to look at surrogates that will furnish similar information, or gases which might be easier to sample in volume, to study this zone. Regarding the equilibrium at the groundwater/UZ interface, one project in this CRP (High Plains Aquifer in the USA) has sampled  $^{14}C$  in soil gas, but analyses are not yet complete. However, further work should be carried out in other environments to try and determine if gases are in equilibrium, and if any reactions in the SUIR will impact concentrations and equilibria. Pesticides and herbicides were measured in some of the projects of this CRP. These chemicals have reached the water table in some instances, but in the UZ, there appears to be no systematic distribution of these chemicals. The absence of continuous concentrations, unlike other chemicals and tracer, is probably a result of their occasional use and the fact that many of these chemicals are designed to be degraded in the root zone. The best way to study these chemicals may be in a controlled application at an experimental site like that in IARI.

## REFERENCES

- [1] RONEN, D., MAGARITZ, M., ALMON, E., Contaminated aquifers are a forgotten component of the global N<sub>2</sub>O budget, *Nature* **335** (1988) 57–59.
- [2] THORSTENSON, D.C., WEEKS, E.P., HAAS, H., FISHER, D.W., Distribution of gaseous <sup>12</sup>CO<sub>2</sub>, <sup>13</sup>CO<sub>2</sub>, and <sup>14</sup>CO<sub>2</sub> in the sub-soil unsaturated zone of the western U.S. Great Plains, *Radiocarbon* **25** (1983) 315–346.
- [3] MOSIER, A.R., PARTON, W.J., VALENTINE, D.W., OJIMA, D.S., SCHIMEL, D.S., HEINEMEYER, O., CH<sub>4</sub> and N<sub>2</sub>O fluxes in the Colorado shortgrass steppe 2, Long-term impact of land use change, *Glob. Biogeochem. Cycles* **11** (1997) 29–42.
- [4] HOULE, D., CARIGNAN, R., ROBERGE, J., The transit of <sup>35</sup>SO<sub>4</sub><sup>2-</sup> and <sup>3</sup>H<sub>2</sub>O added in situ to soil in a boreal coniferous forest, *Water Air Soil Pollut. Focus* **4** (2004) 501–516.
- [5] MOSER, H., RAUERT, W., “Isotopic tracers for obtaining hydrologic parameters”, *Isotopes in the Water Cycles* (AGGARWAL, P.K., GAT, J.R., FROEHLICH, K., Eds), (2005) 11–24.
- [6] SUESS, H.E., Tritium geophysics as an international research project, *Science* **163** (1969) 1405–1410.
- [7] MICHEL, R.L., “Tritium in the hydrologic cycle”, *Isotopes in the Water Cycles* (AGGARWAL, P.K., GAT, J.R., FROEHLICH, K., Eds), (2005) 53–66.
- [8] KENDALL, C., “Tracing nitrogen sources and cycling in catchments”, *Isotope Tracers in Catchment Hydrology* (KENDALL, C., MCDONNELL, J.J., Eds), (1998) 519–577.
- [9] COOK, P.G., SOLOMON, D.K., Transport of atmospheric and trace gases to the water table: Implications for groundwater dating with chlorofluorocarbons and krypton 85, *Water Resour. Res.* **31** (1995) 263–270.
- [10] MILLINGTON, R.J., Gas diffusion in porous media, *Science* **130** (1959) 100–102.
- [11] DRISCOLL, F.G., *Groundwater and wells: Saint Paul, Minn., USA*, Johnson Filtration Systems, INC., (1986).
- [12] IZBICKI, J.A., CLARK, D.A., PIMENTEL, M.I., LAND, M., RADYL, J., MICHEL, R.L., Data from a thick unsaturated zone underlying Oro Grande and Sheep Creek Washes in the western part of the Mojave Desert, near Victorville, San Bernardino County, California, 1994–99, U.S. Geological Survey Open-File Report 00-262 (2000) 133, <http://pubs.er.usgs.gov/usgspubs/ofr/ofr00262>.
- [13] IZBICKI, J.A., RADYK, J., MICHEL, R.L., Water movement through a thick unsaturated zone underlying an intermittent stream in the western Mojave Desert, Southern California, USA. *J. Hydrol.* **238** (2000) 194–217.
- [14] IZBICKI, J.A., RADYK, J., MICHEL, R.L., Movement of water through the thick unsaturated zone underlying Oro Grande and Sheep Creek Washes in the western Mojave Desert, USA, *Hydrogeol. J.* **10** (2002) 409–427.
- [15] SCHAAP, M.G., LEIJ, F.J., VAN GENUCHTEN, M.Th., “A bootstrap-neural network approach to predict soil hydraulic parameters” (VAN GENUCHTEN, M.Th., LEIJ, F.J., WU, L., Eds), *Proc. Int. Workshop, Characterization and Measurements of the Hydraulic Properties of Unsaturated Porous Media*, University of California, Riverside, CA. (1999) 1237–1250,
- [16] SCHAAP, M.G., LEIJ, F.J., Improved prediction of unsaturated hydraulic conductivity with the Mualem-van Genuchten, Submitted to *Soil Sci. Soc. Am. J.* (1999).
- [17] HILLEL, D., *Soil Physics*, Harcourt Brace Jovannovich, Publishers, New York (1982).
- [18] JURY, W.A., GARDNER, W.R., GARDNER, W.H., *Soil Physics*, John Wiley & Sons, Inc., New York, (1991) 328 .
- [19] MICHEL, R.L., IZBICKI, J.A., Measurements of CFC's in the unsaturated zones of recharge sites in the Mojave Desert, USA, *Proceedings of IAH Conference on Balancing the Groundwater Budget*, Darwin, Australia (2002) CD-Rom.
- [20] VAN GENUCHTEN, M.Th. A closed-form equation for predicting the hydraulic conductivity of unsaturated soils, *Soil Sci. Am. J.* **44** (1980) 892–898.
- [21] BROOKS, R.H., COREY, A.T., Hydraulic properties of porous media, *Hydrol. Pap.* **3**, Colorado State University, Fort Collins, Co (1964).

- [22] NIMMO, J.R., DEASON, J.A., IZBICKI, J.A., MARTIN, P., Evaluation of unsaturated zone water fluxes in heterogeneous alluvium at a Mojave Basin site, *Water Resour. Res.*, **38**, 10 (2002).
- [23] COOK, P.G. WALKER, G., “Evaluation of the use of  $^3\text{H}$  and  $^{36}\text{Cl}$  to estimate groundwater recharge in arid and semi-arid environments”, *Isotopes in Water Resources Management*, IAEA, Vienna, Austria (1996) 397–403.
- [24] SCANLON, B.R., LANDGORD, R.P., GOLDSMITH, R.S., Relationship between geomorphic settings and unsaturated flow in an arid setting, *Water Resour. Res.* **35** (1999) 983–999.

**CHEMICAL, ISOTOPIC, AND MICROBIOLOGICAL EVIDENCE FOR  
NITRIFICATION BELOW THE PLANT ROOT ZONE FROM  
INTENSIVE FERTILIZED AGRICULTURAL AREA IN AUSTRIA**  
*INSIGHTS FROM LYSIMETER STUDIES AND SOIL CORES*

A. LEIS

Joanneum Research Graz,

Institute of Water Resources Research Hydrogeology and Geophysics,

Graz, Austria

**ABSTRACT**

Compared to surface soils, relatively little is known about nitrogen transformation processes below the plant root zone. To investigate the occurrence and rate of nitrification in this zone a combination of chemical, microbial and isotopic techniques are used. Additionally tracer test were conducted with bromide, deuterium and the food dye 'Brilliant Blue FCF'. The mean flow velocity in the unsaturated zone was approximately 1.4 m/y. The maximum velocity was determined to be 1.65 m/y. The residence time in the unsaturated zone was more than 2.5 years. Core incubations under nitrifying conditions demonstrated that nitrifying organisms were present below the plant root and indicated a low, but measurable potential nitrifying activity. Soil samples from a depth of 2.4 m have shown a considerable actual and potential nitrification activity. This conflicts with the widespread idea that nitrification in soils is limited to the plant root zone. Chemical and isotopic analyses of water samples obtained from lysimeters were used to verify the results of the microbiological investigations. Isotopic analyses primarily included the oxygen and nitrogen isotopes of the dissolved nitrate ( $\delta^{18}\text{O}-\text{NO}_3^-$  and  $\delta^{15}\text{N}-\text{NO}_3^-$ ). In addition, selected samples also were analyzed for the carbon isotopic composition ( $\delta^{13}\text{C}-\text{DIC}$ ) of dissolved inorganic carbon and the sulphur isotopic composition ( $\delta^{34}\text{S}$ ) of sulphate-sulphur. Analysis of the  $\delta^{13}\text{C}$  and  $\delta^{34}\text{S}$  of these other constituents help to determine the geochemical processes which are controlling the nitrogen transformation process. The  $\delta^{15}\text{N}-\text{NO}_3^-$  and  $\delta^{18}\text{O}-\text{NO}_3^-$  data confirmed that  $\text{NO}_3^-$  in the unsaturated zone was predominately derived from microbial nitrification and to a much lesser extent from atmospheric deposition. The  $\delta^{15}\text{N}-\text{NO}_3^-$  and  $\delta^{18}\text{O}-\text{NO}_3^-$  data further suggested that nitrification can occur in the whole profile of the unsaturated zone. Nitrification can occur below the plant root zone and can play a significant role in the speciation and transport of nitrogen compounds through the unsaturated zone.

**1. INTRODUCTION**

The intensive use of organic and inorganic fertilizers has led to increased loads of nitrate in groundwater in many regions of Europe. The Leibnitzer Field aquifer of Styria in southern Austria has seen a strong increase in groundwater nitrate concentrations over the past decades. This aquifer is extremely susceptible to surface derived contamination because of its largely unconfined nature and highly permeable sands and gravels. The source of nitrate contamination in the aquifer is attributed to local, long term agricultural land use practices such as spreading large amounts of liquid manure (mainly from pigs) above the soils. To determine what action should be taken to reduce nitrate contamination of groundwater, it is important to identify the sources and the fate of nitrate in unsaturated zone, as well as the relevant microbiological processes. Previous studies have demonstrated that the application of pig manure can strongly influence the ammonia oxidising bacteria [1, 2]. It was found that additions of swine manure to soil plots increased both the number of ammonia oxidising bacteria as well as increasing their potential ammonia oxidising activity. The nitrogen and oxygen isotope ratios of dissolved nitrate can be used to distinguish sources of nitrate [3] and evaluate whether nitrate concentrations are changing due to mixing of different sources or to denitrification processes [4–6]. Nitrogen and oxygen isotopes have been used in previous studies to distinguish whether the observed nitrate contamination in an aquifer was from manure used as fertilizer or from inorganic nitrogen fertilizer [7, 8]. The precise value of the oxygen isotopic component of the nitrate molecule probably varies somewhat in time and space. However, as long as the variability is small relative to the separation between  $\delta^{18}\text{O}$  of nitrate from atmospheric deposition and microbial nitrification,  $\delta^{18}\text{O}$  can be useful for determining relative contributions of the two sources [9].

The objective of this study was to evaluate the main nitrogen transformation processes within and below the plant root zone using standard biogeochemical, isotopic and microbiological methods.

## 2. DESCRIPTION OF THE STUDY AREA

The investigation area, the so called Leibnitzer Feld, is situated in the lower Mur valley in Styria (Austria) (Fig. 1). The valley is filled with quaternary gravels and sands with a thickness of 10 to 15 m. The Quaternary glacial deposits are comprised of gravels and occupy a depth between 0.3 and 2.5 m. The soil cover varies between 1 to 2 m in the alluvium of the river Mur and reaches up to 7 m under the erosional terraces of Pleistocene age. At the lysimeter test site the water table commonly varies from 3.5 to 5 m below the soil surface [10, 11]. Mean annual precipitation between 1992 and 2004 was 920 mm, and the annual air temperature (1901–1980) was 8.9°C. Recharge to the aquifer is primarily by precipitation. Due to the permeable soils and coarse-grained aquifer material, recharge is on the order of 38% of the annual precipitation. The land use in the study area is primarily agriculture, dominated by maize monoculture.

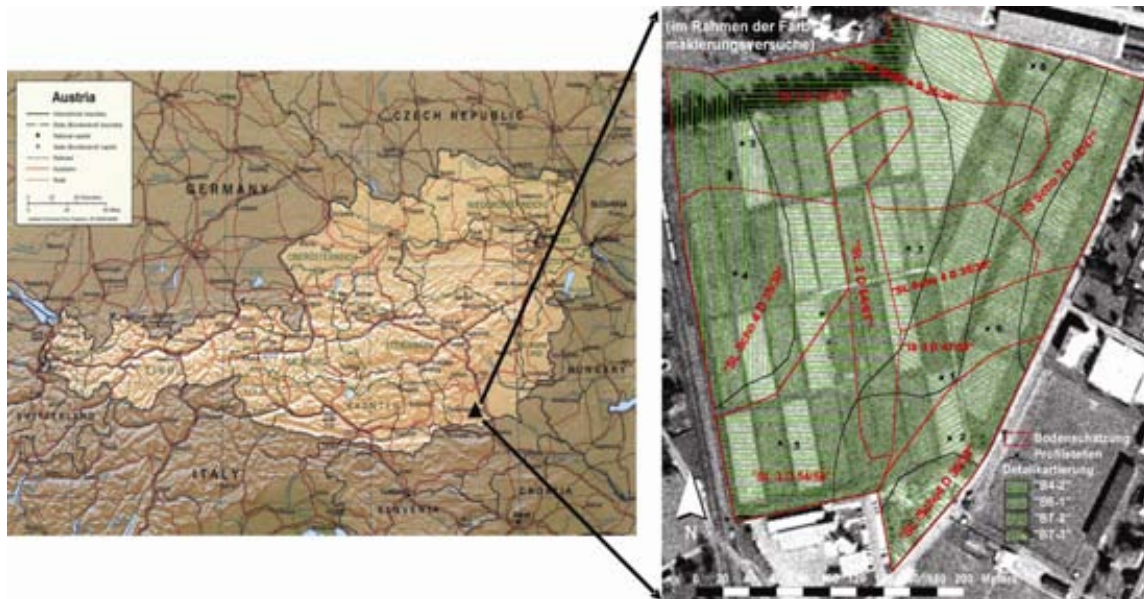


FIG. 1. Location of the study area.

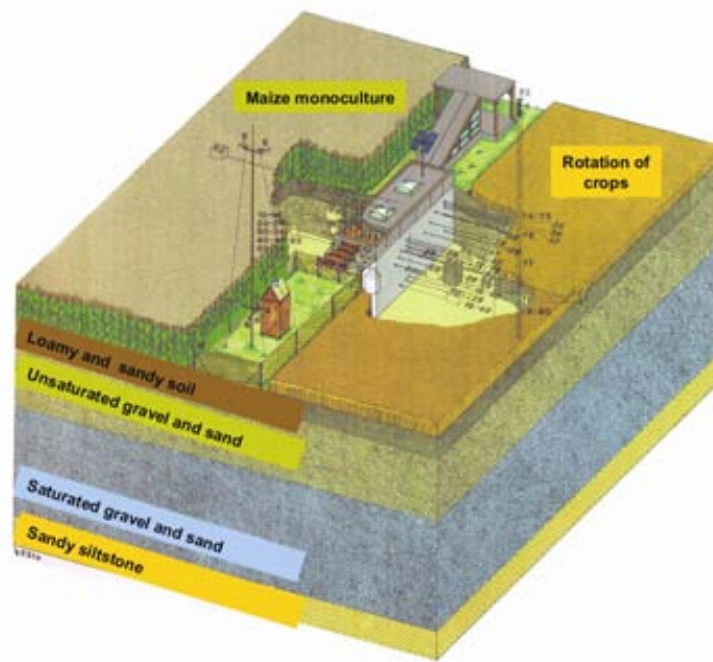


FIG. 2. Schematic plot of the lysimeter station.

### 3. MATERIALS AND METHODS

#### 3.1. Field test site (Operating from 1991–2004)

Based on the knowledge that key processes which contributed to the nitrate problem in the Leibnitzer Feld predominantly take place in the unsaturated zone, an experimental lysimeter station was built in 1991. The station was designed to monitor the movement of water and solids from the atmosphere through the soil (~100 cm) and unsaturated sand and gravel (~450 cm) into the saturated quaternary valley fill [12].

The lysimeter station itself is located between two different cropped plots. One field was cultivated with single-crop farming with complete fallow (maize) and the other with a crop rotation (maize, winter corn, rape). Planting on this second plot was with interspersed with crops that were intended to prevent significant nitrate leaching. The station includes two non-weighable backfilled gravitation lysimeters (operating since 1991), six non-weighable monolithic field lysimeters [13] (operating from 1991–2004), five seepage water samplers [14] (operating from 1991–2004, two are still in operation) and various open field measurements. These included time-domain reflectometry (TDR) probes, gypsum blocks, tensiometers, and chemical sensors and suction cups and plates. The lysimeter station includes also a full automatic climatic station. Depending on the different soil layers we have installed these probes on both sites in five different depths. Several tracer tests were conducted with Bromide, Deuterium and the food dye Brilliant Blue FCF as tracers [15, 16].

A detailed description of the station can be found at the website of the Austrian Lysimeter study group [17, 18]. The most important function of the station is its ability to explore the movement of water and solids by means of hydrochemical and isotope-hydrological analyses based on natural land use practices.

#### 3.2. Water in the unsaturated zone

The collected outflow of the suction plates and cups was analyzed over a number of years for hydrochemical (major cations and anions, DOC) and isotope contents ( $\delta^{18}\text{O}$ ,  $\delta^2\text{H}$ ,  $\delta^{13}\text{C}$ -DIC,  $\delta^{15}\text{N}$ - $\text{NO}_3^-$  and  $\delta^{18}\text{O}$ - $\text{NO}_3^-$ ). The parameters pH, dissolved oxygen, specific electric conductivity and temperature were measured in the field using appropriate meters and electrodes. The water samples for nitrogen and oxygen isotopes analysis were preserved with a few drops of chloroform. In addition to the nitrogen and oxygen isotopes, selected samples also were analyzed for the sulphur isotopic composition ( $\delta^{34}\text{S}$ ) of sulphate sulphur ( $\delta^{34}\text{S}$ - $\text{SO}_4$ ), and  $\delta^{13}\text{C}$  in dissolved inorganic carbon ( $\delta^{13}\text{C}$ -DIC).

#### 3.3. Soil cores

Soil samples were taken from eight sampling points within the test field. Six locations outside of the test field were also sampled as a control. The samples were collected every 30 cm from undisturbed soil profiles (0–240 cm). The soil samples collected for determination of the actual and potential nitrification activity, quantification of nitrifying bacteria and DNA-analyses were sieved (5 mm), cooled and deep-frozen in the laboratory. The actual and potential nitrification activity was evaluated using a nitrification assay similar to that described by Schinner and co-workers [19]. The number of nitrifying bacteria were determined according to [19] using the “most pro number” method [20]. The numerical taxonomy of the nitrifying bacteria were evaluated according to the methods described by Holt [21–23]. A commercially available PCR template preparation kit (Roche ‘High Pure’) was used for the isolation of bacterial DNA.

## 4. RESULTS

### 4.1. Nitrate distribution in the unsaturated zone

The nitrate distribution in the unsaturated zone waters showed an unexpected trend. The mean nitrate concentrations increase with increasing soil depth (Fig. 3) and the highest nitrate concentration can be found at the deepest sampling point at 3 m below surface. This same trend was observed beneath both of the cropping regimes.

This trend can not be explained by simple leaching of nitrate from the plant root zone. The comparison of the 2D distribution of nitrate and chloride concentration in the unsaturated zone clearly shows differences between the behaviour of the conservative tracer chloride and the transport of nitrate (Fig. 3).

The unexpected distribution of nitrate indicates that there must be some nitrification in the deeper parts of the unsaturated zone.

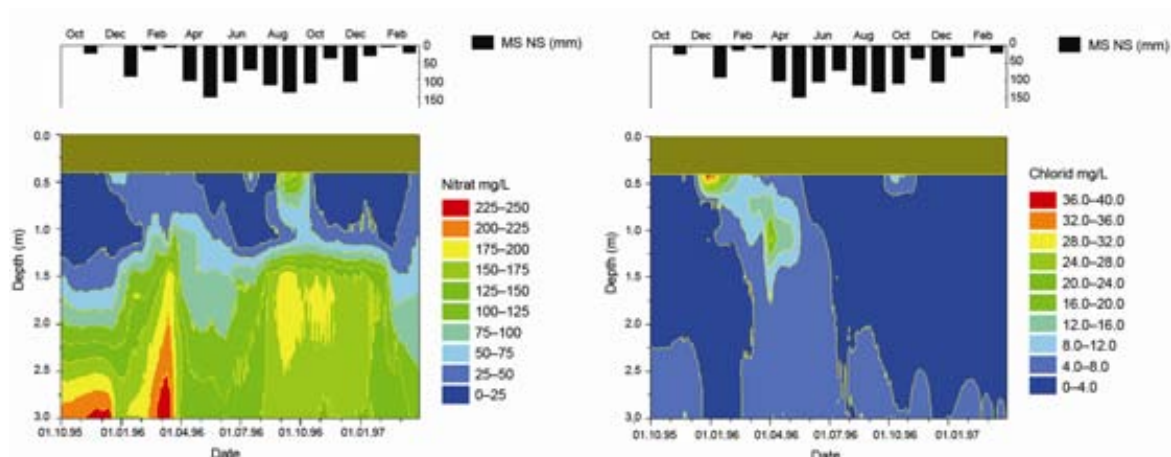
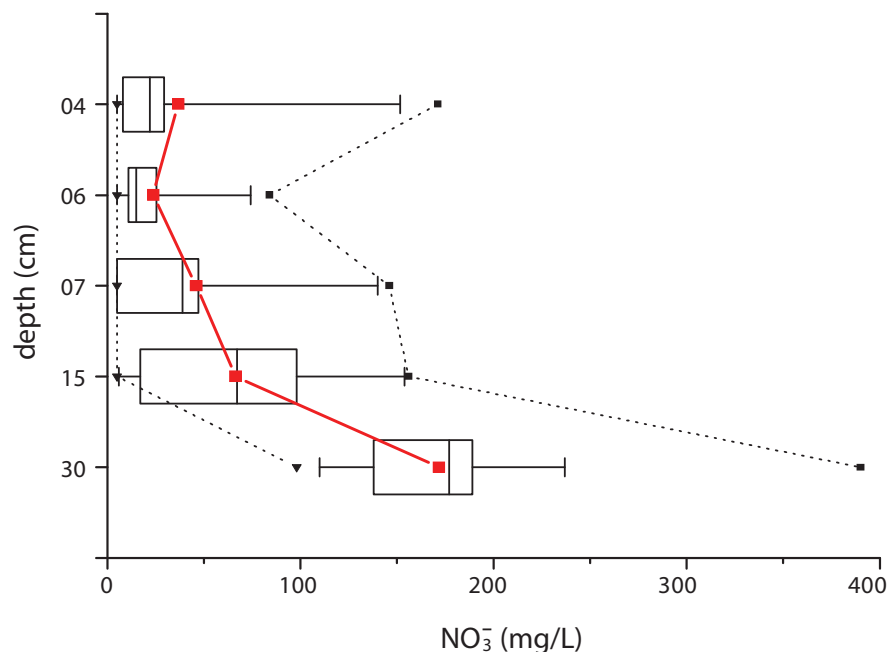


FIG. 3. 2D-profile of nitrate and chloride concentrations and monthly precipitation data (crop rotation).

## 4.2. Microbiological Investigations

To prove the assumption that nitrification is occurring in the deeper parts of the unsaturated zone, various microbiological investigations were carried out. All soil profiles have shown that nitrifying bacteria occur along the entire range of the sampling interval (Fig. 4).

Core incubations under aerobic conditions indicated a low, but measurable actual and potential nitrifying activity below the plant root zone. Additionally, soil samples from a depth of 2.4 m have shown still a considerable actual and potential nitrifying activity (Fig. 5).

## 4.3. Isotopic Investigations

To verify these results with an independent method we have used  $\delta^{15}\text{N}$  and  $\delta^{18}\text{O}$  isotope ratios of nitrate in unsaturated zone water samples obtained from the lysimeters (Appendix I).

Samples for  $\delta^{15}\text{N}$  and  $\delta^{18}\text{O}$  of nitrate were analysed monthly at the outflows of the suction plates and cups (Fig. 6 and 7).

As mentioned before the application of the  $\delta^{15}\text{N}\text{-NO}_3^-$  and  $\delta^{18}\text{O}\text{-NO}_3^-$  isotope ratios is a useful technique to identify sources and fate of nitrate. Due to the large oxygen isotopic difference between nitrate produced in the atmosphere and that produced by microbial processes in the soil (nitrification), the oxygen isotopes in nitrate are particularly powerful for distinguishing between nitrate originating from fertilizer application and nitrate from atmospheric deposition. In addition, changes in the concentration and isotopic composition of nitrate can be used to identify processes such as denitrification [6]. The isotope ratios in the unsaturated zone will be also influenced by mixing processes from different nitrate sources. In our case, the two main sources of nitrate are from nitrification in the soil and from atmospheric deposition. During nitrification in soil, the  $\delta^{18}\text{O}$  values in the resulting nitrate normally decrease because the amount and availability of isotopically heavy atmospheric nitrate decreases with increasing depth. The mean isotopic composition of atmospheric nitrate was determined as 9.1‰ for  $\delta^{15}\text{N}\text{-NO}_3^-$  and 37‰ for  $\delta^{18}\text{O}$ . The outflow of the suction plates and cups ranged from approximately 2‰ to 12.6‰ for  $\delta^{15}\text{N}\text{-NO}_3^-$  and 2.2‰ to 19.1‰ for  $\delta^{18}\text{O}\text{-NO}_3^-$ . The lysimeter samples collected during the study period, together with groundwater and the atmospheric composition of  $\delta^{15}\text{N}\text{-NO}_3^-$  and  $\delta^{18}\text{O}\text{-NO}_3^-$  are plotted in Fig. 8. The unsaturated zone water samples show a clear trend of increasing nitrate concentration accompanied by decreasing  $\delta^{18}\text{O}$  values of nitrate with increasing depth. This trend could be explained by continuously admixing of nitrate originating from nitrification along the whole profile in the unsaturated zone (Fig. 9).

## 5. CONCLUSIONS

The isotopic composition of nitrate is not only a powerful tool to determining its sources, but can also provide information about nitrogen transformation processes such as nitrification and denitrification in the unsaturated zone. The combined use of  $\delta^{15}\text{N}\text{-NO}_3^-$  and  $\delta^{18}\text{O}\text{-NO}_3^-$  data confirmed that nitrate in the unsaturated zone was predominately derived from microbial nitrification and to a much lesser extent from atmospheric deposition. The  $\delta^{15}\text{N}\text{-NO}_3^-$  and  $\delta^{18}\text{O}\text{-NO}_3^-$  data further suggested that nitrification can occur in the whole profile of the unsaturated zone. From this study it is concluded that nitrification can occur below the plant root zone also and therefore plays a significant role in the speciation and transport of nitrogen compounds in the unsaturated zone.

## ACKNOWLEDGEMENTS

Discussions with the colleagues in the CRP are acknowledged. I wish to thank my colleagues Mr. W. Berg and M. Koinigg for assistance in soil sampling, Ms. B. Zirngast for sampling of seepage water and Mr. J. Fank and Mr. A. Stuhlbacher for providing data. I am also grateful to the Hydroisotop laboratory staff for the  $\delta^{13}\text{C}\text{-DIC}$ ,  $\delta^{15}\text{N}\text{-NO}_3^-$  and  $\delta^{18}\text{O}\text{-NO}_3^-$  isotope analyses.

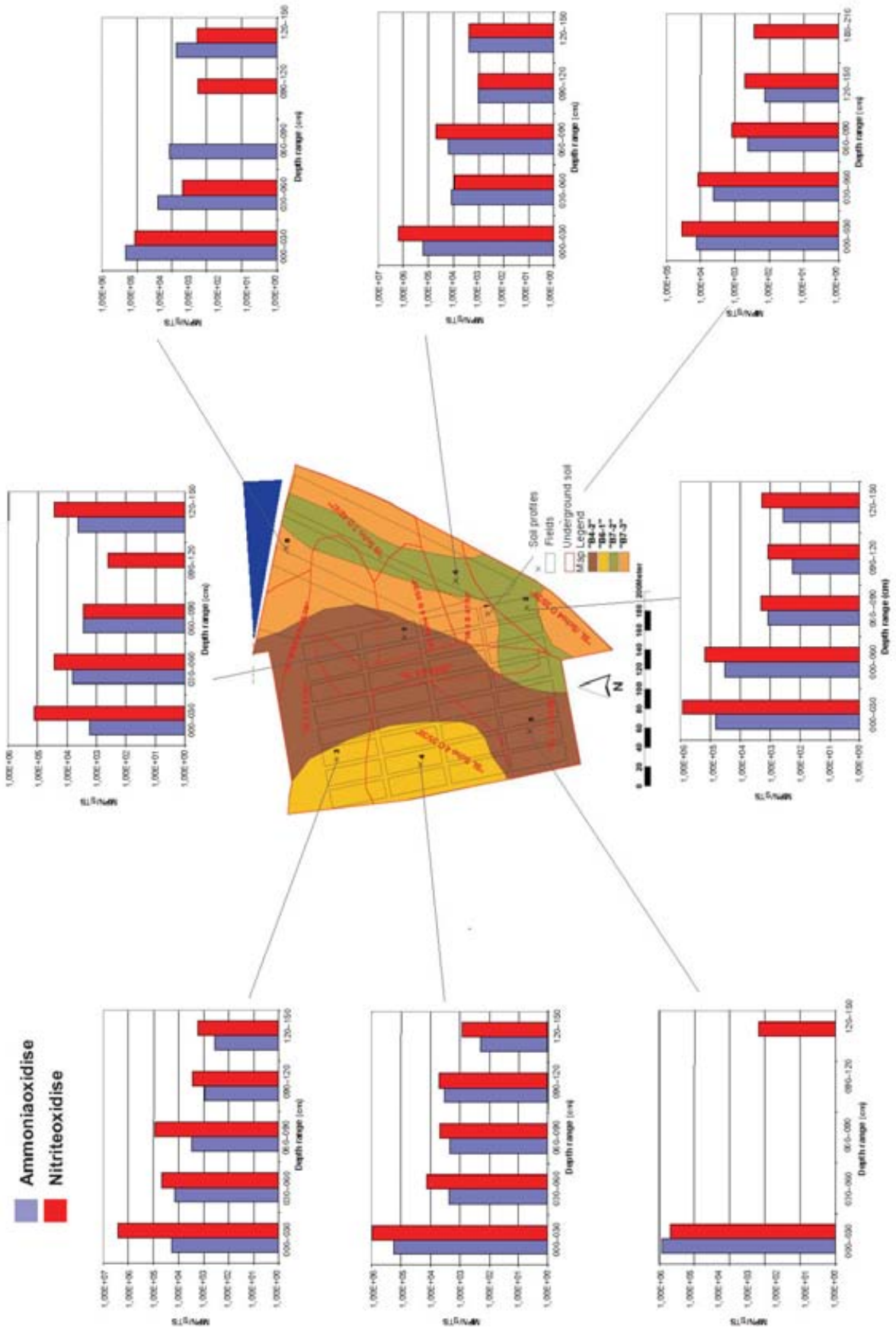


FIG. 4. Distribution of nitrifying bacteria in several soil profiles (0-1.5 m).

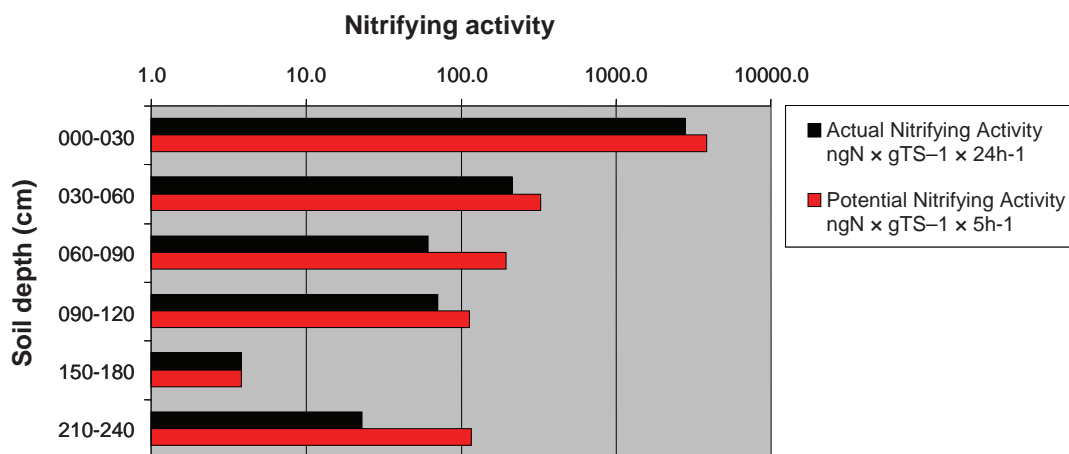


FIG. 5. Actual and potential nitrifying activity of soil profile STW09.

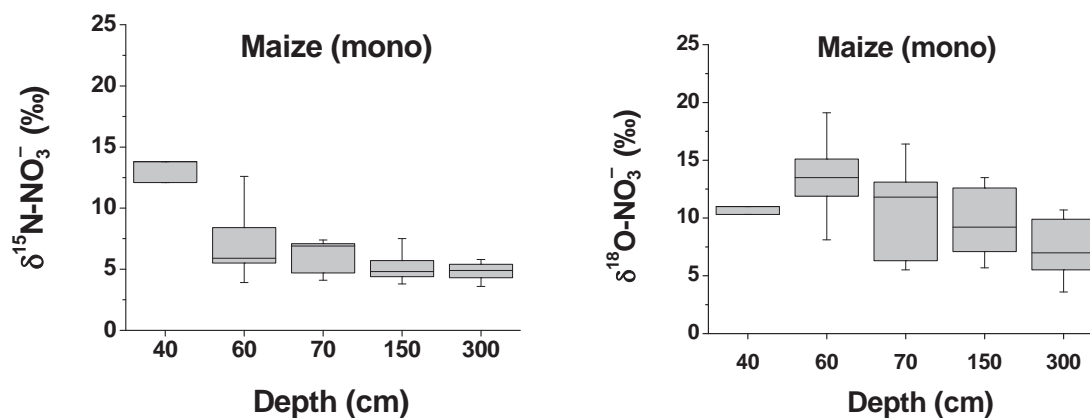


FIG. 6. Box plot of  $\delta^{15}\text{N}-\text{NO}_3^-$  and  $\delta^{18}\text{O}-\text{NO}_3^-$  from lysimeters beneath crop rotation site for the period between May 1998 and April 1999.

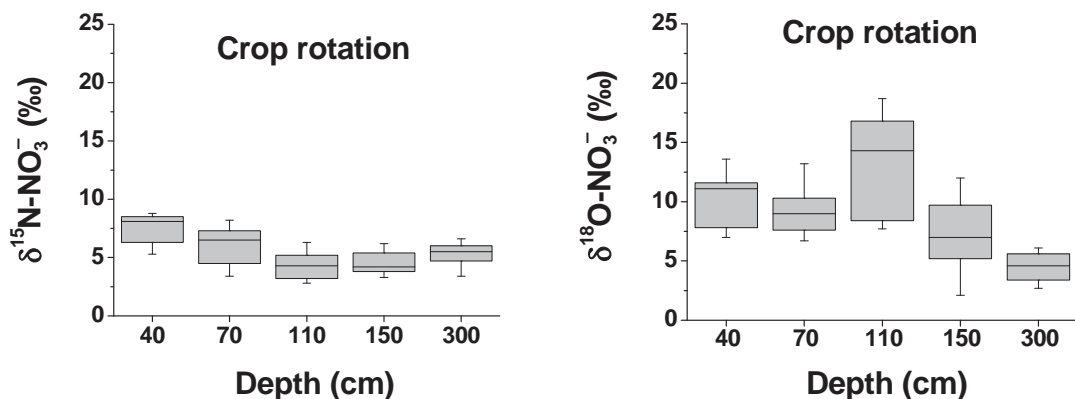


FIG. 7. Box plot of  $\delta^{15}\text{N}-\text{NO}_3^-$  and  $\delta^{18}\text{O}-\text{NO}_3^-$  from lysimeters beneath crop rotation site for the period between May 1998 and April 1999.

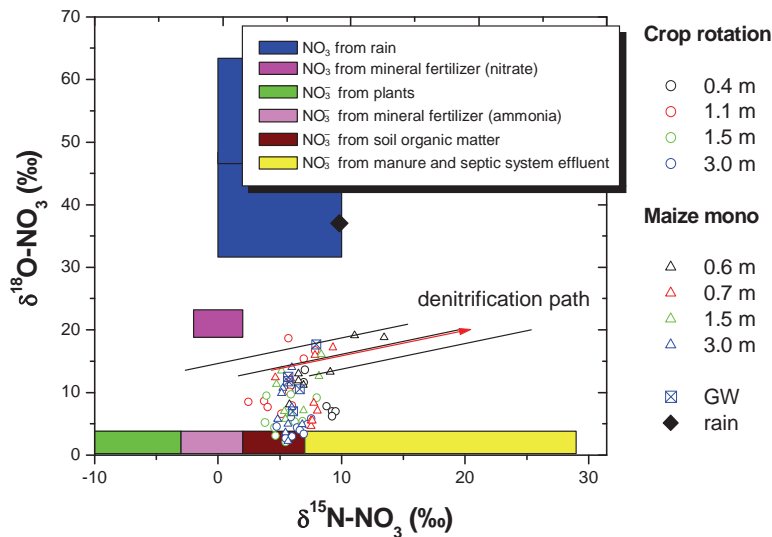


FIG. 9. Typical ranges for  $\delta^{15}N$  and  $\delta^{18}O$  values of nitrate from atmospheric deposition, nitrate containing mineral fertiliser and nitrification of ammonia derived from plant material, mineral fertiliser, soil organic matter, manure and septic system effluents. Also shown are the unsaturated zone water samples obtained from the lysimeters, groundwater and rain.

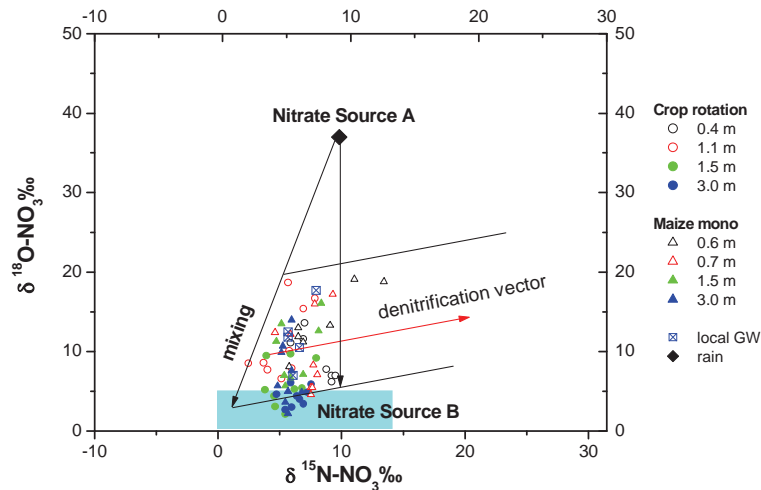


FIG. 10. Mixing between two different sources of nitrate in the unsaturated zone. Source A is nitrate in atmospheric deposition and source B is nitrate originating from nitrification

## REFERENCES

- [1] HASTINGS, R.C., CECCHERINI, M.T., MICLAUS, N., SAUNDERS, J.R., BAZZICALUPO, M., MCCARTHY A.J., Direct molecular biological analysis of ammonia oxidising bacteria population in cultivated soil plots treated with swine manure, *FEMS Microbiol. Ecol* **23** (1997) 45–54.
- [2] CECCHERINI M.T., CASTALDINI M., PIOVANELLI C., HASTINGS R., MCCARTHY A.J., BAZZICALUPO M. AND N.MICLAUS, Effects of swine manure fertilization on autotrophic ammonia oxidizing bacteria in soil, *Applied Soil Ecology* **7** (1998) 149–157.
- [3] AMBERGER, A., SCHMIDT, H.-L., Natürliche Isotopengehalte von Nitrat als Indikatoren für dessen Herkunft, *Geochim. Cosmochim. Acta* **51** (1987) 2699–2705.
- [4] KENDALL, C., “Tracing nitrogen sources and cycling in catchments”, *Isotope Tracers in Catchment Hydrology* (KENDALL, C., MCDONNELL, J.J., Eds.), Elsevier Science B.V., Amsterdam, (1998) 517–576.

- [5] CLARK, I., FRITZ, P., *Environmental Isotopes in Hydrogeology*, Lewis Publishers, New York, NY (1997).
- [6] BÖTTCHER, J., O. STREBEL, VOERKELIUS, S., SCHMIDT, H.-L., Using isotope fractionation of nitrate-nitrogen and nitrate-oxygen for evaluation of microbial denitrification in a sandy aquifer, *J. Hydrol.* **114** (1990) 413–424.
- [7] WASSENAAR, L.I., Evaluation of the Origin and Fate of Nitrate in the Abbotsford Aquifer using the Isotopes  $^{15}\text{N}$  and  $^{18}\text{O}$  in  $\text{NO}_3^-$ , *Appl. Geochem.* **10** (1995) 391–405.
- [8] ARAVENA, R., EVANS, M.L., CHERRY, J.A., Stable isotopes of oxygen and nitrogen in source identification of nitrate from septic systems, *Ground Water*, **31** (1993) 180–186.
- [9] CAMPBELL, D.H., KENDALL, C., CHANG, C.C.Y., SILVA, S.R., TONNESSEN, K.A., Pathways for nitrate release from an alpine watershed: Determination using  $\delta^{15}\text{N}$  and  $\delta^{18}\text{O}$ , *Water Resour. Res.* **38** 5 (2002) 1052.
- [10] HARUM. T., FANK, J., “Solute transport and water movement in the unsaturated zone of a gravel filled valley: tracer investigations under different cultivation types”, *Future Groundwater Resources at Risk, Proc. of the Helsinki Conference, June 1994, IAHS-Pub. No 222, Wallingford, UK* (1994) 341–354.
- [11] FANK, J., Die Bedeutung der ungesättigten Zone für Grundwasserneubildung und Nitratbefrachtung des Grundwassers in quartären Lockersediment-Aquiferen am Beispiel des Leibnitzer Feldes (Steiermark, Österreich), *Beiträge zur Hydrogeologie* **49/50** (1999) 101–388.
- [12] ZOJER, H., RAMSPACHER, P., FANK, J., „Die kombinierte Lysimeteranlage Wagna“, Art der Sickerwassergewinnung und Ergebnisinterpretation, Bericht über die Gumpensteiner Lysimetertagung, Gumpenstein (1991) 55–62.
- [13] FEICHTINGER, F., „Erste Erfahrungen beim Einsatz eines modifizierten Feldlysimeters“, Lysimeter und ihre Hilfe zur umweltschonenden Bewirtschaftung landwirtschaftlicher Nutzflächen, 2. Gumpensteiner Lysimetertagung, BAL Gumpenstein, 28–29.4.1992, Gumpenstein (1992) 59–62.
- [14] EDER, G., „Lysimeteranlagen in Österreich“, Lysimeter — Demands, Experiences, Technical Concepts, *Beiträge zur Hydrogeologie* (LEIS, A., Ed.), Graz (2002) 15–232.
- [15] BERG, W., ČENČUR CURK, B., FANK, J., FEICHTINGER, F., NÜTZMANN, G., PAPESCH, W., RAJNER, V., RANK, D., SCHNEIDER, S., SEILER, K.-P., STEINER, K.-H., STENITZER, E., STICHLER, W., TRČEK, B., VARGAY, Z., VESELIČ, M., ZOJER, H., Tracers in the Unsaturated Zone, *Beiträge zur Hydrogeologie* **52** (2001) 7-102.
- [16] FANK, J., “Tracer investigations at the research station Wagna (Leibnitzer Feld, Austria) to detect the role of the unsaturated zone for groundwater protection”, *New Approaches Characterizing Groundwater Flow* (SEILER, K.P., WOHNLICH, S. Eds.). Proc. of the XXXI. IAH International Association of Hydrogeologists Congress Munich, Germany, Vol. I, München, Swets & Zeitlinger, Lisse (2001) 55–58.
- [17] [http://www.lysimeter.at/HP\\_EuLP/web/austria/at27a.html](http://www.lysimeter.at/HP_EuLP/web/austria/at27a.html)
- [18] LANTHALER, C., Lysimeter Stations and Soil Hydrology Measuring Sites in Europe — Purpose, Equipment, Research Results, Future Developments, Diploma Thesis ([http://www.lysimeter.at/Publikationen/THESIS\\_LYSIMETERS.pdf](http://www.lysimeter.at/Publikationen/THESIS_LYSIMETERS.pdf)) Uni Graz (2004) 145.
- [19] SCHINNER, F., ÖHLINGER, R., KANDELER, E., MARGESIN, R. *Bodenbiologische Arbeitsmethoden*, Springer Verlag, Berlin, Heidelberg, New York, (1993).
- [20] DUNGER, W., FIEDLER, H.J., *Methoden der Bodenbiologie*, Gustav Fischer Verlag, Stuttgart New York (1989).
- [21] HOLT, J.G., *Bergey’s manual of systematic bacteriology*, Vol.1, Williams & Wilkins Co., Baltimore (1984).
- [22] HOLT, J.G., *Bergey’s manual of systematic bacteriology*, Vol.2, Williams & Wilkins Co., Baltimore (1986).
- [23] HOLT, J.G., *Bergey’s manual of systematic bacteriology*, Vol.3 and 4, Williams & Wilkins Co., Baltimore (1989).

## Appendix 1

### $\delta^{15}\text{N}-\text{NO}_3^-$ AND $\delta^{18}\text{O}-\text{NO}_3^-$ DATA IN WATER SAMPLES

Sample type	Date	$\delta^{15}\text{N}-\text{NO}_3^-$ (‰)	$\delta^{18}\text{O}-\text{NO}_3^-$ (‰)
Seepage water 40 cm (crop rotation)	20.05.1998	6.3	11.6
Seepage water 40 cm (crop rotation)	23.06.1998	6.4	13.6
Seepage water 40 cm (crop rotation)	21.09.1998	8.5	7
Seepage water 40 cm (crop rotation)	20.10.1998	8.1	7.8
Seepage water 40 cm (crop rotation)	17.11.1998	8.8	7
Seepage water 40 cm (crop rotation)	16.12.1998	8.5	6.2
Seepage water 40 cm (crop rotation)	28.01.1999	5.3	11.1
Seepage water 40 cm (crop rotation)	20.04.1999	22	22.7
Seepage water 40 cm (crop rotation)	25.02.1999	4.2	11.3
Seepage water 40 cm (crop rotation)	26.03.1999	7.5	12.6
Seepage water 40 cm (crop rotation)	19.05.1999	8.6	8.1
Seepage water 40 cm (crop rotation)	21.06.1999	5.6	7.8
Seepage water 70 cm (crop rotation)	23.06.1998	4	13.2
Seepage water 70 cm (crop rotation)	21.07.1998	7.3	8.9
Seepage water 70 cm (crop rotation)	21.09.1998	6.8	10.3
Seepage water 70 cm (crop rotation)	20.10.1998	8	6.7
Seepage water 70 cm (crop rotation)	17.11.1998	8.2	7.6
Seepage water 70 cm (crop rotation)	21.12.1998	3.4	9
Seepage water 70 cm (crop rotation)	28.01.1999	3	10
Seepage water 70 cm (crop rotation)	25.02.1999	6.5	10.2
Seepage water 70 cm (crop rotation)	26.03.1999	6.6	7.4
Seepage water 70 cm (crop rotation)	19.05.1999	5	10.4
Seepage water 70 cm (crop rotation)	21.06.1999	4.5	4.6
Seepage water 110 cm (crop rotation)	05.05.1998	2	8.5
Seepage water 110 cm (crop rotation)	26.05.1998	3.2	8.6
Seepage water 110 cm (crop rotation)	23.06.1998	5.2	10.1
Seepage water 110 cm (crop rotation)	21.07.1998	5.4	7.9
Seepage water 110 cm (crop rotation)	27.09.1998	7.2	16.7
Seepage water 110 cm (crop rotation)	20.10.1998	5.1	18.7
Seepage water 110 cm (crop rotation)	20.11.1998	6.3	15.4
Seepage water 110 cm (crop rotation)	19.12.1998	3.5	7.7
Seepage water 110 cm (crop rotation)	28.01.1999	4.6	6.6
Seepage water 110 cm (crop rotation)	19.05.1999	2.8	19.1
Seepage water 110 cm (crop rotation)	25.02.1999	4.3	14.3
Seepage water 110 cm (crop rotation)	26.03.1999	3.5	16.8
Seepage water 110 cm (crop rotation)	21.06.1999	4.1	8.4
Seepage water 110 cm (crop rotation)	29.07.1999	2.8	17.5

Sample type	Date	$\delta^{15}\text{N}-\text{NO}_3^-$ (‰)	$\delta^{18}\text{O}-\text{NO}_3^-$ (‰)
Seepage water 150 cm (crop rotation)	05.05.1998	3.3	5.2
Seepage water 150 cm (crop rotation)	26.05.1998	4	4.4
Seepage water 150 cm (crop rotation)	23.06.1998	3.4	9.5
Seepage water 150 cm (crop rotation)	21.07.1998	4.1	3.1
Seepage water 150 cm (crop rotation)	21.09.1998	5.3	9.7
Seepage water 150 cm (crop rotation)	20.10.1998	7.3	9.2
Seepage water 150 cm (crop rotation)	17.11.1998	6.2	5.4
Seepage water 150 cm (crop rotation)	16.12.1998	4.9	2.1
Seepage water 150 cm (crop rotation)	28.01.1999	5.6	5.3
Seepage water 150 cm (crop rotation)	25.02.1999	3.3	10.6
Seepage water 150 cm (crop rotation)	26.03.1999	5.4	2.1
Seepage water 150 cm (crop rotation)	20.04.1999	4.7	13.7
Seepage water 150 cm (crop rotation)	26.05.1999	3.8	7
Seepage water 150 cm (crop rotation)	21.06.1999	4.2	12
Seepage water 150 cm (crop rotation)	29.07.1999	3.7	7.2
Seepage water 300 cm (crop rotation)	05.05.1998	5.8	4.4
Seepage water 300 cm (crop rotation)	26.05.1998	6.6	4.9
Seepage water 300 cm (crop rotation)	23.06.1998	6	4
Seepage water 300 cm (crop rotation)	21.07.1998	5.3	6.1
Seepage water 300 cm (crop rotation)	21.09.1998	4.9	2.7
Seepage water 300 cm (crop rotation)	20.10.1998	6.3	3.4
Seepage water 300 cm (crop rotation)	17.11.1998	6.9	5.9
Seepage water 300 cm (crop rotation)	16.12.1998	4.2	4.6
Seepage water 300 cm (crop rotation)	28.01.1999	5.4	3
Seepage water 300 cm (crop rotation)	25.02.1999	5.5	5.2
Seepage water 300 cm (crop rotation)	26.03.1999	5.7	3.5
Seepage water 300 cm (crop rotation)	20.04.1999	4.7	1
Seepage water 300 cm (crop rotation)	21.06.1999	3.4	5.6
Seepage water 300 cm (crop rotation)	29.07.1999	3.2	7
Seepage water 40 cm (maize)	21.09.1998	13.8	10.3
Seepage water 40 cm (maize)	25.10.1998	12.1	11
Seepage water 60 cm (maize)	05.05.1998	5.9	11.9
Seepage water 60 cm (maize)	26.05.1998	6.3	11.2
Seepage water 60 cm (maize)	23.06.1998	5.9	13
Seepage water 60 cm (maize)	21.09.1998	8.4	13.2
Seepage water 60 cm (maize)	20.10.1998	5.2	8.1
Seepage water 60 cm (maize)	25.11.1998	12.6	18.8
Seepage water 60 cm (maize)	28.12.1998	10.3	19.1
Seepage water 60 cm (maize)	25.02.1999	5.5	13.5
Seepage water 60 cm (maize)	19.05.1999	5.9	15.1
Seepage water 60 cm (maize)	21.06.1999	3.9	13.8

Sample type	Date	$\delta^{15}\text{N}-\text{NO}_3^-$ (‰)	$\delta^{18}\text{O}-\text{NO}_3^-$ (‰)
Seepage water 70 cm (maize)	05.05.1998	6.9	4.6
Seepage water 70 cm (maize)	26.05.1998	6.9	5.5
Seepage water 70 cm (maize)	23.06.1998	7.1	8.3
Seepage water 70 cm (maize)	21.07.1998	8.6	17.2
Seepage water 70 cm (maize)	21.09.1998	7.2	16
Seepage water 70 cm (maize)	20.10.1998	7	5.5
Seepage water 70 cm (maize)	17.11.1998	7.4	7.1
Seepage water 70 cm (maize)	21.12.1998	4.1	12.4
Seepage water 70 cm (maize)	28.01.1999	5.3	12.2
Seepage water 70 cm (maize)	20.04.1999	4.3	13.1
Seepage water 70 cm (maize)	25.02.1999	4.8	11.8
Seepage water 70 cm (maize)	26.03.1999	4.7	16.4
Seepage water 70 cm (maize)	19.05.1999	4.7	6.3
Seepage water 70 cm (maize)	21.06.1999	3.4	9.5
Seepage water 150 cm (maize)	05.05.1998	4.9	5.7
Seepage water 150 cm (maize)	26.05.1998	5.3	6.7
Seepage water 150 cm (maize)	04.07.1998	6.3	7.13
Seepage water 150 cm (maize)	21.07.1998	7.5	12.6
Seepage water 150 cm (maize)	21.09.1998	4.6	13.5
Seepage water 150 cm (maize)	20.10.1998	7.7	16.1
Seepage water 150 cm (maize)	16.12.1998	4.8	7
Seepage water 150 cm (maize)	28.01.1999	4.2	11.3
Seepage water 150 cm (maize)	25.02.1999	5.1	7.4
Seepage water 150 cm (maize)	26.03.1999	4.4	9.2
Seepage water 150 cm (maize)	20.04.1999	3.8	13.1
Seepage water 150 cm (maize)	19.05.1999	4.2	10.1
Seepage water 150 cm (maize)	21.06.1999	4.7	2.8
Seepage water 150 cm (maize)	29.07.1999	5.7	7.1
Seepage water 300 cm (maize)	05.05.1998	5.1	5
Seepage water 300 cm (maize)	26.05.1998	6.2	4.9
Seepage water 300 cm (maize)	23.06.1998	4.7	10.7
Seepage water 300 cm (maize)	21.07.1998	5.4	14
Seepage water 300 cm (maize)	21.09.1998	5.4	7.6
Seepage water 300 cm (maize)	20.10.1998	4.9	3.6
Seepage water 300 cm (maize)	17.11.1998	5.1	2.2
Seepage water 300 cm (maize)	16.12.1998	4.3	5.7
Seepage water 300 cm (maize)	28.01.1999	4.6	9.9
Seepage water 300 cm (maize)	25.02.1999	4	5.9
Seepage water 300 cm (maize)	26.03.1999	5.8	8.6
Seepage water 300 cm (maize)	20.04.1999	5.6	7.2
Seepage water 300 cm (maize)	19.05.1999	3.4	5.5

Sample type	Date	$\delta^{15}\text{N-NO}_3^-$ (‰)	$\delta^{18}\text{O-NO}_3^-$ (‰)
Seepage water 300 cm (maize)	21.06.1999	3.6	9.9
Seepage water 300 cm (maize)	29.07.1999	4.2	7
Ground water	21.09.1998	6	10.5
Ground water	16.12.1998	5.5	7
Ground water	05.05.1998	7.3	17.7
Ground water	23.06.1998	5.1	11.8
Ground water	07.07.1998	5.1	12.5
Ground water	25.02.1999	3.8	12.5
Ground water	20.04.1999	4.3	13.7
Ground water	21.06.1999	3.1	13.5

## Appendix II

### $\delta^{13}\text{C}$ -DIC DATA IN WATER SAMPLES

Sample type	Date	$\delta^{13}\text{C}$ -DIC (‰)
Seepage water 40 cm (crop rotation)	14.09.1998	-9.9
Seepage water 40 cm (crop rotation)	09.11.1998	-12.5
Seepage water 40 cm (crop rotation)	13.01.1999	-12.1
Seepage water 40 cm (crop rotation)	17.03.1999	-11.5
Seepage water 40 cm (crop rotation)	12.05.1999	-11.6
Seepage water 40 cm (crop rotation)	12.07.1999	-6.9
Seepage water 70 cm (crop rotation)	30.06.1998	-11.7
Seepage water 70 cm (crop rotation)	14.09.1998	-8.5
Seepage water 70 cm (crop rotation)	09.11.1998	-10.7
Seepage water 70 cm (crop rotation)	13.01.1999	-11.5
Seepage water 70 cm (crop rotation)	17.03.1999	-8.8
Seepage water 70 cm (crop rotation)	12.05.1999	-10.5
Seepage water 70 cm (crop rotation)	12.07.1999	-7.9
Seepage water 110 cm (crop rotation)	09.06.1998	-13.2
Seepage water 110 cm (crop rotation)	14.09.1998	-10.4
Seepage water 110 cm (crop rotation)	09.11.1998	-11.7
Seepage water 110 cm (crop rotation)	13.01.1999	-12.4
Seepage water 110 cm (crop rotation)	17.03.1999	-10.5
Seepage water 110 cm (crop rotation)	12.05.1999	-13.6
Seepage water 110 cm (crop rotation)	12.07.1999	-9.1
Seepage water 150 cm (crop rotation)	20.09.1998	-6.3
Seepage water 150 cm (crop rotation)	08.06.1998	-12.7
Seepage water 150 cm (crop rotation)	30.06.1998	-12.3
Seepage water 150 cm (crop rotation)	03.08.1998	-9.3
Seepage water 150 cm (crop rotation)	14.09.1998	-10.4
Seepage water 150 cm (crop rotation)	09.11.1998	-10.8
Seepage water 150 cm (crop rotation)	13.01.1999	-10.6
Seepage water 150 cm (crop rotation)	17.03.1999	-10.2
Seepage water 150 cm (crop rotation)	12.05.1999	-12.6
Seepage water 300 cm (crop rotation)	03.08.1998	-10.9
Seepage water 300 cm (crop rotation)	14.09.1998	-10.7
Seepage water 300 cm (crop rotation)	09.11.1998	-10.5
Seepage water 300 cm (crop rotation)	13.01.1999	-10.1
Seepage water 40 cm (maize)	18.09.1998	-11.3
Seepage water 40 cm (maize)	17.03.1999	-10.7
Seepage water 40 cm (maize)	12.05.1999	-12.7
Seepage water 60 cm (maize)	09.06.1998	-10.2
Seepage water 60 cm (maize)	14.09.1998	-8.4
Seepage water 60 cm (maize)	09.11.1998	-11.3

Sample type	Date	$\delta^{13}\text{C-DIC}$ (‰)
Seepage water 60 cm (maize)	13.01.1999	-12.5
Seepage water 60 cm (maize)	17.03.1999	-11.5
Seepage water 60 cm (maize)	12.05.1999	-9.9
Seepage water 60 cm (maize)	12.07.1999	-7.1
Seepage water 70 cm (maize)	09.06.1998	-11.3
Seepage water 70 cm (maize)	14.09.1998	-7.1
Seepage water 70 cm (maize)	09.11.1998	-11.5
Seepage water 70 cm (maize)	13.01.1999	-13.7
Seepage water 70 cm (maize)	17.03.1999	-15.4
Seepage water 70 cm (maize)	12.05.1999	-13.1
Seepage water 70 cm (maize)	12.07.1999	-6.6
Seepage water 150 cm (maize)	04.07.1998	-5.6
Seepage water 150 cm (maize)	03.08.1998	-7
Seepage water 150 cm (maize)	15.09.1998	-7.1
Seepage water 150 cm (maize)	09.11.1998	-7.7
Seepage water 150 cm (maize)	13.01.1999	-8.3
Seepage water 300 cm (maize)	27.07.1998	-5.9
Seepage water 300 cm (maize)	03.08.1998	-5.8
Seepage water 300 cm (maize)	14.09.1998	-3.9
Seepage water 300 cm (maize)	09.11.1998	-4.8
Ground water	09.06.1998	-11.8
Ground water	03.08.1998	-11.1
Ground water	14.09.1998	-10.8
Ground water	09.11.1998	-11.2
Ground water	13.01.1999	-12.5
Ground water	17.03.1999	-11.2
Ground water	12.05.1999	-11.4
Ground water	12.07.1999	-10

### Appendix III

#### $\delta^{34}\text{S-SO}_4$ AND $\delta^{18}\text{O-SO}_4$ DATA IN WATER SAMPLES

Sample type	Date	$\delta^{34}\text{S-SO}_4$ (‰)	$\delta^{18}\text{O-SO}_4$ (‰)
Seepage water 110 cm (crop rotation)	03.07.1998	9	
Seepage water 150 cm (crop rotation)	03.07.1998	6.2	
Seepage water 300 cm (crop rotation)	12.07.1998	8.7	
Seepage water 60 cm (maize)	07.07.1998	5.2	
Seepage water 70 cm (maize)	03.07.1998	3.5	
Seepage water 150 cm (maize)	05.07.1998	3.7	4.2

# NITRATE IN GROUNDWATER AND THE UNSATURATED ZONE, SHIJIAZHANG CITY, CHINA

GUO YONGHAI<sup>a</sup>, XU GUOQING<sup>a</sup>, GAO ZHENYU<sup>b</sup>, LIU SHUFEN<sup>a</sup>, JIANG GUILIN<sup>a</sup>

<sup>a</sup> Beijing Research Institute of Uranium Geology  
Beijing, China

<sup>a</sup> Shijiazhuang Prospecting Institute of Hydrogeology and Engineering Geology,  
Shijiazhuang, China

## ABSTRACT

In 2001, nitrate concentrations in water from wells in Shijiazhuang City, China ranged from 15 to about 160 mg/L as nitrate, with a median concentration of 50 mg/L. Agricultural return waters from lands irrigated with sewage or groundwater are believed to be the source of increasing nitrate, chloride, sulphate, and dissolved solids concentrations. Recharge rates estimated from chemical and tritium data are about 130 mm/y for non-irrigated agricultural land and exceed 200 mm/y for irrigated land. Nitrate concentrations in pore water in the unsaturated zone were as high as 930 mg/L. As much as 350 kg/ha of nitrogen is stored in the upper 18 m of the unsaturated zone beneath a groundwater irrigated site. As much as 780 kg/ha of nitrogen could be stored in thicker unsaturated zones within the study area and nitrogen storage beneath sewage irrigated sites is even probably greater. About 60% of the nitrate stored in the unsaturated zone is in the form of nitrate and 36% is in the form of ammonia. Denitrification in near-saturated fine-grained layers reduces the concentration of nitrate in with depth and at 18 m below land surface 60% of the nitrogen is in the form of ammonia. The  $\delta^{15}\text{N}$  composition of water from sampled wells ranged from 2.2 to 11.7‰, with median value of 6.1‰. Water from wells in the urban area had the highest average  $\delta^{15}\text{N}$  compositions with progressively lower values in the village and farmland areas.  $\delta^{15}\text{N}$  values in surficial soils averaged 1.0‰ in natural sites, 9.5‰ in sewage and manure amended sites, and 7.3‰ in the chemically fertilized sites. Most  $\delta^{15}\text{N}$  values in water from wells are in the range of compositions expected from sewage and manure sources of nitrogen—with some denitrification, although extensive denitrification of nitrogen from chemical fertilizers also could produce observed  $\delta^{15}\text{N}$  values.

## 1. INTRODUCTION

Shijiazhuang City is the capital of Hebei province, in north eastern China about 260 km southwest of Beijing (fig. 1). Groundwater from the underlying Quaternary aquifer is the only water supply source for the city. There are seven groundwater treatment plants drawing groundwater from a total of 108 wells. In addition, there are about 640 private wells, mainly for industrial use. The combined extraction of these wells exceeds recharge to the aquifers, and the water table has been dropping by 1 meter annually for many years. Overlying land use practices, especially practices related to the disposal and use of sewage for irrigation, have resulted in a deterioration of the groundwater quality. Hardness and total dissolved solids (TDS),  $\text{Cl}^-$ ,  $\text{NO}_3^-$ , and  $\text{SO}_4^{2-}$  concentrations, as well as concentrations of some heavy metals such as Hg, and Cr have increased since 1959.

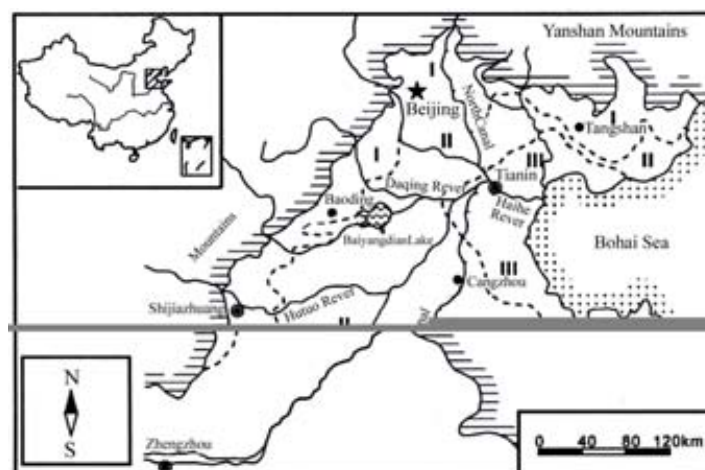


FIG. 1. Location of Shijiazhuang City, China.

Pollutants released to the land surface have to pass through the unsaturated zone (UNZ) before entering the ground-water system. Ground-water pumping and land use practices that have resulted in ground-water quantity and quality issues in Shijiazhuang City are typical for cities in northern China, as a consequence this city was chosen for inclusion in the International Atomic Energy Agency (IAEA) Coordinated Research Project (CRP) on the use of isotopes for understanding the migration of contaminants through the unsaturated zone.

## **2. HYDROLOGIC SETTING**

The climate of the study area is semi-arid, with a mean annual rainfall of about 520 mm. About 70% of the precipitation occurs between July and September. The mean annual temperature is about 13°C and the temperature difference between summer and winter is large. The potential mean annual evaporation is 1200 mm.

Shijiazhuang City, about 72 km<sup>2</sup>, is located in the Hutuo river alluvial fan, east of the Taihang Mountains (Fig. 1). The plain slopes gently to the east from about 100 m to about 50 m above sea level. The topographic gradient is smooth, about 4‰ in the west and 2‰ in the east.

The underlying quaternary deposits are divided into 4 aquifers (I, II, III and IV, Fig. 2). The shallow aquifers, I and II, are composed mainly coarse sand and gravel with total thickness of 34–70 m and are extensively pumped. Aquifer I has been almost completely dewatered; as a consequence, aquifer II is presently (2001) the main aquifer pumped water supply. The deep aquifers III and IV are composed mainly of fine sand. A continuous aquitard separates these aquifers from the overlying aquifers and the groundwater is confined. Recharge to the deeper aquifers is limited and they have not been extensively pumped for water supply.

Under predevelopment conditions (50 years ago), groundwater recharge was through infiltration of precipitation and lateral inflow from the mountain front to the west. Discharge was mainly through lateral outflow to the east. With the development of an irrigation canal system, irrigation return flow has become another recharge source. At present (2001), groundwater pumping is the main method of discharge, smaller amounts of water discharge through lateral outflow to the east.

### **2.1. Groundwater pumping and water table drawdown**

In 1959, the depth of groundwater underlying Shijiazhuang City was between 1 m to 5 m and groundwater flowed mainly from northwest to southeast (Fig. 3). Beginning in the 1970s, about  $3.46 \times 10^8$  m<sup>3</sup> groundwater has been extracted annually from aquifers underlying Shijiazhuang City. And a large cone of depression has developed in the regional water table. Groundwater levels have decreased about 1 meter per year in the centre of the cone of depression (Appendix I, Fig. 4). By 2000, the depth to groundwater was from 30 m to 40 m in the centre of the pumping depression and the groundwater flowed mainly from periphery towards the centre of the pumping depression (Fig. 5).

### **2.2. Sewage utilization and discharge**

The discharge of sewage and industrial wastewater increased yearly with increasing population, industrial growth, and pumping of groundwater. The total discharge in 2000, was more than 540 000 m<sup>3</sup> per day for industrial wastewater and 200 000 m<sup>3</sup> per day for urban sewage.

Before 1970, there was no sewage discharge system in residential areas in Shijiazhuang city. Even at present, most of sewage is discharged through open ditches without liners to prevent leakage. The main sewage ditches are East open ditch and West open ditch in south part of the city. The two ditches join and then discharge to the Xiaoxiaohu River south of the city. Sewage not discharged to the river is used for irrigation without treatment, south of Shijiazhuang City.

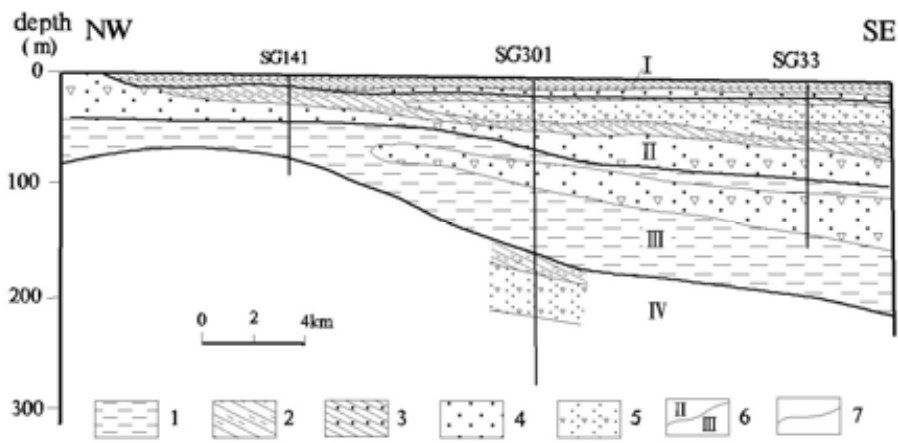


FIG. 2. The hydrogeological cross section of Shijiazhuang City. 1. clay; 2. clayey soil; 3. clay contained gravel; 4. sand and gravel; 5. sand; 6. boundary line of aquifer; 7. boundary line of stratum.

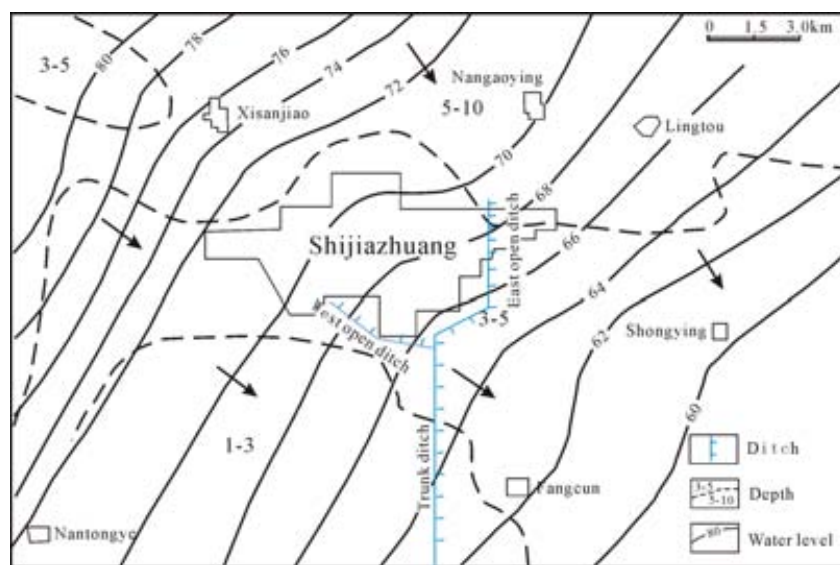


FIG. 3. Water levels and depths to groundwater, Shijiazhuang City, China, 1959.

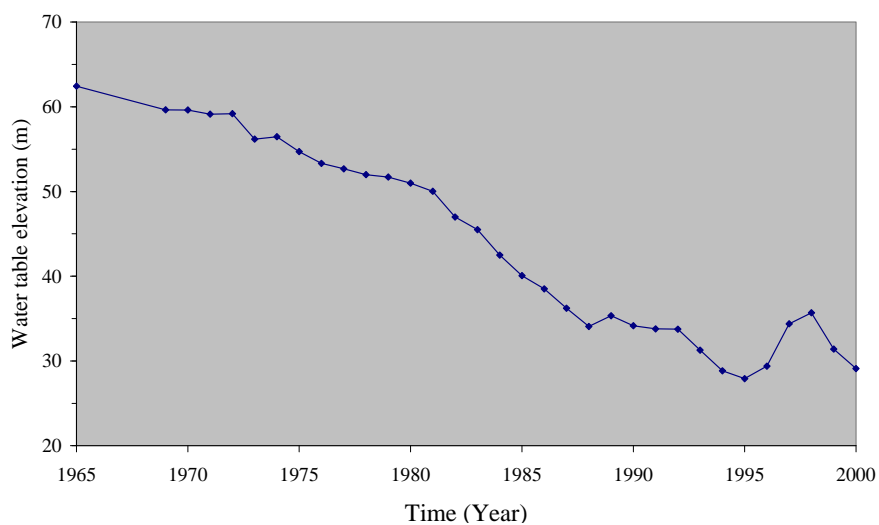


FIG. 4. Groundwater levels in the centre of the pumping depression underlying, Shijiazhuang City, China.

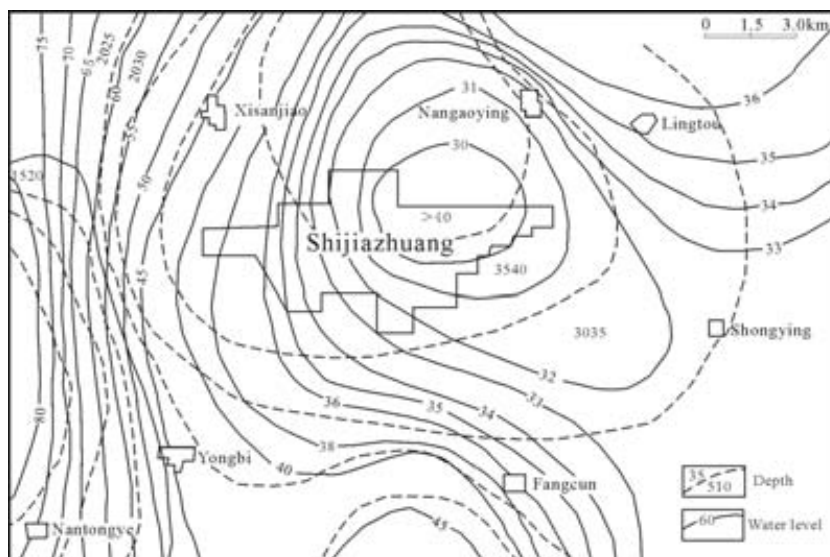


FIG. 5. Water levels and depths to groundwater, Shijiazhuang City, China, 2000.

### 2.3. Predevelopment and 1992 major-ion chemistry

From 1958 to 1959, 21 wells were drilled for water supply in Shijiazhuang City. Groundwater samples from each well were analyzed for pH, major ions, nitrate, hardness and dissolved solids (Appendix II). These are the earliest groundwater chemical data in the study area and they reflect background groundwater chemistry without (or with only mild) pollution. At that time, most of groundwater had TDS values around 300 mg/L, and only one sample had a TDS concentration greater than 600 mg/L.

Hardness of most groundwater samples was less than 300 mg/L and only one sample had a value over 400 mg/L. Water chemical types were mainly  $\text{HCO}_3\text{-Ca}$  and  $\text{HCO}_3\text{-CaMg}$  (Fig. 7).

Groundwater chemical concentrations have increased annually since 1959. The concentrations of groundwater constituents in 1992, the latest year for which comprehensive chemical data are available, are listed in Appendix III. At that time average concentrations for selected constituents were: dissolved solid = 710 mg/L; hardness = 502 mg/L;  $\text{Cl}^- = 118$  mg/L; and  $\text{SO}_4^{2-} = 163$  mg/L. Concentrations from selected well that were sampled as part of this study in 2001 are given in Appendix IV. Concentrations of measured constituents were higher in sewage irrigated area than in areas that were not irrigated with sewage (Fig. 7), and water chemical types had changed since 1959 (Fig. 8). Some of the increase in calcium, magnesium, bicarbonate, and sodium concentrations has been attributed to increased dissolution of minerals within the unsaturated zone and subsequent cation exchange as a result of water table decline (Appendix V). These reactions are driven by high partial pressures of  $\text{CO}_2$  in the unsaturated zone atmosphere resulting from oxidation of organic carbon in sewage used for irrigation. In addition, trace pollutants from industrial activity, such as  $\text{Cr}^{6+}$ , phenol and  $\text{CN}^-$ , were found in groundwater in high concentrations.

### 2.4. Predevelopment and present-day (2001) nitrate concentrations

In 1959, water from most sampled wells in Shijiazhuang City had nitrate concentrations less than 2 mg/L, with a maximum concentration of 6.6 mg/L (Appendix II). By 1978, the average nitrate concentration was 15.7 mg/L. Since 1978, groundwater quality monitoring has been done routinely in about 90 wells in the city. Concentrations of nitrate increased steadily in water from these wells between 1978 and 2000 (Fig. 9). According to the data, by 1996, the average nitrate concentration was 44.8 mg/L. Histograms showing nitrate concentrations in water from wells in Shijiazhuang City between 1980 and 2001 show a consistent shift to higher concentrations and a marked decrease in the number of wells yielding lower nitrate concentrations (Fig. 10). Nitrate concentrations were higher in areas irrigated with sewage than in non-sewer irrigated areas (Fig. 7) and in general nitrate

concentrations are lower in the northern part of the study area and higher in the southern part of the study area (Fig. 11). As previously discussed, sewage from disposal ditches is commonly used for irrigation in the southern part of the study area.

Water from wells in the vicinity of borehole B03 in the area of high nitrate contamination south of Shijiazhuang City has been contaminated by nitrate since 1982. Sewage irrigation started in this area in 1965 and stopped in 1980. Only 15 years elapsed between sewage irrigation and the onset of groundwater nitrate contamination in this area. In 1982, the groundwater table depth was around 14 m. and nitrate must have moved downward at a rate of more than 0.9 m/y. Assuming an average volumetric water content of 23%, the recharge rate must be at least 200 mm/y. This calculation probably greatly underestimates the actual recharge rate since a large amount of high-nitrate water would have had to accumulate near the top of the water table before contaminating wells.

### 3. PURPOSE AND SCOPE

The purpose of this study was to evaluate the source and movement of water and surface contaminants, especially nitrate, in the unsaturated zone overlying the I, II aquifers. Special attention was paid to processes that may increase or decrease the concentrations of nitrate as it moved through the unsaturated zone.

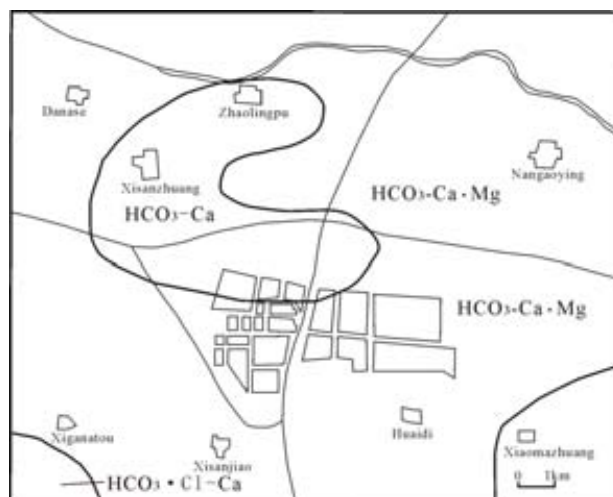


FIG. 6. Groundwater chemical types, Shijiazhuang City, China, 1958 to 1959.

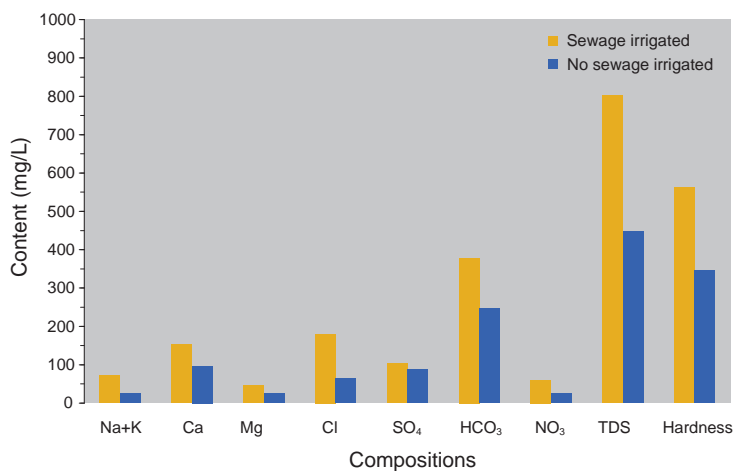


FIG. 7. Comparison of groundwater chemistry between sewage irrigated and non-sewer irrigated areas, Shijiazhuang City, China, 1992.

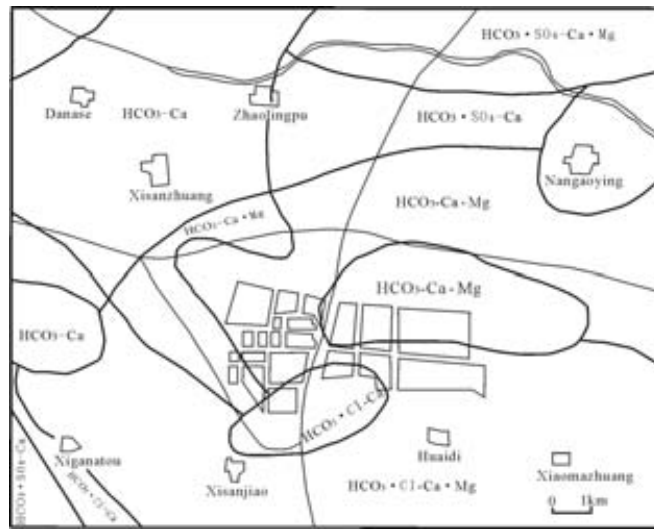


FIG. 8. Groundwater chemical types, Shijiazhuang City, China, 1992.

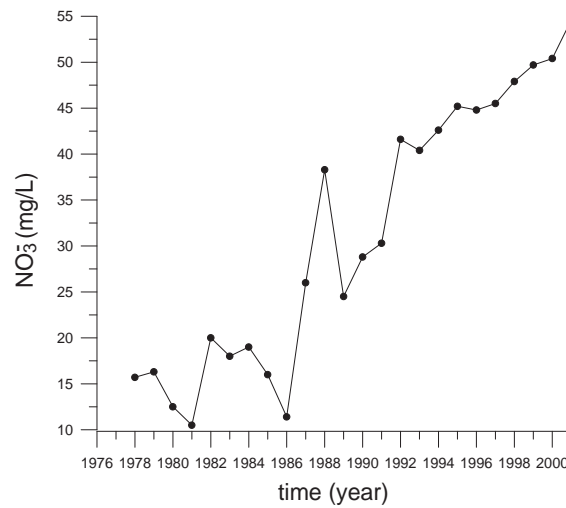


FIG. 9. Average nitrate concentrations in water from wells, Shijiazhuang City, China, 1992.

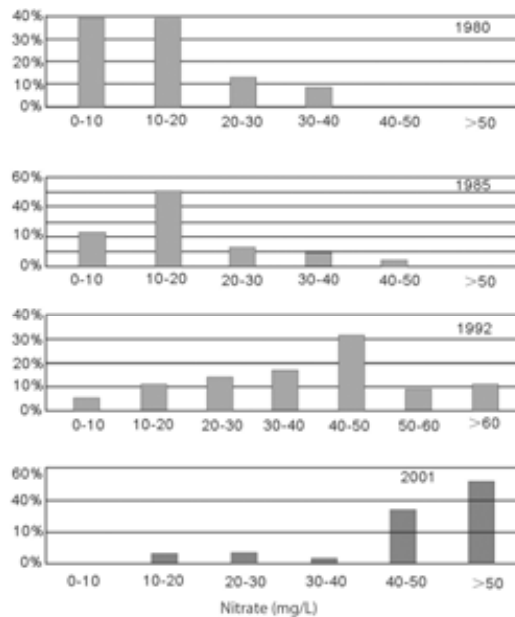


FIG. 10 . Frequency histograms of nitrate concentrations in water from wells, Shijiazhuang City, China, 1980 to 2001.

Scope of the study included drilling and sample collection from the unsaturated zone. Lithology, water content, the stable isotopes of oxygen and hydrogen, and tritium were measured at 50 cm intervals in three boreholes drilled to a depth of about 18 m. Samples from one borehole were analyzed for selected chemical constituent (chloride, nitrate, nitrite, and ammonia). Samples of surficial material (less than 150 cm depth) were collected from 8 sites having native, sewage (and manure) amended, and chemically fertilized soils. These samples were analyzed for nitrate and nitrogen isotopes. Samples were collected at an additional 7 sites to a depth of 5 m were analyzed for nitrate, and nitrogen isotopes. Borehole and sample site locations are shown on Fig. 11.

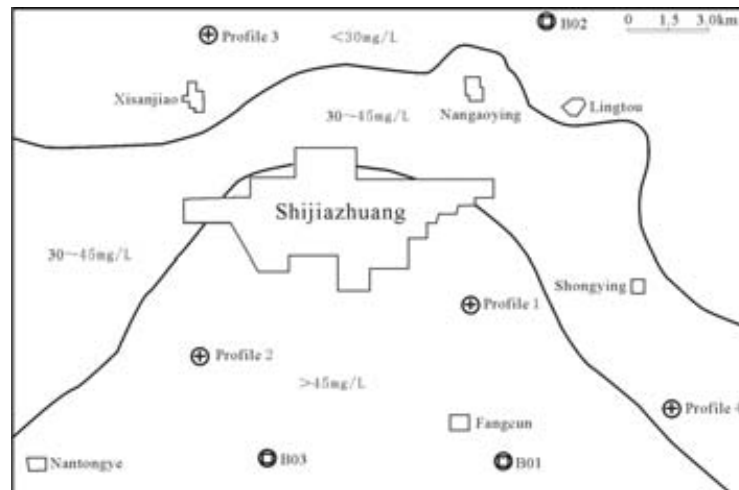


FIG. 11. Distribution of nitrate in water from wells, Shijiazhuang City, China, 2001.

## 4. RESULTS OF UNSATURATED ZONE DATA COLLECTION

### 4.1. Regional characterization of the unsaturated zone

The lithologic character, thickness and texture of unsaturated zone are important factors affecting the groundwater vulnerability to pollution. Because of pumping in excess of recharge and water-level declines, the thickness of unsaturated zone has increased through time and presently is between 15 and 40 m thick (Fig. 12). The thickest unsaturated deposits overlie the centre of the pumping depression and the unsaturated zone thins to the edges of the study area. The unsaturated zone can be broadly grouped into two lithologic assemblages. The first assemblage, present in the south and west part of the city, is composed of clay or fine sand. Between clay layers there are occasional thin layers of sandy clay. The thickness of the clay layers occupies 90% of the total unsaturated zone. The second assemblage, present in the north and central part of the study area, is composed of alternating clay, sandy clay and fine sand. The thickness of clay or sandy clay occupies 35–65 % of the total unsaturated zone.

### 4.2. Borehole B01

Borehole B01 is drilled in an unirrigated area in the south part of the study area (fig. 11). The altitude is about 75 m above sea level and the depth of borehole is 18.2 m. Data from this borehole reflect natural background conditions and serve as a control to evaluate data collected at other sites.

#### 4.2.1. Lithology and water content

The upper part unsaturated zone at borehole B01 is composed of agricultural soil 0.7 m thick, underlain by a 3.1 m thick clay layer. Below 3.8 m the borehole is composed primarily of silt loam with alternating layers of fine to coarse sand (Table 1). This borehole is representative of the finer-grained unsaturated deposits found in the study area.

Gravimetric water content ranged from 2.2 to 26.4%, with a median water content of 8.6% (Appendix VI, Fig. 13). Water contents were higher in the finer-grained clay and silt loam and lower in the sand. The lower values from the coarse-grained sands are consistent with values expected from sand in arid areas in other parts of the world [1, 2]. The higher values in the finer-grained silt loam are comparatively wet but consistent with the semiarid climate of the study area. Assuming a bulk density of about 1.8 g/cm for the silt loam [3], the volumetric water content of these units may be as high as 48% and may be approaching saturation. If the deposits are saturated, reducing conditions may be present.

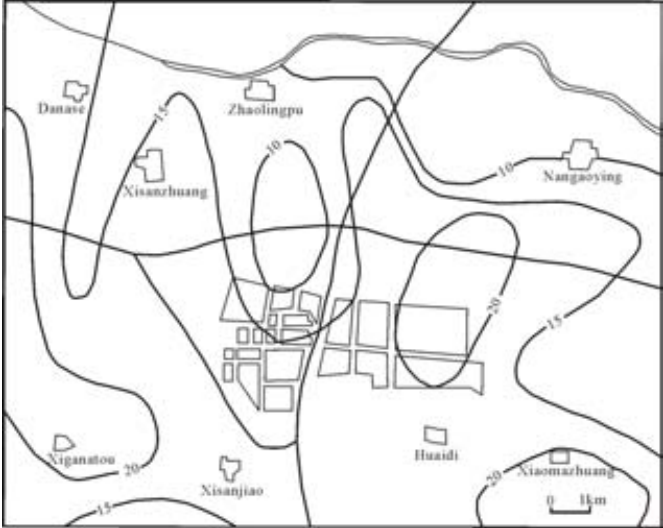


FIG. 12. The thickness of clay in unsaturated zone (in meters) underlying Shijiazhuang City, China, 2000.

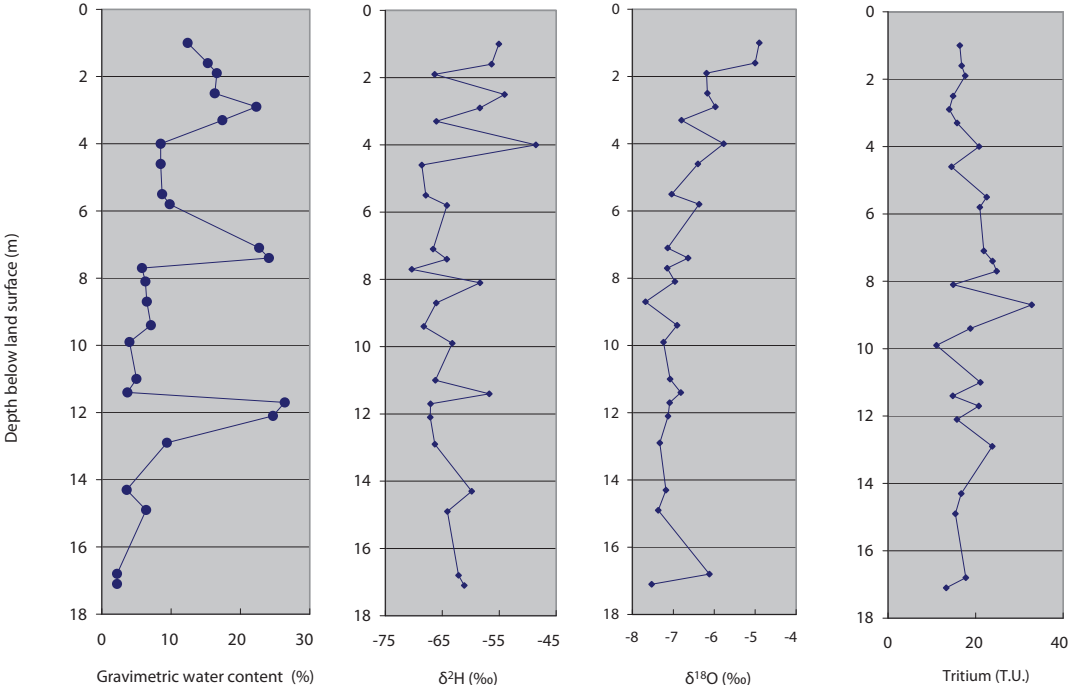


FIG. 13. Gravimetric water content, deuterium, oxygen-18, and tritium data from the unsaturated zone at borehole B01, Shijiazhuang City, China, 2001.

TABLE 1. LITHOLOGY OF THE UNSATURATED DEPOSITS AT BOREHOLE B01, SHIJIAZHANG CITY, CHINA

Sampling depth (m)	Lithology
0—0.7	Agricultural soil
0.7—3.8	Clay
3.8—5.8	Silt loam
5.8—6.6	Coarse sand
6.6—7.4	Silt loam
7.4—11.6	Fine sand
11.6—12.3	Silt loam
12.3—13.7	Fine sand
13.7—18.2	Coarse sand

#### 4.2.2. The $^{18}\text{O}$ , $^2\text{H}$ and $^3\text{H}$ composition of unsaturated zone water in borehole B01

The oxygen-18 ( $\delta^{18}\text{O}$ ) and deuterium ( $\delta^2\text{H}$ ) composition of water extracted from borehole B01 ranged from  $-4.9$  to  $-7.7$  and  $-49$  to  $-70\text{‰}$ , with median compositions of  $-6.9$  and  $-64\text{‰}$ , respectively (Appendix VI, Fig. 13). The heavier (less negative) values are in the upper part of the borehole to a depth of about 4 m. This is consistent with previous work in the study area that suggested the maximum depth of bare soil evaporation in the study area is about 4 m [4]. The  $\delta^2\text{H}$  profile shows pronounced spikes of heavier values at about 4 m intervals, generally without similar spikes in the  $\delta^{18}\text{O}$  profile. Given an average annual precipitation of about 520 mm and an average gravimetric water content in the borehole of 11.4% (about 20% by volume), these heavier values cannot be the result of seasonal differences in the isotopic composition of infiltrating precipitation.

The isotopic composition of water from borehole B01 plots 10 to 25‰ below the Global Meteoric Water Line, in  $\delta^2\text{H}$  and as much as 3‰, in  $\delta^{18}\text{O}$ , to the right of the composition of native groundwater (Fig. 14). The distribution of the data is bimodal, with several samples distributed along a line having a slope of about 8 parallel to and about 10‰ below the global meteoric water line. Distributions of data along a line having a slope of 8 have been shown to result from vapour movement within the dry unsaturated zones found in arid areas [1]. The remainder of the samples plot along an evaporative trend line. The intersection of the 2 lines at a  $\delta^{18}\text{O}$  and  $\delta^2\text{H}$  composition of about  $-9$  and  $-72\text{‰}$  reflects the original composition of water infiltrated at this site. The composition is different from that of ground water sampled in the study area, suggesting that areal recharge from infiltration of precipitation was not the dominant recharge process in this area under predevelopment conditions. This is common in arid and semiarid areas where focused recharge from infiltration of surface water dominates.

The tritium composition of water extracted from borehole B01 ranged from 11 to 32.8 T.U., with median composition of 17.6 TU (Appendix VI, Fig. 13). Tritium concentrations are relatively uniform to a depth of about 8 m, with an average concentration of about 18 TU, reflecting the return to natural background conditions in recent years after the cessation of atmospheric testing of nuclear weapons. The highest concentration is at a depth of 8.7 m. If this high value were the result of infiltration of water during about 1963 having the highest concentrations of tritium from the atmospheric testing of nuclear weapons, then the downward rate of movement would be about 0.22 m/y (calculated as depth of peak concentration divided by the time since infiltration) with a recharge rate of 17 mm/y, about 3% of the total precipitation (calculated as the rate of movement divided by the average volumetric water content in that part of the profile). These rates are much lower than rates estimated previously on the basis of the timing of increased nitrate concentrations in ground water. Given that the highest tritium concentrations in precipitation in the study area was around 2,000 TU in 1963, then the peak concentration in borehole B01 is too low to have resulted from infiltration of precipitation at that time. The 1963 tritium peak must have moved through the unsaturated zone at borehole B01 and actual recharge rates must be closer to the rates indicated by the onset of nitrate contamination and greater than rates indicated on the basis of tritium data.

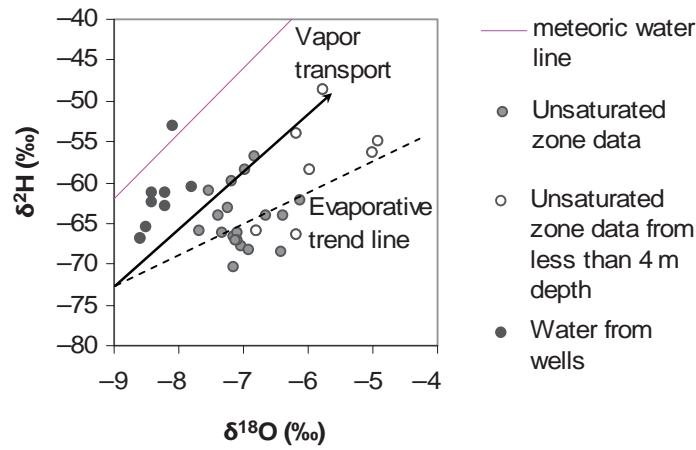


FIG. 14. The  $\delta^2\text{H}$  and  $\delta^{18}\text{O}$  in water from wells, and from the unsaturated zone at borehole B01, Shijiazhuang City, China, 2001.

### 4.3. Borehole B02

Borehole B02, in the northern part of the study area (Fig. 11), is in an area irrigated with groundwater. The altitude is about 70 m above mean sea level and the depth of the borehole is 16.5 m.

#### 4.3.1. Lithology and water content

The upper part of the unsaturated zone at borehole B02 is composed of agricultural soil 0.6 m thick, underlain by a 2.7 m thick clay layer. Below 3.3 m the unsaturated zone is composed largely of sandy material with a 2.9 m thick clay layer at 9.3 m (Table 2). This borehole is representative of the coarser-grained unsaturated deposits found in the northern part of the study area.

TABLE 2. LITHOLOGY OF BOREHOLE B02, SHIJIAZHUANG CITY, CHINA, 2002

Sampling depth (m)	Lithology
0—0.6	Agricultural soil
0.6—3.3	Clay with intercalated silty clay
3.3—5.2	Fine sand with intercalated silt loam
5.2—5.4	Fine sand
5.4—9.3	Medium-grained sand
9.3—12.2	Clayey loam with silt
12.2—12.9	Medium-grained sand
12.9—13.8	Coarse sand
13.8—16.5	Medium-grained sand

Gravimetric water content ranged from 2 to 24%, with a median water content of 5% (Appendix VII). Similar to borehole B01, water contents were higher in the finer-grained deposits and lower in the sand (Fig. 15). The median water content is lower than the median water content in borehole B01 because of the increased fraction of coarser-grained deposits within the borehole. Similar to borehole B01, water contents within the finer-grained units appear to be saturated.

#### 4.3.2. The $^{18}\text{O}$ , $^2\text{H}$ and $^3\text{H}$ composition of unsaturated zone water in borehole B02

The  $\delta^{18}\text{O}$  and  $\delta^2\text{H}$  composition of water extracted from borehole B02 ranged from  $-5.0$  to  $-7.4$  and  $-47$  to  $-68\text{‰}$ , with median compositions of  $-7$  and  $-59\text{‰}$ , respectively (Appendix VII, Fig. 15). The range in values and median compositions are similar to those measured in borehole B01. The heavier (less negative)  $\delta^{18}\text{O}$  and  $\delta^2\text{H}$  values are in the upper part of the borehole to a depth of about 8 m. The

heavier isotopic compositions are especially evident for  $\delta^2\text{H}$  values. This is deeper than obtained at borehole B01 and suggest that irrigation practices at the site are resulting in significant evaporative losses.

The  $\delta^{18}\text{O}$  and  $\delta^2\text{H}$  composition of water from borehole 02 plots from about 8 to 25‰, with respect to  $\delta^2\text{H}$ , below the global meteoric water line, and as much as 3‰, with respect to  $\delta^{18}\text{O}$ , to the right of the composition of native groundwater (Fig. 16). The distribution of the data to the right of the global meteoric water line is more scattered than the distribution of data from borehole B01. Several samples appear to be distributed along a line parallel to and below the global meteoric water line, and a number of other samples along an evaporative trend line trending toward the composition of native groundwater. A large number of samples plot below this evaporative trend line along the evaporative trend line identified in the unsaturated zone at borehole B01. As previously discussed, this line projects to the composition of precipitation — the only source of water at borehole B01. Values along the evaporative trend line from Fig. 14 probably represent partly evaporated precipitation from wetter than average years when less groundwater was used for irrigation. Some waters plot between the two evaporation line shown on Fig. 16 and appear to be mixtures of partly evaporated groundwater and precipitation.

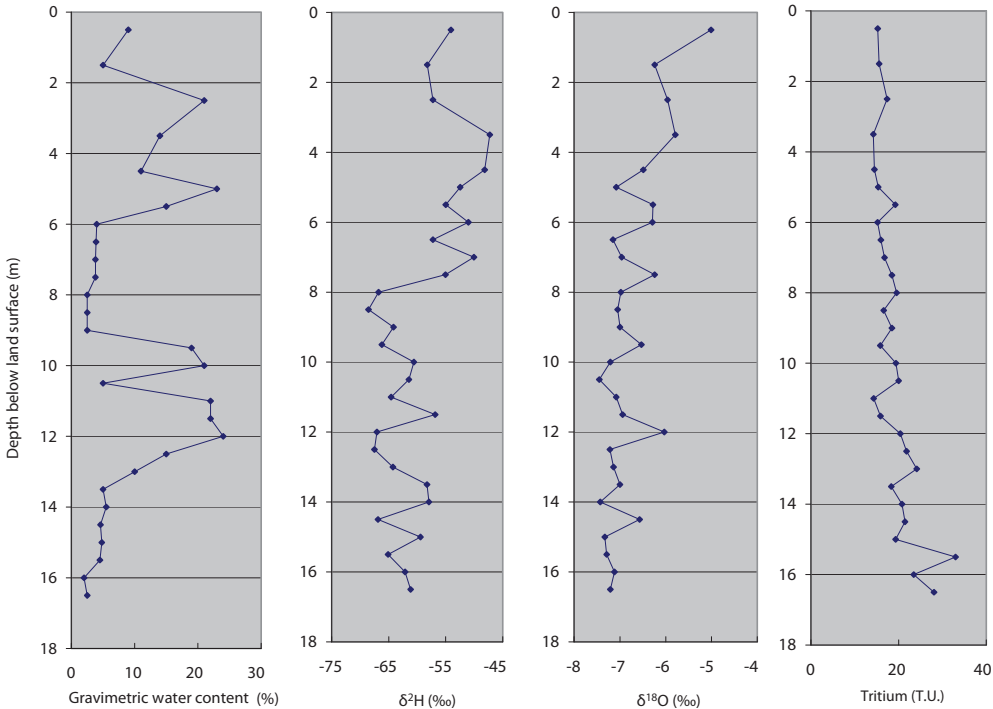


FIG. 15. Gravimetric water content, delta  $\delta^2\text{H}$ ,  $\delta^{18}\text{O}$ , and tritium data from the unsaturated zone at borehole B02, Shijiazhuang City, China, 2002.

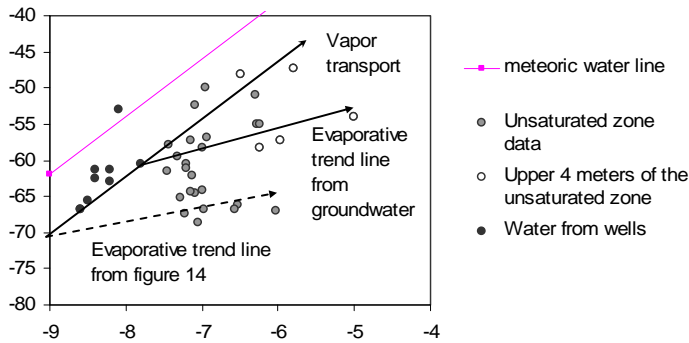


FIG. 16. Deuterium and oxygen-18 in water from wells, and from the unsaturated zone at borehole B02, Shijiazhuang City, China, 2002.

The tritium composition of water extracted from borehole B02 ranged from 14.2 to 33 T.U., with median composition of 18.5 TU (Appendix VII, Fig. 15), similar to the range in borehole B01. The highest concentration is near the bottom of the borehole at a depth of 15.5 m. As in borehole 01, this high value is unlikely to have resulted from the atmospheric testing of nuclear weapons but it may represent water infiltrated at the same time as the high value in borehole B01. If so than the rate of downward movement in borehole 02 is about 80% greater than in borehole 01 and the recharge rate at the irrigated site, normalized for differences in volumetric water content, must be about 55% greater the recharge rate at the unirrigated site in borehole 01.

Assuming the rate of movement and recharge rate from the onset of nitrate contamination (0.9 m/y and 200 mm/y, respectively), than the rate of movement and recharge rate at the unirrigated site B01 must be about 0.6 m/y and 130 mm/y, respectively. As previously discussed, values estimated from the onset of precipitation probably underestimated the rate of downward movement and the recharge rate. It is also not known if the high tritium values in boreholes B01 and B02 infiltrated at the same time.

#### 4.3.3. Chemical composition of unsaturated zone water in borehole 02

Chloride, nitrate, nitrite, and ammonia were measured on water extracts from the unsaturated zone. Results are listed in Appendix VIII. Salts of these ions are highly soluble and it is likely that all the extracted material was dissolved in pore water within the unsaturated zone. Pore water concentrations near the bottom of the borehole provide an estimate of the concentration of water recharging the aquifer beneath irrigated land.

Pore water concentrations of chloride estimated from soil-extract and water-content data ranged from 12 to 130 mg/L, with a median concentration of 46 mg/L (Fig 17). The lowest concentration was just below land surface at 0.5 m and probably represents dilution of groundwater applied for irrigation with precipitation. Chloride concentrations increased to 86 mg/L at 2.5 m just below the root zone. Below 2.5 m, pore water chloride concentrations varied greatly with depth and were independent of water content and lithology. Variations in chloride pore water concentrations probably reflect variations in the chemistry of irrigation water and the amount of precipitation.

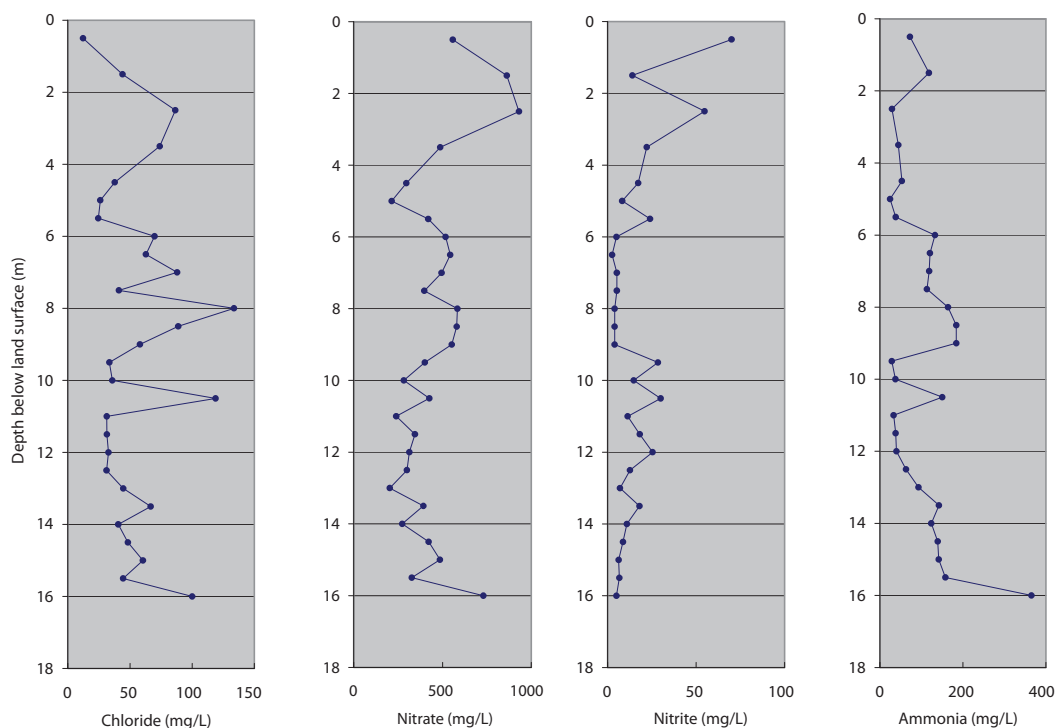


FIG. 17. Chloride, nitrate, nitrite, and ammonia concentrations in pore water from borehole B02, Shijiazhuang City, China, 2002.

Pore water concentrations of nitrate and nitrite ranged from 200 to 930 mg/L and 2.5 to 70 mg/L, with a median concentrations of 420 and 11 mg/L, respectively (Fig. 17). Nitrate concentrations are highest in the upper 2.5 m of the profile and decreased to values of about 520 mg/L between 2.5 m and the clay layer at 9 m. Within the clay layer nitrate concentrations decreased to about 300 mg/L, and then increased gradually to concentrations of exceeding 700 mg/L near the bottom of the borehole. Nitrite concentrations are highest just below land surface and decrease to low values with depth to the clay layer at 9 m where concentrations increase. Decreases in nitrate and increases in nitrite at this depth are consistent with nitrate reduction. Nitrite concentrations decrease to low levels below the clay and remain low to the bottom of the borehole. Pore water concentrations of ammonia ranged from 24 to 365 mg/L, with median concentrations of 115 mg/L (Fig. 17). Ammonia concentrations increased gradually with depth to the clay layer at 9 m, decreased rapidly to low values, and then gradually increased to the highest values near the bottom of the borehole.

On the basis of data from borehole, B02 the total nitrogen stored beneath irrigated land in the study area is about 350 kg/ha. About 60% of the nitrogen is in the form of nitrate, 4% as nitrite, and 36% as ammonia. Nitrate is the more common form in the upper part of the borehole while ammonia is the predominant form in the lower part of the borehole comprising as about 60% of the total nitrogen. Within the borehole nitrate is converted to ammonia, or nitrite and potentially then lost through denitrification. Although the greatest losses in total nitrogen (calculated as the sum of the nitrogen in nitrate, nitrite, and ammonia), a measure of the extent of the denitrification can be made by comparing the mass of nitrate and ammonia to the mass of a conservative (non-reactive) tracer such as chloride (Fig. 18). The ratio of nitrate-to-chloride decreases rapidly within the upper 2.5 m of the borehole. This is the biologically active zone where plant will utilize nitrogen, thereby decreasing its mass. The ratio of nitrate-to-chloride subsequently remains relatively constant with depth to the water table. The ratio of ammonia-to-chloride also shows a rapid decrease within the upper 2.5 m of the borehole. However, unlike nitrate the ammonia to chloride ratio gradually increases with depth to the clay layer at 9.3 m. The ratio then decreases rapidly to low values at the clay at 9.5 m below land surface and then gradually rises toward the water table. The changes in the ammonia-to-chloride ratio are consistent with gradual conversion of nitrate to ammonia (or conversion of organic nitrogen to ammonia) to a depth of about 9 m and a rapid loss of ammonia within the fine-grained clay layer at 9.3 m. Below 9.5 m the gradual conversion of nitrate to ammonia resumes to the water table.

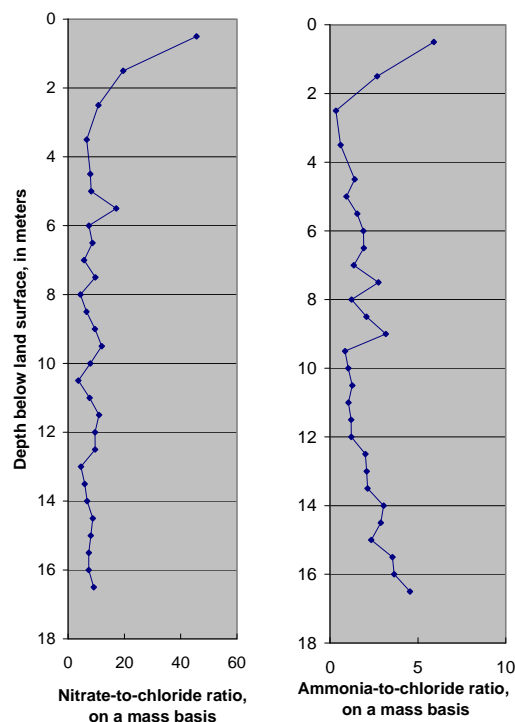


FIG. 18. Nitrate-to-chloride, and ammonia-to-chloride ratios in pore water from borehole B02, Shijiazhuang City, China, 2002.

#### 4.4. Borehole B03

Borehole B03, in the southern part of the study area (Fig. 11), is in an area that was irrigated by sewage before 1980. After 1981, groundwater was used for irrigation. The altitude is about 80 m above mean sea level and the depth of the borehole is 16.5 m.

##### 4.4.1. Lithology and water content

The upper part of the unsaturated zone at borehole B3 is composed of an agricultural soil 0.6 m thick, underlain by clayey units to a depth of 5.3 m (Table 3). Below 5.3 m the unsaturated zone is composed primarily of sand with some silt, with the exception of a clay loam from 9.9 to 12 m depth. This borehole is representative of the finer-grained unsaturated deposits found in the southern part of the study area.

Gravimetric water content ranged from 5 to 26%, with a median water content of 13% (Appendix IX, Fig. 19). The median water content is the highest of the three boreholes studied. Similar to the previous boreholes, water contents were higher in the finer-grained layers and lower in the sand layers. The clay layers between 0.6 and 5.3 m appear to be saturated, the deeper silt layer at 9.9 to 12.1 m, while wetter than most of the borehole, is probably not saturated.

##### 4.4.2. $^{18}\text{O}$ , $^2\text{H}$ and $^3\text{H}$ composition of unsaturated zone water in borehole B03

The  $\delta^{18}\text{O}$  and  $\delta^2\text{H}$  composition of water extracted from borehole B03 ranged from  $-5.4$  to  $-7.6$  and  $-44$  to  $-68\text{‰}$ , with median compositions of  $-6.8$  and  $-59\text{‰}$ , respectively (Appendix IX, Fig. 19). The range in values and median compositions are similar to those measured in boreholes B01 and B02. Similar to borehole B02, the heavier (less negative)  $\delta^{18}\text{O}$  and  $\delta^2\text{H}$  values are in the upper part of the borehole to a depth of about 8 m — possibly reflecting similar irrigation practices at the two sites.

The  $\delta^{18}\text{O}$  and  $\delta^2\text{H}$  composition of water from borehole 03 plots from about 8 to 28‰ in  $\delta^2\text{H}$ , below the Global Meteoric Water Line, and as much as 2.5‰ in  $\delta^{18}\text{O}$ , to the right of the composition of native groundwater (Fig. 20). The distribution of the data to the right of the global meteoric water line is similar to the distribution in borehole B02 and more scattered than the distribution of data from borehole B01. Several samples appear to be distributed along a line parallel to and below the global meteoric water line, and a number of other samples along an evaporative trend.

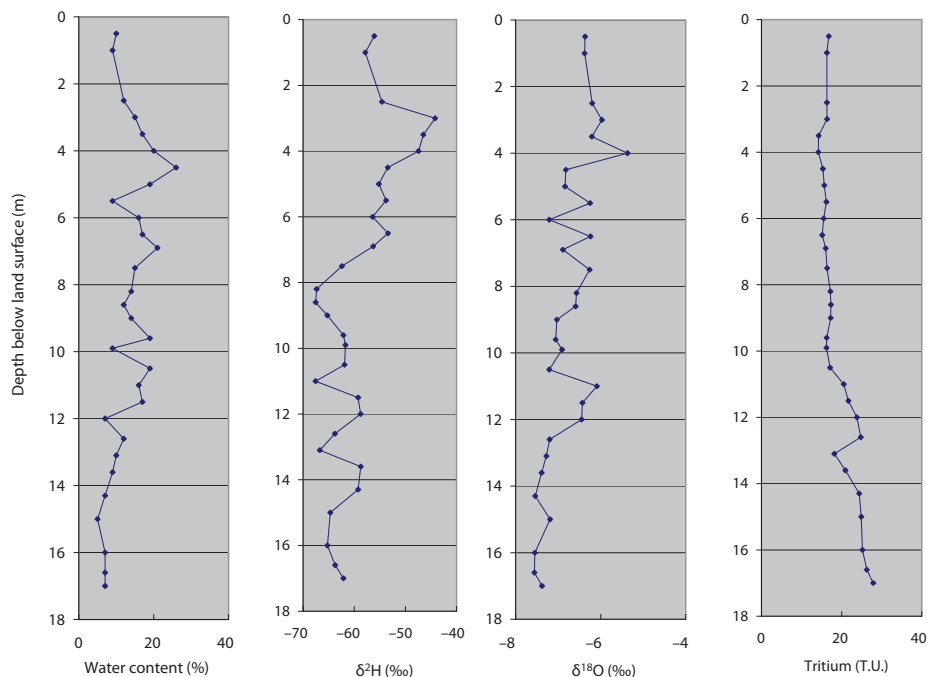


FIG. 19. Gravimetric water content,  $\delta^2\text{H}$ ,  $\delta^{18}\text{O}$  and tritium data from the unsaturated zone at borehole B03, Shijiazhuang City, China, 2003.

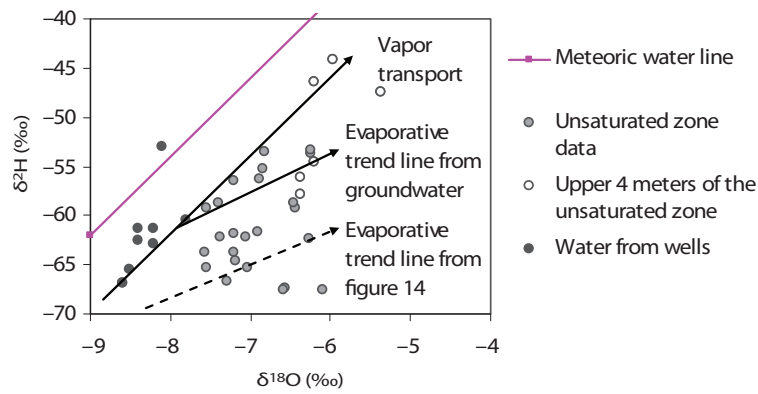


FIG. 20 .  $\delta^2\text{H}$  and  $\delta^{18}\text{O}$  in water from wells, and from the unsaturated zone at borehole B03, Shijiazhuang City, China, 2003.

TABLE 3. LITHOLOGY OF BOREHOLE B03, SHIJIAZHUANG CITY, CHINA

Sampling depth (m)	Lithology
0—0.6	Agricultural soil
0.6—3.0	Clayey loam with silt
3.0—5.3	Clay with intercalated silty clay
5.3—5.6	Fine sand
5.6—6.4	Sand with intercalated silt loam
6.4—9.5	Medium-grained sand
9.5—9.9	Fine sand
9.9—12.1	Clayey loam with silt
12.1—13.6	Medium-grained sand
13.6—14.2	Coarse sand
14.2—17.1	Medium-grained sand

The intersection of the 2 lines at a  $\delta^{18}\text{O}$  and  $\delta^2\text{H}$  composition of about  $-8$  and  $-62\text{‰}$  falls within the range of native groundwater sampled as part of this study and is similar to the values indicated for borehole B02. Similar to borehole B02, a large number of samples plot below the evaporative trend line and some have  $\delta^2\text{H}$  values lighter (less negative) than native groundwater. As previously discussed in borehole B02, these values plot along the evaporative trend line from Fig. 14 and this line projects to the composition of precipitation — the only source of water at borehole B01. Values along the evaporative trend line identified for borehole B01 (Fig. 14) and probably represent partly evaporated precipitation from wetter than average years when less groundwater was used for irrigation. Some waters plot between the two evaporation line shown on Fig. 20 and appear to be mixtures of partly evaporated groundwater and precipitation.

The tritium composition of water extracted from borehole B03 ranged from 14.2 to 33 T.U., with median composition of 18.5 TU (Appendix IX, Fig. 19), similar to the range in borehole B01 and B02. The highest concentration is near the bottom of the borehole at a depth of 15.5 m. As in borehole B01 and B02 this high value is unlikely to have resulted from the atmospheric testing of nuclear weapons. Assuming the year of maximum tritium concentration in rainfall was 1963 and 40 years has elapsed since the precipitation infiltrated the soil, the average rate of downward movement would be about 0.39 m/y. Given an average volumetric water content of 23% the recharge rate would be about 0.09 mm/y. Considering the area is irrigated with groundwater, the actual average recharge rate must be much higher.

Groundwater in the vicinity of this profile has been contaminated by nitrate since 1982. Sewage irrigation started in this area in 1965 and stopped in 1980. Only 15 years elapsed between sewage irrigation and groundwater nitrate contamination in this area. In 1982, the groundwater table depth was around 14 m. and nitrate must have moved downward at a rate of more than 0.9 m/y. Assuming an average volumetric water content of 23%, the recharge rate must be at least 200 mm/y. Although higher than the estimate based on tritium, these calculations probably greatly underestimate the actual recharge rate since a large amount of high-nitrate water would have had to accumulate near the top of the water table before contaminating water from wells.

## 5. $^{15}\text{N}$ ISOTOPIC COMPOSITION OF WATER IN THE UNSATURATED ZONE

The  $\text{NO}_3^-$  concentration and  $\delta^{15}\text{N}$  composition of groundwater samples from 28 public-supply and irrigation wells (Appendix X) ranged from 13 to 148 mg/L and 2.2 to 11.7‰, with median values of 52 mg/L and 6.1‰ respectively. Water from wells in the urban area had the highest average nitrate concentrations with progressively lower concentrations with decreasing population density in the village and farmland areas (Table 4). Sewage was all in the form of ammonia. The  $\delta^{15}\text{N}$  composition of water from wells followed a similar pattern decreasing to lower values with decreasing population densities (Table 4).

TABLE 4. AVERAGE  $\text{NO}_3^-$  CONCENTRATIONS AND RANGES IN  $\delta^{15}\text{N}$  COMPOSITIONS IN WATER FROM WELLS IN URBAN, VILLAGE, AND FARMLAND AREAS, SHIJIAZHUANG CITY, CHINA, 2004

Type of water	Location	$\delta^{15}\text{N}$ (‰)	Mean content of $\text{NO}_3^-$ (mg/L)
Groundwater for city water supply	Urban district	+7.1 ~ +11.67	73.1
Groundwater for village water supply	Village	+5.68 ~ +7.48	65.4
Groundwater for irrigation	Farmland	+2.16 ~ +4.83	53.9
Sewage	Sewage ditch	+7.86 ~ 9.04	0.5 ( $\text{NH}_4^+=82.5$ mg/L)

TABLE 5.  $\text{NO}_3^-$  CONCENTRATIONS AND  $\delta^{15}\text{N}$  COMPOSITIONS OF SOIL-WATER EXTRACTS, SHIJIAZHUANG CITY, CHINA, 2004

Type of soil	Sampling location and depth	lithology	$\text{NO}_3^-$ (mg/L)	$\delta^{15}\text{N}$ (‰)
Natural soil	No. 1 0–20 cm	Silt	77.5	+0.1
	No. 2 100–120 cm	Silt	38.8	+2.1
	No. 3 0–40 cm	Silt	74.8	-0.2
	No. 4 140–150 cm	Clayey silt	16.6	+1.9
Manure soil and sewage irrigated soil	No. 5 0–30 cm	Clay	193.8	+8.8
	No. 6 90–100 cm	Clay	55.4	+8.5
	No. 7 0–40 cm	Sandy clay	188.3	+9.4
	No. 8 0–40 cm	Clayey silt	96.0	+11.3
Chemical fertilizer soil	No. 9 0–20 cm	Loam	199.4	+4.7
	No. 10 0–20 cm	Loam	105.2	+4.6
	No. 11 0–20 cm	Silt	143.9	+4.3

Soil samples were collected from the upper 150 cm at 11 sites. The sites included 4 natural soils, 4 sewage (and manure) amended soils, and 3 chemically fertilized soils. Nitrate was extracted using deionised water. The ratio of air dried, pulverized soil to deionised water was 1/10 by weight. The soil water mixture was shaken for 24 hours and analyzed for  $\text{NO}_3^-$  concentrations and  $\delta^{15}\text{N}$  composition. Results of  $\text{NO}_3^-$  and  $\delta^{15}\text{N}$  analysis from soil extracts are shown in Table 5. Nitrate concentrations were lowest in extracts from the natural soil (average 52 mg/L) and similar in the sewage amended and chemically fertilized soils (133 and 144 mg/L, respectively).  $\delta^{15}\text{N}$  values were lowest in the natural soils (average 1.0‰), highest in the manure amended soils (average 9.5‰), and intermediate in the chemically fertilized soils (average 7.3‰).

Comparison of the nitrate concentrations and  $\delta^{15}\text{N}$  composition of water from wells with natural, sewage (and manure) amended, and chemical fertilizer amended soils shows that most water from wells have higher than expected  $\delta^{15}\text{N}$  compositions assuming only simple mixing with sewage (sewage analysis given in Table 4) and plot within the range of sewage amended soils. This can only occur as a result of denitrification. Denitrification also was indicated on the basis of pore water chemistry data from borehole B02. Water from wells that plot near compositions expected on the basis of addition of nitrate from sewage without denitrification probably are more likely to have originated from chemical fertilizer applications with denitrification than from sewage or manure. Extensive denitrification of nitrate from chemical fertilizer may cause even greater fractionation of  $\delta^{15}\text{N}$  values rendering them indistinguishable from sewage or manure nitrate. Conversion of nitrate to ammonia within the unsaturated zone (also shown to occur in borehole B02) may further complicate the interpretation of  $\delta^{15}\text{N}$  data by producing lighter than expected  $\delta^{15}\text{N}$  values in the remaining nitrate.

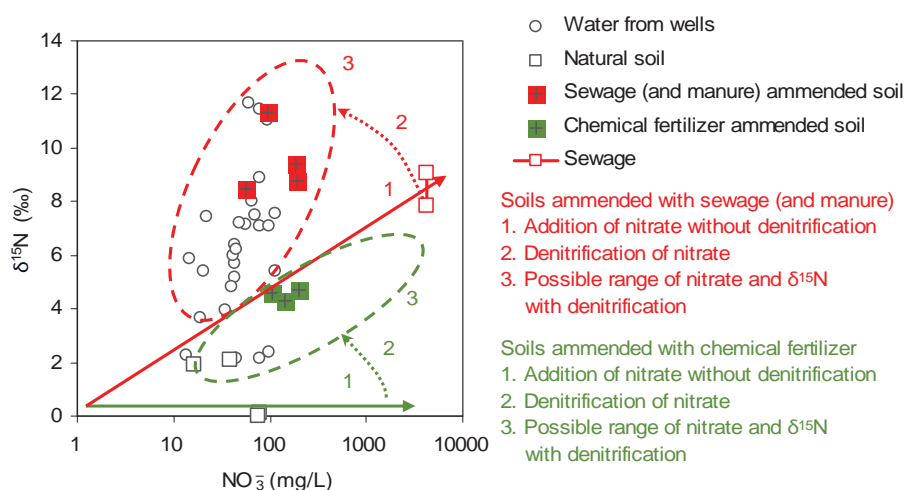


FIG. 21.  $\delta^{15}\text{N}$  as a function of nitrate concentration in water from wells and water extracts from natural soils, sewage (and manure) amended soils, and chemical fertilizer amended soils, Shijiazhuang City, China, 2004.

Samples also were collected from land surface to a depth of 5 m at 7 sites representing natural, sewage (and manure) amended, and chemically fertilized soils. The purpose of the samples was to evaluate if large reductions in nitrate concentrations in the upper part of borehole B02 were the result of denitrification or plant uptake. The samples were extracted with water using the same method as the surficial samples and the extract was analyzed for nitrate concentration and  $\delta^{15}\text{N}$  composition. Lithology and analytical results are listed in Appendix XI.

Nitrate concentrations decreased with depth in all 7 profiles regardless of nitrate applications. However, there was not a consistent increase in  $\delta^{15}\text{N}$  compositions in any of the sampled boreholes with decreasing nitrate concentrations. The profiles  $\delta^{15}\text{N}$  compositions either decreased slightly (largely in sewage amended sites), remained constant (natural sites) or varied randomly (largely in

chemical fertilizer sites. The lack of an increase  $\delta^{15}\text{N}$  compositions with decreasing nitrate concentrations were the result of plant uptake rather than denitrification. The decrease in  $\delta^{15}\text{N}$  compositions is consistent with oxidation of ammonia in sewage to nitrate. Nitrate concentrations in the profile decreased because plant uptake was greater than the addition of nitrate from ammonia.

The groundwater in irrigated areas has a slightly higher value range of  $\delta^{15}\text{N}$  than that of chemical fertilizer soil, which means the nitrogen pollutant source of groundwater in wells for irrigation (in lower population area) is mainly from chemical fertilizer nitrogen.

The groundwater for village water supply has  $\delta^{15}\text{N}$  values little higher than that of chemical fertilizer soil and lower than that of manure and sewage irrigated soil. This may indicate the nitrogen is mainly from human waste and partly from chemical fertilizer. The natural soil nitrate with low  $\delta^{15}\text{N}$  values is not the main cause of nitrate contamination of groundwater in the area.

## 6. DISCUSSION AND CONCLUSIONS

In 1959, water from most sampled wells in Shijiazhuang City had nitrate concentrations less than 2 mg/L, with a maximum concentration of 6.6 mg/L. By 2001, nitrate concentrations in water from wells in Shijiazhuang City, China had increased and ranged from 15 to about 160 mg/L as nitrate, with a median concentration of 50 mg/L. The problem is aggravated by declining water levels that have essentially dewatered the uppermost aquifer. As a result of water level declines there is less groundwater in the aquifers to dilute poor-quality water associated with overlying land uses moving through the unsaturated zone. Return waters from agricultural land irrigated with sewage or groundwater are believed to be the source of increasing nitrate, chloride, sulphate, and dissolved solids concentrations.

The source of water in the unsaturated zone underlying unirrigated land is precipitation having  $\delta^{18}\text{O}$  and  $\delta^2\text{H}$  compositions (after surface evaporation prior to infiltration) is  $-9.0$  and  $72\%$ , respectively. These values are slightly lighter than native groundwater suggesting that native ground water may be recharged from other sources, either infiltration of surface water or recharge sources outside the study area. Sources from outside the study area may render the groundwater vulnerable to contamination from sources outside the study area. Recharge rates through the unsaturated zone, estimated from the onset of nitrate contamination in well water and tritium data are about 130 mm/y for non-irrigated agricultural land, and exceed 200 mm/y for irrigated land. Actual recharge rates for irrigated lands are probably much higher.

Nitrate concentrations in pore water in the unsaturated zone were as high as 930 mg/L. Nitrate concentrations decrease to lower values typically about 500 mg/L with depth in the study boreholes—this may represent an upper limit on potential ground water contamination in the study area given present-day (2001) land use. As much as 350 kg/ha of nitrogen is stored in the upper 18 m of the unsaturated zone beneath a groundwater irrigated site. As much as 780 kg/ha of nitrogen could be stored in thicker unsaturated zones and nitrogen storage beneath sewage irrigated sites is even probably greater. Even if land use practices were changed immediately groundwater quality would not begin to improve until nitrogen from past land use practices has been flushed from the unsaturated zone. About 60% of the nitrate stored in the unsaturated zone is in the form of nitrate and 36% is in the form of ammonia. Denitrification in near-saturated fine-grained layers reduces the concentration of nitrate in with depth and at 18 m below land surface 60% of the nitrogen is in the form of ammonia.

The  $\delta^{15}\text{N}$  composition of water from sampled wells ranged from 2.2 to 11.7‰, with median value of 6.1‰. Water from wells in the urban area had the highest average  $\delta^{15}\text{N}$  compositions with progressively lower values in the village and farmland areas.  $\delta^{15}\text{N}$  values in surficial soils averaged 1.0‰ in natural sites, 9.5‰ in sewage and manure amended sites, and 7.3‰ in the chemically fertilized sites. Most  $\delta^{15}\text{N}$  values in water from wells are in the range of compositions expected from sewage and manure sources of nitrogen — with some denitrification, although extensive denitrification of nitrogen from chemical fertilizers also could produce observed  $\delta^{15}\text{N}$  values.

## REFERENCES

- [1] IZBICKI, J.A., RADYK, J., MICHEL, R.L., Water movement through a thick unsaturated zone underlying an intermittent stream in the western Mojave Desert, southern California, USA, *J. Hydrol.* **238** (2000) 194–217.
- [2] IZBICKI, J.A., J., MICHEL, R.L., Movement of water through the thick unsaturated zone underlying Oro Grande and Sheep Creek Washes in the western Mojave Desert, USA, *Hydrogeology Journal* **10** (2002) 409–427.
- [3] IZBICKI, J.A., CLARK, D.A., PIMENTEL, M.I., LAND, M., RADYK, J., MICHEL, R.L., Data from a thick unsaturated zone underlying Oro Grande and Sheep Creek Washes in the western Mojave Desert, near Victorville, San Bernardino County, California, U.S. Geological Survey Open-File Report 00-262 (2000) 133.
- [4] LIN XUEYU, Scientific Management of Groundwater Resources in Shijiazhuang City, J. Changcun Geological Institute (1987) 1–214.

## Appendix 1

### DEVELOPMENT OF THE GROUNDWATER DEPRESSION UNDERLYING SHIJIAZHUANG CITY, CHINA

Time	Area (km <sup>2</sup> )	Water table depth at the center (m)	Water table elevation (m)
1965	58	7.57	62.43
1969	131	10.36	59.64
1970	154	10.37	59.63
1971	127	11.87	59.13
1972	183	11.81	59.19
1973	177	13.85	56.19
1974	161	13.53	56.47
1975	187	15.29	54.71
1976	170	16.68	53.32
1977	182	18.72	52.67
1978	184	19.40	51.99
1979	185	19.67	51.72
1980	189	20.39	51.00
1981	200	21.36	50.03
1982	245	24.39	47.00
1983	237	25.89	45.50
1984	255	28.89	42.50
1985	259	31.32	40.07
1986	300	32.88	38.51
1987	336	35.16	36.23
1988	314	37.32	34.07
1989	337	36.06	35.33
1990	338	37.22	34.17
1991	326	37.60	33.79
1992	343	37.63	33.76
1993	354	40.11	31.28
1994	360	42.54	28.85
1995	370	43.47	27.92
1996	360	42.00	29.39
1997	315	37.00	34.39
1998	325	35.70	35.69
1999	348	39.98	31.41
2000	340	42.28	29.11

## Appendix II

### GROUNDWATER CHEMICAL COMPOSITION IN mg/L, SHIJIAZHUANG CITY, CHINA, 1958–59

Sample No.	Date of sampling	pH	Na <sup>+</sup> +K <sup>+</sup>	Ca <sup>2+</sup>	Mg <sup>2+</sup>	Cl <sup>-</sup>	SO <sub>4</sub> <sup>2-</sup>	HCO <sub>3</sub> <sup>-</sup>	NO <sub>3</sub> <sup>-</sup>	Hardness	TDS
CKB5	59-1-29	7.5	12.9	79.42	16.68	25.1	35.59	267.02		265	322
CKB6	58-9-10	7.6	1.1	80.58	26.3	26.11	42.89	280.69		311	320
CKB7-1	58-12-10	7.8	8.09	66.55	19.26	21.42	11.09	268.06	1.77	244	322
CKB7-2	59-12-6	7.8	8.9	74.75	20.5	32.12	18.44	273.61	1.77	274	315
CKB8-1	58-11-24	7.7	13.35	80.24	25.86	45.71	9.08	319.01	0.22	300	350
CKB9-1	58-9-23	7.6	29.59	64.51	24.23	33.05	9.03	328.47		267	345
CKB10	59-4-14	7.8	18.36	79.9	17.69	31.89	58.31	253.05	0.0034	276	348
CKB11	59-9-12	7.7	6.6	78.46	20.2	24.61	33.81	265.9	6.64	271	315
CKB13	59-2-22	7.7	7.7	79.64	15.35	28.15	21.81	262.45	1.33	260	295
CKB14-1	58-11-10	7.6	7.04	68.84	23.87	23.33	34.05	264.64		278	300
CKB15-1	59-3-23	7.7	12.99	174.58	19.13	34.76	58.31	224.49	0.02	264	322
CKB16-1	59-1-17	7.8	60.72	121.74	32.83	120.41	56.1	414.63	3.54	436	617
CKB17-1	58-10-3	7.9	7.04	61.44	17.4	21.49	3.17	229.13		221	253
CKB2-2	59-4-27	7.7	17.91	68.08	17.36	22.16	66.14	218.02	1.77	245	314
CKB1-1	59—3-7	7.7	16.78	63.71	15.92	16.56	59.32	214.55		223	322
CKB1-2	59-2-22	7.8	17.91	61.36	15.64	19.86	53.17	211.13		216	283
CKB22-1	58-11-20	7.5	21.78	81.62	19.09	33.33	54.47	276.12		276	388
CKB22-2	58-10-8	7.8	14.0	74.75	24.23	23.15	83.38	240.6		262	356
CKB23	58-12-31	7.6	2.41	65.39	16.83	21.03	36.07	207.96		233	261
CKB21-1	59-1-11	7.7	22.14	80.84	21.64	52.30	37.56	267.08		295	374
CKB21-2	58-12-29	7.5	14.67	58.66	25.49	14.36	7.49	306.87	4.43	248	298

### Appendix III

#### COMPOSITION AND VARIATION OF TYPICAL GROUNDWATER CHEMISTRY IN mg/L, SHIJIAZHUANG CITY, CHINA, 1978, 1985, AND 1992

Well No.	time	Na <sup>+</sup> +K	Ca <sup>2+</sup>	Mg <sup>2+</sup>	Cl <sup>-</sup>	SO <sub>4</sub> <sup>2-</sup>	HCO <sub>3</sub> <sup>-</sup>	NO <sub>3</sub> <sup>-</sup>	Hardness	TDS	Chemical type
3	1978	20	83	20	38	87	229		229	362	
	1985	32	88	21	38	104	244	20	309	426	a
	1992	39	90	23	40	119	225	51	328	474	
50	1978	23	93	23	43	86	271		328	413	
	1985	17	95	28	31	96	290	9	351	422	a
	1992	29	103	28	40	112	290	28	371	484	
47	1978	20	90	24	38	86	266		325	399	
	1985	37	95	21	40	101	290	10	323	450	a
	1992	33	89	31	31	117	293	19	351	467	
88	1985	25	81	22	27	92	256	2	292	377	a
	1992	27	93	21	23	110	273	11	319	422	
40	1980	32	107	24	55	89	300	22	366	479	
	1985	27	131	30	68	88	369	22	449	551	b
	1992	46	150	40	106	122	369	75	544	724	
70	1978	9	97	22	38	65	281		332	371	
	1985	19	112	25	51	79	305	26	383	460	b
	1992	22	134	36	75	110	344	36	483	586	
52	1978	17	98	24	37	80	291		342	413	
	1985	20	103	28	40	88	317	10	373	448	b
	1992	31	107	40	52	108	347	40	433	553	
68	1978	14	99	21	36	63	288		334	391	
	1985	20	106	25	38	85	310	16	366	444	b
	1992	35	123	29	54	110	339	45	430	566	
58	1981	31	129	30	105	86	317	18	440	557	
	1985	53	142	42	145	102	369	40	528	709	c
	1992	75	171	42	162	134	408	75	601	862	
63	1980	35	141	32	122	99	332	14	483	609	
	1985	56	142	35	136	108	361	22	496	679	c
	1992	77	164	39	155	129	405	64	572	831	
66	1985	17	123	29	57	79	356	11	426	493	c

	1992	69	159	37	162	126	359	55	551	788	
112	1985	62	95	36	128	87	283	20	383	570	c
	1992	77	127	39	149	106	339	59	482	727	
106	1985	62	143	36	119	104	425	22	506	699	c
	1992	77	144	40	119	139	412	52	530	778	

a  $\text{HCO}_3\text{-SO}_4\text{-Ca-Mg}$ .

b  $\text{HCO}_3\text{-Ca-Mg}$ .

c  $\text{HCO}_3\text{-Cl-Ca-Mg}$ .

## Appendix IV

### GROUNDWATER CHEMICAL DATA IN mg/L OF SHIJIAZHUANG CITY, CHINA, 2001

No.	Ca <sup>2+</sup>	Mg <sup>2+</sup>	K <sup>+</sup>	Na <sup>+</sup>	Cl <sup>-</sup>	SO <sub>4</sub> <sup>2-</sup>	HCO <sub>3</sub> <sup>-</sup>	NO <sub>3</sub> <sup>-</sup>	SiO <sub>2</sub>	TDS	Hardness
48	161.82	47.83	1.99	63.8	141	165	358.7	80.9	20.45	862.14	604
49	137.28	32.56	1.66	41.84	96.5	145	293.2	44	20.3	665.74	479
43	209.46	45.81	0.83	35.61	222	90	376.8	79.3	18.36	889.77	715
47	74.88	23.35	1.33	18.13	38	105	178.9	14.9	16.27	381.31	284
50	117.52	30.92	5.81	40.06	78	130	160.8	137.8	15.97	636.48	423
23	158.08	33.06	1.33	48.96	73.5	150	371.8	77.7	19.77	748.3	533
26	170.56	36.98	1.99	50.45	77.5	180	345.8	114.3	19.4	824.08	580
29	171.6	27.76	0.66	34.87	79	215	297.5	42.9	15.3	735.84	545
33	200.72	43.29	0.99	54.15	236	110	313	99.7	20.52	921.87	682
45	166.4	31.8	1.66	48.22	97.5	200	283.4	78.2	20.52	786	549
51	119.6	32.43	0.66	23.74	55.5	70	379.9	24.1	19.03	535.01	434
52	66.56	29.66	1.66	17.06	27.5	35	287.9	16.5	20.89	358.78	290
31	161.2	29.4	1.3	38.57	104	175	258.5	71.2	21.27	731.19	526
37	123.76	27.13	0.83	40.8	76.5	95	319	44.5	20.3	588.32	422
53	135.2	27.76	1.33	32.64	72.5	125	297.5	50.2	18.8	612.18	454
54	151.42	36.85	1.33	31.16	79	140	335.2	70.5	18.45	696.31	532
55	143.52	35.34	1.66	36.36	116	125	300.8	46.5	19.43	674.21	506
30	177.84	29.66	3.32	39.32	54.5	420	92.9	65.7	16.39	853.18	568
56	133.12	34.71	1.33	30.42	50.5	170	302.5	49.2	16.92	637.45	477
46	143.52	42.66	1.33	54.15	101.5	185	272.2	99.1	18.14	781.5	537
57	140.4	30.92	0.99	31.9	89.5	100	322.4	56.7	19.81	631.42	480
58	138.94	31.8	1.99	34.87	51	270	189.5	49	16.39	688.74	480
34	143.94	39.5	1.66	35.61	112	90	357.5	59.4	20.2	681.06	524
59	222.56	39.12	0.83	29.67	115.5	170	357.7	156.7	19.05	932.28	719
35	87.36	21.45	1.99	19.29	20.5	140	164.1	42.1	15.24	429.98	308
17	105.04	26.88	1.99	23.74	30	170	202.2	42.7	14.86	516.31	374
60	128.96	47.96	1.99	28.19	114	100	334.1	46.5	16.39	651.04	522
61	85.28	20.82	1.33	22.25	31	135	175.8	20.7	14.1	418.38	300
62	164.32	30.29	0.66	32.64	68.5	145	383.5	47.8	17.91	698.87	537

42	242.94	32.43	0.33	55.64	165	200	382	113.6	16.39	1017.3	742
22	189.28	32.81	0.83	35.61	121.5	155	320.1	95.6	19.43	810.11	610
44	173.68	34.71	1.33	89.02	121	205	382.7	77.4	19.81	913.3	579
36	124.38	21.08	1.66	24.48	43	180	196	44.9	16	553.5	399
24	108.16	26.75	1.33	29.67	36	130	271.2	39.4	15.62	522.53	382
14	100.26	20.95	1.66	22.25	35.5	160	156.9	42.6	16.99	478.66	338

---

## Appendix V

### HYDROGEOCHEMICAL MODELING FOR EXPLANATION OF POLLUTION MECHANISMS, SHIJIAZHUANG CITY, CHINA

#### Model input

From the analysis above, we can see that the percolation of sewage is the basic source of pollution in Shijiazhuang city groundwater. However, what happens in the process of sewage percolation and mixing with groundwater? Is the mixing conservative or do some reactions occur in the process? In order to explore this, hydrogeochemical modeling was carried out as part of the study. The mean chemical compositions of groundwater from 1958 to 1959 is used as the initial groundwater chemistry, and the mean chemical compositions of groundwater in 1992 taking from 30 wells located in south part of the city is used as the final water, and the mean chemical compositions of sewage measured from 1980 to 1992 is taken as another end member. The chemical data of three waters are shown in Table V-1.

Calcite, dolomite, gypsum, and quartz are the common minerals in the unsaturated zone. Considering the TDS and hardness are the main two pollutants in groundwater, calcite, dolomite, gypsum and Ca-Na exchange are chosen as the mineral phases in the model. Meanwhile, for the open groundwater system, we also choose CO<sub>2</sub> as the input item in the model.

Mineral-water relationship for three waters is analyzed using the computer program WATEQ2 [1]. The calculated results of saturation indexes for three waters are given in Table V-2.

Mass-balances of mineral-water interactions in the mixing process of sewage with groundwater are calculated using the computer program BALANCE [2] and the results are shown in Table V-3.

TABLE V-1. CHEMICAL COMPOSITIONS OF GROUNDWATER AND SEWAGE (mg/L)

water	Na <sup>+</sup> +K	Ca <sup>2+</sup>	Mg <sup>2+</sup>	Cl <sup>-</sup>	SO <sub>4</sub> <sup>2-</sup>	HCO <sub>3</sub> <sup>-</sup>	T(°C)	pH
sewage	113.6	131.9	23.5	136.9	160.8	451.9	19.5	6.56
Mean contents from 1958to1959	15.3	74.5	20.8	30.9	37.6	268.8	14.7	7.69
Mean contents in 1992	49.5	147.2	34.5	98.5	127.3	395.5	16.4	7.44

TABLE V-2 SATURATION INDEXES (SI) FOR THREE WATERS

water	calcite	dolomite	gypsum
sewage	-0.793	-2.408	-1.272
Groundwater from 1958to1959	+0.357	+0.368	-1.963
Groundwater in 1992	+0.500	+0.610	-1.310

TABLE V-3 RESULTS OF MASS BALANCE CALCULATION

Mineral phase	calcite	dolomite	gypsum	CO <sub>2</sub>	exchange
Mass transfer	-0.032790	+0.49318	+0.11598	-7.82930	-0.62019

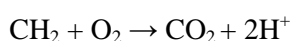
**Note:** The unit is in millimoles per kilogram of water. Positive values indicate dissolution, and negative values indicate precipitation. For ion exchange of Ca-Na, negative values indicate Ca is released to solution and Na is removed from solution

## Model results

Table V-2 shows that calcite and dolomite are oversaturated and gypsum is undersaturated in groundwater, that meaning groundwater both in 1959 and 1992 had lost the ability to dissolve calcite and dolomite but maintained the dissolution ability for gypsum. From 1959 to 1992, the saturation indexes increased notably for three minerals. For sewage, calcite, dolomite and gypsum are all undersaturated, which indicate the sewage in Shijiazhuang city has a high dissolution ability for carbonate and sulphate minerals distributed in the geological formation.

From the results in Table V-3, it can be seen that there are water-rock interactions occurring during mixing process of sewage and groundwater, mainly resulting in the dissolution of dolomite and gypsum, the precipitation of calcite, the outgassing of CO<sub>2</sub> and ion exchange of Ca<sup>2+</sup> – Na<sup>+</sup> (Na<sup>+</sup> in water exchange Ca<sup>2+</sup> in solids).

In addition, the reaction for organic oxidation should happened during the infiltration of sewage as follows:



This reaction increases the acidity of infiltrated water and thus calcium and magnesium carbonates can be dissolved more easily, resulting in an increase in groundwater TDS and hardness.

As mentioned above the TDS and hardness are the main pollution items in Shijiazhuang city. The mechanism of TDS and hardness pollution can be explained by the modeling like this: in the process of sewage percolating and mixing with groundwater, the dissolution of dolomite and gypsum (0.60916 mmol per kilogram water) is much greater than the precipitation of calcite (0.32790 mmol per kilogram water), resulting in an increase of Ca<sup>2+</sup>, Mg<sup>2+</sup>, SO<sub>4</sub><sup>2-</sup> and HCO<sub>3</sub><sup>-</sup> in groundwater beyond that from pure mixing process. Meanwhile, ion exchange of Ca-Na forms another source of Ca<sup>2+</sup> for groundwater, which leads to increasing of groundwater hardness. The increased Cl<sup>-</sup> most likely is directly derived from the sewage.

Many researchers have carried out experimental studies with regard to the Ca–Na ion exchange occurring during the process of sewage percolation. The results shown that the exchange occurs when the sodium absorption ratio (SAR) of sewage is more than 1.25. For the sewage of, the mean SAR is 2.39, so that the reaction in which Na<sup>+</sup> in sewage exchange the Ca<sup>2+</sup> absorbed by solid phase will happens easily. The hydrogeochemical modeling results are identical with this.

## REFERENCES

- [1] BALL, J. W., NORDSTROM, D. K., JENNE, E.A., Additional and revised thermochemical data and computer code for WATEQ2 — A computerized chemical model for trace and major element speciation and mineral equilibria of natural waters (1980).
- [2] PARKHURST D.L., PLUMMER L.N., THORSTENSON D.C., BALANCE — A computer program for calculation mass transfer for geochemical reactions in groundwater, U.S Geol. Surv. Water Resour. Invest. Report., ca 82-14 (1982).

## Appendix VI

### **$\delta^2\text{H}$ , $\delta^{18}\text{O}$ , $^3\text{H}$ , AND GRAVIMETRIC WATER CONTENT DATA FOR BOREHOLE B01, SHIJIAZHUANG CITY, CHINA, 2001**

Sample No.	Depth	$\delta^2\text{H}$ (‰)	$\delta^{18}\text{O}$ (‰)	$^3\text{H}$ (TU)	Water Content (%)
1	1	-55.08	-4.90	16.37	12.4
2	1.6	-56.36	-5.00	16.80	15.3
3	1.9	-66.33	-6.19	17.63	16.6
4	2.5	-54.07	-6.17	14.86	16.3
5	2.9	-58.41	-5.97	13.97	22.3
6	3.3	-66.02	-6.80	15.76	17.4
7	4.0	-48.56	-5.77	20.78	8.5
8	4.6	-68.61	-6.40	14.51	8.5
9	5.5	-67.90	-7.04	22.52	8.7
10	5.8	-64.19	-6.37	20.98	9.8
11	7.1	-66.62	-7.14	21.89	22.7
12	7.4	-64.20	-6.64	23.87	24.1
13	7.7	-70.35	-7.15	24.81	5.8
14	8.1	-58.37	-6.96	14.90	6.3
15	8.7	-66.06	-7.68	32.83	6.5
16	9.4	-68.24	-6.91	18.82	7.1
17	9.9	-63.26	-7.24	11.05	4.0
18	11.0	-66.2	-7.08	21.09	5.0
19	11.4	-56.74	-6.82	14.78	3.7
20	11.7	-67.05	-7.09	20.71	26.4
21	12.1	-67.10	-7.13	15.72	24.7
22	12.9	-66.30	-7.33	23.82	9.4
23	14.3	-59.83	-7.18	16.70	3.6
24	14.9	-64.10	-7.37	15.36	6.4
25	16.8	-62.14	-6.12	17.76	2.2
26	17.1	-61.15	-7.53	13.28	2.2

## Appendix VII

### **$\delta^2\text{H}$ , $\delta^{18}\text{O}$ , $^3\text{H}$ , AND GRAVIMETRIC WATER CONTENT DATA FOR BOREHOLE B02, SHIJIAZHANG CITY, CHINA, 2002**

Sample No.	Depth (m)	$\delta^2\text{H}$ (‰)	$\delta^{18}\text{O}$ (‰)	$^3\text{H}$ (TU)	Water Content (%)
1	0.5	-54.07	-5.01	15.22	9
2	1.5	-58.24	-6.24	15.55	5
3	2.5	-57.25	-5.96	17.38	21
4	3.5	-47.26	-5.79	14.22	14
5	4.5	-48.17	-6.49	14.46	11
6	5.0	-52.45	-7.08	15.34	23
7	5.5	-54.98	-6.28	19.25	15
8	6.0	-51.03	-6.29	15.21	4
9	6.5	-57.24	-7.15	15.96	3.9
10	7.0	-50.04	-6.96	16.78	3.8
11	7.5	-55.05	-6.24	18.46	3.8
12	8.0	-66.78	-6.98	19.54	2.5
13	8.5	-68.54	-7.05	16.59	2.5
14	9.0	-64.16	-7.00	18.46	2.5
15	9.5	-66.20	6.53	15.82	19
16	10.0	-60.59	-7.21	19.38	21
17	10.5	-61.46	-7.45	19.99	5
18	11.0	-64.58	-7.08	14.31	22
19	11.5	-56.85	-6.94	15.86	22
20	12.0	-67.06	-6.03	20.38	24
21	12.5	-67.50	-7.22	21.79	15
22	13.0	-64.27	-7.14	24.14	10
23	13.5	-58.28	-7.00	18.31	5
24	14.0	-57.96	-7.43	20.76	5.5
25	14.5	-66.89	-6.57	21.45	4.6
26	15.0	-59.43	-7.33	19.32	4.8
27	15.5	-65.10	-7.29	32.98	4.5
28	16.0	-62.13	-7.12	23.46	2.0
29	16.5	-61.15	-7.21	28.05	2.5

### Appendix VIII

#### CHEMICAL ANALYSES OF WATER EXTRACTS FROM THE BOREHOLE B02, SHIJIAZHANG CITY, CHINA, 2002

Sample No.	Depth (m)	TDS (mg/ kg)	Cl <sup>-</sup> (mg/kg)	NO <sub>3</sub> <sup>-</sup> (mg/kg)	NO <sub>2</sub> <sup>-</sup> (mg/kg)	NH <sub>4</sub> <sup>+</sup> (mg/kg)
1	0.5	700	1.10	50.2	6.3	6.5
2	1.5	880	2.20	43.1	0.7	5.9
3	2.5	1808	18.16	195.4	11.5	6.1
4	3.5	1121	10.35	68.2	3.1	6.2
5	4.5	882	4.15	32.6	1.9	5.8
6	5.0	1078	6.01	49.2	1.9	5.6
7	5.5	1025	3.68	62.9	3.6	5.7
8	6.0	452	2.79	20.7	0.2	5.3
9	6.5	407	2.45	21.2	0.1	4.7
10	7.0	425	3.34	18.8	0.2	4.5
11	7.5	410	1.56	15.1	0.2	4.3
12	8.0	545	3.34	14.6	0.1	4.1
13	8.5	457	2.22	14.5	0.1	4.6
14	9.0	473	1.45	13.8	0.1	4.6
15	9.5	505	6.35	76.0	5.4	5.4
16	10.0	998	7.51	59.2	3.1	7.8
17	10.5	649	5.94	21.3	1.5	7.5
18	11.0	706	6.90	52.6	2.5	7.2
19	11.5	628	6.91	75.8	4.0	8.3
20	12.0	756	7.86	75.2	6.1	9.5
21	12.5	701	4.68	44.9	1.9	9.4
22	13.0	604	4.46	20.3	0.7	9.3
23	13.5	404	3.33	19.6	0.9	7.1
24	14.0	379	2.23	15.0	0.6	6.8
25	14.5	509	2.22	19.4	0.4	6.4
26	15.0	785	2.90	23.3	0.3	6.8
27	15.5	507	2.00	14.7	0.3	7.1
28	16.0	509	2.00	14.6	0.1	7.3
29	16.5	425	1.67	15.2	0.1	7.6

## Appendix IX

### **$\delta^2\text{H}$ , $\delta^{18}\text{O}$ , $^3\text{H}$ , AND GRAVIMETRIC WATER CONTENT DATA FOR BOREHOLE B03, SHIJIAZHANG CITY, CHINA, 2003**

Sample No.	Depth (m)	$\delta^2\text{H}(\text{‰})$	$\delta^{18}\text{O}(\text{‰})$	$^3\text{H}$ (TU)	Water Content (%)
1	-0.5	-56.09	-6.37	16.79	10
2	-1	-57.83	-6.38	16.33	9
3	-2.5	-54.6	-6.2	16.34	12
4	-3	-44.2	-5.97	16.38	15
5	-3.5	-46.5	-6.21	14.29	17
6	-4	-47.45	-5.37	14.2	20
7	-4.5	-53.46	-6.82	15.34	26
8	-5	-55.19	-6.84	15.68	19
9	-5.5	-53.78	-6.25	16.19	9
10	-6	-56.42	-7.21	15.54	16
11	-6.5	-53.4	-6.24	15.17	17
12	-6.9	-56.32	-6.89	16.04	21
13	-7.5	-62.41	-6.26	16.38	15
14	-8.2	-67.35	-6.57	17.21	14
15	-8.6	-67.56	-6.59	17.34	12
16	-9	-65.27	-7.03	17.29	14
17	-9.6	-62.12	-7.06	16.3	19
18	-9.9	-61.73	-6.91	16.23	9
19	-10.5	-61.9	-7.21	17.12	19
20	-11	-67.57	-6.09	20.55	16
21	-11.5	-59.24	-6.43	21.7	17
22	-12	-58.75	-6.45	23.83	7
23	-12.6	-63.79	-7.2	24.79	12
24	-13.1	-66.74	-7.28	18.18	10
25	-13.6	-58.73	-7.39	20.97	9
26	-14.3	-59.25	-7.54	24.4	7
27	-15	-64.7	-7.19	24.9	5
28	-16	-65.25	-7.55	25.2	7
29	-16.6	-63.74	-7.56	26.3	7
30	-17	-62.13	-7.38	27.9	7

## Appendix X

### NITRATE CONCENTRATION AND $\delta^{15}\text{N}$ COMPOSITION OF WATER FROM SELECTED WELLS, SHIJIAZHUANG CITY, CHINA, 2004

Sample No.	Location	$\text{NO}_3^-$ (mg/L)	$\delta^{15}\text{N}$ (‰)
1	Dongpingle	19.3	+3.654
2	Xibaizhuang	13.5	+2.265
3	Caocun	56.8	+7.136
4	Quyongqiao	47.9	+7.226
5	Angu	43.3	+6.416
10	Zilaishui	22.3	+7.430
12	Beiguan	147.6	+4.223
14	Shilipu	42.6	+5.677
15	Xizhaotong	20.7	+5.407
16	Takou	34.9	+3.965
17	Xiaomazhuang	42.7	+5.185
22	Chengjiaozhuang	95.6	+11.043
23	Erjianyu	77.7	+7.096
24	Pijiuchang	39.4	+4.826
26	Zhenzhichang	114.3	+7.546
30	Nangaoying	65.7	+8.017
31	Huaidi	71.2	+7.480
33	Dongliangxiang	99.7	+2.365
35	Huafeichang	42.1	+6.006
36	Nangaoji	44.9	+2.162
37	Gongjiazhuang	44.5	+6.200
41	Hengshan	60.7	+11.666
42	Shangzhuang	113.6	+5.380
43	Datan	79.3	+2.164
44	Yanchang	77.4	+11.430
45	Dieryinranchang	78.2	+8.904
46	Fangbei	99.1	+7.110
47	Liucun	14.9	+5.865

## Appendix XI

### NITRATE CONCENTRATIONS AND $\delta^{15}\text{N}$ COMPOSITION WITH DEPTH IN SELECTED PROFILES, SHIJIAZHUANG CITY, CHINA

Profile 1 (cotton field fertilized with manure)				Profile 2 (wheat field fertilized with chemical fertilizer)			
Depth (m)	Lithology	$\text{NO}_3^-$ (mg/L)	$\delta^{15}\text{N}$ (‰)	Depth (m)	Lithology	$\text{NO}_3^-$ (mg/L)	$\delta^{15}\text{N}$ (‰)
0	Soil	165.1	13.2	0	Soil	197.4	4.4
0.5	Soil	162.3	12.8	0.5	Soil	185.2	4.5
1.0	Clay	154.2	13.5	1.0	Clayey loam	197.3	4.7
1.5	Clay	148.4	12.6	1.5	Clayey loam	197.1	4.5
2.0	Sub-sandy soil	132.1	11.2	2.0	Sub-sandy soil	165.9	4.0
2.5	Sub-sandy soil	100.5	11.3	2.5	Sub-sandy soil	161.2	3.9
3.0	Clayey loam	112.7	12.7	3.0	Clay	173.1	4.4
3.5	Clayey loam	121.3	13.1	3.5	Clay	182.4	4.2
4.0	Clayey loam	121.4	12.4	4.0	Sub-sandy soil	161.6	4.7
4.5	Clayey loam	105.2	11.8	4.5	Clayey loam	165.4	3.9
Profile 3 (natural soil)				Profile 4 (corn field irrigated with sewage)			
Depth (m)	Lithology	$\text{NO}_3^-$ (mg/L)	$\delta^{15}\text{N}$ (‰)	Depth (m)	Lithology	$\text{NO}_3^-$ (mg/L)	$\delta^{15}\text{N}$ (‰)
0	Soil	56.3	2.3	0	Soil	74.5	8.7
0.5	Soil	54.5	1.8	0.5	Soil	72.3	8.5
1.0	Clayey loam	62.4	1.9	1.0	Clay	74.5	8.6
1.5	Clayey loam	61.8	2.3	1.5	Clay	72.6	8.4
2.0	Sub-sandy soil	58.9	2.1	2.0	Sub-sandy soil	68.3	7.9
2.5	Clayey loam	58.2	1.8	2.5	Clayey loam	71.5	7.8
3.0	Silt	50.3	1.6	3.0	Sub-sandy soil	65.4	8.4
3.5	Clayey loam	52.9	2.5	3.5	Sub-sandy soil	69.7	8.1
4.0	Clay	54.6	2.1	4.0	Silt	64.5	8.6
4.5	Clay	55.4	2.2	4.5	Sub-sandy soil	69.5	8.5
Profile 5 (wheat field irrigated with sewage)				Profile 6 (corn field fertilized with chemical fertilizer)			
Depth (m)	Lithology	$\text{NO}_3^-$ (mg/L)	$\delta^{15}\text{N}$ (‰)	Depth (m)	Lithology	$\text{NO}_3^-$ (mg/L)	$\delta^{15}\text{N}$ (‰)
0	Soil	85.6	8.5	0	Soil	186.4	4.3
0.5	Soil	82.3	8.4	0.5	Soil	187.6	4.4
1.0	Clayey loam	78.9	8.6	1.0	Clay	196.3	4.6
1.5	Clay	87.5	8.7	1.5	Clayey loam	192.5	4.2
2.0	Clay	87.1	8.6	2.0	Sub-sandy soil	171.8	4.0
2.5	Sub-sandy soil	76.7	8.0	2.5	Sub-sandy soil	170.4	3.9
3.0	Clayey loam	74.6	7.0	3.0	Clay	179.7	4.2

3.5	Clayey loam	72.3	7.3	3.5	Clay	176.1	4.2
4.0	Clayey loam	73.4	7.8	4.0	Sub-sandy soil	163.4	4.0
4.5	Clayey loam	70.3	8.3	4.5	Sub-sandy soil	164.7	3.8
5.0	Clayey loam	69.2	7.1	5.0	Clayey loam	170.2	3.7

Profile 7  
(natural soil area)

Depth (m)	Lithology	NO <sub>3</sub> <sup>-</sup> (mg/L)	δ <sup>15</sup> N (‰)
0	Soil	62.3	2.1
0.5	Soil	62.6	2.0
1.0	Clay	64.1	1.8
1.5	Clay	64.9	1.9
2.0	Sub-sandy soil	60.2	1.7
2.5	Clayey loam	62.1	1.8
3.0	Silt	60.0	1.6
3.5	Clayey loam	55.3	1.7
4.0	Clayey loam	54.5	1.7
4.5	Clayey loam	52.1	1.5
5.0	Clay	56.3	1.8

## Appendix XII

### CFC ANALYSES OF WATER FROM WELLS, SHIJIAZHUANG CITY, CHINA, 2002

CFC determinations on samples collected from wells in Shijiazhuang City in 2002 are listed in Table XII-1. Using the software developed by the Isotope Hydrology Laboratory of the IAEA, the recharge date of the groundwater has been calculated. From Table XII-1, it appears that the CFC-113 data provide a more useful estimate of the recharge date of the investigated groundwater. We can see for most groundwater samples in the Table the recharge date is after 1985. If the mean thickness of unsaturated zone is 17 m a little before 1985, the recharge rate must be around 1 m/a. This also gives us an important evidence to show why there is no tritium peak in the profiles of boreholes B01 and B02 represents the real residue bomb-peak tritium.

Note that in the calculation of groundwater recharge date in Table XII-1, the lag of CFCs diffusion through the unsaturated zone as a gas is not considered. But according to previous study, when the thickness of unsaturated zone is more than 10 m, CFCs diffusion through the unsaturated zone is lagged, and when the thickness of unsaturated zone is about 30 m, the calculated groundwater recharge age without considering the lag of CFCs diffusion may be 7 years older than the real age. The mean thickness of unsaturated zone is about 17 m a little before 1985 in Shijiazhuang city, so the real groundwater recharge date may be several years older than that in Table XII-1.

TABLE XII-1. CFC'S RESULTS OF SELECTED WELLS IN SHIJIAZHUANG CITY, CHINA, 2002

Sample	Concentration (pmol/kg)			Apparent recharge date (PFM)			Remarks
	CFC-11	CFC-12	CFC-113	CFC-11	CFC-12	CFC-113	
1	C <sup>a</sup>	C	0.51	C	C	M <sup>b</sup>	Sample contaminated by CFC-11 and CFC-12. CFC-113 indicates modern water (Age=0).
2	C	9.25	3.69	C	C	C	Sample contaminated by all three CFCs. Dating impossible.
3	4.57	8	0.37	1987	C	1988	Suggested recharge date 1987.
4	3.76	1.91	0.27	1983	1984	1986	This sample may have some old water contribution.
5	C	C	C	C	C	C	Sample contaminated by all three CFCs. Dating impossible.
6	C	C	C	C	C	C	Sample contaminated by all three CFCs. Dating impossible.
7	C	2.48	0.38	C	1990	1989	Suggested recharge date 1989.
8	4.92	1.73	0.36	1989	1984	1988	Most probably this is a mixture having old water contribution and the sample is slightly contaminated by CFC-11.
9	C	C	0.31	C	C	1987	Suggested recharge date 1987 based on CFC-113.
10	9.52	1.8	0.24	C	1983	1985	Most probably this is a mixture having old water contribution and the sample is contaminated by CFC-11.
11	C	3.04	0.39	C	C	1989	Suggested recharge date 1989 based on CFC-113.

12	7.69	2.5	0.34	C	1990	1988	Suggested recharge date 1988.
13	4.76	2.46	0.31	1988	1990	1987	Suggested recharge date 1987.
	C	2.19	0.37	C	1987	1989	Suggested recharge date 1987.
15	4.08	1.85	0.28	1985	1983	1986	Suggested recharge date 1985.
16	8.36	1.46	0.25	C	1979	1985	Old water contribution in this sample seems to be higher.
17	5.06	1.81	0.29	1990	1983	1987	See remarks for Sample 8.

<sup>a</sup> C: contaminated.

<sup>b</sup> M: Modern water (Age=0).

# REGULATION FUNCTION OF THE UNSATURATED ZONE ON DISCHARGE AND THE EXPORT OF INORGANIC AGROCHEMICALS FROM ARABLE LANDS IN SOUTH GERMANY

K.-P. SEILER, W. STICHLER

GSF, National Research Centre, Neuherberg, Germany

## ABSTRACT

A representative experimental site has been equipped in Bavaria/Germany to study scale related flow and contamination pathways in the unsaturated zone of Tertiary sands/gravels and Quaternary loess. In these sediments both preferential- and matrix-flow occur and preferential-flow produces interflow. Deuterium tracer experiments show that preferential-flow velocities exceed 0.5 m/day, in contrast matrix-flow was 0.7 m/year in Loess, 1.2 m/year in Tertiary sands/gravels and 2 m/year in Quaternary gravels. Preferential-flow penetrates to depths of less than 1.5 m b.g. in fine grained sands and more than 3 m b.g. in gravels before it either incorporates into matrix-flow or generates interflow in hilly areas. Preferential-flow depends upon geologic, biologic, pedologic, and in arable lands, also on anthropogenic factors; since these factors underlie seasonal variations. Interflow also has a seasonal characteristic with low and high mean residence times during the year. In hilly terrains, preferential- and inter-flow favours the export of agrochemicals especially from the effective root zone; in contrast, in flat lands preferential-flow accelerates the input of agrochemicals to groundwater. From hydrograph, chemical and environmental isotope analysis, as well as from tracing percolation water in the study area, an average of 21% of infiltration produces inter-flow and about 75% groundwater recharge; only 4% discharges as overland-flow. In the study area, the partitioning of overland- and inter-flow is significantly influenced by ploughing techniques and the field sizes. Groundwater recharge is not measurably changed by these factors. Interflow pathways also transport DOC, which strongly favours the export of agrochemicals. Since DOC forms large "molecules", it is subject to mechanical filtering, and thus follows wide preferential flow paths during interflow. Because DOC has a high sorption capacity, it can promote exportation of many agrochemicals during storm events through direct discharge to surface water. Hence, while interflow and DOC may reduce the potential for groundwater contamination, it may also cause contamination pulses to reach surface waters.

## 1. INTRODUCTION

The unsaturated zone between the land and groundwater surface acts to regulate discharges and the fate of contaminants on the way to adjacent water resources. At the interface atmosphere/lithosphere, precipitation turns into overland-flow, infiltrates into the subsurface, or evaporates. The infiltrate is either stored for transpiration or discharges downward or laterally to neighbouring groundwater and surface compartments. Hence, discharge on continents is made up of four components (Fig. 1)

- Evapotranspiration
- Overland-flow
- Interflow
- Groundwater recharge.

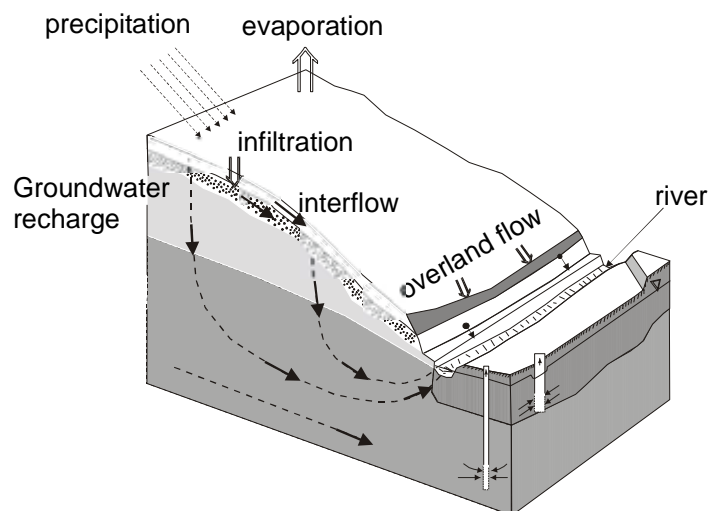


FIG. 1. Block diagram of a landscape with the four most important discharge components.

Overland flow, interflow, and groundwater recharge transport pollutants either as dissolved or particle bound phases and may result in adverse impacts on surface and groundwater quality. The main pools of contaminants are releases from waste disposals, traffic, industrial and urban areas, as well as agrochemicals from arable lands.

Porous media often exhibit a variety of small scale heterogeneities, such as cracks, macropores, interaggregate pores, and destruction features from humans, animals and plants. They all may affect water, particle and solute movement at the macroscopic level by creating widely different flow-velocities, often referred to as slow matrix [1, 2] and fast preferential-flow [3, 4, 5]. They may also create changes of flow directions from downward to lateral [14]. These phenomena have been studied in the past in structured [5] and seemingly homogeneous coarse-textured soils/sediments [6, 7].

Fast-flow in the unsaturated zone also leads to an apparent disequilibrium situation with respect to the pressure head or the distribution of solute concentrations and thus severely limits our ability to define initial boundary conditions to simulate flow and to reliably forecast contaminant transport in unsaturated media.

Preferential-flow was first recognized at the end of the 19th century, but has never been systematically defined (see below) or quantified. It interacts with matrix-flow by means of diffusion and incorporation (mostly into the matrix water) or produces inter-flow in hilly terrains [13, 14, and 19]. However, it is not well understood

- How much of the infiltrating water contributes to preferential-flow?
- What is its penetration depth, and how is it affected by the types of sediments and the intensity of the infiltration process?
- How much is the interaction of preferential- and matrix-flow governed by the changing array of capillary water and surface tensions?
- What is the export potential of the discharge components for agrochemicals?

To answer some of these questions, an experimental field (Fig. 2) has been set up in south Germany (Bavaria, Scheyern) with facilities to perform and evaluate small scale tracer experiments with non-reactive tracers; these results have been compared with large scale hydrograph, chemical and environmental isotope discharge analysis, with monitoring results of contaminants in agro-pools, and the changing chemical composition of brook, spring, and groundwater as a response on precipitation input and land use.



FIG. 2. Hydro-geological observation stations at the test site of the Research Station Scheyern and the areas with organic and integrated farming activities during the investigation time (1992-2001).

## 2. RESEARCH AREA

The Research Station Scheyern (Fig. 2) is located in the central part of south Bavaria, Germany. In this area Tertiary and Pleistocene sediments crop out. Tertiary sediments have been deposited by a limno-fluvial run-off system in the late Tertiary time; they developed with grain sizes ranging from clay to fine grained gravels, are horizontally layered and have the typical fabrics of fluvial sediments; sediment and hydraulic conductivity changes are always quite abrupt in this sequence. During the Pleistocene, loess accumulated on east sloping hills to a thickness of 2 m [15] on Tertiary sediments, permafrost changed fabrics of Tertiary and Quaternary sediments close to the surface and frost-thaw avalanches characterize hill slopes.

The regional groundwater level was found at 450m asl or at 2–24 m below the test site surface; therefore, in the study area regional groundwater does not contribute to the actual surface run-off. However, some perched groundwater develops temporarily or constantly upon local clay lenses. Perched groundwater contributes basically to the base-flow of brooks as well as to perennial and sporadic springs and drains.

The previous conventional farming and landscape management (before 1990) was completely changed in 1992/1993 and systematic chemical surface and subsurface water monitoring begun in 1994 [16]. At the Research Station Scheyern, mineral phosphorous fertilizer has not been applied since 1989, because of an over-P-fertilization in the antecedent years, and the application of nitrogen fertilizers in the area of integrated crop production (see below) was steered by soil-N analyses.

Two different farming systems have been established in 1992. In the south part of the research station (Fig. 2) loess sediments prevail and plant production followed the principles of an integrated crop production (ICP). Hence, a 4 years potato–wheat–maize–wheat rotation together with mulching and minimum tillage applied. In the north part (Fig. 2), where Tertiary sands/gravels dominate, crop production was carried out according to guidelines of the German Association for Organic Farming (AGÖL). The organic farming system (OF) required a diversified 7 years crop rotation with legumes, as well as intensive green manuring and extensive live stock production. In contrast to the ICP part of the research station, the OF part allowed ploughing, but there was a severe risk of nutrient losses through seepage [17].

## 3. METHODS

### 3.1. Tracing percolation water

Pairs of shaft lysimeters (Fig. 3) have been constructed along the border line of two to four fields by digging vertical shafts of 2.5 m depth and 5 m distant from one another. From these shafts 5 m slightly inclined drills have been placed in three replicates at 10 cm, 20 cm, 50 cm, 90 cm, 130 cm and 180 cm below ground to the different fields, in order to install probes in the sediment/soil at the end of each open end full tube drill:

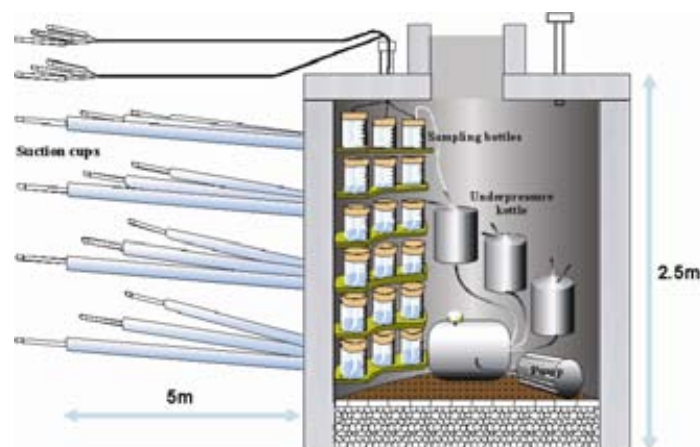


FIG. 3. Design of a natural lysimeter with suction cups, which were located 5m away from the shaft wall in the unsaturated zone. At each depth three replicates have been installed at distances of 50 cm.

- In one shaft lysimeter suction cups for continuous water sampling from the unsaturated zone, and
- In the neighbouring shaft lysimeter TDRs, thermometers and tensiometers have been placed, to control the changing hydraulic properties of the unsaturated zone.

### 3.2. Inter-flow

Often tracer experiments are performed using the sorbing tracer brilliant blue FCF to colour percolation flow paths and to visualize any fingering of flow by excavating the propagation front of this tracer: This fingering has been named preferential-flow [12], but could also be attributed to an inhomogeneous matrix-flow. Thus, it becomes clear that a reliable out-sourcing of matrix and preferential-flow is needed, which is not an easy task [20]. In this paper we call preferential all percolation flow velocities exceeding the slow matrix flow by at least two orders of magnitude.

Inter-flow occurs as saturated and close to saturation flow. It represents a quick subsurface run-off, which parallels morphology and originates from fast preferential-flow; the change from preferential vertical down to lateral flow (inter-flow) happens along inclined hydraulic discontinuities, paralleling morphology. Such hydraulic discontinuities occur natural and man made:

- Natural discontinuities are related to:
  - The remnants of permafrost, which changed sediment fabrics and produced fossil hill slides,
  - The decompression of rocks according to a change from a tri-axial state of stress in depth to an one-axial stress at the land surface, which favours rock/sediment physical disintegration, followed by chemical weathering,
  - The deposition of aeolian sediments, and
  - Bioactivities in the effective root zone.
- Humans add such discontinuities by:
  - Ploughing agro-lands, and
  - Earth movements.

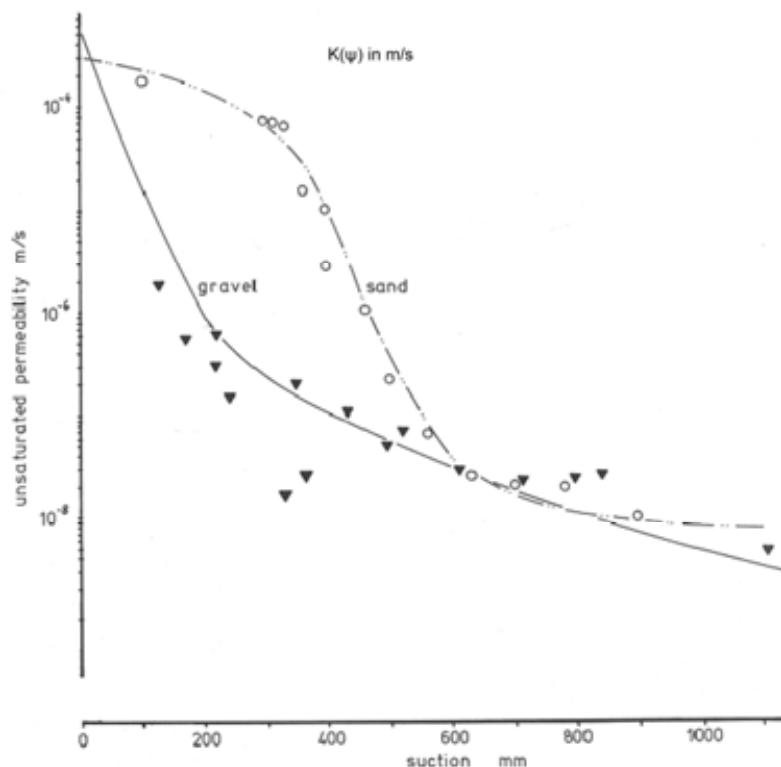


FIG. 4. Hydraulic functions of an unsaturated gravel and sand, measured under laboratory conditions.

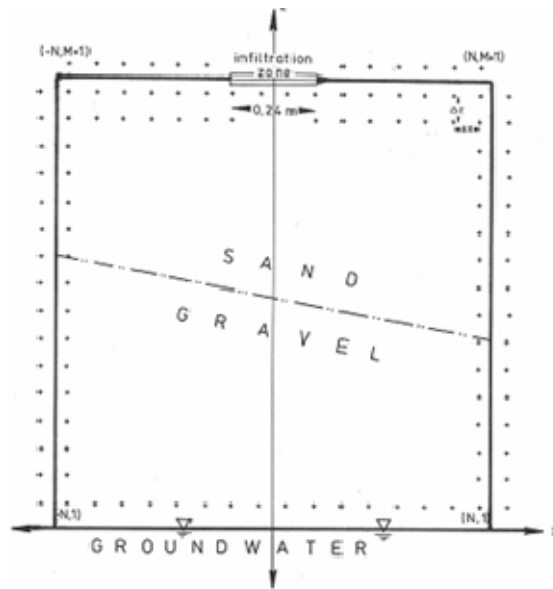


FIG. 5. The model plan with an inclined interface between sands and gravels.

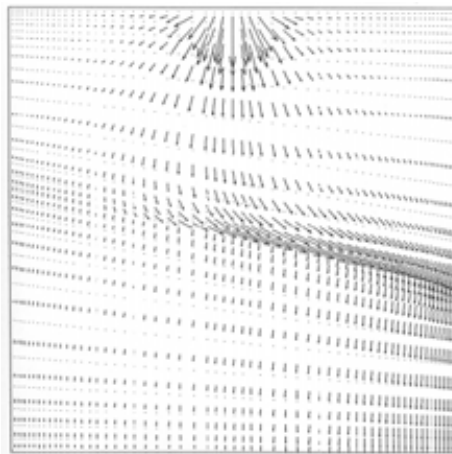


FIG. 6. Flow vectors showing the role of the interface between sands and gravels at an infiltration of 50 mm/day. Infiltration is of line type as in the case of river-infiltration.

Hydraulic discontinuities behave under special boundary conditions like capillary barriers, turning flow along hydraulic discontinuities from vertical down into lateral [13, 14]. As an example, Fig. 4 presents the  $K(\psi)$ -suction function for a gravel and a sand, measured in laboratory experiments, and shows that hydraulic conductivities reach in a certain suction range lower values in gravels than in sands; in the special case of Fig. 4 at suctions  $<100$  mm respectively.  $>600$  mm hydraulic conductivities of the unsaturated sand and gravel do not differ; hence, the inclined interface between sand and gravel (Fig. 5) does not act as a hydraulic barrier; however, between these two suctions significant differences in hydraulic conductivities exist (Fig. 4), thus producing interflow along the inclined interface between sands and gravels (Fig. 6); hence, the functioning of this interface as a capillary barrier cannot be considered as constant [14]; it varies according to changes in hydraulic functions with seasons, with time and input conditions as well.

### 3.3. Hydrograph separation

Water fluxes produced by precipitation in excess of evapotranspiration (Fig. 1) move rather quickly as overland-flow or inter-flow to surface water, but rather slowly down to groundwater (matrix-flow) (section 4). Overland- and inter-flow are usually summed as the direct run-off response to precipitation events, superimposing base-flow from groundwater reservoirs (indirect response).

There exist well established methods in separating discharge components applying either hydrograph [9] or chemical/environmental isotope methods [18, 10], but both these methods, often refer only to two and not multi-component systems and are based on quite different assumptions; therefore these methods do not lead to comparable results:

- Hydrograph methods distinguish between quick and slow discharge;
- Chemical/environmental isotope methods between event and prevent water.

The discharge analysis to quantify inter-flow in rivers is best performed using chemical/environmental tracers in combination with hydrograph methods. By definition, environmental tracer based discharge analysis results in the determination of one component without (precipitation) and one from subsurface water (Fig. 7). Among the run-off components only overland-flow had no contact with subsurface water; in contrast, inter-flow and base-flow had. Therefore environmental tracers allow as a good approximation to separate the sum of inter-flow ( $Q_I$ ) and base-flow ( $Q_G$ ) from overland-flow ( $Q_O$ ).

$$Q = (Q_G + Q_I) + Q_O \quad (1)$$

and hydrograph methods differentiate between slow ( $Q_G$ ) and quick run-off components ( $Q_I + Q_O$ )

$$Q = Q_G + (Q_I + Q_O) \quad (2)$$

Combining both equations allows approximating inter-flow.

Fig. 7 presents one of many examples of a sampled discharge event in the experimental area, showing that consecutive storm events produce quite different responses on the field sites:

- A first and second storm event produced strong and similar responses on both fields,
- But during a third storm event only acre 16 showed a respective  $\delta^{18}\text{O}$  decline, missing from observations in the surface run-off (inter- and overland-flow) of acre 18.

Hence, for the first and second rain event the contribution of pre-event water to the run-off is small, however, it is large for acre 18 during the third rain event.

## 4. RESULTS

### 4.1. Flow velocities in the unsaturated zone

Tracing the melting snow cover produces an initial Dirac signal along the infiltration front. As far as percolation was homogeneous this Dirac signal produced a Gauss-distribution of concentrations at defined time steps all over the profile; this, however, has never been observed in all tracer experiments (Fig. 8). Obviously flow in the investigated unsaturated zones was always non-homogeneous.

It also came out from all these tracer experiments in the unsaturated zone that an instantaneous tracer signal (Dirac signal), starting at the ground surface, produces

- Always an extended tracer-break-through (TBT) response (Figs. 8, 9),
- Sometimes TBT peaks at the beginning of a tracer exercise followed by the already mentioned extended TBT (Fig. 9), or
- Followed by short-term low concentration peaks in the extended TBT; these low concentration peaks always parallel infiltration events (Fig. 9).

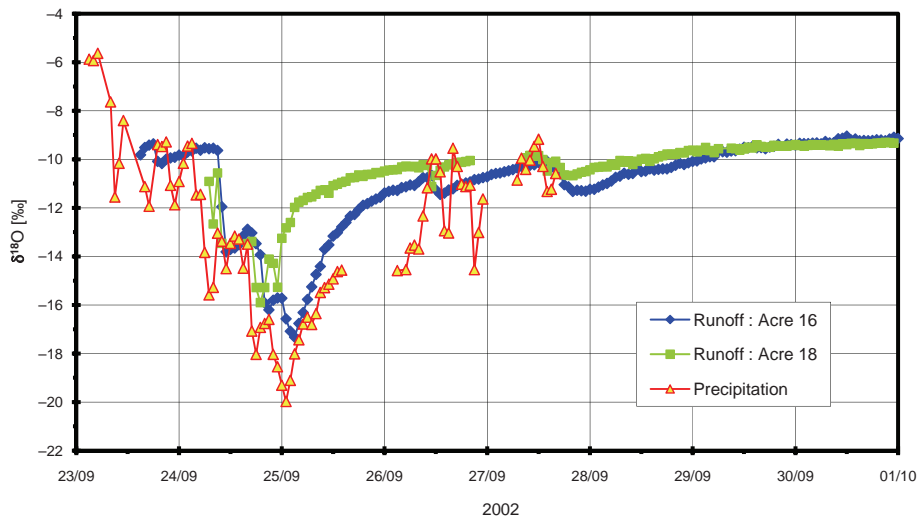


FIG. 7. Surface run-off from two fields, acre 16 and 18, as influenced by a precipitation event.

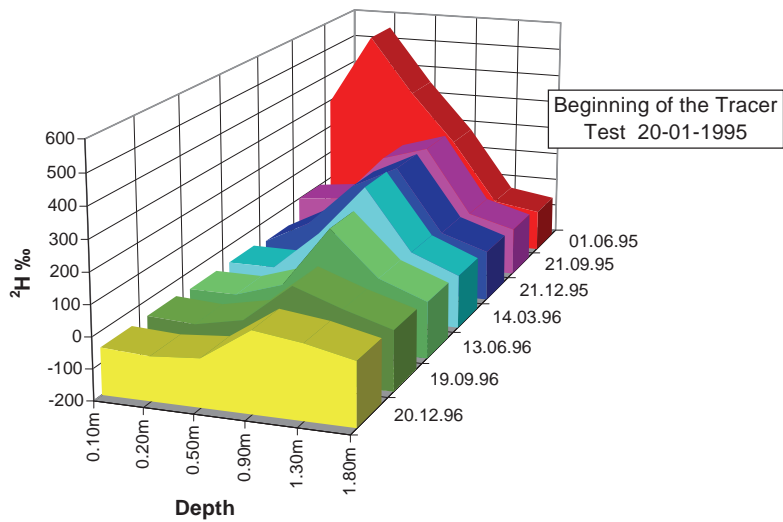


FIG. 8. Concentration distribution of  $\delta^2\text{H}$  throughout the profile at given time intervals.

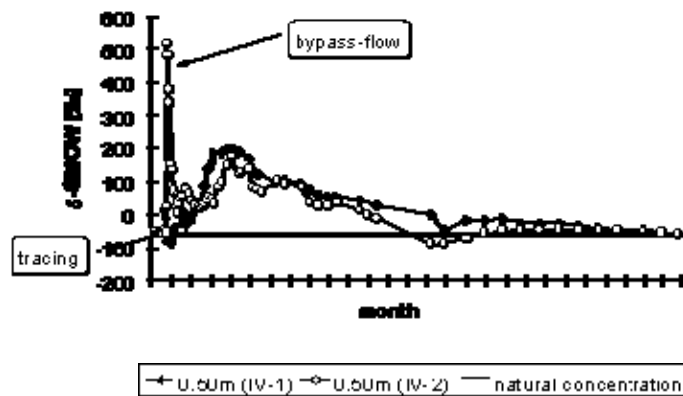


FIG. 9. Quick and slow tracer-break-through (TBT) from a tracer experiment in Quaternary loess of the Scheyern experimental site in south Germany. Deuterium ( $^2\text{H}$ ) was used as a tracer and sampling was performed continuously at two points at 0.5 m b.g. and distant of about 50cm from one another. Preferential-flow is indicated by a positive pulse at the beginning and many negative pulses during TBT in 50 cm b.g. at the position IV-2. Tracing started in 2000.

The single short-term high and the many short-term low concentration peaks in the extended TBT (Fig. 9) indicate preferential-flow, increasing respectively diluting as a flux-pulse the prevailing tracer concentration in the unsaturated zone.

The evaluation of TBTs from one tracer exercise in replicate sampling points (Fig. 9), however, shows that short-term high or low concentration peaks appear only if very high tracer input concentrations have been applied, because preferential-fluxes are smaller in amount than matrix-fluxes (section 4.1, 4.2); hence, matrix-flow always dominates the mix of matrix- and preferential-flow; as compared to the tracer Deuterium ( $^2\text{H}$ ) concentrations should exceed the background concentration by about 10 to 20 times.

Traditional calculations of seepage velocities based on tensiometer- and TDR-observations do not allow any differentiation between slow and quick flow. Thus, the approximate calculation of percolation flow velocities ( $v$ ) using infiltration ( $R$ ) and mean water content ( $\theta$ ) applies well for matrix, but not for bypass-flow.

$$v = \frac{R}{\theta} \quad (3)$$

From all small scale tracer experiments it comes out that matrix-flow ranges in

- Loess at 0.7 m/year,
- Tertiary sands/gravels at 1.2 m/year and
- Quaternary gravels at 2 m/year.

Taking the mean water content over the period 1992–2001 and using equation 3, infiltration was calculated at

- 150 mm/ year at the Loess,
- 200 mm/year at the Tertiary and
- 300 mm/year at the Quaternary gravel site.

These numbers are in good agreement with water balance studies.

In contrast to matrix-flow, preferential-flow ranges in all studied sediments from 0.5 m/day to >2 m/day and was observable till 1 m below ground in Loess, 1.5 m in Tertiary sands/gravels and more than 3 m in coarse grained Quaternary gravels.

Considering the slow matrix flow and the thickness of the unsaturated zone, ranging from 2 to 24m, it becomes clear that the impact of any change in land use appears delayed by years to decades in groundwater resources (see below). Therefore, any early warning estimate of such changes can only be monitored in time in the effective root zone.

#### **4.2. Discharges from the study area**

The amount and mean residence time of interflow changes not only with the  $k(\psi)$ -suction function (Fig. 4), but also with the season. Analyzing repeated tracer experiments in one site shows that preferential-flow may be or may be not a reproducible phenomenon, indicating that the flow-path-way of preferential-flow is not constant in extent, position and functioning. During the vegetation period bioactivities and the mulching or ploughing of fields produces preferential flow paths with high water through put; in contrast in the non-vegetation period preferential flow paths narrow by silting and compaction, which both document in a change of mean residence times with the season (Fig. 10). This was recognized by a systematic evaluation of hydrographs, showing lower slopes for interflow in the winter as compared to the summer season; thus producing longer lasting discharge responses in winter than during summer.

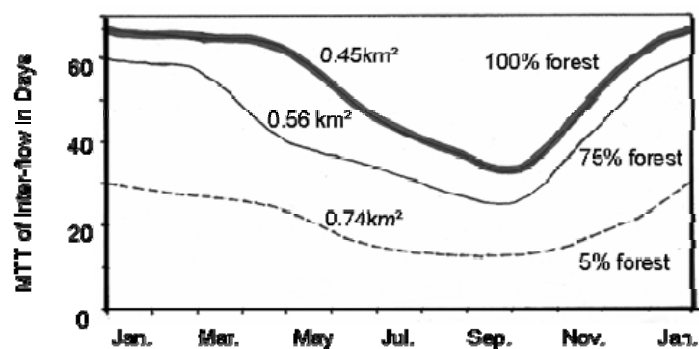


FIG. 10. The seasonal change of means residence times of interflow in the experimental site of Scheyern with 100%, 75% and 5% forest respectively 0%, 25%, 95% of arable land. MTT = mean transit time. Mean values over the run of the years 1998–2000.

As a result of field studies in the experimental watershed and adjacent catchments of 1 to 36 km<sup>2</sup> in size [18], a discharge of 200 mm/year, which is typical for Loess, will produce on an 8 year average 4% overland-flow (8 mm/year), 21% inter-flow (42 mm/year) and 75% groundwater recharge (150 mm/year).

The annual mean of 21% of inter-flow, however, can fluctuate from 0 to 60% in individual infiltration events, depending on the water content or suction conditions along the atmosphere/ lithosphere interface and within the effective root zone, and the intensity, duration and quantity of rain events as well. From detailed observations [18] it was found that only precipitation exceeding 2–4 mm/day produce overland and inter-flow, and that inter-flow becomes strongest under very wet and very dry moisture conditions and is less pronounced in between these two extremes.

Moving from the Loess to the Tertiary sands/gravels, direct run-off diminishes and groundwater recharge increases respectively; in the Quaternary gravels no direct run-off is produced.

In contrast, the partitioning of overland- and inter-flow depends significantly from the crop, the season and human activities, specially ploughing or mulching. This changing partitioning had no measurable influence on the amount of groundwater recharge in the study area.

#### 4.3. Co-transport of agrochemicals by preferential-flow and inter-flow

It is often observed in hilly terrains that concentrations and loads of DOC and agrochemicals increase in river discharges following rain events. Therefore, DOC in the soil solution of the effective root zone

and in discharge events has been monitored. Typical yearly means and standard deviations of concentrations of DOC in soil solutions out of Loess and Tertiary sands/gavels are plotted in Fig. 1. As can be seen by the data, within the effective rote zone DOC well exceeds 2 to 4 mg/L carbon. The groundwater of the same area, however, has <2 mg/L. This is due mainly to mechanical filtering of the “DOC molecule” and microbial metabolisms of DOC.

Since macro-pores play an important role in the effective root zone and are mostly missing in the unsaturated zone beneath, they favour mechanical DOC filtering and accumulation as well. During rain events DOC-concentrations increase (Fig. 12); this increase is proportional to the amount of discharge, higher in forest areas than in arable lands of the study area and concentration always exceeding those beneath 100 cm b.g. (Fig.11). Obviously, DOC is mainly leached from the effective root zone (0–100 cm b.g.), which is also an important source area of preferential- and inter-flow.

Either the DOC production is stronger in forest than arable lands, or the effective root zone of arable lands is more leached than in forest areas.

In addition to DOC, high loads of nitrogen, sulphur and chloride reach surface water during discharge events. For chlorides/sulphates, loads (Fig. 13) more or less partition similarly to the flow components that contribute to run-off (section 4.2). In contrast, DOC travels to surface water preferentially within inter-flow (Fig. 13), because of the before mentioned mechanical filtering effect for the big “DOC-molecule”. Nitrogen seems to play an intermediate role (Fig. 13) in between solute chlorides/sulphates and particulate DOC. It is hypothesized that the nitrogen export starts with ammonia fixed on DOC and ammonia oxidizes on this flow path to nitrate. Monitoring of pesticides also showed an increase during discharge events, which was approximately proportional to the DOC-export. Hence, discharge events produce impacts to surface run-off through sorbing agro-chemicals, and thus contribute to groundwater protection if inter-flow develops.

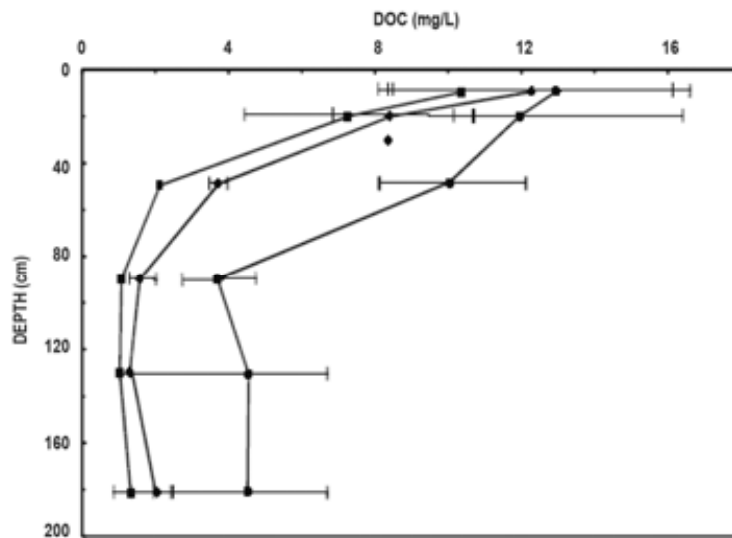


FIG. 11. DOC-concentrations in soil typical loess (right and centre) and Tertiary gravel profiles (left) in the study area. Mean values over the run of one year and standard deviations (horizontal lines).

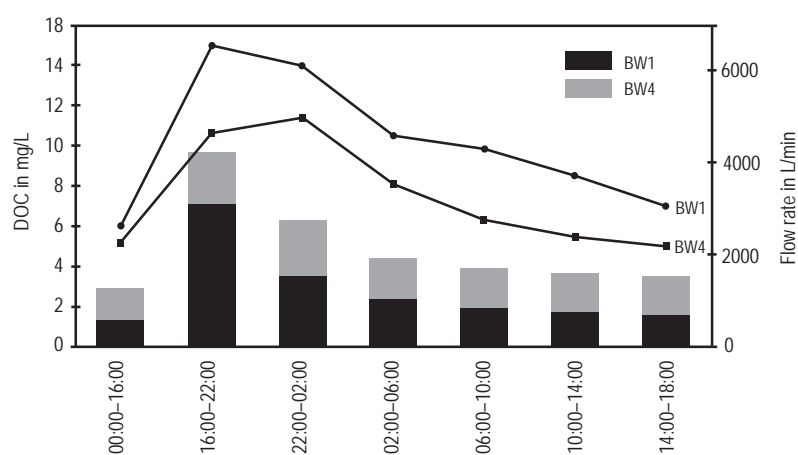


FIG. 12. Discharge (columns) and DOC-concentrations (curve) in a river during one discharge event. BW1 = 100% forested, BW2 = 60% forested and 40% arable land.

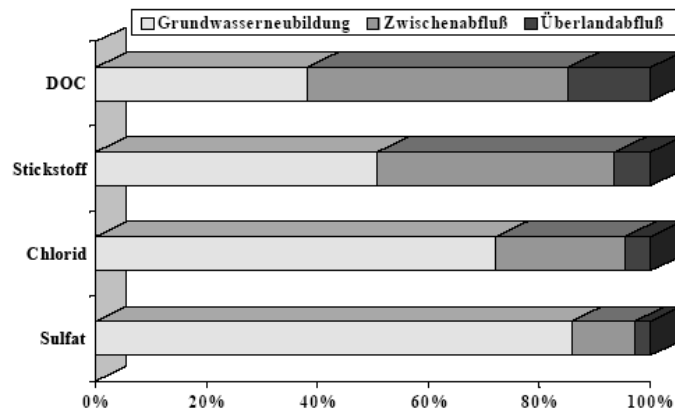


FIG. 13. The export of sulphate, chloride, nitrogen and DOC with groundwater recharge, inter-flow and overland-flow as compared to the total discharge. Mean values over the run of years 1994 to 2001.

High contaminant and nutrient concentrations in rivers and groundwater in agricultural areas have also been reported by Brown et al. (1995) [7] and Haria et al. (1994) [8]. As this export of agrochemicals was better attributed to discharge components, it was possible to efficiently contribute to the development of mathematically based strategies for soil cultivation and the application of agrochemicals. Such strategies should:

- Minimize the export of contaminants from arable land to surface and groundwater;
- Make applied agrochemicals more available for plants and better safeguard the microbial degradation capacity of the subsurface by adapting application methods of agrochemicals.

#### 4.4. Nitrate concentration in multilevel groundwater wells

Since 1992, inorganic water chemistry has been monitored in multilevel wells to assess groundwater quality. Nitrate results are presented in Fig. 14 for wells II, III, IV and V, which have been positioned along “a main flow line” in the regional aquifer. In these multi level wells, undisturbed sampling was possible meter by meter.

Tritium monitoring showed that only the 15 m of groundwater depth belongs to the active groundwater recharge zone [22], which is highly susceptible to groundwater contamination. Beneath this zone, groundwater ages increase rapidly and the susceptibility with respect to groundwater contamination becomes low; therefore this zone with high water ages was always free of agrochemicals from present and past agro-activities.

Low nitrate concentrations have been monitored all the time in the active groundwater recharge zone in the south of the experimental area (ML II), because of a forest in the upstream area of this multi-level well. From here and following groundwater flow direction nitrate concentrations increased significantly and reached concentrations of 50 mg NO<sub>3</sub><sup>-</sup>/L and more (ML IV and ML V); the same is true for chloride (data not shown) reaching 30 to 50 mg Cl<sup>-</sup>/L.

Since the beginning of a change in agricultural practice in 1992, mean nitrate concentrations decreased in all multilevel wells. This trend in multi-level-wells, however, is much weaker than in the effective root zone, because of the low matrix flow velocities in the unsaturated zone, the depth of the groundwater surface below ground (2 to 24 m b.g.) and the positioning of the fields with respect to the selected groundwater flow path.

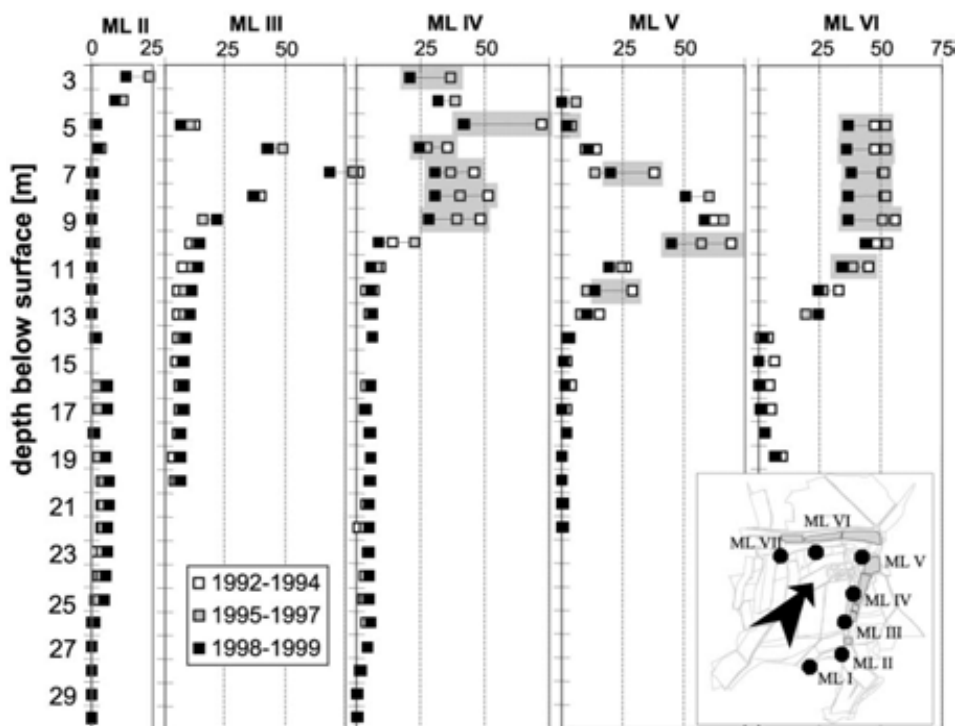


FIG. 14. Changes of nitrate concentrations ( $\text{mg NO}_3/\text{L}$ ) in five multilevel wells. Mean values of three different periods with two to five observations for each period. The map in the right corner indicates the direction of the regional groundwater flow.

#### 4.5. A comparison of two farming systems

In the integrated plant crop area (IPC) fertilizers, except P (chapter 2), and pesticides have been applied according to crop needs. In the organic farming area (OF) only manure and no pesticides have been distributed. One aspect of these different modes of farming is shown in Table 1.

TABLE 1. THE EXPORT OF INORGANIC AGROCHEMICALS BY OVERLAND-, INTER-FLOW AND GROUNDWATER RECHARGE UNDER INTEGRATED CROP PRODUCTION (ICP) AND ORGANIC FARMING (OF). MEAN VALUES OVER THE RUN OF THE YEARS 1994 TO 2001.

	N [kg/ha year]		DOC [kg/ha year]		S [kg/ha year]		Cl <sup>-</sup> [kg/ha year]	
	OF	ICP	OF	ICP	OF	ICP	OF	ICP
Overland-flow	1.4	1.7	0.9	2.1	0.5	0.9	0.4	1.0
Inter-flow	3.9	14	12	6.7	2.6	4.4	3.9	3.3
Groundwater recharge	10	11	2.3	4.9	46	28	7.5	15
Summe	16	27	15	14	49	34	12	19

The export of N and Cl is higher in the ICP than in the OF area, in contrast S- and DOC-export to neighboring water compartments is strongest in the OF area.

As shown, the N-export from ICP is linked mainly to inter-flow. This is, however, not the case in the OF area although the DOC-export from OF is much stronger than from ICP. DOC from manure and DOC from plant disintegration in soils have obviously different co-transport capabilities.

## 5. CONCLUSIONS

In the study area the partitioning of overland- and inter-flow changes with agro activities; these changes, however, do not influence groundwater recharge within the measurement accuracy. Groundwater recharge is much more governed by sediment fabrics.

Only mass transport studies contribute to distinguish clearly between preferential- and different forms of matrix-flow in the unsaturated zone; classical hydraulic observations in the unsaturated zone do not. The velocities of preferential-flow are in the same order of magnitude as overland-flow and produce in hilly terrains inter-flow with a high export potential for sorbing agrochemicals.

DOC reaches surface waters preferentially thorough interflow. Since many agrochemicals are sorbing substances and DOC has a strong sorption capacity, many agrochemicals move through particle transport. Thus, DOC export produces contaminant pulses for surface water, which simultaneously favors groundwater protection. This export potential has shorter mean residence times in the growing season than in the winter season. However, the co-transport capability of DOC depends also on the DOC origin; manure DOC co-transport less agrochemicals than plant DOC.

## REFERENCES

- [1] FEDDES, R.A., KADAT, P., VAN BAKEL, P.J.T., BRONSWYK, J.J.B., HALBERTZSMA, J., Modeling Soil Water Dynamics in the Unsaturated Zone: State of the Art, *J. Hydrol.* **100** (1988) 69–111.
- [2] HILLEL, D., Soil and Water, Acad. Press, New York, London (1971).
- [3] VAN GENUCHTEN, M. Th., “New Issues and Challenges in Soil Physics Research”, Proc. 15th World Congress of Soil Science, Acapulco, Mexico, Vol. 1, Inaugural and State of the Art Conferences (1994) 5–27.
- [4] SCOTTER, D. R., Preferential solute movement through larger soil voids, I: Some computations using simple theory, *Austr. J. Soil. Res.* **16** (1978) 257–267.
- [5] BEVEN, K., GERMAN, P., Macropores and water flow in soils, *Water Resour. Res.* **18** (1982) 1311–1325.
- [6] BAKER, R.S., HILLEL, D., “Observations of fingering behaviour during infiltration into layered soils”, Preferential-flow (GISH, T.J., SHIRMOHAMMADI, A., Eds), Am. Soc. Agricult. Engineers (1991) 87–99.
- [7] BROWN, C.D. et al., Movement of pesticides to surface waters from a heavy clay soil, *Soil Pest Sci* **43** (1995) 131–140.
- [8] HARIA A.H. et al., Water movement and isotopuron behaviour in a drained heavy clay soil: Preferential flow processes, *J. Hydrol.* **163** (1994) 203–216
- [9] NATERMANN, E., Die Linie des langjährigen Grundwassers und der Trockenwetterabflußlinie (TWL), *Die Wasserwirtschaft* **41** (1951) 12–14.
- [10] SKLASH, M.G., FARVOLDEN, R.N., FRITZ, P., A conceptual model of watershed response to rainfall, developed through the use of oxygen-18 as a natural tracer, *Can. J. Earth Science* **13** (1976) 271–283.
- [11] EICHINGER, L., SALVAMOSER, J., STICHLER, W., MERKEL, B., NEMETH, G., “Seepage Velocity Determinations in Unsaturated Quaternary Gravel”, Proc. Recent Investigations in the Zone of Aeration (1984) 303–313.
- [12] BERG, W., FANK, J., LEIS A., “Digitale Bildverarbeitung als Hilfsmittel zur Quantifizierung von bevorzugten Fließwegen in der ungesättigten Zone”, Ber. 8. Lysimetertagung, BAL Gumpenstein, Irding (1999)
- [13] BEHRENS, H., SEILER, K.-P., NEUMAIER, F., Geländeversuche mit Fluoreszens-Tracern zur Wasserbewegung im wasserungesättigten Lockergestein in den Talern der Bayerischen Alpen, *Z. dt. geol. Ges.* **131** (1980) 129–138.
- [14] SEILER, K.-P., BAKER, D., Der Einfluss der Schichtung auf die Sickerwasserbewegung bei punkt- und linienförmiger Infiltration, *Z. dt. geol. Ges.* **136** (1985) 659–672.

- [15] SCHEINOST, A., SINOWSKI, W., AUERSWALD, K., SCHWERTMANN, U., “Flächenhafte und punktverdichtete Erfassung von Bodenparametern”, Forschungsverbund Agrarökosysteme München: Abschlußbericht der Aufbauphase 1990–1992. FAM -Bericht, Vol. 3 (HANTSCHHEL, R., KAINZ, M., Eds.), GSF Research Centre, Neuherberg (1993) 37–59.
- [16] HANTSCHHEL, R., LENZ, R., “Management induced changes in agroecosystems — aims and research approach of the Munich research network on agroecosystems”, Soil and Environment: Integrated Soil and Sediment Research, A Basis for Proper Protection (EIJSSACKERS, H.J.P., HAMERS, T., Eds.), Kluwer Academic Publishing, Maastricht (1993) 142–144.
- [17] HELLMEIER, C., Stofftransport in der ungesättigten Zone unter landwirtschaftlich genutzten Flächen im Tertiärhügelland, GSF-Ber. 05/01 Neuherberg (2001) 1–170.
- [18] LOEWENSTERN v., S., Separierung und Bewertung von Abflusskomponenten für den Stoffaustrag aus Einzugsgebieten mit Tertiärsedimenten (Scheyern, Oberbayern), GSF-Ber. 7/98 Neuherberg (1998) 1–42.
- [19] SEILER, K.-P., LOEWENSTERN v., S., SCHNEIDER, S., Matrix and bypass-flow in quaternary and tertiary sediments of agricultural areas in south Germany, *Geoderma* **105** (2002) 299–306.
- [20] SEILER, K.-P., GAT J.R., Groundwater recharge from run-off, infiltration and percolation, Springer (in preparation).
- [21] SEILER, K.-P., LINDNER, W., Near surface and deep groundwater, *J. Hydrol.* **165** (1995) 33–44.

# MULTI-TRACER TECHNIQUE AND HYDRO-GEOCHEMICAL APPROACH TO ASSESS POLLUTANTS DYNAMICS IN THE UNSATURATED ZONE AT THE IARI FARM SITE, NEW DELHI, INDIA

U.P. KULKARNI, U.K. SINHA, S.V. NAVADA, U. SARAVANA KUMAR  
Isotope Hydrology Section, Isotope Applications Division,  
Bhabha Atomic Research Centre, Mumbai, India

Y.K. SUD, P.S. DATTA  
Nuclear Research Laboratory, Indian Agricultural Research Institute,  
New Delhi, India

## ABSTRACT

Soil and groundwater pollution from agricultural activity is becoming an important topic of interest worldwide as a result of the increasing public and regulatory concern on groundwater contamination and its impacts on human health and ecological systems. Contaminant behaviour in the soil, and ultimately in the groundwater is governed by coupled complex processes. Quantitative and qualitative knowledge of such processes is essential to develop optimal strategies to prevent or remedy the adverse effects of these pollutants. While considerable efforts have been made to understand pollutant dynamics in the saturated zone, very little information is available about their behaviour below root zone and up to the saturated zone. Hence, a study was carried out at the farm site of Indian Agricultural Research Institute (IARI), New Delhi to understand the pollutant dynamics and to protect the groundwater from pollution. Extensive agricultural activities were undertaken at the IARI farm for over 5–6 decades with a history of agrochemical loadings onto its soil. In order to understand the pollutant behaviour in two different conditions, two locations in the farm site was selected; one in an irrigated area and the other in a non-irrigated (rainfed) area. Soil cores were taken from these sites and the samples were analyzed for pH, EC, moisture content, major-ions and isotopes ( $^2\text{H}$ ,  $^{18}\text{O}$ ,  $^{13}\text{C}$ ). Chemical and radioisotope tracers were injected to estimate the mobility of pollutants. Results of the study are reported here. The results of analyses of soil solution, soil pore gas and the injected tracer experiments indicated that the pollutants may reach the saturated zone in the study area in 7–8 years time. The investigation also indicated absence of reducing environment in the vadose zone and decay of the plant residues in the top layers in the study area. The borehole instrumentation carried out during the investigation helped immensely in understanding the pollutant dynamics in real time mode at the study site.

## 1. INTRODUCTION

Due to the rise in human population, the demand for good quality of water for industrial, agricultural and domestic purposes is increasing tremendously over the last few decades, with groundwater being the major source. Over-exploitation of groundwater for various purposes has resulted in pollution of the groundwater resources in a few countries and hence has become a major concern as it has a direct impact on human health and ecological systems. The behaviour of contaminants in the soil and, ultimately, in the groundwater is governed by various coupled complex processes. A quantitative and qualitative assessment of such processes is essential for developing optimal strategies to prevent or remedy the adverse effects of these pollutants. While considerable efforts have been made to understand pollutant dynamics in the root zone and in the saturated zone, very little information is available about their behaviour in the unsaturated zone beneath the root zone. The study of this topic requires a multi-disciplinary approach involving physics, biology, chemistry, mathematics, geology, hydrogeology, hydrology, agriculture, soil science etc. The driving force for pollutant transport in the unsaturated zone is recharge (natural, artificial). Hence, a thorough understanding on the recharge processes is highly essential for abating groundwater pollution. Tracers (environmental, artificial) can provide an insight about the recharge processes taking place in the unsaturated zone.

Under the International Atomic Energy Agency (IAEA), Vienna, Austria funded Co-ordinated Research Project on “Isotopes in the Study of Pollutant Behaviour in Unsaturated Zone for Groundwater Protection”, environmental ( $^2\text{H}$ ,  $^{18}\text{O}$ ,  $^{13}\text{C}$ ) and artificial ( $\text{Li}^+$ ,  $\text{Br}^-$ ,  $\text{HTO}$ ,  $^{60}\text{Co}$ ) tracers were used to understand the various complex processes occurring in the unsaturated zone at the farm site of Indian Agricultural Research Institute (IARI), New Delhi. Also, an estimate on the recharge, mobility of pollutants and related parameters was made. The study was carried out in collaboration with the Nuclear Research Laboratory, IARI.

## 2. STUDY AREA

The study area (~2.8 km<sup>2</sup>) is located in the farm of Indian Agricultural Research Institute, New Delhi (Fig.1). It has two major geomorphic units, a sloping plain in the south and an alluvial plain in the central and northern parts. The irrigation system consists of underground pipelines with a chain of twenty interlinked tube wells connected to the storage reservoir. Water is supplied to the fields through surface channels. During the last five decades, the area has been subjected to intensive agricultural activities with different fertilizers, pesticides, insecticides and water management practices.

The climate is semi-arid, with average annual rainfall of 703 mm (80% during June to September) and is generally non-uniform and erratic with heavy rainfalls occasionally. Groundwater occurs under unconfined and semi confined conditions. During the last two decades, due to increased pumping of groundwater, there has been a significant decline in the water table. Water table in the study area fluctuates between 13 to 14 m. Groundwater chemistry is generally Na-Cl- HCO<sub>3</sub> type.

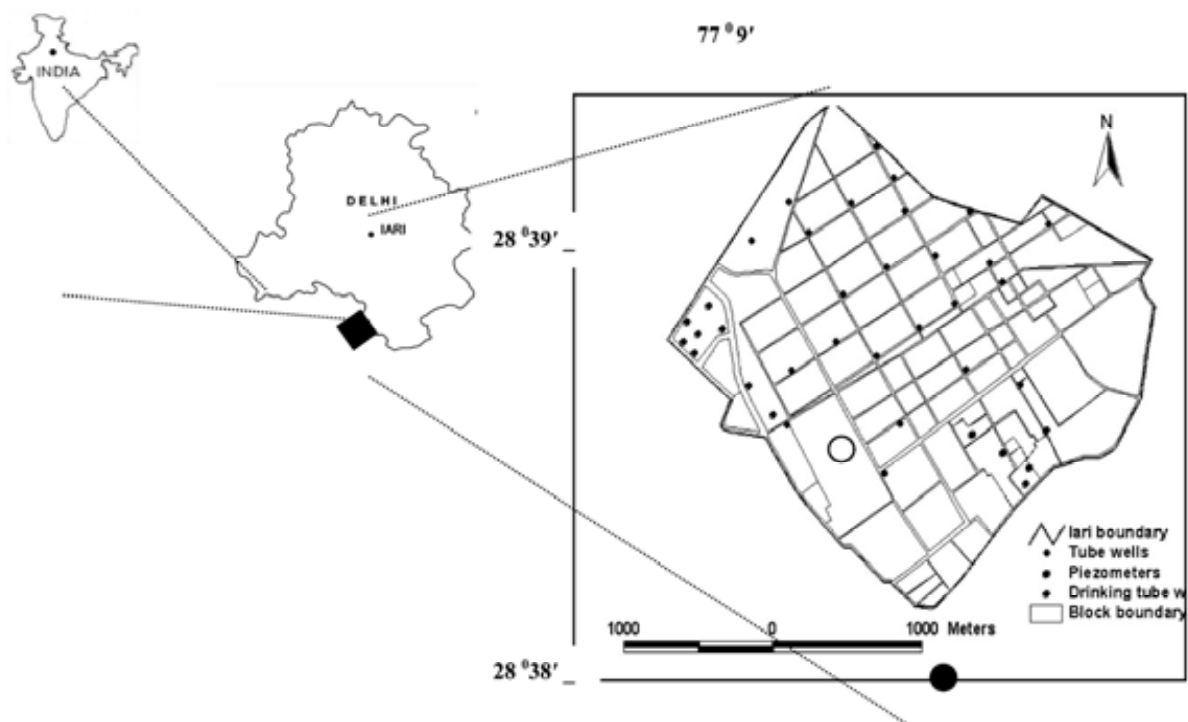


FIG. 1. Location map of study area (◆ — IARI farm area; ○ — Irrigated site; ● — Non-irrigated site; • — Tube wells).

## 3. EXPERIMENTAL DETAILS AND METHODS

Three soil cores (2 nos. — irrigated site; 1 no. — non-irrigated site) up to 7 m (at 40 cm interval) and one soil core up to 13 m (at 50 cm interval) were collected in April 2002 and February 2005, respectively using a hydraulic drilling machine. Soil core samples were analyzed for pH, EC, moisture content, major-ion chemistry and isotopes ( $\delta^{13}\text{C}_{\text{DIC}}$ ,  $\delta^{18}\text{O}$ ,  $\delta^2\text{H}$ ).

One to one mixture (weight/weight) of soil and distilled water was prepared. The mixture was filtered using 0.45 $\mu$  filter paper and the filtrate was used for chemical analysis of the soil water samples using Dionex Ion Chromatograph. pH and EC of the soil water samples were measured by preparing 1:2.5 mixture. Analyses of  $\delta^{13}\text{C}_{\text{DIC}}$  (phosphoric acid method),  $\delta^{18}\text{O}$  and  $\delta^2\text{H}$  in soil solutions and groundwater samples were carried out using Geo 20–20 isotope ratio Mass Spectrometer. Pore gas samples were measured by Gas Chromatography.

Two boreholes (8" Ø) were drilled up to 20 m depth during February 2005 and July 2006. They were used for collecting the real-time data on the pollutant transport in the vadose zone by installing several instruments as listed in Table 1. (The depth to water table was 13 and 14 m, respectively, during the borehole instrumentation work in 2005 and 2006.) After the drilling of the boreholes, a 2" Ø PVC pipe with various sensors tied at every alternate metre length was lowered into the boreholes. Before lowering the PVC pipe, testing and calibration of the various sensors, as per the guidelines given by the suppliers, were successfully carried out. (The layout of borehole instrumentation in the two boreholes is shown in Figs. 2–3). As seen in Figs. 2–3, sealing of the various instruments (HDP, lysimeter, Gas collection device), were carried out at different depths with alternating sand and bentonite layers. Also, finally the top of the boreholes were properly sealed.

TABLE 1. DETAILS OF VARIOUS SENSORS INSTALLED IN THE BOREHOLES.

Sensor	Purpose	Information collected
Heat Dissipation Probe (HDP Model 229)	Measurement of soil water matric potential	<b>Physical processes</b> -Movement of water (movement of pollutant)
Lysimeter (1920F1)	Collection of pore water	<b>Chemical processes</b> -Chemical and isotopic fluxes
Gas collection device	Collection of pore gases	<b>Biochemical/microbiological processes</b> -Oxidation, reduction processes

A few tracer (chemical, radioactive) experiments were carried out at the irrigated site to obtain information such as recharge, mobility etc.  $^{60}\text{Co}$  [ $\text{K}_3\text{CO}(\text{CN})_6$ ]  $\sim <1$  mCi,  $^3\text{H}$  (tritiated water  $\sim 10$   $\mu\text{Ci}$ ) and LiBr 10% solution were injected in June 2002 using peristaltic pump at a depth of 60 cm from the surface.  $^{60}\text{Co}$  tracer was injected at eight points as shown in the Fig. 4a, while the other tracers ( $^3\text{H}$ , Li, Br) were injected about 2 m away from the  $^{60}\text{Co}$  injection location at four locations (60 cm apart).

At the four locations, the tracers were injected at five points (four on the circumference and one at the centre of a circle with a radius 15 cm). The layout of tracer injection is given in Fig. 4.

For in-situ measurement of the movement of the  $^{60}\text{Co}$  tracer, an access tube was installed at the centre. The displacement of the tracer was monitored using a water-proof NaI(Tl) scintillation detector. Soil core samples were collected after 5 irrigation events ( $\sim 6$  months) and soil moisture was extracted by vacuum distillation method.  $^3\text{H}$  tracer concentration in the soil moisture was measured on liquid scintillation counter and measurement of Li and Br tracer using Dionex Ion Chromatograph.

#### 4. RESULTS

The results of the analyses of the samples from soil cores (core-I, core-II from irrigated site (April 2002), core from non-irrigated site (April 2002), core from tracer injected site (January 2003), core from irrigated site (February 2005), physical properties of soil from irrigated site), soil solutions (lysimeters), pore gas and groundwater collected during different periods for pH, EC, moisture content, major-ion chemistry and isotopes ( $\delta^{13}\text{C}_{\text{DIC}}$ ,  $\delta^{18}\text{O}$ ,  $\delta^2\text{H}$ ) are given in Tables 2-13.

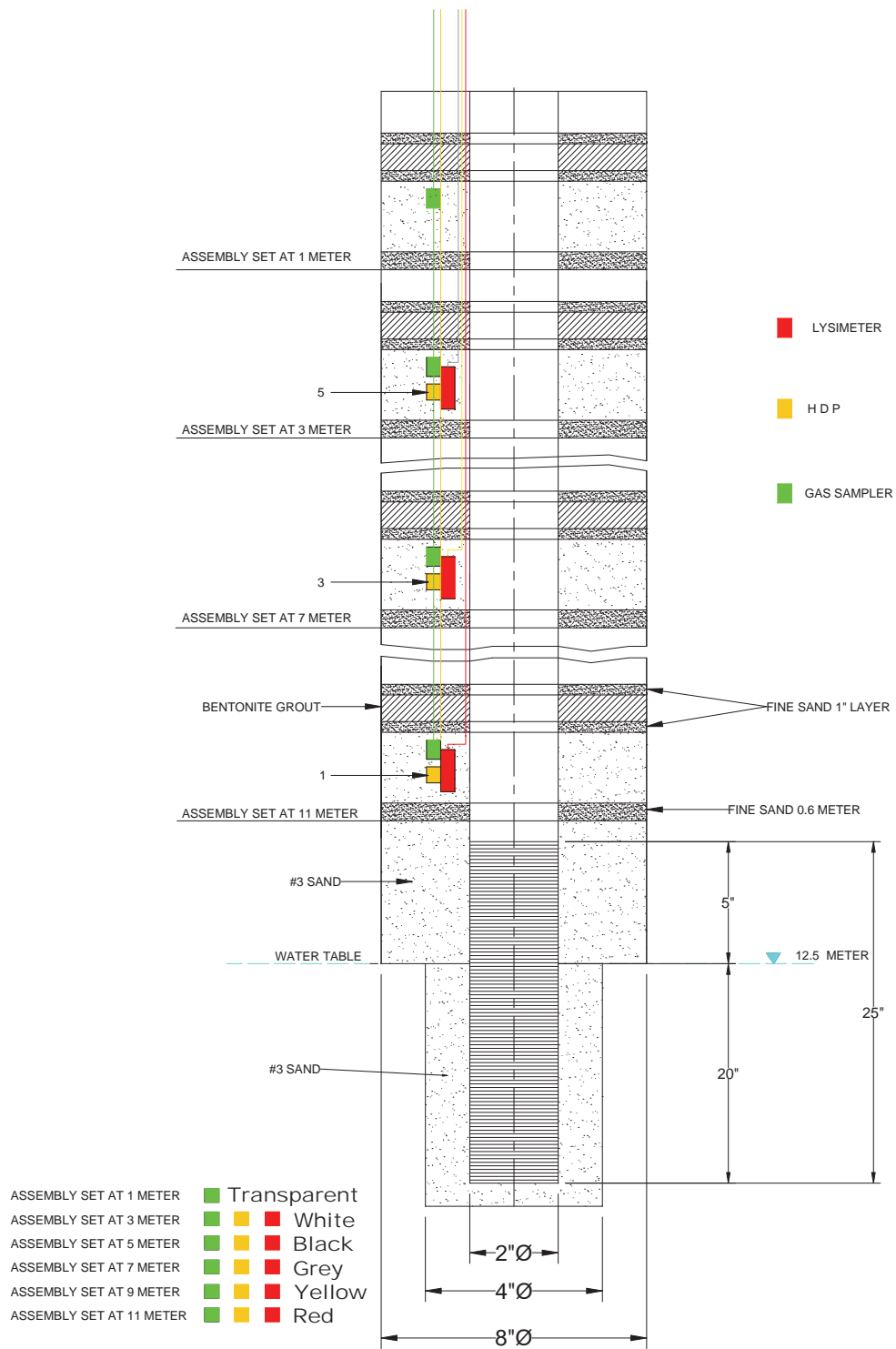


FIG. 2. Layout for instrumentation installation at Borehole 1.

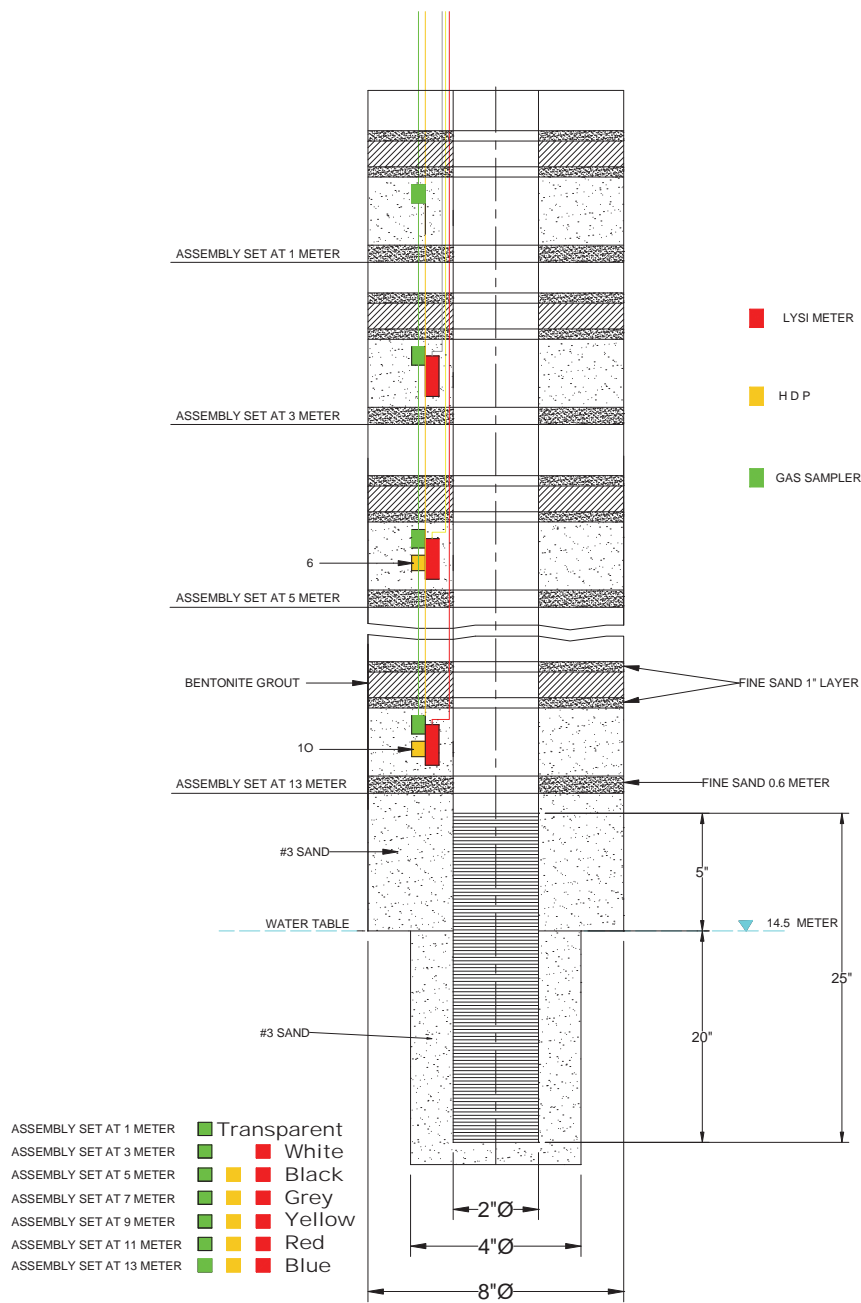


FIG. 3. Layout for instrumentation installation at Borehole 2.

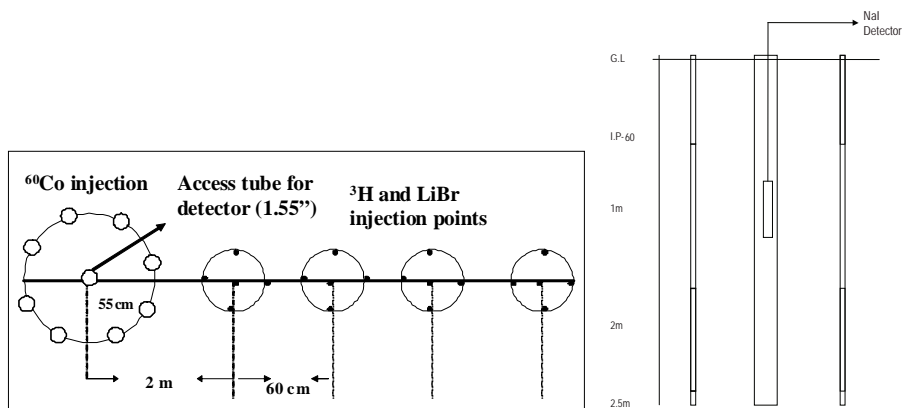


FIG. 4. (a) Layout of tracer (chemical, radioactive) injection; (b). <sup>60</sup>Co tracer movement (sectional view).

TABLE 2. RESULTS OF SOIL CORE-1 FROM THE IRRIGATED SITE IN APRIL 2002.

Depth (cm)	F	Cl	Br	NO <sub>3</sub> <sup>-</sup>	SO <sub>4</sub>	PO <sub>4</sub>	Na	K	Mg	Ca	Moisture (%)	pH	EC ( $\mu$ S/cm)	$\delta^{13}\text{C}$ (‰)	$\delta^{18}\text{O}$ (‰)
0-40	7	925	22	18	1367	-	-	-	-	-	11.1	8.3	352	6.0	-2.0
40-80	29	347	-	12	141	-	-	-	-	-	8.4	8.1	176	-	-5.0
80-120	10	1000	39	-	1093	2.0	-	-	-	-	14.3	7.9	264	-	-2.0
120-160	10	530	-	72	942	3.0	-	-	-	-	10.8	8.1	284	-	-1.5
160-200	19	372	-	37	548	-	511	-	61	392	14.8	8.2	362	0.3	-1.6
200-240	20	499	-	71	415	-	508	0.1	4	31	13.2	8.3	421	1.1	-3.0
240-280	26	564	-	69	179	-	486	0.9	54	312	12.2	8.4	372	0.8	-3.7
280-320	30	711	-	30	233	0.4	567	5.0	71	290	12.6	8.4	362	1.3	-4.0
320-360	28	324	-	7	265	-	456	0.9	52	229	10.9	8.4	343	1.2	-1.4
360-400	26	97	-	1	195	-	271	1.2	41	222	9.0	8.4	333	1.5	-2.3
400-440	24	94	-	6	128	-	233	6.6	39	197	8.2	8.5	245	0.7	+0.1
440-480	21	125	-	29	120	-	58	1.5	33	143	7.6	8.5	235	1.8	+0.1
480-520	20	91	-	16	88	-	212	1.1	23	119	6.3	8.5	253	0.6	-0.4
520-560	24	288	-	133	121	0.3	365	1.7	39	172	8.3	8.5	284	1.8	-1.2
560-600	32	507	-	187	242	0.1	508	2.4	73	326	12.0	8.5	402	1.3	-3.6
600-640	23	447	-	124	135	-	407	2.7	67	264	8.9	8.4	382	0.8	-1.6

**NOTE:** Units of chemical species concentration is in mg/L.

TABLE 3. RESULTS OF SOIL CORE – II FROM THE IRRIGATED SITE IN APRIL 2002.

Depth (cm)	F	Cl	Br	NO <sub>5</sub>	SO <sub>4</sub>	PO <sub>4</sub>	Na	NH <sub>4</sub>	K	Mg	Ca	Moisture (%)	pH	EC ( $\mu$ S/cm)
0-40	8	154	-	108	58	1.2	28	7.8	6	15	46	3.2	7.2	206
40-80	7	166	-	49	85	-	-	-	-	-	-	5.6	7.3	255
80-120	13	76	-	100	94	3.5	-	-	-	-	-	5.0	8.0	304
120-160	16	25	-	100	98	-	32	8.8	7.2	17	53	3.1	8.0	421
160-200	8	99	-	153	89	-	-	-	-	-	-	5.0	8.1	421
200-240	14	23	-	107	87	-	76	-	6.6	3	125	6.7	8.3	323
240-280	13	36	-	147	125	0.2	-	-	-	-	-	5.2	8.3	401
280-320	13	7	-	37	0	-	171	-	17.5	29	-	4.5	8.6	313
320-360	7	28	-	209	54	-	123	3.6	1.7	15	48	3.1	8.6	313
360-400	8	49	-	41	61	0.3	-	-	-	-	-	3.0	8.2	421
400-440	-	-	-	-	-	-	-	-	-	-	-	3.3	8.7	294
440-480	9	19	-	137	60	-	117	-	0.7	15	62	3.6	8.4	353
480-520	21	62	-	19	92	0.8	-	-	-	-	-	6.5	8.8	382
520-560	42	34	-	26	545	4.0	-	-	-	-	-	12.0	8.8	490
560-600	33	122	-	90	396	0.3	524	-	5.2	38	150	8.7	8.7	441
600-640	48	68	-	119	410	1.3	-	-	-	-	-	13.0	8.9	568
640-680	57	172	-	24	594	2.8	-	-	-	-	-	14.0	9.0	656

**NOTE:** Units of chemical species concentration is in mg/L.

TABLE 4. RESULTS OF SOIL CORE FROM THE NON-IRRIGATED SITE IN APRIL 2002

Depth (cm)	F	Cl	Br	NO <sub>3</sub> <sup>-</sup>	SO <sub>4</sub>	PO <sub>4</sub>	Na	K	Mg	Ca	Moisture (%)	pH	EC ( $\mu$ S/cm)	$\delta^{18}\text{O}$ (‰)
0-40	24	560	-	96	157	-	341	10.0	50	247	11.0	8.4	469	-3.1
40-80	38	990	0.6	1	2304	-	615	-	86	397	12.3	8.0	509	+1.1
80-120	62	634	-	58	152	-	503	-	53	94	13.0	8.0	430	+2.3
120-160	75	273	-	95	318	1.0	-	-	-	-	14.2	8.2	509	-4.0
160-200	76	425	-	58	661	-	-	-	-	-	14.0	8.4	578	+2.3
200-240	25	970	0.8	1	184	1.0	684	-	58	185	12.0	8.5	627	-2.4
240-280	46	567	-	32	189	-	-	-	-	-	11.0	8.4	499	-1.1
280-320	48	327	-	69	233	2.4	489	2.4	31	157	12.0	8.5	421	-2.5
320-360	17	287	0.3	0	135	2.0	375	1.0	19	125	10.3	8.5	392	-2.8
360-400	15	245	0.1	0	135	-	312	1.1	21	107	8.3	8.5	401	-2.2
400-440	17	136	-	12	106	1.3	215	0.7	13	89	6.7	8.5	362	+0.6
440-480	11	174	-	12	153	-	221	1.2	21	112	6.1	8.6	352	+1.0
480-520	24	158	-	5.5	197	1.3	326	2.2	24	141	11.0	8.5	294	+1.8
520-560	13	114	0.1	0	137	1.3	182	1.0	18	64	4.5	8.5	450	-

**NOTE:** Units of chemical species concentration is in mg/L

TABLE 5. RESULTS OF SOIL CORE FROM THE TRACER INJECTED SITE IN JANUARY 2003.

Depth (cm)	Li	Na	NH <sub>4</sub>	K	Mg	Ca	F	Cl	Br	NO <sub>3</sub> <sup>-</sup>	SO <sub>4</sub>	PO <sub>4</sub>	Moisture (%)	δ <sup>18</sup> O (‰)	δ <sup>13</sup> C (‰)
0-60	0.1	478	10	14	126	323	17	277	0	49	391	4	14.0	-6.5	-4.0
60-75	0.7	436	-	19	112	273	20	561	0	220	366	0	8.6	-5.0	-10.0
75-90	0.2	412	-	10	74	176	16	369	0	90	265	0	11.7	-7.0	-10.0
90-105	0.1	404	-	5	42	105	31	381	0	29	160	0	10.5	-7.7	-1.0
105-120	0.1	344	-	6	37	105	17	243	0	13	144	0	15.5	-11.0	-5.0
120-135	0.4	202	-	9	61	165	8	194	0	65	158	0	17.2	-12.0	-2.0
135-150	2.2	388	8	13	60	244	12	104	0	8	280	6	17.9	-10.0	-6.0
150-165	0.4	448	8	12	55	275	15	82	0	4	331	6	16.3	-8.0	-5.3
165-180	0.4	475	8	11	43	340	8	83	0	0	314	3	17.5	-8.0	-1.0
180-195	0.2	485	8	10	18	323	15	110	0	0	308	2	16.6	-6.2	0
195-210	0.1	440	-	10	7	29	18	127	0	0	331	0	15.1	-7.0	+0.4
210-225	0.3	560	10	15	59	473	17	250	0	0	330	2	12.7	-8.0	+6.0
225-240	0.3	435	10	20	46	227	10	203	12	0	301	0	15.6	-2.7	+1.0
240-255	0.3	362	-	16	32	256	16	194	19	63	269	0	14.4	-2.0	+1.0
255-270	0.6	461	9	31	61	366	15	271	33	94	402	3	12.6	-1.0	+1.0
270-285	0.4	498	-	21	49	257	21	275	27	195	419	0	11.2	-1.0	-1.0

NOTE: Units of chemical species concentration is in mg/L

TABLE 6A. RESULTS OF SOIL CORE FROM THE IRRIGATED SITE IN FEBRUARY 2005.

Depth (cm)	F	Cl	NO <sub>3</sub> <sup>-</sup>	SO <sub>4</sub>	Moisture (% )	EC ( $\mu$ S/cm)	pH	$\delta^{13}\text{C}$ (‰)	$\delta^{18}\text{O}$ (‰)
0–50	11.0	484	10	627	15.3	770	8.5	-4.4	-
50–100	4.8	100	37	106	17.7	210	8.6	-	-1.5
100–150	20.6	1436	110	1485	4.5	610	8.3	-	-0.5
150–200	36.0	491	70	479	7.9	430	8.1	-0.5	-4.5
200–250	8.4	336	10	385	9.4	380	8.0	-3.0	-4.3
250–300	13.8	2619	9	525	10.1	1000	8.1	+0.1	-1.8
300–350	23.2	4700	17	23	6.1	2030	8.1	-0.5	-1.7
350–400	34.0	446	54	443	7.7	410	8.1	+3.5	-4.3
400–450	10.0	803	62	2093	4.0	910	8.4	-8.7	-0.6
450–500	38.0	598	11	202	6.5	420	7.6	-0.5	-14.5
500–550	73.4	1782	18	660	4.7	660	7.8	-6.7	-5.0
550–600	49.6	4395	13	41	3.8	1220	8.2	+1.9	-2.1
600–650	7.7	1277	8	64	10.6	1020	7.9	-0.1	-7.7
650–700	13.9	334	30	627	14.2	670	8.0	-1.3	-7.0
700–750	20.3	1885	6	361	9.7	960	7.7	+0.4	-7.6
750–800	25.5	173	0	384	11.6	370	7.9	+0.6	-2.9
800–850	14.8	220	4	322	14.8	470	7.9	+1.8	-6.8
850–900	36.7	1858	8	693	5.9	710	8.1	-0.2	-4.4
900–950	27.0	171	13	435	10.1	340	8.2	-1.3	-9.7
950–1000	12.6	403	6	550	10.8	670	8.1	-1.2	-3.3
1050–1100	16.0	1392	5	777	6.8	1030	8.1	-1.6	-5.8
1100–1150	12.2	326	0	73	12.1	490	8.3	-3.0	-4.4
1150–1200	6.9	557	6	126	16.5	650	8.1	-4.0	-7.4
1200–1250	10.7	19	0	144	15.6	470	8.3	-3.0	-5.9
1250–1300	10.6	795	4	540	17.0	800	8.4	-6.0	-5.0

**NOTE:** Units of chemical species concentration is in mg/L.

TABLE 6B. RESULTS OF PHYSICAL PROPERTIES OF SOIL FROM THE IRRIGATED SITE.

Soil depth (cm)	Particle size distribution (%)			Bulk density (g/cm)	Soil moisture retention at matric potentials		Saturated water content (cm <sup>3</sup> /cm <sup>3</sup> )	Organic carbon (%)
	Sand	Silt	Clay		[0.33 bar] (cm <sup>3</sup> /cm <sup>3</sup> )	[-0.15 bar] (cm <sup>3</sup> /cm <sup>3</sup> )		
0–15	76.4	11.8	1.51	1.54	0.26	0.09	0.38	0.65
15–30	74.4	10.8	1.56	1.56	0.25	0.09	0.40	0.61
30–60	77.4	9.8	1.58	1.58	0.26	0.10	0.40	0.36
60–90	71.4	12.8	1.57	1.57	0.25	0.10	0.39	0.38
90–120	68.4	13.8	1.50	1.50	0.27	0.12	0.40	0.54
120–150	63.4	11.8	1.49	1.49	0.27	0.12	0.39	0.42
150–180	64.4	14.8	1.52	1.52	0.30	0.12	0.42	0.36

TABLE 7. RESULTS OF ANALYSES OF SOIL SOLUTION COLLECTED FROM LYSIMETER

BH-1	Date	Depth (m)	Volume (ml)	EC (μS/cm)	F	Cl	NO <sub>3</sub>	SO <sub>4</sub>	δ <sup>18</sup> O (‰)
	21/7/05	5	60	3590	2.8	380	22	259	-5.6
		7	60	5620	4.5	692	75	730	-5.8
	21/9/05	5	400	2350	2.2	250	38	111	-5.9
		7	200	4720	3.4	584	84	539	-5.9
	24/10/05	3	10	5650	1.5	733	175	860	-7.0
		5	400	2040	1.8	191	61	174	-5.9
		7	250	4220	3.7	567	91	109	-5.7
		9	10	–	4.0	414	94	109	-5.8
	31/5/06	5	400	1672	–	190	90	279	–
		7	100	3902	–	1060	165	314	–
	29/6/06	5	200	1653	–	184	89	296	–
		7	200	3360	–	1126	187	321	–
		11	10	–	–	110	32	23	–
	22/8/06	3	500	748	3.2	120	56	287	–
		7	500	1724	1.2	698	129	451	–
		11	20	734	0.7	304	100	69	–
	4/12/06	3	10	–	1.0	417	382	488	-6.2
		5	150	853	1.0	266	148	181	-5.6
		7	1000	1181	2.0	329	151	127	-6.8
		11	60	748	1.0	603	134	140	-4.7
BH-2	25/8/06	3	1000	217	1.7	5.5	57	18	-2.8
		7	200	1117	1.9	312	190	326	-8.8
		9	30	3710	1.5	154	104	212	-6.2
		11	100	798	1.6	184	120	248	-7.0
	4/12/06	3	100	650	9.4	62	205	34	-3.0
		7	200	1405	1.3	526	157	406	-4.5
		9	200	2760	14.3	895	309	1230	-8.9
		11	250	1070	9.5	545	236	548	-8.0

NOTE: Units of chemical species concentration is in mg/L.

TABLE 8. RESULTS OF SOIL PORE- GAS ANALYSIS (ND-NOT DETECTABLE).

Bore Hole No.	Date	Depth (m)	CO (mg/L)	CO <sub>2</sub> (mg/L)	CH <sub>4</sub> (mg/L)
BH-1	24/10/05	1	ND	336	1
		3	ND	388	1
		5	ND	10785	1
		7	ND	6712	1
		9	ND	388	1
		11	ND	5830	1
	21/6/06	1	ND	530	ND
		3	ND	4125	ND
		5	ND	6910	ND
		7	140	2793	ND
		9	ND	210	ND
		11	ND	745	ND
	22/8/06	1	ND	11045	ND
		3	ND	10618	ND
		5	ND	480	ND
		7	ND	575	ND
		9	ND	650	ND
		11	50	2445	ND
BH-2	22/8/06	1	ND	2745	ND
		3	ND	655	ND
		5	ND	1106	ND
		7	ND	625	ND
		9	ND	755	ND
		11	ND	685	ND
		13	ND	745	ND
	23/8/06	1	ND	2405	ND
		3	ND	1517	ND
		5	ND	3760	ND
		7	ND	1055	ND
		9	ND	2445	ND
		11	ND	1035	ND
		13	ND	3870	ND

TABLE 9. RESULTS OF GROUND WATER SAMPLES IN JUNE 2001.

Location	Alkalinity (CaCO <sub>3</sub> )	EC (µS/cm)	δ <sup>18</sup> O (‰)	δD (‰)	F	Cl	NO <sub>3</sub>	SO <sub>4</sub>	Na	K	Mg	Ca	pH	Water type
TW-1	340	2700	-7.0	-43	0.6	711	6.5	45	414	8.5	28	130	7.1	Na-Mg-Ca- Cl-HCO <sub>3</sub>
TW-2	431	2530	-7.0	-38	1.2	538	11.0	79	376	9.3	40	168	7.1	Na-Ca-Cl- HCO <sub>3</sub>
TW-4	358	4510	-6.8	-45	0.6	128	1.2	44	615	9.3	93	273	7.1	Na-Ca-HCO <sub>3</sub>
TW-6	408	2070	-7.3	-45	1.3	408	6.7	60	315	2.1	54	106	7.3	Na-Ca-Mg- Cl-HCO <sub>3</sub>
TW-7	400	1140	-7.2	-45	-	-	-	-	-	-	-	-	7.8	-
TW-8	388	1937	-6.6	-44	0.9	351	34.5	70	217	1.0	29	96	7.5	Na-Ca-Cl- HCO <sub>3</sub>
TW-10	374	1382	-7.0	-50	0.6	200	23.5	55	112	3.3	46	102	7.2	Ca-Na-Mg- HCO <sub>3</sub> -Cl
TW-14	319	1207	-7.0	-44	-	-	-	-	-	-	-	-	7.2	-
TW-17	365	1842	-7.0	-41	-	-	-	-	-	-	-	-	7.3	-
TW-NT	384	1565	-6.8	-43	0.5	270	5.8	16	134	3.9	45	123	7.4	Ca-Na-Mg- Cl-HCO <sub>3</sub>

NOTE: Units of chemical species concentration is in mg/L.

TABLE 10. RESULTS OF GROUND WATER SAMPLES IN APRIL 2002.

Sample ID	F	Cl	NO <sub>3</sub>	SO <sub>4</sub>	Na	K	Mg	Ca	NH <sub>4</sub>	Alkalinity	pH	EC ( $\mu\text{S}\cdot\text{cm}^{-1}$ )	$\delta^{18}\text{O}$ (‰)	Water type
TW-GEN	1.6	236	21	93	145	1.4	20	113	2.5	210	7.6	1303	-6.0	Na-Ca-Cl-HCO <sub>3</sub>
TW-SPB	0.8	571	9	29	143	9.6	89	160	-	215	7.6	2130	-6.0	Ca-Mg-Na-Cl-HCO <sub>3</sub>
TW-NT	0.7	325	19	36	108	4.6	65	114	2.3	275	7.7	1539	-6.3	Ca-Mg-Na-Cl-HCO <sub>3</sub>
TW-10	0.8	226	33	65	90	4.4	63	95	2.6	285	7.9	1375	-5.8	Mg-Ca-Na-Cl-HCO <sub>3</sub>
Tank water	1.1	243	39	57	133	2.9	49	78	2.8	275	7.9	1422	-5.6	Na-Mg-Ca-Cl-HCO <sub>3</sub>
TW-16	0.7	339	177	80	217	3.2	57	88	-	310	8.0	1866	-6.2	Na-Mg-Ca-Cl-HCO <sub>3</sub>
TW-17	0.9	260	55	88	187	2.7	52	75	-	310	8.1	1607	-6.1	Na-Mg-Ca-Cl-HCO <sub>3</sub>
TW-14	0.1	159	23	36	81	2.5	30	75	2.0	220	7.9	1075	-6.1	Ca-Na-Mg-Cl-HCO <sub>3</sub>
TW-8	1.2	258	29	43	169	1.6	47	76	2.0	300	8.1	1506	-6.1	Na-Mg-Ca-Cl-HCO <sub>3</sub>
TW-7	0.8	188	22	29	96	2.3	49	75	1.7	310	7.9	1228	-5.9	Na-Mg-Ca-Cl-HCO <sub>3</sub>
TW-2	0.9	556	17	82	279	8.3	70	109	-	315	7.7	2400	-5.3	Na-Mg-Ca-Cl-HCO <sub>3</sub>
TW-TB6	0.1	1811	12	53	599	10.3	135	337	-	158	7.6	5700	-5.9	Na-Ca-Mg-Cl
TW-TB4	0.8	712	21	52	294	6.4	70	153	-	260	7.6	2690	-6.3	Na-Ca-Mg-Cl
TW-ENG	0.1	323	25	28	209	2.9	43	84	-	320	7.9	1738	-6.3	Na-Ca-Mg-Cl-HCO <sub>3</sub>
TW-CPWD-1	0.1	257	130	66	243	2.3	39	58	-	370	8.1	1675	-6.3	Na-Cl-HCO <sub>3</sub>
TW-CPWD-2	2.6	297	49	86	263	2.3	37	52	-	330	8.1	1770	-6.1	Na-Cl-HCO <sub>3</sub>
TW-MB	0.6	248	12	59	147	5.7	55	77	3.2	330	8.0	1490	-6.0	Na-Mg-Ca-Cl-HCO <sub>3</sub>

**NOTE:** Units of chemical species concentration is in mg/L.

TABLE 11. RESULTS OF GROUND WATER SAMPLES IN JANUARY 2003.

Well no.	F	Cl	NO <sub>3</sub>	SO <sub>4</sub>	Na	K	Mg	Ca	EC ( $\mu\text{S}\cdot\text{cm}^{-1}$ )	pH	Alkalinity	$\delta^{18}\text{O}$ (‰)	Water type	Location (Ref. Fig. 1)
TW-1	0.5	721	6	53	273	4	71	167	2750	7.2	326	-6.7	Na-Ca-Mg-Cl	N 23° 8.333' E 77° 09.741'
TW-2	1.3	574	14	103	307	11	61	56	2480	7.3	420	-6.0	Na-Mg-Cl-HCO <sub>3</sub>	N 28° 38.171' E 77° 09.422'
TW-Tb4	1.4	743	1	51	323	9	71	74	2920	7.3	416	-5.7	Na-Mg-Cl-HCO <sub>3</sub>	N 28° 38.813' E 77° 09.440'
TW-Tb6	1.8	853	3	55	342	9	75	131	3140	7.1	394	-6.6	Na-Ca-Mg-Cl-HCO <sub>3</sub>	N 28° 38.967' E 77° 09.514'
TW-7	1.2	184	20	31	103	3	44	55	1220	7.6	406	-6.6	Na-Mg-Ca-HCO <sub>3</sub> -Cl	N 28° 38.450' E 77° 09.561'
TW-8	1.2	252	23	61	163	2	50	53	1510	7.5	466	-6.5	Na-Mg-HCO <sub>3</sub> -Cl	N 28° 38.374' E 77° 09.295'
TW-10	0.5	228	27	77	91	5	59	64	1404	7.4	346	-6.4	Mg-Na-Ca-Cl-HCO <sub>3</sub>	N 28° 38.625' E 77° 09.553'
TW-14	0.5	241	28	69	141	2	29	42	1412	7.3	210	-5.8	Na-Mg-Cl-HCO <sub>3</sub>	N 28° 38.574' E 77° 09.167'
TW-16	0.6	478	75	58	305	6	47	93	2230	7.5	390	-6.5	Na-Ca-Cl-HCO <sub>3</sub>	N 28° 38.833' E 77° 09.167'
TW-17	0.7	169	33	67	163	4	32	26	1299	7.7	374	-5.2	Na-Mg-HCO <sub>3</sub> -Cl	N 28° 38.789' E 77° 09.246'
TW-MB	0.7	359	29	90	211	4	47	68	1966	7.4	390	-6.4	Na-Mg-Cl-HCO <sub>3</sub>	N 28° 38.161' E 77° 09.129'
TW-SPB	0.4	931	2	17	189	20	100	193	3190	7.0	368	-6.4	Ca-Mg-Na-Cl-HCO <sub>3</sub>	N 28° 38.629' E 77° 09.810'
TW-NT	0.4	320	12	40	114	5	57	81	1623	7.5	360	-6.6	Na-Mg-Ca-Cl	N 28° 38.523' E 77° 09.634'
Rain Water	0.2	4	2	5	2	1	1	3	40	6.6	-	-	Li-Ca-Na- Ca	N 28° 38.333' E 77° 09.741'
CPWD-2	2.0	282	44	92	291	3	27	61	1747	7.5	402	-6.5	Na-Cl-HCO <sub>3</sub>	N 28° 38.244' E 77° 09.923'
CPWD-1	1.0	266	27	73	278	3	33	49	1757	7.7	470	-6.4	Na-HCO <sub>3</sub> -Cl	N 28° 38.034' E 77° 09.039'

**NOTE:** Units of chemical species concentration is in mg/L.

TABLE 12 RESULTS OF GROUND WATER SAMPLES IN APRIL 2004.

Well No	pH	Alkalinity (mg/L)	Ec ( $\mu$ S/cm)	Temp ( $^{\circ}$ C)	$\delta^{18}\text{O}$ ( $\text{‰}$ )	$\delta^{13}\text{C}$ ( $\text{‰}$ )
Shadipur	7.1	330	2410	23.6	-6.7	-10.7
TW- Genetics	7.3	250	1513	23.6	-6.5	-9.2
TW-10	7.4	320	1309	23.2	-6.3	-9.9
TW-2	7.4	380	1707	23.6	-6.5	-10.9
TW-17	7.6	350	1463	23.3	-6.4	-10.1
TW-NA	7.3	220	1340	23.5	-6.5	-13.5
TW-14	7.3	310	1107	24.1	-6.4	-9.7
TW-7	7.3	360	1162	23.8	-6.8	-8.7
TW-8mb, 8c	7.4	400	1361	24.1	-6.8	-9.9
TW-MB	7.3	460	1399	24.8	-6.9	-9.5
TW-cpwd1	7.4	450	1644	23.7	-6.8	-10.8
TW-Attic	7.3	325	1593	23.7	-6.6	-10.0
TW- cpwd2	7.5	380	1625	23.8	-6.6	-10.5
WTC	7.3	300	1633	24.1	-6.9	-10.1
TW-1	7.1	320	2330	25.0	-6.9	-12.6

TABLE 13. RESULTS OF GROUND WATER SAMPLES IN OCTOBER 2005.

Tube well	$\delta^{18}\text{O}$ ( $\text{‰}$ )	F	Cl	$\text{NO}_3$	$\text{SO}_4$	$\text{PO}_4$
TW-1	-7.0	1.01	607	18.0	87	0
TW-2	-6.4	1.79	681	29.0	156	0
TW-7	-6.5	1.36	214	52.0	51	0
TW-8	-6.7	1.56	279	58.9	112	0
TW-10	-6.4	0.83	261	72.0	97	0
TW-14	-6.8	0.60	198	47.0	82	0
TW-15	-6.5	1.07	287	47.0	114	0
TW-17	-6.5	1.34	273	118.0	149	0
TW-GANETICS	-6.3	2.93	210	42.3	152	0
TW-INDO-ISR	-6.7	3.95	335	1.0	52	0
TW-GH	-6.5	0.92	385	30.0	61	0
TW-CPWD	-6.6	1.18	330	56.0	110	0
TW-TB	-6.4	1.22	783	-	81	0
Irrigation Water (24/02/05)	-5.7	1.11	231	47.6	82	0
TW-2 (24/02/05)	-6.6	1.56	645	25.9	151	0

NOTE: Units of chemical species concentration is in mg/L.

## 5. DISCUSSION

The analysis of results (Tables 2–13) indicated that the gravimetric water content varied from ~3 to 15 % in April 2002. The water content in the non-irrigated site was relatively low at 40–500 cm depth and below this depth an increase was seen which may due to the previous year's rain. At the irrigated sites, soil moisture water content ranged from ~6 to 15 % and identical trends were seen in both cores (Fig. 5). The higher water content in the upper part of the profile is the result of the frequent application of irrigation water. (Each irrigation event is equal to 50 mm of water and minimum five irrigations are applied per year. Irrigation depends upon crop sown (soybean/wheat)). Soil core-II, collected from the experimental site, where higher fertilizer inputs were applied, indicated higher EC values ranging (~294 to 627  $\mu\text{S}/\text{cm}$ , Table 3). There is not much variation in pH (Fig. 5) for three cores except at the top layer.

At the non-irrigated site, the nitrate content varies from 19 to 209 mg/L (Fig. 5). In the nitrate profiles, soil cores I and II show that the nitrate is moving in a pulse-like fashion and hence distinct pulses are seen clearly depth wise. In soil core-III, high nitrate values are observed compared to the profiles of soil cores-I and II. As the crops are not cultivated in this area, no fertilizer is applied and hence no nitrate uptake by the plants and thus resulted in higher nitrate values.

The values of chloride, a conservative ion, range from 7 to 172 mg/L at the non-irrigated site (Fig. 5). In soil cores-I and II, the chloride values are high (up to ~1000 mg/L) and decline after 3 m depth. The concentration of fluoride up to 5 m in soil cores-I and III showed similar trend (with values  $>30$  mg/L) whereas in soil core-II, the values get enriched (up to 80 mg/L in the top zone (2 m)) and then a decline. All plots show movement of ions due to rainfall and irrigation. The concentration of sulphate showed similar trend as that of fluoride.  $\delta^{18}\text{O}$  and  $\delta^{13}\text{C}$  of the soil water show cyclic variation with depleted values at 0.6, 3 and 6m and enriched values at 0.4, 2, 3.6 and 4.8 m.

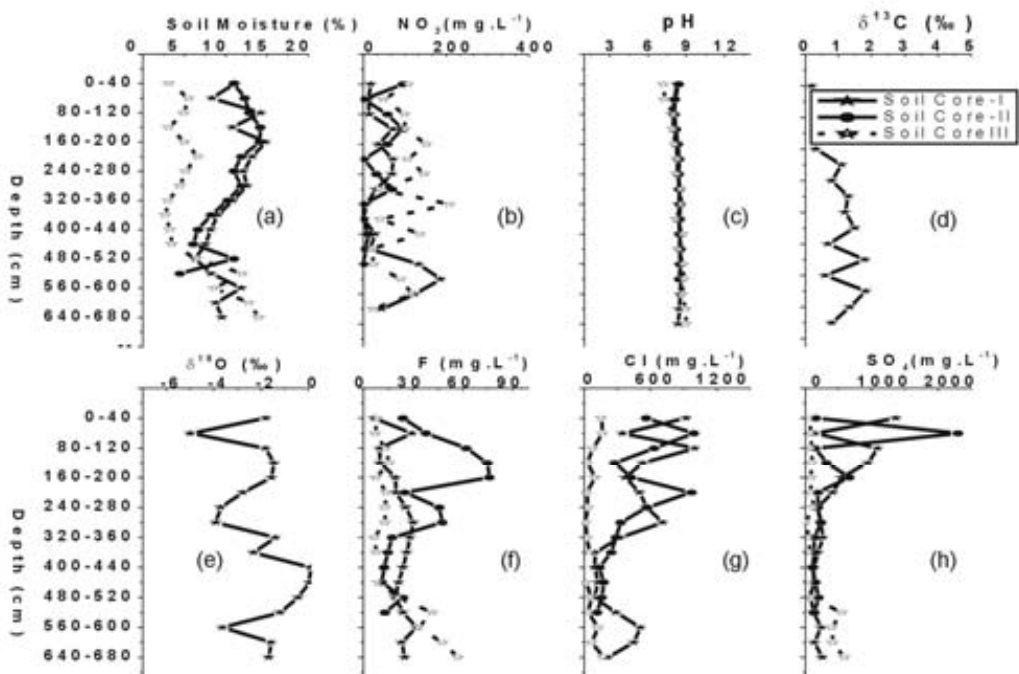


FIG. 5. Profiles in soil cores from the irrigated (I, II) and non-irrigated sites (III) (April 2002).

The analysis of results of soil cores, collected from the irrigated site in February 2005, in general, showed higher major-anions compared to the groundwater samples. This information will be useful as background information. Profiles of soil moisture content,  $\delta^{18}\text{O}$ ,  $\delta^{13}\text{C}$ , pH, F, Cl,  $\text{NO}_3^-$  and  $\text{SO}_4$  are presented in (Fig. 6).

Comparison between soil core collected from the irrigated site in April 2002 and February 2005 (Figs. 5, 6) indicated;

- Similar nitrate values in both the years,
- Low fluoride (max. 20 mg/L) in 2002 compared to 2005 (max. 70 mg/L at 5.5 m),
- Peak chlorides levels (~1000 mg/L) at 0.4 and 1.2 m in 2002 shifted to 3.5 and 6 m with enhancement (> 4000 mg/L) in 2005,
- Sulphate concentration high in the top zone (0–1 m) and then declined steadily to ~200 mg/L in 2002 whereas in 2005 the levels were higher (max. ~2000 mg/L) and
- $\delta^{18}\text{O}$  and  $\delta^{13}\text{C}$  showed similar trend and depleted values at ~5 m.

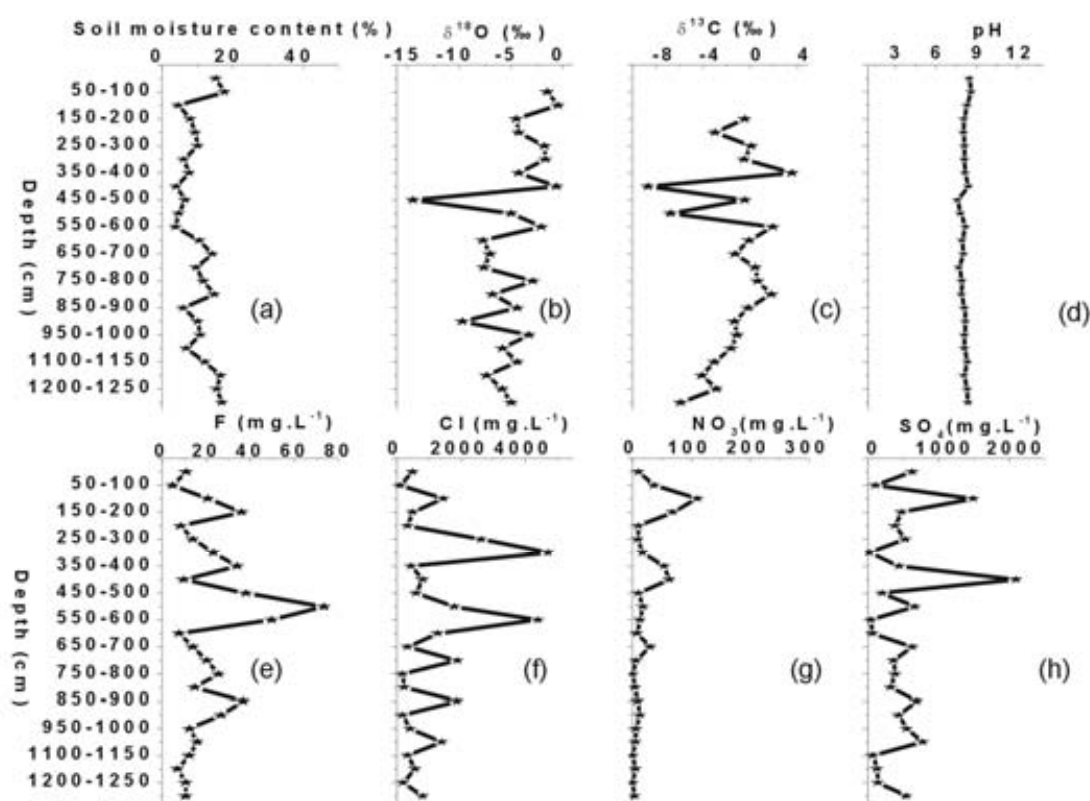


FIG. 6. Profiles in soil cores from the irrigated site (Feb. 2005).

Comparison between soil water from the lysimeters in October 2005 and soil core in February 2005 indicated;

- Low fluoride levels (max. 4 mg/L at 8 m) in October 2005 whereas 60 mg/L at 5.5 m in February 2005,
- Similar trend in chloride levels (max. 500 mg/L at 7 m) in October 2005 where as ~ 4000 mg/L at 6 m in February 2005 and
- Similar trends in the nitrate and sulphate levels.

## 5.1. Mobility of Pollutants

To determine the mobility of pollutants, soil cores were collected by hand auger from the tracer injection sites and tracers were extracted from the soil core. The results of analyses of chemical ( $\text{Li}^+$ ,  $\text{Br}^-$ ) and isotopic ( $\delta^{18}\text{O}$ ) and injected artificial radioactive tracers ( $^{60}\text{Co}$ ,  $^3\text{H}$ ) of the soil core are given in Table 5 and Table 14, respectively.

TABLE.14.  $^{60}\text{Co}$  AND  $^3\text{H}$  TRACER DATA

Depth (cm)	$^{60}\text{Co}$ –Mean activity (cpm)	$^{60}\text{Co}$ –Net activity (cpm)	Normalized $^{60}\text{Co}$ –activity (cpm)	Depth (cm)	$^3\text{H}$ –activity (dpm)	Normalized $^3\text{H}$ activity (dpm)
40	13886	7159	0.229	0–60	418	0.259
50	15612	8884	0.029	60–75	1117	0.694
60	16376	9648	0.031	75–90	428	0.263
70	16125	9397	0.031	90–105	1107	0.688
80	16437	9710	0.031	105–120	638	0.396
90	17286	10559	0.034	120–135	540	0.335
100	18221	11494	0.037	135–150	714	0.460
110	19322	12595	0.040	150–165	657	0.408
120	21126	14398	0.046	165–180	803	0.499
130	22715	15987	0.051	180–195	953	0.592
140	26562	19835	0.063	195–210	1526	0.948
150	30486	23759	0.076	210–225	995	0.618
160	38817	32089	0.103	225–240	1610	1.000
170	48977	42249	0.136	240–255	1352	0.839
180	64111	57383	0.184	255–270	1178	0.732
190	98213	91485	0.293	270–285	1089	0.676
200	139686	132958	0.427			
210	196508	189780	0.609			
220	252588	245860	0.788			
230	299873	293145	0.940			
240	318449	311721	1.000			
250	293672	286944	0.920			
260	236941	230213	0.730			
270	182635	175908	0.560			

Findings of the tracer study are as follows;

- Displacements of the tracers (due to recharge and irrigation) were observed after 187 days from the injection depth and from the displacement the rate of mobility for all the tracers were found to be different ( $\text{Br}^-$ : 0.011;  $\text{Li}^+$ : 0.005;  $^{60}\text{Co}$ : 0.009 and  $^3\text{H}$ : 0.009 m/d). The displacement of all the tracers is due to 550 mm of rainfall including five irrigation events equivalent of 250 mm of rainfall.
- From the tracer displacements average recharge was estimated to be ~17%,
- Pollutants may reach the saturated zone in about 7-8 years time,
- $\text{Li}^+$  ion tracer has been retarded in the formation, possibly due to absorption or exchange with soil matrix,
- After ~ two year  $^{60}\text{Co}$  tracer has moved to 4.4 m and
- Tritium has four peaks possibly due to exchange with immobile water.

## 5.2. Soil solution

Soil solution from BH–1 and BH–2 were collected at different dates and results of chemical, isotopic etc. analysis is tabulated in Table 7. Depth profile plots of the ions in the soil solution (lysimeters) collected from BH–1 in October 2005; June 2006, August 2006 and December 2006 are presented in

Fig. 8, 9, 10 and 11 respectively. Depth profiles of the ions in the soil solutions collected from BH-2 in August 2006 and December 2006 are presented in Fig. 12 and 13, respectively.

Comparison of the analyses of the soil water samples collected in October 2005 (post monsoon) and June 2006 (pre monsoon) leads to the following observations;

- Chloride peaks in both the cases at 7 m with an increase in concentration from 500 to 1000 mg/L, respectively,
- Nitrate peaks in 2005 and 2006 are at 7 m with an increase in concentration from 100 to 200 mg/L and
- Sulphate peaks in 2005 and 2006 are at 7 m with an increase in concentration from 100 to 300 mg/L.

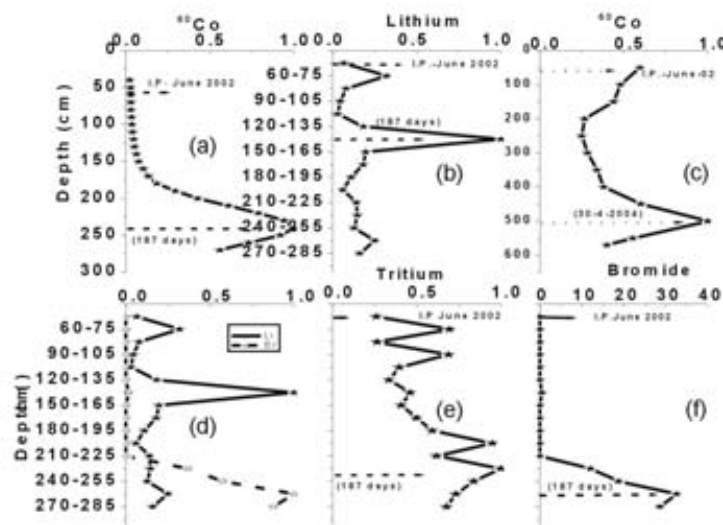


FIG. 7. Tracer displacement profiles during 2003 and 2004. (Tracer concentrations are normalized).

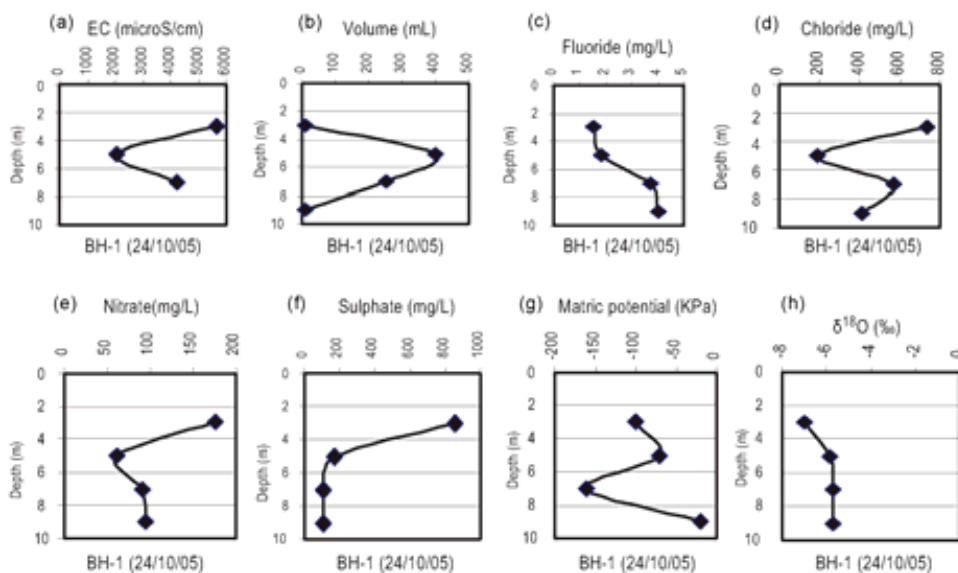


FIG. 8. Depth profile plots of ions (a to f), matric potential (g), and  $\delta^{18}O$  (h) in soil solutions collected from the lysimeters in Borehole No.1 during 24/10/05.

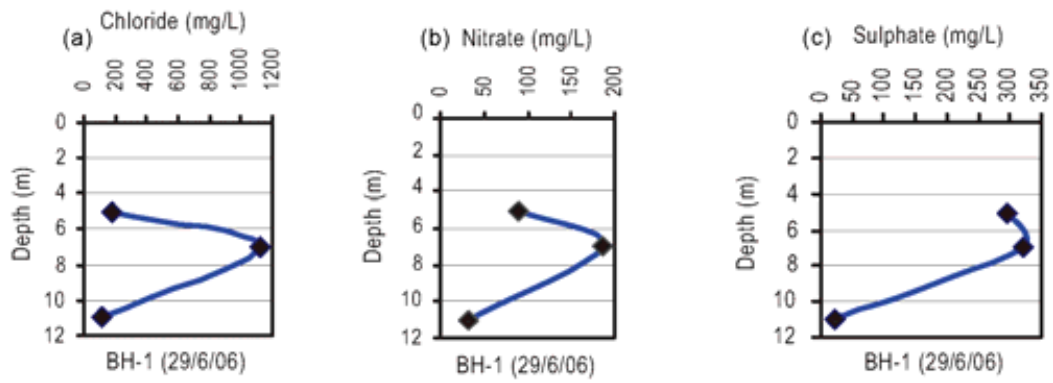


FIG. 9. Depth profile plots of ions in soil solutions collected from the lysimeters in Borehole No.1 during 29/6/06.

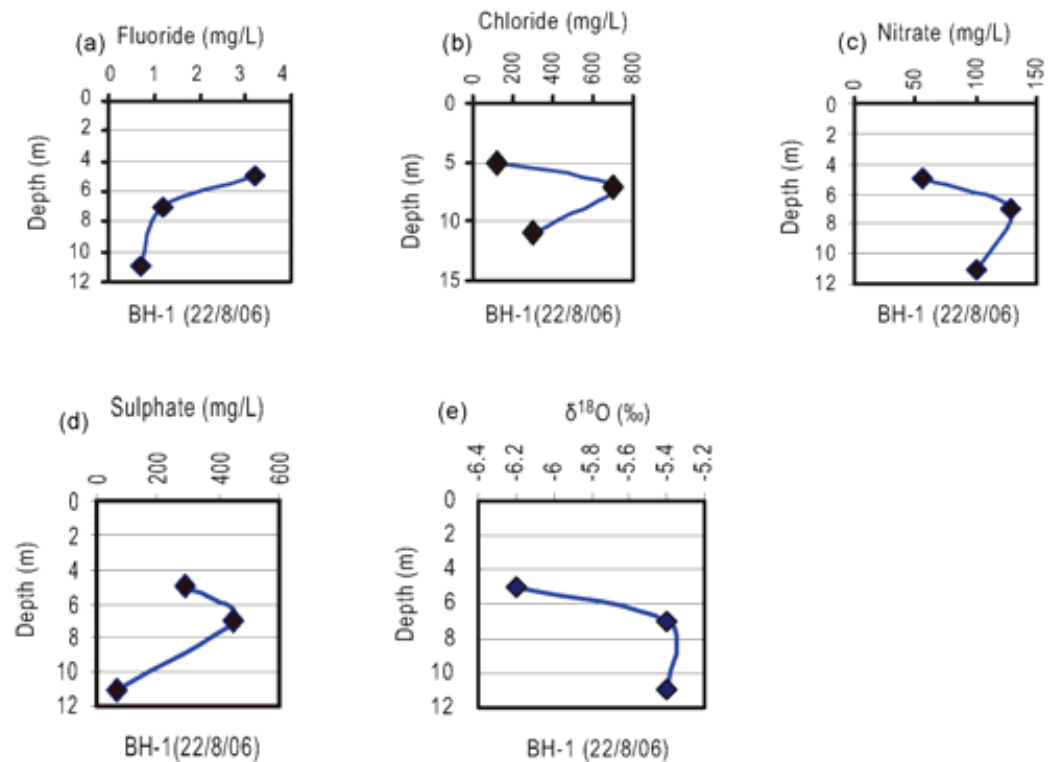


FIG. 10. Depth profile plots of ions (a to d) and  $\delta^{18}O$  (e) in the soil solutions collected from the lysimeters in Borehole No.1 during 22/8/06.

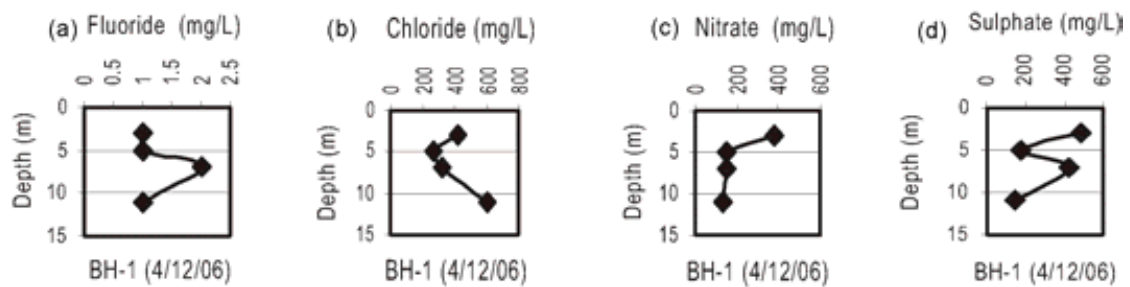


FIG. 11. Depth profile plots of ions (a to d) in soil solutions collected from the lysimeters in Borehole No.1 during 4/12/06.

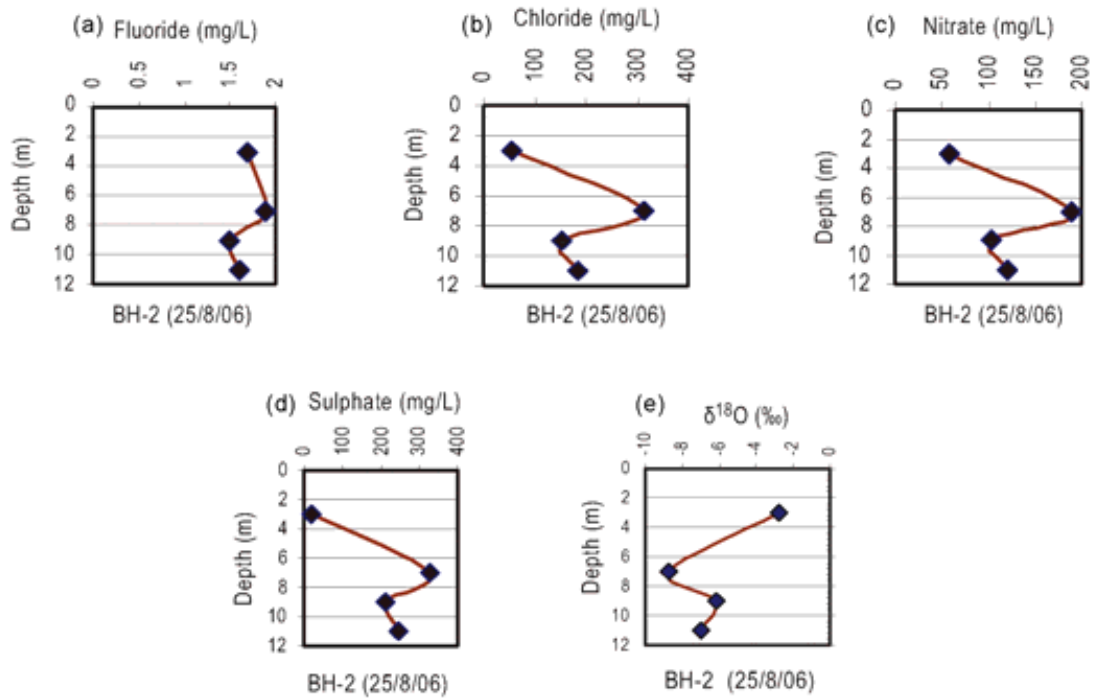


FIG. 12. Depth profile plots of ions (a to d) and  $\delta^{18}O$  (e) in soil solutions ( Borehole No.2 during 25/8/06).

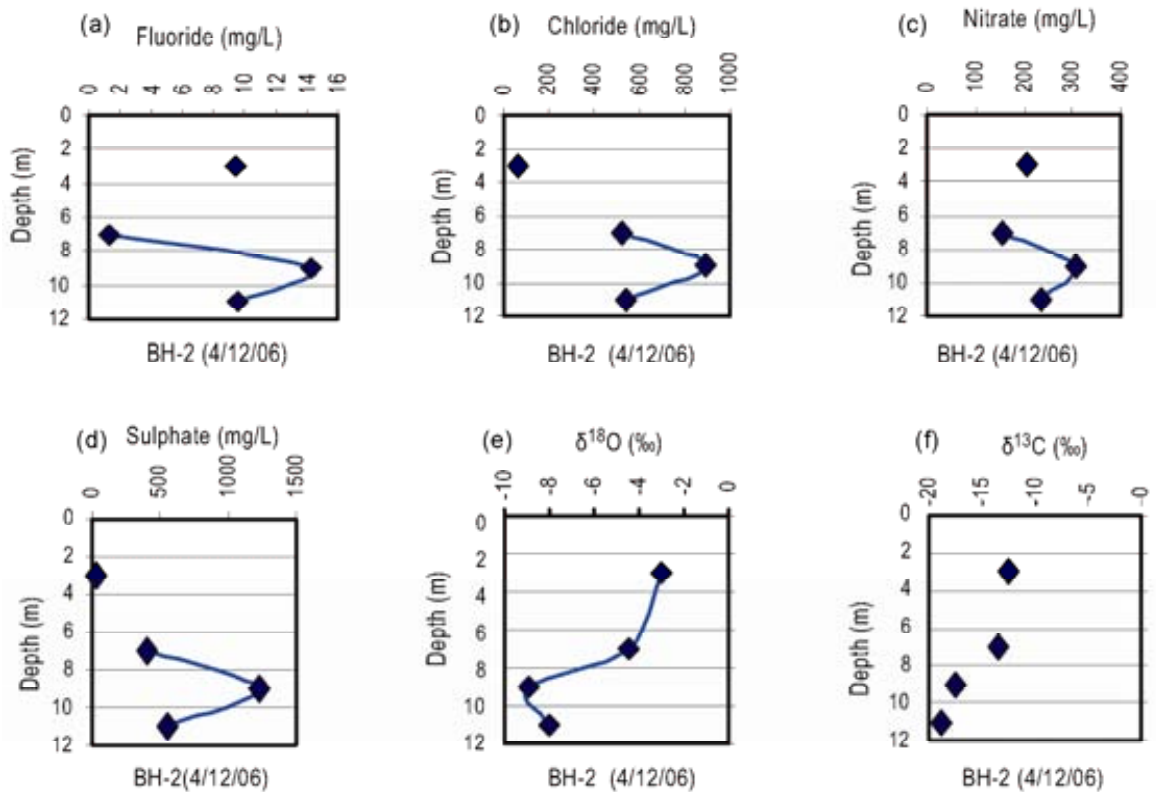


FIG. 13. Depth profile plots of ions (a to d),  $\delta^{18}O$  (e), and  $\delta^{13}C$  (f) in soil solutions collected from the lysimeters in Borehole No.2 during 4/12/06.

### 5.3. Findings from the soil solutions collected from BH-1 and BH-2

From the depth profiles of ions ( $\text{NO}_3^-$ ,  $\text{SO}_4$ ,  $\text{Cl}^-$ ) and  $\delta^{18}\text{O}$ , peaks are observed at 7 m in June 2006 and August 2006 (BH-1) and in August 2006 in BH-2.

- In December 2006 (BH-2), ions and  $\delta^{18}\text{O}$  peaks are shifted to 9 m
- In December 2006 (BH-1), ion peaks are observed at 7 m but possibly may be at 9 m as from 9 m depth soil solution could not be collected.

### 5.4. Soil pore gas

Soil pore gas samples were collected from BH-1 and BH-2 in October 2005 and June, August 2006 respectively, in the pre-evacuated glass bottles. Glass bottle volume was ~ three times the respective volume of gas collecting tube. Results are given in Table 8 and as shown in the Fig.14 gas samples were collected and analysed for carbon dioxide and methane. Depth profile plots are given in Fig.15.

The main findings from pore gas analysis results are:

- Depth wise methane concentrations (Table 8) were closer to the atmospheric concentration and thus indicating absence of reducing environment in the vadose zone and
- Carbon dioxide concentrations were higher in the top layers of the soil (~up to 5 m, ranging from ~7 000 to 10 000 mg/L (Fig. 15)). Higher concentration is due to decay of the plant residues as they are present in top layers.

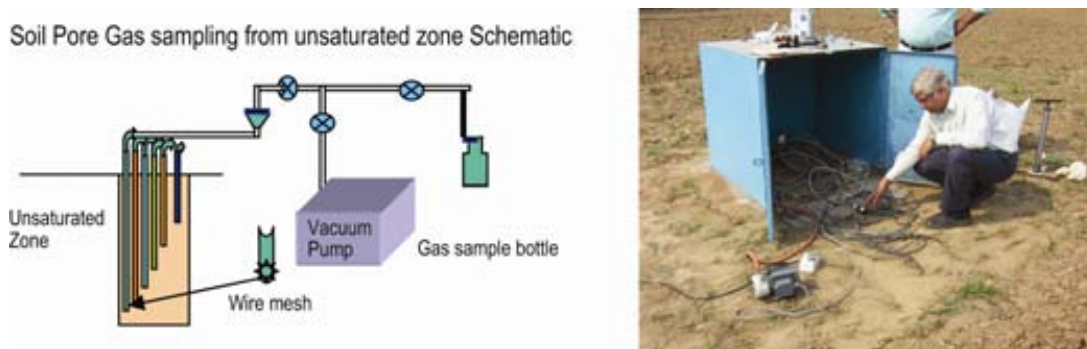


FIG. 14. Pore gas collection schematic and actual installation.

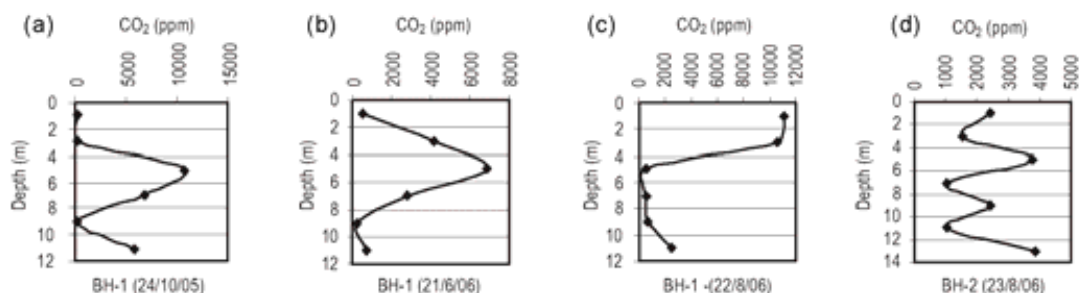


FIG. 15. Depth profile distributions of  $\text{CO}_2$  measured in boreholes BH-1 and BH-2 in four campaigns, from 24/10/2005 (a) to 23/08/2006 (d).

## 5.5. Chemical Quality of Groundwater

Five sets of groundwater were collected during study period and were analyzed for field parameters such as alkalinity, pH, temperature, conductivity, major-ion chemistry and isotopes (Table 9–13). Groundwater quality types were calculated using AquaChem software. The quality is generally Na–Cl–HO<sub>3</sub>. The Piper diagram for groundwater samples collected in June 2001 and May 2003 are given in Fig. 16. During the last decade, annual variations in the concentration of major-ions in the groundwater are not significant. The  $\delta^{18}\text{O}$  of the groundwater during the last decade ranged between  $-6.2$  to  $-7.8\text{‰}$  and is relatively depleted compared to the long-term weighted average value ( $-6.1\text{‰}$ ) of Delhi rainfall. The levels of nitrate (1.2–100 mg/L) and fluoride (1–4 mg/L) in groundwater vary spatially and showed 2–3 fold increase in all the tube wells in a decade. Tank water which is used for irrigation purpose measures a nitrate concentration of  $\sim 48$  mg/L.

Absence of nitrate and fluoride minerals in the geological formation (unsaturated zone) of the study area, suggest considerable leaching of pollutants through the unsaturated zone beneath the root zone. Farms are irrigated from the tank water and all the tube well water samples are pumped in to the tank before irrigation. Due to this system, all tube well waters are clustered in one group which is reflected in  $\delta\text{D}$ – $\delta^{18}\text{O}$  plot also (Fig. 16).

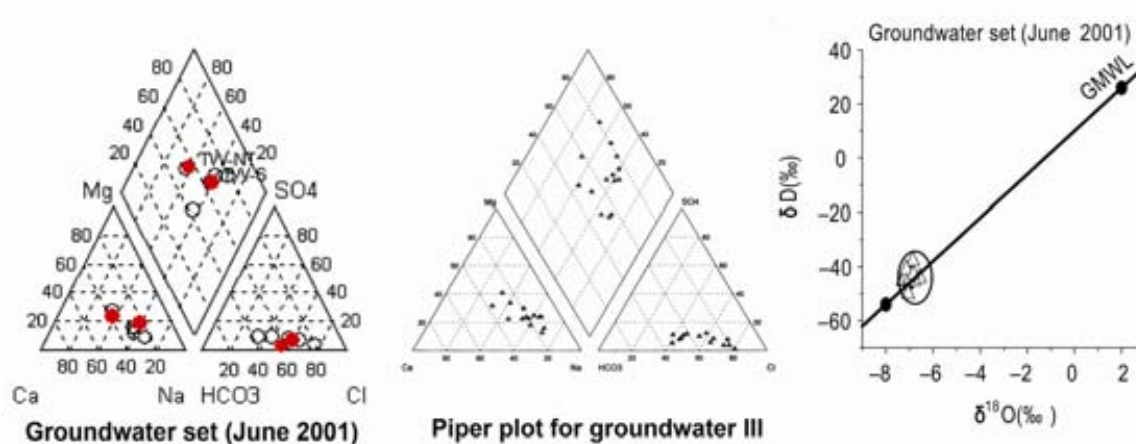


FIG. 16. Piper diagram for groundwater samples collected in 2001 and 2003, and  $\delta\text{D}$ – $\delta^{18}\text{O}$  plot.

## 6. CONCLUSIONS

The injected tracer study indicated that the movement of pollutants is up to 5 m in the study area during June 2002 to April 2004 owing to irrigation and rainfall events. Since no crops were cultivated in the irrigated area after 2004, the driving forces of the pollutant movement was only rainfall. Thereby the observed movement of pollutants was up to 9 m during April 2004 to December 04, 2006. The results of the soil solution indicate that the pollutants would reach the saturated zone in the study area in 7–8 years time. The investigation also indicated absence of reducing environments in the vadose zone and decay of the plant residues in the top layers in the study area. For unsaturated zone pollutant studies, installation of borehole instrumentation for real time data collection and lysimeters for depth sampling of pore waters can be a powerful approach for understanding water and pollutant movement.

## ACKNOWLEDGEMENT

We thank Dr. Gursharan Singh Head, Isotope Applications Division for his interest during the investigation. Thanks are also due to the International Atomic Energy Agency for the financial support extended for carrying out borehole instrumentation work.

**APPENDIX I: DAILY AND MONTHLY RAINFALL DISTRIBUTION (in mm) IN THE STUDY SITE (2002-2005)**

Year 2002 dd/mm/yy	Rainfall (mm)	Year 2003 dd/mm/yy	Rainfall (mm)	Year-2004 dd/mm/yy	Rainfall (mm)	Year 2005 dd/mm/yy	Rainfall (mm)
26/05/02	16	01/01/03	14.2	21/01/04	4.8	23-01/05	2
28/05/02	46	28/01/03	13.6	22/01/04	1.5	28/01/05	0.2
29/05/02	51.2	29/01/03	3.6	23/01/04	3.6	Jan – Total	2.2
May – Total	113.2	31/01/03	10.2	30/01/04	2	06/02/05	7.2
05/06/02	2.4	Jan –Total	41.6	31/01/04	2.2	08/02/05	18.8
20/06/02	1.2	01/02/03	14.7	Jan – Total	14.1	11/02/05	2
22/06/02	1.4	18/02/03	2.3	Feb – Total	0	15/02/05	2.4
25/06/02	17.6	19/02/03	10.8	March - Total	0	16/02/05	1
29/06/2	9.6	28/02/03	0.6	23/04/04	1.2	18/02/05	0.8
30/06/02	6.8	Feb – Total	28.4	24/04/04	2.2	Feb – Total	32.2
June -Total	39	01/03/03	28.2	30/04/04	16.2	05/03/05	3.8
20/7/02	2	03/03/033	1.4	April – Total	19.6	10/03/05	1.8
21/07/02	12.8	March – Total	29.6	01/05/04	16.8	21/03/05	3.4
July - Total	14.8	April – Total	0	26/05/04	4	22/03/05	4
02/08/02	1.5	23/05/03	6.4	28/05/04	4	Mar - Total	13
09/08/02	0.7	25/05/03	1	May – Total	24.8	25/04/05	0.3
10/08/02	0.6	May- Total	7.4	05/06/04	1	28/04/05	4.5
12/08/02	0.7	06/06/03	2	06/06/04	19.6	April	4.8
13/08/02	49.6	20/06/03	20.4	19/06/04	58.4	02/05/05	0.2
23/08/02	0.2	21/06/03	0.6	20/06/04	9.6	03/05/05	1.2
26/08/02	1.2	24/06/03	0.4	22/06/04	1.2	05/05/05	0.2
28/08/02	14.2	25/06/03	2.6	June – Total	89.8	May – Total	1.6
30/08/02	6.6	28/06/03	5.2	04/07/04	0.2	06/06/05	7
Aug – Total	75.3	29/06/03	0.3	07/07/04	5	07/06/05	3.2
06/09/02	0.2	June - Total	31.5	16/07/04	2	10/06/05	0.2
07/09/02	5.8	05/07/03	55.2	July - Total	7.2	24/06/05	18.4
11/09/02	0.7	06/07/03	65	02/08/04	14.2	26/06/05	5
12/09/02	19.8	08/07/03	3	03/08/04	42.6	27/06/05	8.8
13/09/02	102	09/07/03	4	04/08/04	24.2	29/06/05	1
14/09/02	29.8	10/07/03	33.2	10/08/04	10.2	30/06/05	3
16/09/02	9	11/07/03	165.4	11/08/04	10.8	June – Total	46.6
19/09/02	2.5	12/07/03	40.4	14/08/04	7.2	03/07/05	8
Sept - Total	169.8	16/07/03	2	17/08/04	9.4	July - Total	8
13/10/02	2	17/07/03	10.6	19/08/04	2		
Oct – Total	2	18/07/03	32	21/08/04	24.2		
Nov - Total	0	19/07/03	11.2	23/08/04	12.6		
25/12/02	2.8	21/07/03	38	24/08/04	41.6		

Year 2002 dd/mm/yy	Rainfall (mm)	Year 2003 dd/mm/yy	Rainfall (mm)	Year-2004 dd/mm/yy	Rainfall (mm)	Year 2005 dd/mm/yy	Rainfall (mm)
31/12/02	14	22/07/03	12.6	25/08/04	28.8		
Dec - Total	16.8	24/07/03	18.4	26/08/04	57.2		
		28/07/03	63.6	Aug - Total	285.0		
		30/07/03	9	16/08/04	5.4		
		31/07/03	15	Sept - Total	5.4		
		July-Total	578.6	03/10/04	64.4		
		Aug - Total	148	11/10/04	16.2		
		Sept - Total	44.5	29/10/04	5		
		Oct - Total	0	Oct - Total	85.6		
		Nov- Total	0	Nov - Total	0		
		Dec - Total	21.3	Dec - Total	0		

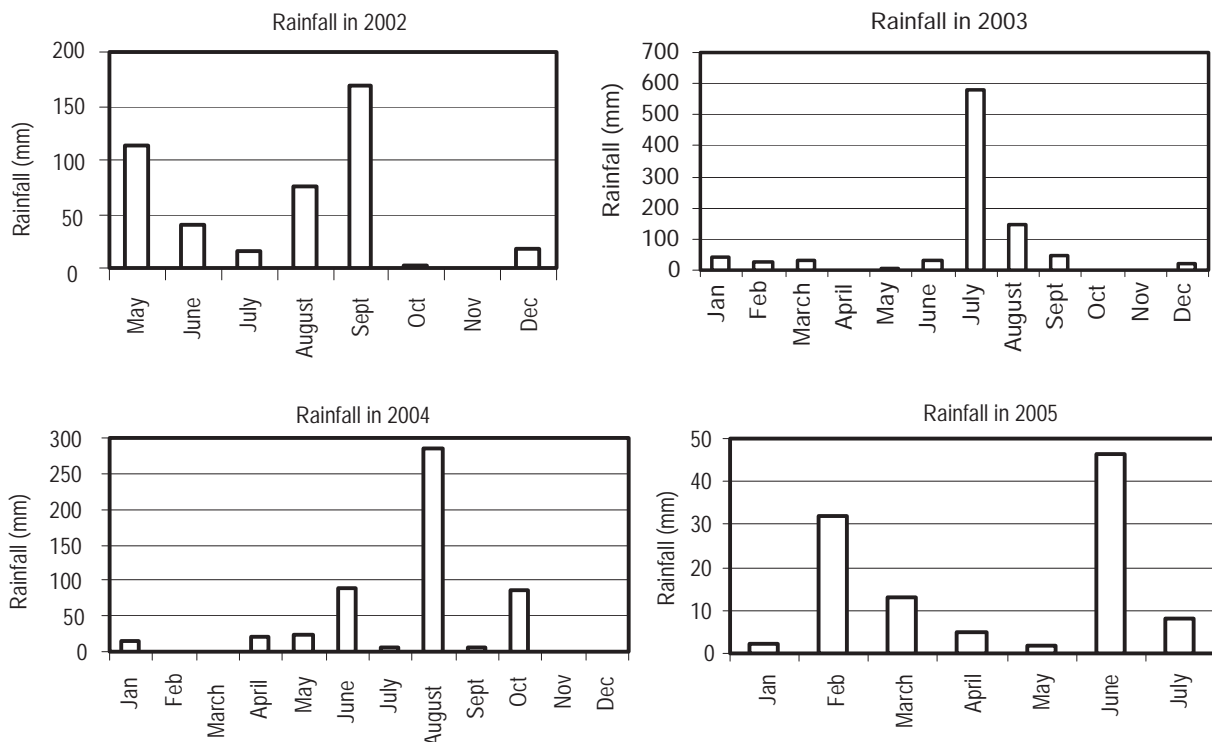


FIG. A-1 Distribution of monthly rainfall in the study site 2002 to 2005

#### APPENDIX II: ESTIMATION OF RECHARGE RATE BASED ON TRACER EXPERIMENT DATA

Period	Rain fall (cm)	Irrigation (cm)	C.G of <sup>60</sup> Co (cm)	C.G of Tritium (cm)	Recharge (%)
30/6/ 02 – 4/1/ 03	30.0	25.0	162.5		18.8
30/6/ 02 – 4/1/ 03	30.0	25.0		125.4	14.45
30/6/02 – 30/4/04	128.95	70.0	283.14		

APPENDIX III. TRACER EXPERIMENTS (Co-60 AND TRITIUM): CALCULATIONS OF CENTERS OF GRAVITY

Depth (cm)	Count (cpm)	Depth × Count		Depth range (cm)	Count (cpm)	Mean depth (cm)	Depth × Count	
40	7159	286360	162.1247 cm	60-75	1117	67.5	75397.5	125.4551 cm
50	8884	444200		75-90	428	82.5	35310	
60	9648	578880	C.G.-Co-60	90-105	1107	97.5	107932.5	C.G - Tritium
70	9397	657790		105-120	638	112.5	71775	
80	9710	776800		120-135	540	127.5	68850	
90	10559	950310		135-150	714	142.5	101745	
100	11494	1149400		150-165	657	157.5	103477.5	
110	12595	1385450		165-180	803	172.5	138517.5	
120	14398	1727760		180-195	953	187.5	178687.5	
130	15987	2078310		195-210	1526	202.5	309015	
140	19835	2776900		210-225	995	217.5	216412.5	
150	23759	3563850		225-240	1610	232.5	374325	
160	32089	5134240	240-255	1352	247.5	334620		
170	42249	7182330	255-270	1178	262.5	309225		
180	57383	10328940	270-285	1089	277.5	302197.5		
190	91485	17382150		14707	2587.5	2727488		
200	132958	26591600						
210	189780	39853800						
220	245860	54089200						
230	293145	67423350						
240	311721	74813040						
250	286944	71736000						
260	230213	59855380						
270	175908	47495160						
	2243160	498261200						
50	0.597	29.85	283.1472 cm					
100	0.48	48						
150	0.44	66	C.G. Co-60					
200	0.2667	53.34						
250	0.25	62.5						
300	0.2848	85.44						
350	0.341	119.35						
400	0.38	152						
450	0.602	270.9						
500	1	500						
550	0.554	304.7						
570	0.4	228						
	5.5955	1920.08						



# SALINITY AND METAL TRANSPORT THROUGH THE UNSATURATED ZONE, KASUR, PAKISTAN

M.A. TASNEEM, M. ALI, Z. LATIF, M. AHMAD, T. JAVED,  
A. MASHIATULLAH, W. AKRAM  
Isotope Application Division,  
Pakistan Institute of Nuclear Science and Technology,  
P.O. Nilore, Islamabad, Pakistan

## ABSTRACT

The area surrounding Kasur, 60 km east of Lahore, Pakistan, has been contaminated with salinity and trace elements by waste disposal from about 300 tanneries. Over the years, tannery wastes were discharged to open land which eventually became a pond. Sewage from Kasur city also is discharged to the waste pond. Water from 43 wells in the study area had  $\delta^{18}\text{O}$  and  $\delta^2\text{H}$  compositions ranging from about  $-2.8$  to  $-10$  ‰ and  $-25$  to  $-72$ ‰, respectively. The lightest values were from high-quality low specific conductance water ( $<1,300$   $\mu\text{S}/\text{cm}$ ) infiltrated from a canal carrying water from the river Chenab. The heaviest value was poor-quality, high specific conductance water ( $>4,000$   $\mu\text{S}/\text{cm}$ ) infiltrated from the waste pond. Native groundwater had specific conductance less than  $2,000$   $\mu\text{S}/\text{cm}$  and  $\delta^{18}\text{O}$  and  $\delta^2\text{H}$  compositions of ranging from  $-5.4$  to  $-7.9$ ‰ and  $-34$  to  $-54$ ‰, respectively. Water from most wells sampled had specific conductance greater than  $2,000$   $\mu\text{S}/\text{cm}$  and  $\delta^{18}\text{O}$  and  $\delta^2\text{H}$  compositions consistent with mixing of native water with water from the overlying unsaturated zone having compositions ranging from  $-1.5$  to  $-3.5$ ‰ and  $-21$  to  $-35$ ‰, respectively — rather than mixing with water from the waste pond. The unsaturated zone near the tanneries also is contaminated with soluble salts, chromium, copper, and zinc from the tanneries. The highest chromium and zinc concentrations in the unsaturated zone ( $1,920$  and  $4,580$  mg/kg of sample, respectively) was within  $0.25$  m of land surface. High copper concentrations (between  $200$  and  $400$  mg/kg of sample) were present in silt deposits to a depth of about  $3$  m. Chromium, zinc, and copper concentrations at the water table surface were  $<10$ ,  $0.18$ , and  $0.22$  mg/L, respectively. The absence of chromium at the water table was consistent with strongly reducing conditions in the overlying unsaturated zone indicated by the absence of oxygen and the presence of hydrogen sulfide and methane gasses.

## 1. INTRODUCTION

Groundwater contamination is a serious threat to public health in Pakistan and other places throughout the world. In part, this concern has emerged because traditional land use management did not recognize the links between groundwater quality and land use practices. Groundwater quality is now recognized as being closely tied to land use; however, that knowledge has come too late to prevent growing groundwater contamination problems. Altering land use practices, such as sewer lines, landfills and settling ponds to reduce or eliminate the release of contaminants into groundwater is an enormous undertaking. Groundwater management to improve water-quality is complicated by the long residence times of most groundwater systems. Because of these long residence times, even if all contamination sources were eliminated today, it may take many decades for the groundwater quality to improve.

The transport of solutes and gases through the unsaturated zone and into the water table is a complex process which ultimately determines the quality of groundwater. The quantitative relationship between the amount of a contaminant and/or geochemical tracer applied to the soil surface and its concentration in groundwater may be highly uncertain. This is due to the lack of knowledge and data concerning the physical, chemical, and biological transport processes undergone by contaminants and tracers in the unsaturated zone and at the Saturated-Unsaturated Interface Region (SUIR).

The study area, Kasur, Pakistan (Fig. 1) contains a cluster of about 300 tanneries that process the hides and skins up to the wet-blue stage (Table 1). The unprocessed waste from the tanneries has been discharged to open land, for the last four/five decades, creating a pond (Fig. 2). The sewage from the Kasur city also is discharged to the pond along with the tannery waste. The tannery waste and sewage have increased the salinity and trace element concentrations in the surrounding groundwater.

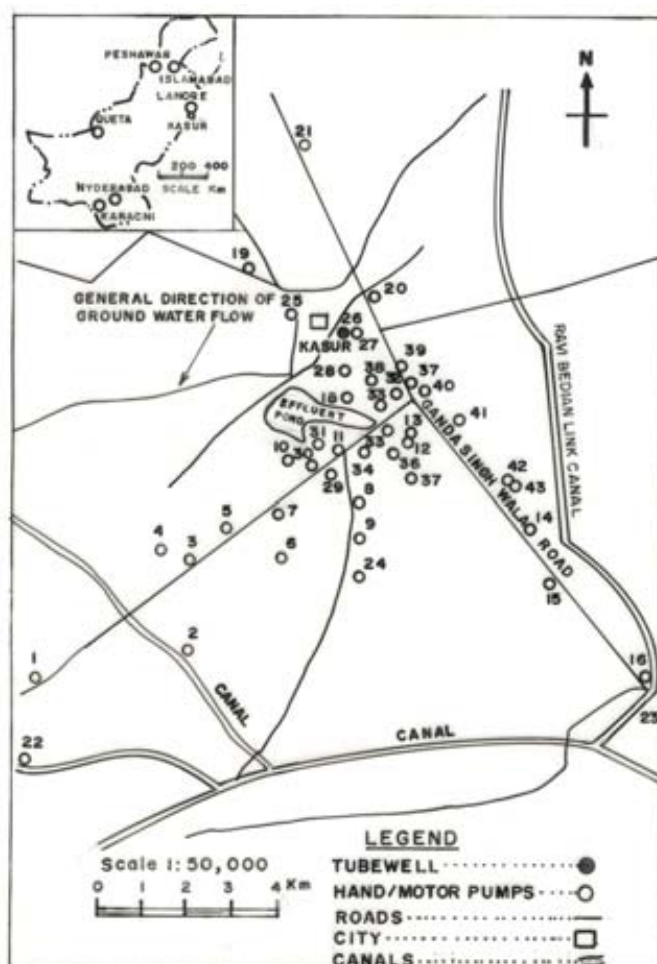


FIG. 1. Location map of groundwater sampling points.

TABLE 1. HIDE PROCESSING, CHEMICALS USED, AND WASTE PRODUCED AT TANNERIES NEAR KASUR. FLOW DIAGRAM

Process	Chemicals Used	Waste Contents
Washing and Water Soaking		Blood, Dirt, Salt
↓		
Liming and Hair removal	CaO, Na <sub>2</sub> S	Lime, Protein, Hair, Sulphide
↓		
Fleshing		Fleshing, BOD
↓		
Bating	(NH <sub>4</sub> ) <sub>2</sub> SO <sub>4</sub> , Na HSO <sub>3</sub>	Protein, Ca, BOD
↓		
Chrome Tan	H <sub>2</sub> SO <sub>4</sub> , Chrome Salt	Chromium, BOD
↓		
Colouring	Oils and Dyes	Oil, Dye
↓		
Finishing		



*FIG. 2. Pond formed by tannery effluents and sewage waste near Kasur, Pakistan.*

## **2. PURPOSE AND SCOPE**

The purpose of this study was to determine the source of water and contamination to wells in the Kasur area. Scope of the study included collection and analysis of water from wells and the collection and analysis of solid, material, water, and gasses from the overlying unsaturated zone. The data were intended to determine if the tannery waste and sewage disposal pond was the primary source of contamination or if water movement and contaminant transport through contaminated soils and the unsaturated zone also was contributing to groundwater contamination.

## **3. THE KASUR STUDY AREA**

The study area lies in Bari Doab, which is a part of Punjab plain. Punjab plain covers major portion of the cultivated land in Indus Plain. Kasur area is adjacent to Lahore city whose climate is semi-arid with average precipitation about 520 mm/a. High temperatures approach or exceed 40°C from April to October and low temperatures near 0°C in December to February. The Bamnawala Ravi Bedian Depalpur Canal crosses the study area. Water in the canal is diverted from the river Chenab at the Marala Head Works.

Quaternary alluvium underlying the Punjab Plain has been deposited on semi-consolidated Tertiary rocks or on the pre-Cambrian basement. The alluvial deposits of the Punjab, in spite of heterogeneous composition, form a unified, highly transmissive aquifer, in which groundwater occurs essentially under water table conditions. The uppermost 90 meters of aquifer compose the most productive zones. The lateral permeability of the alluvium ranges from  $1.5 \times 10^{-4}$  to  $1.5 \times 10^{-3}$  m/sec and is roughly of an order of magnitude higher than the vertical permeability,  $0.3 \times 10^{-5}$  to  $0.3 \times 10^{-3}$  m/sec [1].

## **4. FIELD METHODS**

### **4.1. Groundwater sample collection**

The groundwater samples were collected from thirty four sampling points distributed across the area of waste disposal (Fig. 1). The sampling points consisted shallow hand pumps, tube wells and effluent water. Four water samplings were carried out. The water samples were also collected from the experimental site, just from the water table and at a depth of about 200 feet. Specific conductance, pH, temperature and dissolved oxygen were measured in the field. The water samples were analyzed for stable isotopes of oxygen and hydrogen. Water samples from selected locations were analyzed for  $\delta^{15}\text{N}$  and  $\delta^{34}\text{S}$  also.

## **4.2. Drilling and installation of piezometers and unsaturated zone gas sampling**

A borehole was drilled by hand auger to the water table, 6.5 meters below land surface. During the study period the water table in the area declined from 6.5 m to 8.5 m below land surface. Tygon tubing (I.D. ~3 mm) of various lengths ranging from 0.5 meter to 6.0 meters with an interval of 0.5 m, was lowered into the unsaturated zone to collect gasses at different depths. The top portion of all tubes were aligned and fitted with rubber septa. Small pieces of nylon mesh were wrapped around the bottom of all tubes to avoid entry of insects etc. The tubing was marked for each sample depth and the hole was back-filled with native material. After installation, the tubes were evacuated to adequate volumes so that the internal air in the tubing is excluded. The tubing nest was then covered with a PVC closed end pipe. An additional borehole was drilled and used for monitoring the water table and measurement of soil moisture with Neutron moisture gauge. Because of water-level declines during the study, an additional gas collection tube was installed in a separate bore hole at a depth of 7.0 meter.

## **4.3. Collection of core material**

The samples from the unsaturated zone were collected using a hand auger at an interval of 25 cm from land surface to the water table. The samples were analyzed for the following:

- grain size analysis
- soil moisture content
- $\delta^{18}\text{O}$  and  $\delta^2\text{H}$  isotopic analyses
- EC measurement
- chemical analysis

Samples intended for grain-size distribution and chemical analyses were packed in polyethylene bags. Samples intended for analysis of water content and extraction of water for isotopic analyses were packed in polyethylene bags and then put in leak-tight metal boxes.

## **4.4. Collection of unsaturated zone gases**

During sample collection, 50 ml of air was removed from the air-sampler tubing with a hypodermic syringe. The syringe needles were closed with rubber plugs to exclude external air. Concentrations of  $\text{O}_2$  and  $\text{CO}_2$  collected in the syringe were measured using a portable gas analyzer. Concentrations of hydrogen sulfide and methane were measured for the last two sample sets.

# **5. LABORATORY METHODS**

## **5.1. Grain size distribution and water content**

Grain size distribution was determined on polyethylene bagged samples by the Geotechnical Testing laboratory at Lahore through Sieve and Hydrometric analyses. Gravimetric water content was measured on polyethylene bagged samples protected from evaporation in air-tight containers. Ten gram sample was dried in an oven overnight at a temperature of  $105^\circ\text{C}$ , the dry soil sample was then weighed and soil moisture content (weight percent) was calculated.

## **5.2. Pore water extraction for isotopic analyses**

A moisture extraction system (Fig. 3) was designed and fabricated locally to extract water from the unsaturated core samples without any isotopic fractionation. To extract water a wide mouth, round bottom, one-liter flask containing 60 to 80 g of sample is connected to a vacuum line at the entry of the extraction system. The system, containing three moisture traps, is evacuated with rotary vacuum pump. The moisture traps are cooled to  $-196^\circ\text{C}$  using liquid nitrogen. The round bottom flask containing the sample is gradually heated in a water-bath at  $95^\circ\text{C}$ . Gases evolved from the samples are evacuated and water from the moisture traps is collected in clean air tight glass bottles.



*FIG. 3. Soil moisture extraction system.*

### **5.3. Measurement of electrical conductivity (EC) of soil samples**

For measurement of EC, 40 g sample was placed in a 300 ml titration flask with 100 ml of distilled water. The flask and its contents were shaken for 10 minutes. Then the supernatant liquid was poured into a 150 ml test tube and the conductivity was measured using a conductivity meter LF 91 from Karl Kolb, Germany.

### **5.4. Chemical analyses of soil samples**

Soil samples were oven dried at 105°C for 24 hours and homogenized by grinding. 2.5 g dried and homogenized sample was treated with 10 ml aliquots of concentrated HNO<sub>3</sub> at 90°C for 30 minutes and diluted to 50 ml with 1% HNO<sub>3</sub>. The solution, thus prepared, was analyzed for selected metals by atomic absorption spectrophotometry.

### **5.5. Nitrate and <sup>15</sup>N analyses**

For nitrate and  $\delta^{15}\text{N}$  analyses, 10 g of soil in a bottle with 100 ml of 2M KCl. was shaken in a mechanical shaker. The soil-KCl solution was allowed to settle until the supernatant liquid was clear. The supernatant was filtered using Whatman filter paper No. 42. The Bremner and Kenny (1966) method, with certain modifications, was used to extract nitrate nitrogen. Ammonium-N was distilled by using 0.2 g magnesium oxide for 20 ml of soil extract. Distillate was collected in the flask up to 30 ml mark containing 5 ml boric acid indicator. Nitrite was destroyed by using sulfamic acid. Nitrate-N was distilled by the addition of 0.2 g ball milled Devarda alloy. Nitrogen contents were determined by titration with 0.05 N H<sub>2</sub>SO<sub>4</sub> and sample was concentrated by using 0.2 ml 1 N sulfuric acid. Ammonium concentrates were converted to nitrogen gas using potassium hypobromide solution in Rittenberg ampoules.

## **6. RESULTS OF GROUND WATER DATA COLLECTION**

### **6.1. Specific conductance of groundwater**

The specific conductance of water from 45 sampled wells ranged from 127 to 9,800  $\mu\text{S}/\text{cm}$ , with a median value of about 1,900  $\mu\text{S}/\text{cm}$ . Specific conductance of pond water was 13,800  $\mu\text{S}/\text{cm}$ . The lower specific conductance was from well 22 adjacent to the Bambanwala Ravi Bedian Depalpur Canal. The specific conductances of water from wells 23, and 16 adjacent to the canal also were low. The highest values were from well 35.

## 6.2. Oxygen-18 and deuterium composition of groundwater

The  $\delta^{18}\text{O}$  values of groundwater range from  $-10.0\text{‰}$  to  $-2.77\text{‰}$  and  $\delta^2\text{H}$  values range from  $-71.8\text{‰}$  to  $-24.7\text{‰}$ . Values are similar for both shallow and deeper groundwater. Results from the four sample collection trips are presented in Tables 1, 8, 9, 10 and the average data from each sampled well are plotted in Fig. 4. The range of isotopic data along meteoric water line suggests that the groundwater is characterized by several different isotopic compositions reflecting different sources of recharge.

Lighter (more negative) isotopic values measured in water from wells 22, 23, and 16 (Fig. 4) correspond to recharge from the Bambanwala Ravi Bedian Depalpur Canal, diverted from the river Chenab at the Marala Head Works. Previous work by Tasneem et al. (1994) showed that isotopic composition of river Chenab at Marala Headworks was about  $-10.0\text{‰}$  for  $\delta^{18}\text{O}$  and  $-61.0\text{‰}$  for  $\delta^2\text{H}$ . The specific conductances of water from these wells are generally less than  $1,300\ \mu\text{S}/\text{cm}$  and these wells are not contaminated by infiltration from the effluent pond. As previously discussed, water from well 22 had the lowest average specific conductance.

A number of wells having heavier (less negative)  $\delta^{18}\text{O}$  and  $\delta^2\text{H}$  contents that plot along the Meteoric Water Line and comparatively low specific conductance (Fig. 4) were not associated with the canal or with infiltration of water from the Chenab River (Fig. 1). These wells include wells 43, 26, and 25. Values from these wells probably reflect the isotopic composition of native ground water recharged primarily by the infiltration of precipitation.

The heaviest (least negative) isotopic values reflect infiltration of water from the effluent pond. The isotopic composition of water from the pond has been enriched by evaporation. As a group, water from these wells has higher specific conductances and water from well K-35 has the highest specific conductance.

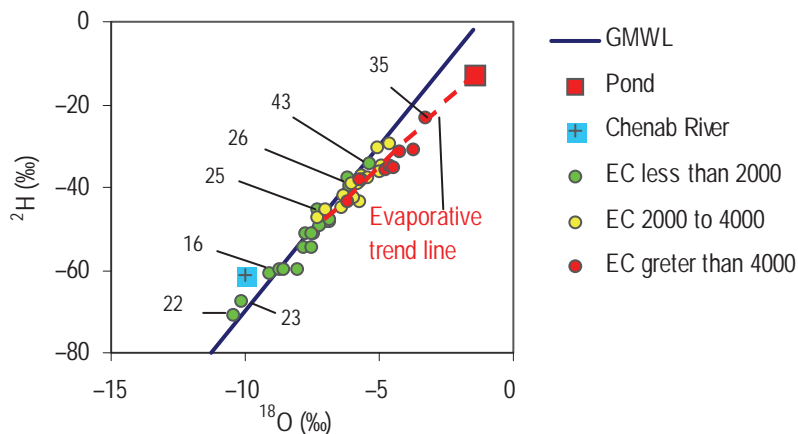


FIG. 4. Plot of  $\delta^{18}\text{O}$  vs.  $\delta^2\text{H}$  of groundwater collected in 2002-03 from Kasur area.

TABLE 1. ISOTOPIC AND PHYSICO-CHEMICAL DATA OF WATER SAMPLES

Sample No.	EC ( $\mu\text{S/cm}$ )	Temp. ( $^{\circ}\text{C}$ )	pH	Dissolved $\text{O}_2$ ( $\text{mg/L}$ )	$\delta^{18}\text{O}$ ( $\text{‰}$ )	$\delta^2\text{H}$ ( $\text{‰}$ )
KS-0	13830	27	8.42	4.13	-1.42	-12.78
KS-01	1905	25	7.20	4.28	-8.74	-61.33
KS-02	1310	25	Collected for EC only			
KS-03	1685	25	7.17	4.03	-7.80	-58.39
KS-03A	1750	15	Collected for EC only			
KS-04	538	18	Collected for EC only			
KS-05	1619	25	7.04	4.03	-7.42	-53.35
KS-06	2222	24	Collected for EC only			
KS-07	3373	24	7.23	4.03	-6.48	-45.59
KS-08	1780	25	7.31	3.48	-6.68	-46.14
KS-09	1772	25	7.33	4.10	-7.37	-50.62
KS-10	3125	25	7.42	3.38	-5.39	-36.39
KS-11	1660	25	Collected for EC only			
KS-12	4923	25	7.44	3.75	-5.92	-42.37
KS-13	1072	24	Collected for EC only			
KS-14	930	24	Collected for EC only			
KS-15	1290	26	7.42	2.98	-7.82	-54.88
KS-16	2757	25	7.70	3.10	-6.52	-45.77
KS-17	6153	25	7.61	3.13	-4.58	-34.55
KS-18	625	26	8.22	3.23	-6.21	-35.47
KS-19	4005	26	8.04	4.15	-5.00	-36.15
KS-20	1452	25	7.41	3.05	-7.43	-51.70
KS-21	1175	25	7.44	3.30	-8.89	-61.27
KS-22	722	25	7.87	3.07	-9.97	-65.96
KS-22 A	813	24	6.87	3.30	-9.00	-62.83
KS-23	2090	28	8.09	3.63	-7.76	-49.25
KS-24	2930	26	7.70	4.60	-4.13	-31.03
KS-24 A	2920	27	8.01	3.90	-5.15	-41.00
KS-24 B	5380	27	7.01	4.30	-4.26	-33.81
KS-25	1111	26	8.03	4.85	-7.96	-53.62
KS-26	1889	26	7.92	2.98	-7.75	-50.74
KS-27	1541	25	7.85	2.83	-6.28	-43.92
KS-28	4890	27	7.93	2.10	-5.58	-36.24
KS-29	815	31	7.83	3.95	-6.44	-37.39
KS-30	1862	27	7.38	3.80	-7.60	-50.76

TABLE 2. RESULTS OF TEXTURAL AND ORGANIC MATTER ANALYSIS OF SOIL SAMPLES

Depth (m)	Sand (%)	Silt (%)	Clay (%)	Organic matter (%)
0.00	11	66	23	0.82
0.25	1	59	40	0.09
0.50	2	60	38	0.14
0.75	25	61	14	0.08
1.00	33	55	12	0.19
1.25	10	65	25	0.12
1.50	7	74	19	0.29
1.75	10	71	19	0.21
2.00	13	76	11	0.11
2.25	11	74	15	0.28
2.50	14	72	14	0.26
2.75	7	54	39	0.10
3.00	25	39	36	0.09
3.25	36	51	13	0.18
3.50	90	8	2	0.21
3.75	85	12	3	0.16
4.00	92	7	1	0.09
4.25	94	4	2	0.12
4.50	94	4	2	0.06
4.75	93	7	–	0.13
5.00	95	4	1	0.09
5.25	91	7	2	0.13
5.50	97	3	–	0.10
5.75	55	41	4	0.06

TABLE 3. ELECTRICAL CONDUCTIVITY AND MOISTURE CONTENTS OF SOIL WITH DEPTH

Depth (cm)	EC ( $\mu\text{S}/\text{cm}$ )	Moisture content (%)	Depth (cm)	EC ( $\mu\text{S}/\text{cm}$ )	Moisture content (%)
0	7010	25.5	300	1080	17.5
25	7260	29.7	325	1298	18.4
50	5460	24.9	350	489	5.6
75	4760	19.4	375	875	10.1
100	4210	18.7	400	653	5.6
125	5270	27.6	425	447	4.9
150	5700	29.1	450	676	9.0
175	4530	24.3	475	506	5.2
200	5210	33.0	500	475	5.4
225	5000	29.1	525	770	10.9
250	3900	30.0	550	541	7.5
275	2930	27.0	575	892	14.4

TABLE 4. ISOTOPIC CONCENTRATION OF WATER FROM THE UNSATURATED ZONE WITH DEPTH

Depth (cm)	$\delta^{18}\text{O}$ (‰)	$\delta^2\text{H}$ (‰)	Depth (cm)	$\delta^{18}\text{O}$ (‰)	$\delta^2\text{H}$ (‰)
0	-2.71	-26.60	325	-3.35	-29.91
25	-2.89	-28.19	350	-2.61	-28.77
50	-2.90	-27.93	375	-2.25	-24.71
75	-1.49	-21.44	400	-1.72	-23.65
100	-2.68	-25.92	425	-2.36	-26.26
125	-2.63	-26.17	450	-2.65	-25.93
150	-2.84	-28.63	475	-2.78	-25.49
175	-3.01	-27.86	500	-2.49	-26.02
200	-2.97	-27.69	525	-3.40	-29.89
225	-2.66	-27.63	550	-2.56	-29.67
250	-2.78	-28.01	575	-3.87	-34.85
275	-3.25	-29.42	Effluents	-4.11	-34.06
300	-3.82	-34.49			

TABLE 5. CONCENTRATIONS OF MAJOR AND TRACE ELEMENTS IN SOIL

Depth (cm)	Na (mg/L)	K (mg/L)	Ca (mg/L)	Mg (mg/L)	Cr (mg/L)	Fe (mg/L)	Zn (mg/L)	Cu (mg/L)
0	3849	9340	7690	ND	96	15084	229	20
25	3516	9861	4776	ND	28	15616	71	19
50	2580	8180	9440	ND	16	13926	48	15
75	2206	8058	6260	ND	15	11446	39	12
100	1912	7070	6792	ND	12	10523	36	10
125	2102	6924	10958	ND	12	11506	52	12
150	2425	7380	13442	ND	13	14142	53	15
175	1951	6520	9960	ND	12	13014	45	10
200	2047	7164	10512	ND	14	13560	49	15
225	1863	7320	10152	ND	15	13467	50	13
250	1760	6642	9084	ND	28	12240	41	12
275	1164	9160	2788	ND	17	16610	55	16
300	902	8153	3222	ND	19	15336	51	15
325	643	5420	4930	43	11	10158	36	9
350	247	2460	7302	198	12	7233	24	4
375	303	2220	7548	211	7	6993	32	5
400	293	2012	9246	248	14	5046	17	5
425	211	1884	7748	316	8	4192	16	4
450	373	2564	7578	245	13	4508	45	7
475	250	3170	7814	224	6	4974	20	7
500	212	2282	8320	310	11	4018	16	5
525	329	2570	9410	294	13	4114	22	6
550	234	1320	10504	301	5	3574	17	4
575	399	2714	8586	282	9	5654	23	7
G.W.	1827	408	43.4	31.3	ND	6.9	0.18	0.22
G.W.	766	184.7	48.23	33.2	ND	1.6	0.22	0.02

Note: ND — not detected.

TABLE 6. CONCENTRATION OF PORE GASES WITH DEPTH (FIRST SAMPLING)

Depth (m)	CO <sub>2</sub> (%)	O <sub>2</sub> (%)
0.50	1.41	18.40
1.50	2.24	16.90
2.00	2.09	17.40
2.50	2.59	18.00
3.00	3.11	16.50
3.50	2.32	17.50
4.00	3.12	16.60
4.50	3.85	15.00
5.00	3.51	15.40
5.50	3.32	15.70
6.00	3.57	15.40
6.50	3.91	15.20

TABLE 7. CONCENTRATION OF PORE GASES WITH DEPTH. (SECOND SAMPLING)

Depth (m)	CO <sub>2</sub> (%)	O <sub>2</sub> (%)
0.50	1.35	17.80
1.00	1.81	17.00
1.50	1.63	16.50
2.00	1.00	17.40
2.50	1.83	16.30
3.00	2.00	15.40
3.50	2.32	15.30
4.00	2.46	15.20
4.50	2.47	15.20
5.50	2.45	15.30
6.50	2.42	14.60
7.00	2.56	14.50

TABLE 8. ISOTOPIC AND PHYSICO-CHEMICAL DATA OF GROUNDWATER SAMPLES (SEPTEMBER 2002)

Sample No.	EC ( $\mu\text{S}/\text{cm}$ )	$\delta^{18}\text{O}$ (‰)	$\delta^2\text{H}$ (‰)	Sample No.	EC ( $\mu\text{S}/\text{cm}$ )	$\delta^{18}\text{O}$ (‰)	$\delta^2\text{H}$ (‰)
K-1	2220	-7.22	-48.69	K-14	1599	-7.47	-52.22
K-2	1591	-7.44	-54.62	K-15	663	-8.77	-60.16
K-3	1620	-7.64	-51.90	K-16	880	-9.93	-65.09
K-4	3480	-6.40	-45.66	K-17	1928	-7.69	-49.05
K-5	1644	-6.94	-46.88	K-18	2925	-4.10	-30.50
K-6	1833	-7.44	-50.87	K-19	1014	-7.99	-56.28
K-7	3070	-5.17	-35.05	K-20	1938	-7.76	-51.77
K-8	4900	-6.22	-43.01	K-21	1591	-6.18	-43.69
K-9	1491	-7.55	-52.50	K-22	145	-12.36	-83.27
K-10	3080	-6.19	-44.27	K-23	127	-12.52	-86.07
K-11	6680	-4.66	-34.36	K-24	4890	-5.58	-36.24
K-12	653	-6.38	-35.44	K-25	830	-6.67	-37.12
K-13	3960	-5.22	-36.63				

TABLE 9. ISOTOPIC AND PHYSICO-CHEMICAL DATA OF WATER SAMPLES (DECEMBER 2002)

Sample No.	EC ( $\mu\text{S/cm}$ )	$\delta^{18}\text{O}$ (‰)	$\delta^2\text{H}$ (‰)	Sample No.	EC ( $\mu\text{S/cm}$ )	$\delta^{18}\text{O}$ (‰)	$\delta^2\text{H}$ (‰)
K-1	1810	-9.21	-64.90	K-21	1661	-5.97	-43.81
K-2	2030	-9.43	-71.75	K-26	567	-5.23	-34.02
K-3	1640	-7.43	-55.86	K-27	3010	-5.42	-42.36
K-4	4010	-6.45	-43.79	K-28	4780	-5.81	-38.64
K-5	2010	-6.57	-44.93	K-29	3540	-5.42	-40.32
K-6	1863	-7.67	-51.75	K-30	8220	-3.01	-27.74
K-7	3290	-5.06	-35.07	K-31	4320	-3.58	-24.72
K-8	5130	-5.84	-42.20	K-32	7660	-4.17	-30.65
K-9	1098	-8.31	-57.72	K-33	1760	-7.25	-47.15
K-10	3320	-5.94	-42.45	K-34	3730	-5.62	-38.93
K-11	5940	-4.62	-34.25	K-35	9800	-3.94	-30.15
K-12	615	-6.18	-36.21	K-36	2710	-6.04	-39.08
K-13	4010	-4.87	-36.33	K-37	1204	-6.99	-48.3
K-14	1401	-7.14	-50.00	K-38	2830	-4.95	-29.1
K-15	1570	-9.09	-61.48	K-39	2040	-7.38	-47.71
K-16	587	-10.00	-66.49	K-40	2790	-5.65	-35.82
K-17	2280	-7.84	-47.87	K-41	3900	-4.38	-28.53
K-18	2930	-4.13	-31.03	K-42	1345	-5.87	-37.45
K-19	1170	-7.86	-50.35	K-43	1792	-5.6	-37.73
K-20	1820	-7.92	-49.96				

TABLE 10. ISOTOPIC AND PHYSICO-CHEMICAL DATA OF WATER SAMPLES (MARCH 2003)

Sample No.	EC ( $\mu\text{S/cm}$ )	$\delta^{18}\text{O}$ (‰)	$\delta^2\text{H}$ (‰)	Sample No.	EC ( $\mu\text{S/cm}$ )	$\delta^{18}\text{O}$ (‰)	$\delta^2\text{H}$ (‰)
K-1	1793	-9.08	-64.93	K-20	1876	-7.98	-51.24
K-2	1651	-7.20	-53.17	K-21	1520	-6.38	-43.56
K-3	1575	-7.19	-52.19	K-26	605	-5.49	-33.82
K-4	3680	-6.40	-45.59	K-27	3120	-5.56	-43.80
K-5	1818	-6.50	-45.57	K-28	4620	-5.92	-38.96
K-6	1567	-7.57	-50.05	K-29	3350	-5.57	-39.80
K-7	3130	-5.15	-35.07	K-30	8360	-2.77	-26.62
K-8	5530	-5.90	-41.82	K-31	4200	-3.04	-21.41
K-9	1103	-8.25	-56.41	K-32	7040	-4.31	-32.24
K-10	2840	-6.44	-46.08	K-33	1840	-7.06	-44.88
K-11	6140	-4.54	-35.35	K-33 (a)	4830	-4.73	-33.57
K-12	597	-6.16	-35.97	K-34	3670	-5.65	-37.47
K-13	3970	-4.90	-35.45	K-35	9770	-3.55	-31.48
K-14	1310	-7.69	-50.89	K-38	2810	-5.16	-31.60
K-15	1632	-9.10	-62.24	K-39	2020	-7.24	-46.63
K-16	698	-9.99	-66.31	K-40	2640	-5.72	-38.77
K-17	2080	-7.89	-49.46	K-41	3880	-4.83	-29.93
K-18 (a)	2920	-5.15	-41.00	K-42	1350	-5.69	-39.79
K-19	1130	-8.06	-54.28	K-43	1720	-5.14	-30.35

Note: Water table at 28 feet, measurement was carried out at 26 feet.

### 6.3. Nitrate and $\delta^{15}\text{N}$ composition of groundwater

$\delta^{15}\text{N}$  and  $\text{NO}_3^-$  were measured in selected groundwater samples (Fig. 5 and 6). The  $\delta^{15}\text{N}$  values of the groundwater samples ranged from  $-3.14$  to  $+37.10\%$  and the  $\text{NO}_3^-$  concentration varies from 1 to 310 mg/L. Highly positive  $\delta^{15}\text{N}$  values are consistent with the source of  $\text{NO}_3^-$  from sewage, or manure. The sampling points with low  $\text{NO}_3^-$  concentration and enriched  $\delta^{15}\text{N}$  values may indicate denitrification.

## 7. RESULTS OF UNSATURATED ZONE DATA COLLECTION

### 7.1. Particle-size and water content

The upper 3.5 m of the unsaturated zone consists primarily of silt with smaller amounts of clay (Table 2, Fig. 7). The unsaturated zone below a depth of about 3.5 m is composed primarily of sand.

Gravimetric water content ranges from about 5 to 33%. Water contents are higher in the finer-grained surficial units and lower in the underlying sand. After the depth of 5 m, the soil moisture again starts increasing because of the presence of the saturated zone at 5.75 m below land surface (Fig. 8).

### 7.2. $\delta^{18}\text{O}$ and $\delta^2\text{H}$ composition of water in the unsaturated zone

The  $\delta^{18}\text{O}$  and  $\delta^2\text{H}$  isotopic composition of water extracted from soil samples from different depths is presented in Table 4 and plotted as a function of depth in Fig. 11. The isotopic composition of the water does not show any consistent shift with depth, water content, or salinity (as measured by specific conductance of the water extract) and appears to vary primarily as a function of the composition of the infiltrated water and evaporation prior to infiltration.

Comparison of the  $\delta^{18}\text{O}$  and  $\delta^2\text{H}$  composition of unsaturated zone water with groundwater and water in the effluent pond (Fig. 12) shows that the isotopic composition of water in the pond is different from that of water in the unsaturated zone and that water from most wells appears to lie on a mixing line with unsaturated zone waters rather than with water from the effluent pond. These data suggest that high specific conductance in water from wells is related to infiltration of water through the unsaturated zone and dissolution of soluble salts within the unsaturated zone. The exception is water from well 35 having the highest specific conductance measured in any well. Data from well 35 shows that infiltration from the tannery and sewage waste pond is locally important.

The concentrations of major and trace elements in  $\text{HNO}_3$  extracts from unsaturated zone at various depths are given in Table 5. The concentrations of the trace elements chromium, copper, and zinc are of greatest concern in the Kasur area and are shown as a function of depth in Fig. 13. Chromium and

zinc have similar distributions with depth and the highest concentrations are within 0.5 m of land surface, this is consistent with a lack of movement of these elements with infiltrating water through the unsaturated zone. The distribution of copper is different and copper concentrations are higher in the upper 3 m of the unsaturated zone where silt contents are high. Copper concentrations decrease to lower values in the underlying sandy layer. The distribution of copper in the  $\text{HNO}_3$  extracts from unsaturated zone is similar to the distribution of iron suggesting that copper mobility is controlled by sorption on iron hydroxides distributed on the surface of mineral grains. Chromium was not detected in groundwater below the profile at about 6 m below land surface. Copper and zinc were detected in groundwater at the water table surface below the sample profile at concentrations of 0.22 and 0.18 mg/L, respectively. These data are consistent with immobilization and storage of chromium, copper, and zinc contamination within the unsaturated zone.

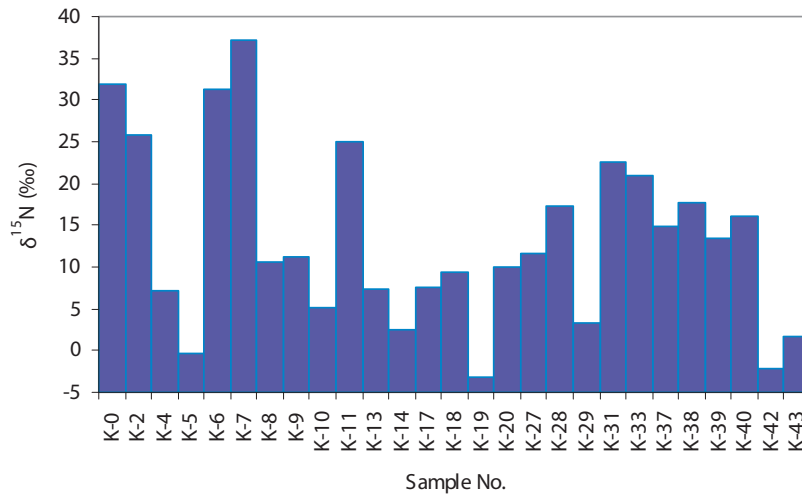


FIG. 5. Variation of  $\delta^{15}N$  in water samples.

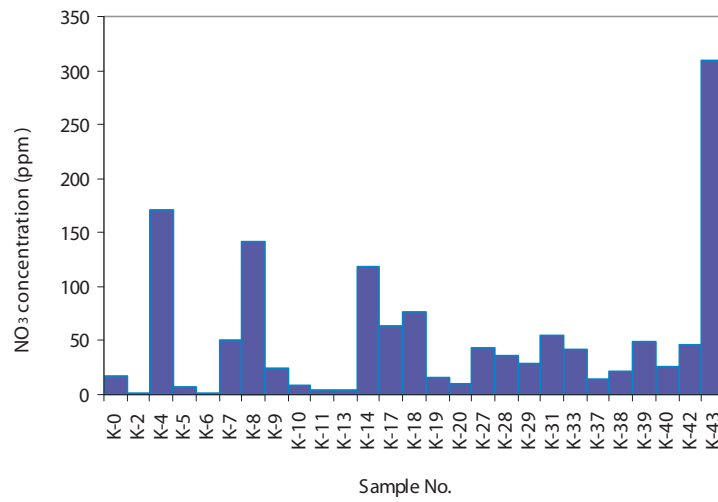


FIG. 6. Variation of  $NO_3$  concentration in water samples.

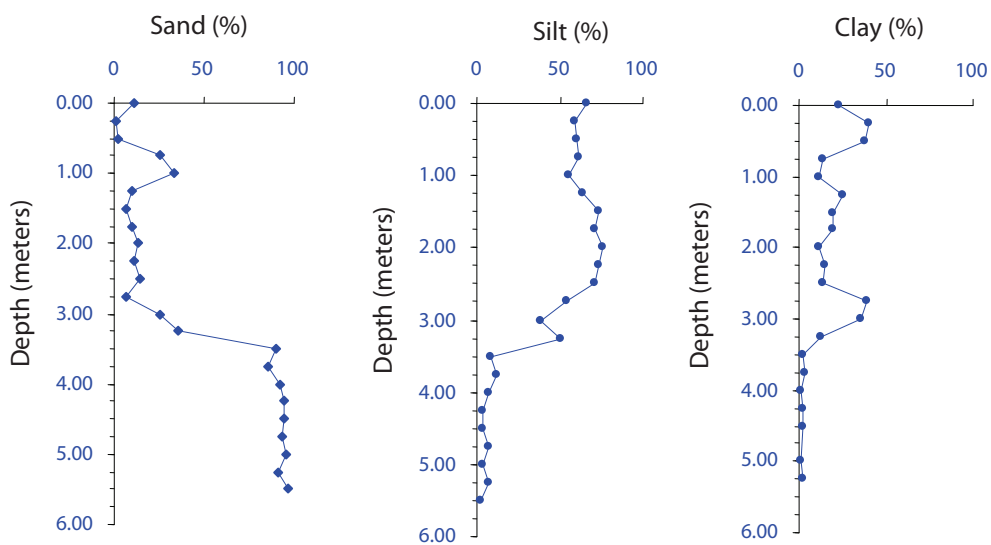


FIG. 7. Grain size distribution in soil samples at different depth.

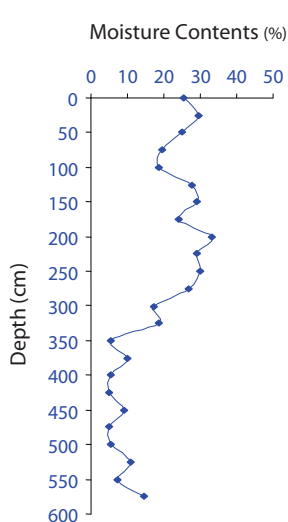


FIG. 8. Soil Moisture content with depth.

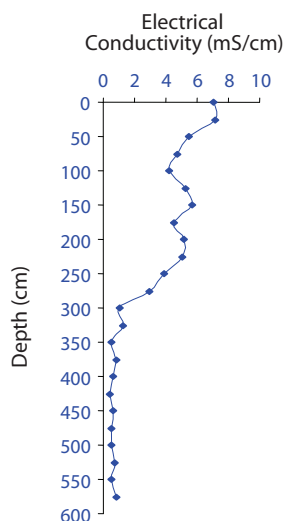


FIG. 9. EC of soil with depth.

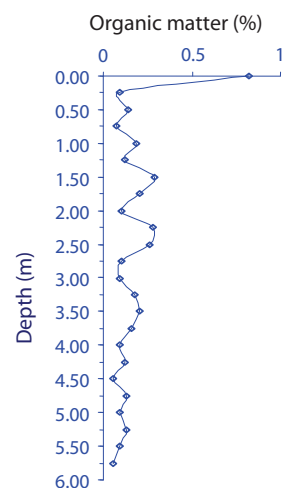


FIG. 10. Variation of organic contents with depth.

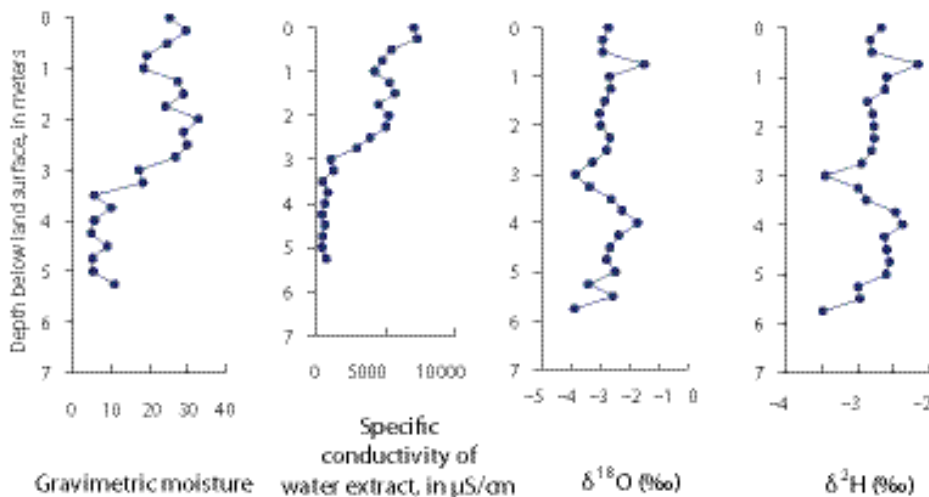


FIG. 11. Gravimetric water content, specific conductance of water extract,  $\delta^{18}O$  and  $\delta D$  composition of water from the unsaturated zone, Kasur, Pakistan.

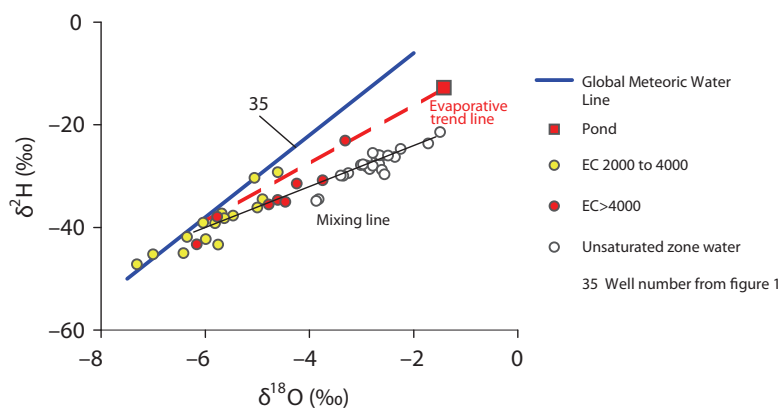


FIG. 12. Comparison of the  $\delta^{18}O$  and  $\delta^2H$  composition of unsaturated zone water with water from wells having high specific conductance, Kasur, Pakistan.

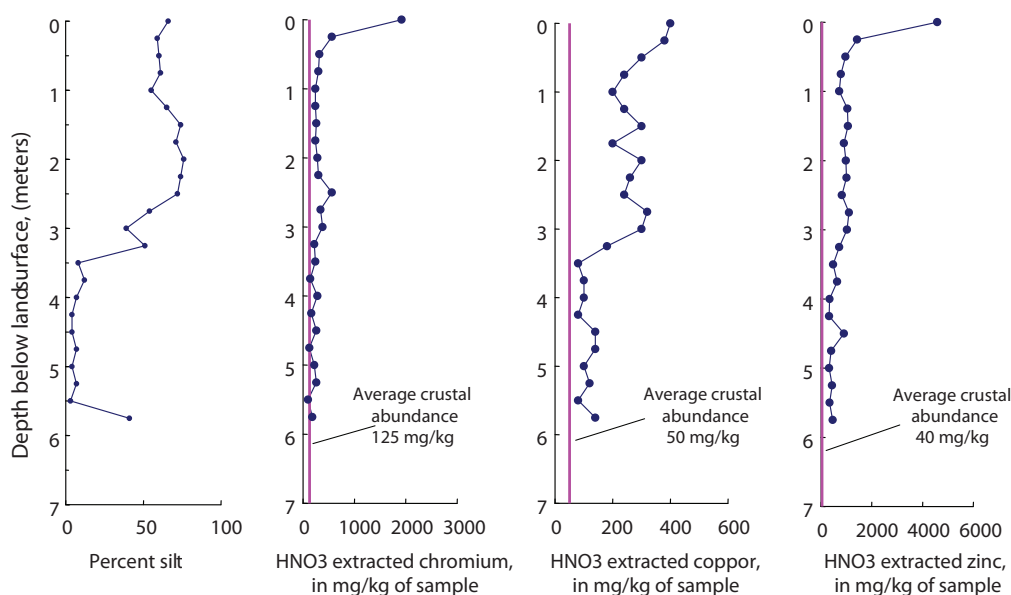


FIG. 13. Percent silt,  $\text{HNO}_3$  extracted chromium, copper, and zinc with depth in the unsaturated zone, Kasur, Pakistan.

Sodium and potassium are distributed in the unsaturated zone similar to copper and iron with high concentrations in the silty layer to a depth of about 3 m and lower concentrations in the underlying sandy layer (Table 4). The distribution of calcium and magnesium with depth is different with higher concentrations in the sandy layer below 3.0 meters of depth (Table 4). It is possible that some of the sands are either calcareous or that the sands are partly consolidated with a calcareous cement and the  $\text{HNO}_3$  extract dissolved calcareous material. Sodium and potassium concentrations at the water table beneath the unsaturated zone profile were about 1830 and 410 mg/L, consistent with high specific conductance in groundwater resulting from infiltration and recharge through the overlying unsaturated zone.

### 7.3. Unsaturated zone gas composition

The concentration of pore gases are given in Table 13 & 14 and plotted in Fig. 14. Reducing conditions within the unsaturated zone are indicated by low oxygen concentrations. Oxygen is absent at some depths and hydrogen sulfide and methane, indicative of strongly reducing conditions are present. Reducing conditions within the unsaturated zone are consistent with the rapid immobilization of chromium. Chromium in the hexavalent form ( $\text{Cr}^{+6}$ ) is mobile in oxic, alkaline environments. In the reducing environment present in the unsaturated zone underlying Kasur, chromium would be rapidly reduced to  $\text{Cr}^{+3}$ . Chromium, as  $\text{Cr}^{+3}$ , would be immobile and rapidly precipitated in the unsaturated zone, consistent with the data in Fig. 13.

The organic contents are also plotted in Fig. 14. The  $\text{CO}_2$  gas was collected from initially installed systems at four depths. The  $\delta^{13}\text{C}$  was measured in soil  $\text{CO}_2$  and has been plotted in Fig. 15. The  $\delta^{13}\text{C}$  values vary from  $-20\text{‰}$  to  $-14\text{‰}$ . During third sampling, the concentration of  $\text{CO}_2$  was high (nearly 10%) and it was consistent up to the water table. The depleted  $\delta^{13}\text{C}$  values show that source of  $\text{CO}_2$  is respiration from plants. The experimental site is surrounded by a large number of plants.

### 7.4. Nitrate and $\delta^{15}\text{N}$ in the unsaturated zone

The results of  $\text{NO}_3^-$  and  $\delta^{15}\text{N}$  of soil core samples collected from the unperturbed site and experimental site are plotted in Fig. 16 and 17. At unperturbed site the  $\delta^{15}\text{N}$  values are almost near to zero which is atmospheric concentration, the  $\text{NO}_3^-$  concentration has a range from 1.15 to 8.19 mg  $\text{NO}_3^-$  /kg soil. At experimental site,  $\delta^{15}\text{N}$  values vary from 7.5 to 31.7‰, nitrate varies from 2 to 33 mg  $\text{NO}_3^-$  /kg soil.

TABLE 11. <sup>34</sup>S CONCENTRATIONS IN WATER SAMPLES OF SELECTED POINTS

Sample No.	$\delta_{\text{CDT}}^{34}\text{S}$ (‰)	Sample No.	$\delta_{\text{CDT}}^{34}\text{S}$ (‰)
K-26	3.51	K-35	15.6
K-27	5.72	K-37	4.33
K-28	10.92	K-38	3.06
K-29	3.58	K-39	2.22
K-30	7.92	K-40	2.62
K-31	1.92	K-41	9.48
K-32	19.53	K-42	3.74
K-33	2.86	K-43	2.73
K-34	10.02		

TABLE 12. ISOTOPIC DATA OF NITROGEN OF WATER SAMPLES

Sample No.	$\delta^{15}\text{N}$ (‰)	Depth (cm)	$\delta^{15}\text{N}$ (‰)
K-27	11.57	0	34.61
K-28	17.37	50	28.40
K-29	3.28	100	18.35
K-31	22.66	150	6.74
K-33	20.99	200	25.85
K-37	14.85	250	20.94
K-38	17.60	300	18.12
K-39	13.50	350	19.86
K-40	16.05	400	23.79
K-42	-2.25	450	22.17
K-43	1.74	500	26.83

TABLE 13. CONCENTRATIONS OF VARIOUS GASES WITH RESPECT TO DEPTH

Depth (m)	CH <sub>4</sub> (%)	CO <sub>2</sub> (%)	O <sub>2</sub> (%)	H <sub>2</sub> S (mg/L)	CO (mg/L)	SO <sub>2</sub> (mg/L)	NO <sub>2</sub> (mg/L)	Cl <sub>2</sub> (mg/L)
0.50	0.25	9.92	3.7	0	5	1	0.1	0.3
1.00	0.09	9.10	1	0	0	0	0	0.1
1.50	0.19	9.25	0.89	0	0	0	0	0.4
2.00	0.42	9.99	0.4	2	0	0	0	0.5
2.50	0.29	9.99	1.7	0	0.5	0	0	0.2
3.00	0.38	9.99	0.4	0	0	0	1	0
3.50	0.55	9.99	0.2	0.1	0.5	0	0	0.4
4.00	0.67	9.99	0.1	0	1	0	0	0.1
4.50	0.66	9.99	0.1	1	0	0	0	0.1
5.00	0.62	9.99	0.4	1	0.5	0	0	0
5.50	0.54	9.99	0.4	0	0.5	0	0.1	0.5
6.43	0.42	9.99	0.2	0	4	0	0.1	0

TABLE 14. CONCENTRATIONS OF VARIOUS GASES IN SOIL WITH RESPECT TO DEPTH (THIRD SAMPLING)

Depth (m)	CH <sub>4</sub> (%)	CO <sub>2</sub> (%)	O <sub>2</sub> (%)	H <sub>2</sub> S (mg/L)	CO (mg/L)	SO <sub>2</sub> (mg/L)	NO <sub>2</sub> (mg/L)	Cl <sub>2</sub> (mg/L)
0.50	0.25	9.92	3.7	0	5	1	0.1	0.3
1.00	0.09	9.10	1	0	0	0	0	0.1
1.50	0.19	9.25	0.89	0	0	0	0	0.4
2.00	0.42	9.99	0.4	2	0	0	0	0.5
2.50	0.29	9.99	1.7	0	0.5	0	0	0.2
3.00	0.38	9.99	0.4	0	0	0	1	0
3.50	0.55	9.99	0.2	0.1	0.5	0	0	0.4
4.00	0.67	9.99	0.1	0	1	0	0	0.1
4.50	0.66	9.99	0.1	1	0	0	0	0.1
5.00	0.62	9.99	0.4	1	0.5	0	0	0
5.50	0.54	9.99	0.4	0	0.5	0	0.1	0.5
6.43	0.42	9.99	0.2	0	4	0	0.1	0

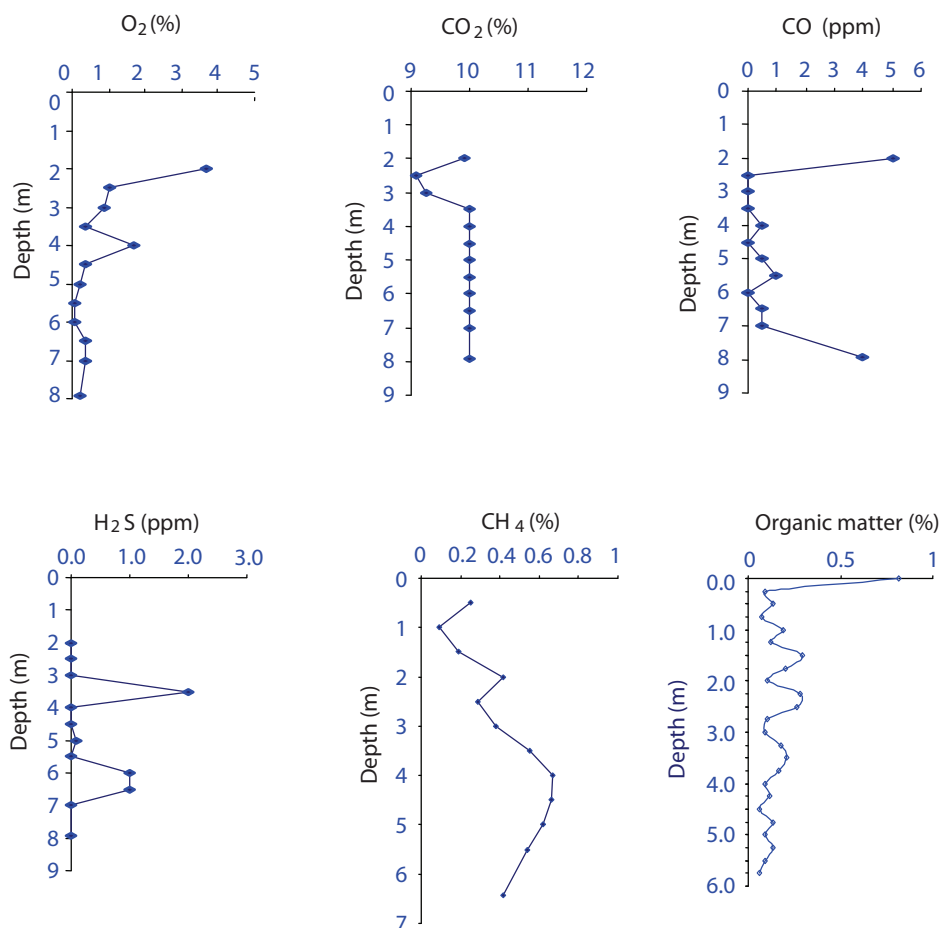


FIG. 14. O<sub>2</sub>, CO<sub>2</sub>, CO, H<sub>2</sub>S, CH<sub>4</sub> and organic matter concentrations with depth in the unsaturated zone, Kasur, Pakistan.

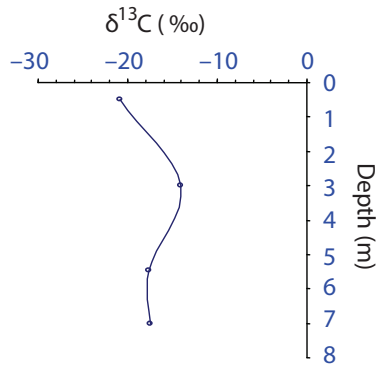


FIG. 15. Variation of  $\delta^{13}\text{C}$  of soil  $\text{CO}_2$  with depth.

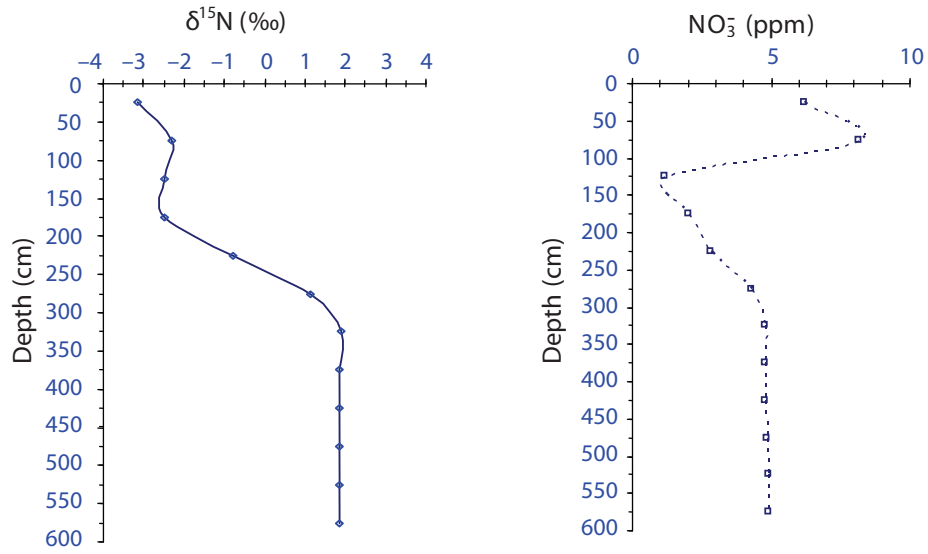


FIG. 16. Variation of  $\delta^{15}\text{N}$  and  $\text{NO}_3^-$  in soil at unperturbed site, Kasur, Pakistan.

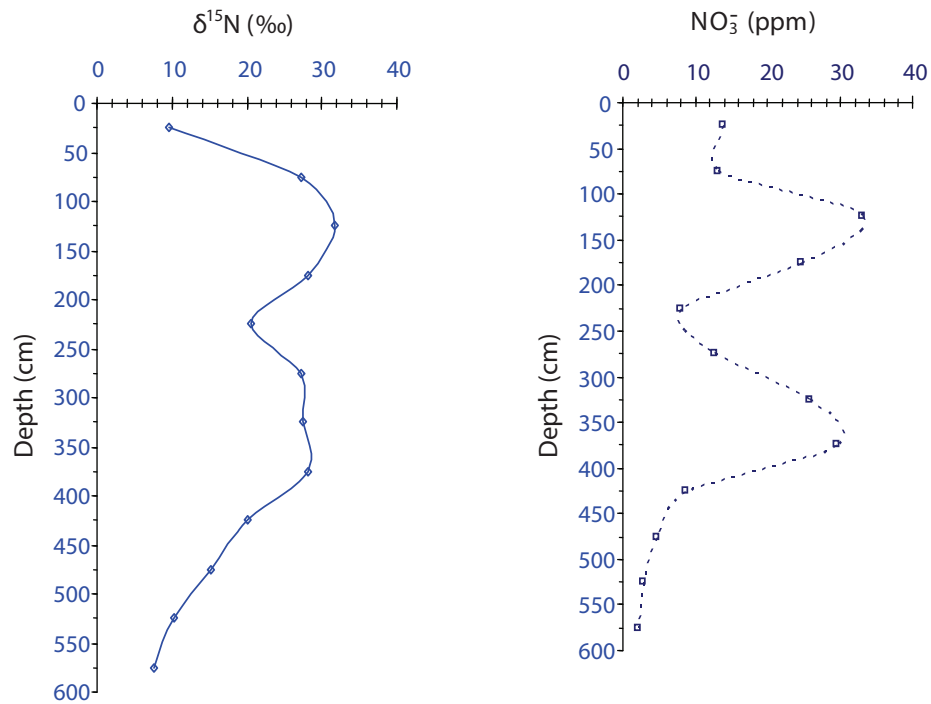


FIG. 17. Variation of  $\delta^{15}\text{N}$  and  $\text{NO}_3^-$  in soil at experimental site, Kasur, Pakistan.

TABLE15. CHEMICAL ANALYSIS OF SOIL CORE SAMPLES FROM SAMBRIAL SITE

Depth (cm)	Na (mg/L)	K (mg/L)	Ca (mg/L)	Mg (mg/L)	Cr (mg/L)	Fe (mg/L)	Zn (mg/L)	Cu (mg/L)	Mn (mg/L)
0–25	3824	2140	19400	5472	2136	9988	74	23.8	380
25–50	4828	1772	7420	5023	1024	9996	47	18.8	404
50–75	3592	2836	608	5496	260	10428	63	28	204
75–100	1652	1636	4184	5400	36	10192	44	23	592
100–125	1532	1352	900	5452	25.4	10340	47	30.4	428
125–150	2088	1348	1420	6308	23.8	10288	45	25	492
150–175	2208	1252	3108	5240	22.6	10008	42	18.2	372
175–200	1507	1452	3804	1784	34.8	10320	46	20.2	474
200–225	1424	1088	6996	5531	33.7	10328	43	20.8	433
225–250	1344	1068	4292	5284	32.2	10296	48	19.2	302

TABLE 16. ISOTOPIC AND PHYSICO-CHEMICAL DATA OF WATER SAMPLES

Sample No.	EC ( $\mu\text{S}/\text{cm}$ )	Temp. ( $^{\circ}\text{C}$ )	pH	$\delta^{18}\text{O}$ (‰)	$\delta^2\text{H}$ (‰)
K–26	594	32.6	6.47	–5.94	–34.09
K–27	3520	28.1	7.10	–5.52	–36.93
K–28	5240	26.1	6.97	–5.78	–35.61
K–29	3290	26.5	7.55	–5.55	–40.15
K–30	7870	22.7	7.50	–3.13	–24.90
K–30 (A)	757	–	–	–6.64	–43.15
K–31	4090	25.0	7.58	–3.10	–20.61
K–32	8950	25.1	7.33	–3.70	–29.53
K–33	1810	26.7	7.50	–7.06	–46.46
K–34	4150	26.9	7.65	–5.37	–36.97
K–35	10180	26.6	7.27	–3.55	–27.93
K–38	2950	27.6	7.56	–6.03	–40.74
K–39	2160	27.9	7.35	–6.64	–44.09
K–40	2790	26.5	7.68	–5.64	–39.50
K–41	3420	23.9	7.61	–5.19	–36.56
K–42	1384	26.0	7.27	–5.84	–38.81
K–43	1800	26.3	7.23	–5.35	–35.14
K–44	8420	26.2	7.57	–4.80	–34.61
T. Effluents	–	–	–	–5.70	–37.97
Sambrial Site					
S–1	1045	18.0	–	–7.08	–46.06
S–2	475	17.7	–	–8.89	–56.67
S–3	250	16.2	–	–9.37	–60.68
S–4	478	16.4	–	–9.48	–63.40
S–5	236	16.5	–	–9.82	–65.26
S–6	1057	16.5	–	–5.49	–36.42

S-7	370	17.0	-	-9.84	-64.53
S-8	1374	17.0	-	-8.12	-53.43
S-9	774	18.0	-	-7.05	-47.50
S-10	1253	18.3	-	-7.41	-51.54
S-11	864	16.7	-	-9.47	-60.87
S-12	437	17.2	-	-9.57	-61.31
S-13	2170	15.6	-	-9.35	-61.10
S-14	1075	16.4	-	-9.88	-62.95

TABLE 17. CHEMICAL DATA OF WATER SAMPLES FROM KASUR SITE (MARCH 2003)

Sample No.	EC ( $\mu$ S/cm)	HCO <sub>3</sub> (mg/L)	Cl (mg/L)	SO <sub>4</sub> (mg/L)	Ca (mg/L)	Fe (mg/L)	K (mg/L)	Mg (mg/L)	Na (mg/L)
K-26	605	223	51	170	14.9	0	2.5	10.4	84
K-27	3120	797	501	261	4.8	0	10.3	52.7	475
K-28	4620	842	1068	221	39.1	0	35.0	90.2	665
K-29	3350	738	481	241	9.9	0	8.7	76.1	492
K-30	8360	1067	2171	265	23.9	0	31.8	91.6	1594
K-31	4200	1441	576	271	13.7	0	8.0	30.4	782
K-32	7040	1120	1772	325	14.3	0	196.1	69.1	1226
K-33	1840	571	167	155	21.8	0	13.4	21.2	265
K-33 (a)	4830	1153	728	376	22.7	0	241.6	39.9	760
K-34	3670	849	731	227	4.6	0	46.6	48.7	631
K-35	9770	1443	2720	366	5.7	0	124.0	91.3	2096
K-38	2810	849	256	342	7.4	0	114.9	50.3	356
K-39	2020	659	164	185	9.5	0	25.8	36.2	293
K-40	2640	901	239	235	8.4	0	69.5	26.1	398
K-41	3880	1197	337	266	4.4	0	46.8	45.8	673
K-42	1350	439	102	118	24.2	0	7.1	54.9	117
K-43	1720	516	130	149	33.8	0	9.1	64.8	165

TABLE 18. CHEMICAL DATA OF WATER SAMPLES FROM (FEBRUARY 2004)

Sample No.	EC ( $\mu\text{S/cm}$ )	$\text{HCO}_3$ (mg/L)	Cl (mg/L)	$\text{SO}_4$ (mg/L)	Ca (mg/L)	Fe (mg/L)	K (mg/L)	Mg (mg/L)	Na (mg/L)	Zn (mg/L)
K-26	594	234	43	34	7.7	<.02	3.1	7.2	101	<0.1
K-27	3520	955	525	286	2.9	ND	17.2	50.8	637	<0.1
K-28	5240	894	1380	231	47.6	0.4	34.9	127.0	998	<0.1
K-29	3290	694	552	372	8.2	0.2	12.3	58.7	683	0.1
K-30	7870	1037	1843	669	30.7	7.0	33.6	112.0	1623	2.7
K-31	4090	1325	488	210	18.3	0.6	13.5	25.9	854	<0.1
K-32	8950	1351	2287	363	29.0	0.6	412.0	113.0	1679	0.8
K-33	1810	677	118	157	12.5	0.2	17.2	23.4	327	<0.1
K-34	4150	964	753	220	21.5	<.02	61.1	51.7	775	<0.1
K-35	10180	1467	2761	330	36.4	<.02	197.0	124.0	2087	ND
K-38	2950	860	291	286	27.5	<.02	157.0	36.1	489	<0.1
K-39	2160	784	160	209	29.5	<.02	28.7	34.0	387	ND
K-40	2790	915	214	213	13.7	0.2	96.4	0.0	522	<0.1
K-41	3420	1048	249	418	13.9	0.4	30.8	24.6	696	<0.1
K-42	1384	479	110	92	23.2	ND	11.5	38.0	178	ND
K-43	1800	595	156	146	34.0	<.02	11.5	70.1	228	<0.1
K-44	8420	1302	2119	398	27.8	0.5	161.0	118.0	1689	0.8
T.		-	-	110	11.9	2.2	73.8	57.0	1761	0.6

Sambrial Site

Sample No.	EC ( $\mu\text{S/cm}$ )	$\text{HCO}_3$ (mg/L)	Cl (mg/L)	$\text{SO}_4$ (mg/L)	Ca (mg/L)	Fe (mg/L)	K (mg/L)	Mg (mg/L)	Na (mg/L)	Zn (mg/L)
S-1	1045	406	59	58	18.9	0.2	10.5	47.4	109.0	0.1
S-2	475	234	21	22	21.6	0.3	3.7	22.3	39.8	<0.1
S-3	250	122	17	22	26.6	ND	3.1	16.0	4.2	0.1
S-4	478	125	91	22	52.3	0.3	3.7	25.5	4.0	0.2
S-5	236	118	11	16	31.3	0.3	3.3	7.7	3.0	<0.1
S-6	1057	560	43	22	14.9	1.2	4.7	57.8	109.0	0.1
S-8	1374	398	248	33	28.3	1.2	6.7	56.3	178.0	<0.1
S-9	774	370	66	28	18.9	1.0	4.7	46.8	64.0	ND
S-10	1253	430	178	33	28.0	1.3	7.5	46.0	162.0	ND
S-11	864	175	184	37	43.0	0.2	4.1	24.6	110.0	<0.1
S-12	437	219	21	18	34.5	1.2	4.1	22.4	24.2	0.9
S-13	2170	390	450	127	46.7	1.0	14.8	39.6	359.0	0.2
S-14	1075	194	259	47	56.3	0.3	7.5	29.8	135.0	<0.1

TABLE 19. ISOTOPIC AND PHYSICO- CHEMICAL DATA OF WATER SAMPLES  
(JUNE 2005)

Sample No.	EC ( $\mu\text{S}/\text{cm}$ )	Temp. ( $^{\circ}\text{C}$ )	pH	$\delta^{18}\text{O}$ (‰)	$\delta^2\text{H}$ (‰)
K-26	572	32.6	7.3	-6.41	-35.88
K-27	3390	27.7	7.6	-5.77	-41.89
K-28	5550	28.7	7.7	-6.01	-41.92
K-29	3500	27.9	7.9	-5.70	-46.10
K-30	4580	31.8	7.3	-5.41	-34.61
K-31	2070	28.6	7.1	-6.57	-41.80
K-32	9780	33.7	7.5	-3.08	-22.57
K-33	1828	27.3	7.3	-7.00	-43.12
K-34	4330	26.9	7.6	-5.63	-34.09
K-35	9770	26.1	7.8	-4.34	-28.33
K-36	-	-	-	-5.43	-30.59
K-38	2810	28	7.8	-6.34	-39.14
K-39	2020	27.5	7.5	-6.48	-39.69
K-40	3090	25.8	7.8	-5.87	-37.54
K-41	2360	26.7	7.9	-6.22	-43.26
K-42	1504	26.7	7.2	-5.86	-40.29
K-43	1452	25.2	7.0	-5.77	-38.52
K-44	-	-	-	-4.89	-34.06

Sambrial Site

Sample No.	EC ( $\mu\text{S}/\text{cm}$ )	Temp. ( $^{\circ}\text{C}$ )	pH	$\delta^{18}\text{O}$ (‰)	$\delta^2\text{H}$ (‰)
S-1	926	23.5	7.0	-7.79	-50.65
S-2	809	23.2	7.0	-8.54	-49.01
S-3 (A)	383	22.3	6.7	-9.44	-59.30
S-4	354	21.3	6.5	-9.60	-61.67
S-5	243	22.6	6.5	-9.61	-64.16
S-6	1005	25.4	7.0	-6.05	-44.11
S-7	331	24.8	6.5	-9.83	-63.42
S-8	2580	24.5	7.0	-7.85	-63.82
S-9	915	23.7	7.0	-7.12	-51.55
S-10	1553	23.4	6.7	-7.00	-48.44
S-11	1212	22.9	6.9	-9.56	-59.3
S-12	471	24.5	6.8	-9.49	-63.48
S-14	1110	22.4	6.5	-9.10	-62.74

TABLE: 20. ANALYSIS OF WATER SAMPLES PASSED THROUGH SOIL COLUMN

Code No.	Depth of soil core(meters)	Na (mg/L)	K (mg/L)	Ca (mg/L)	Mg (mg/L)	Mn (mg/L)	Fe (mg/L)	Cr (mg/L)	Cu (mg/L)	Zn (mg/L)	Cl (mg/L)	HCO <sub>3</sub> (mg/L)	SO <sub>4</sub> (mg/L)
S-1	0-1	11200	604	4213	266	2.99	0.99	N.D	0.14	0.13	16899	289	898
S-2	1-2	4920	124	1770	654	0.49	1.6	N.D	0.16	N.D	12445	246	811
S-3	2-3	4940	148	1412	582	0.06	1.2	N.D	N.D	N.D	9080	223	892
S-4	3-4	4220	147	1568	920	0.06	1.2	N.D	N.D	N.D	11928	259	1113
S-6	4-5	4300	358	2680	2360	0.04	7.1	N.D	N.D	0.06	16018	221	1723
S-7	5-6	4810	228	1160	808	0.14	1.5	N.D	N.D	N.D	11238	134	712
S-8	6-7	4740	232	1156	706	0.05	5.2	N.D	N.D	0.11	10896	224	809
S-9	7-8	5400	278	824	964	0.07	0.7	N.D	N.D	N.D	11239	248	911
S-10	8-8.5	984	58.5	274	82.3	N.D	0.6	2.3	N.D	N.D	1223	298	804
Solution passed through soil		5740	450	288	156	0.85	17.3	48.9	3.68	3.1	10906	acidic	604

## **8. DISCUSSION**

The area surrounding Kasur Pakistan has been contaminated with salinity and trace elements by waste disposal from about 300 tanneries. Over the years, tannery wastes were discharged to open land which eventually became a pond. Sewage from Kasur also is discharged to the waste pond. Water from wells in the area has been contaminated from recharge from the waste pond but also from the movement of water through the unsaturated zone in the area. The unsaturated zone also has been contaminated with salinity and metals from the tanneries and other sources near Kasur.

Attempts to clean-up contamination near Kasur that focus the waste pond will remove one locally important source of contamination. The pond itself does not appear to be the most significant source of contamination in the area. Perhaps fine-grained material accumulated on the bottom of the pond limits infiltration and water is lost from the pond primarily by evaporation. Given the discharge of sewage and organic waste from the tanneries, chromium in the pond is not likely to move with water from the pond. It is not known if wind-blown dust from the pond is a source of contamination to nearby soils or a health hazard to local residents.

Movement of water through the unsaturated zone appears to be the major source of salinity to wells in the study area. Chromium does not appear to move through the unsaturated zone in the area surrounding Kasur because of reducing conditions within the unsaturated zone. Copper and zinc are present at the water table surface but like chromium large concentrations of these metals are present in the unsaturated zone. Although these elements do not appear to move readily through the unsaturated zone in the study area they represent a potential source of contamination with time.

## **REFERENCE**

- [1] AHMAD, N., Ground Water Resources of Pakistan, Ripon printing press, Lahore, Pakistan (1974).

# WATER DYNAMICS IN THE UNSATURATED ZONE OF FRACTURED ROCK: TEST SITE SINJI VRH

B. ČENČUR CURK

IRGO – Institute for Mining, Geotechnology and Environment,  
Ljubljana, Slovenia

## ABSTRACT

A research field site (RFS) was established at Sinji Vrh in the western part of Slovenia in order to study flow and solute (particularly pollutant) transport in fractured and karstified rocks, with a focus on the unsaturated zone. RFS consists of surface set-up and a research tunnel, 15 m below the surface. An agrometeorological station and injection boreholes were installed on the surface. A special construction (1.5 m long segments) for collecting water seeping from the ceiling of the research tunnel was developed. Holes for injecting the tracers were located on the basis of a precise cartography of discontinuities on the surface outcrops and within the research tunnel. Isotope techniques were used in long term monitoring of  $^2\text{H}$  and  $^{18}\text{O}$  isotope composition, a tracer experiment with deuterium, and in fertiliser application experiments ( $^{15}\text{N}$ ). The goal of the research was to obtain different paths of the water and pollution through the unsaturated zone and the residence time distribution.

## 1. INTRODUCTION

Fractured and karstified rocks are very heterogeneous and complex in terms of their geometry and void topology. This results in parameter variability and large uncertainties reflecting complicated hydraulic, mechanical, thermal, and chemical processes. Therefore, detailed studies of these processes have to be performed on a macro scale at instrumented field research sites [1]. Such a site was established at Sinji Vrh in the western part of Slovenia [2] (Fig. 1). The main goal of the research field site at Sinji Vrh (RFS Sinji Vrh) was the study of flow and solute (particularly pollutant) transport in fractured and karstified rocks, with a focus on the unsaturated zone.

In hydrogeological systems with karstified aquifers, the unsaturated zone above the water table has physical and chemical retention properties which provide a potential natural protection zone for karstic groundwater. The study of hydrodynamic parameters of water flow through the unsaturated zone and the related transport of pollutants are therefore of extreme importance. Due to the high hydraulic conductivity of karst conduits and fracture networks in the impermeable rock it is difficult to spatially determine the coefficient of hydraulic conductivity of karstified aquifers. The karst conduits in the unsaturated zone provide extremely limited protection of groundwater.

Understanding the structure and specific features of karstic aquifers is only achieved by applying different research methods. The structure of karstic systems can be elucidated through mapping and geophysical techniques. Tracer experiments combined with isotopic and hydrochemical determinations can provide data on groundwater flow and transport processes. Such research can therefore yield the information required for sustainable management of karst groundwater.

The isotope and chemical composition of water at a sampling site reflects the processes taking place with water rock interaction, groundwater mixing and residence times, the portion of water stored in the fractured system and the conditions in the recharge area [5].

Many isotope research studies in karstic regions often use long-term seasonal monitoring and the analysis of input (e.g in precipitation) and output (discharge points such as springs) data. These mainly yield information on base flow of groundwater and an indication of hydrodynamic processes taking place. Since sampling frequency is often low, it is hard to establish the relative contribution of infiltrated precipitation with short residence times [5]. High frequency monitoring of certain isotopes and chemical parameters during key hydrological events (e.g storms, snow) can yield important information on groundwater mixing processes and residence times [6]. This enables the description of flow dynamics with different components of rapid and slow flow and the development of conceptual

models of aquifer processes. This is of great importance for the prediction of pollutant fate and transport. For this purpose, a multiparametric approach is necessary, both on the basis of low and high frequency monitoring of individual hydrological events in different seasons and at multiple depths in the aquifer [5]. Special attention must be paid to the mechanisms of flow and solute transport in the soil and in the unsaturated zone and on the geochemical development of groundwater. Research into aquifers with intergranular porosity has shown that the main part of pollution is reduced in the unsaturated zone. Very little data on karstic aquifers are available. Here we present new data that indicates that certain pollutants may be retained in the unsaturated zone, but this is highly dependent on the structure of the aquifer and the antecedent conditions (e.g., saturation state).

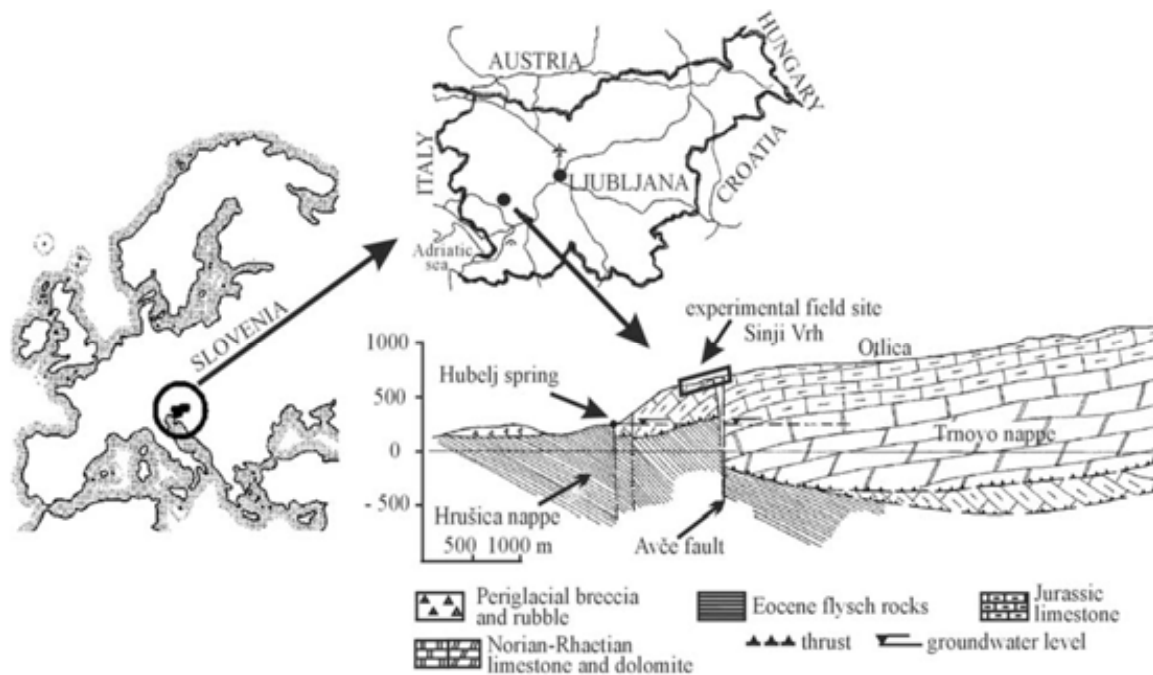


FIG. 1. Location of the research field site Sinji Vrh (RFS Sinji Vrh) with a geological cross-section of the Trnovo plateau [3], [4]).

### 1.1. Research field site Sinji Vrh

RFS Sinji Vrh is located in the western part of Slovenia (Fig. 1) at the edge of the Trnovski Gozd plateau (mean altitude of 900 m.a.s.l), which is an overthrust (Trnovo nappe) of carbonate rock over impermeable Eocene ( $E_{1,2}$ ) flysch rocks (turbidite sediments, mainly changing of marble and sandstone). This area is composed of Jurassic (Lias-Dogger) limestone, which changes laterally into crystalline dolomite. The beds dip in general towards south-west and dip angle changes between  $30^\circ$  and  $60^\circ$ . This territory is crossed by the subvertical Avče fault with a Dinaric direction (NW–SE), resulting in crushed and fractured rock. Within the broader fault area numerous accompanying subvertical faults (stretching in NNW–SSE and NNE–SSW directions) are present, branching from the main fault plane and repeatedly joining it [7]. The geological profile of the Trnovski Gozd plateau is presented in Fig. 1 [8].

The groundwater horizon is extremely deep and appears at the surface at the lowest point of the impermeable flysch border in the karstic spring Hubelj. Water generally flows out of the bedding planes, that have been widened by chemical dissolution [8]. In dry periods the spring outlet is at 240 m.a.s.l. and the minimum discharge is  $0.185 \text{ m}^3/\text{s}$ . During wet periods, the water level rises up to 40 m and the discharge increases to  $59 \text{ m}^3/\text{s}$ . The mean discharge is  $3 \text{ m}^3/\text{s}$  [9]. Average annual precipitation in the catchment is roughly 2450 mm. In this region mainly thin (10–50 cm) carbonate soil types are found. They have low water retention capacities facilitating fast infiltration rates [10].

Hubelj's spring has an average  $\delta^{18}\text{O}$  value of  $-8.45\text{‰}$  [11], [12]. Based on isotopic measurement, the estimated catchment area is roughly  $50\text{ km}^2$  with a mean altitude of  $1000 \pm 100\text{ m}$  ([12], [13], [14]). The mean water transit time is 5.8 months [12]. The spring water is found to be a mixture of two water components, having mean residence times of weeks (through the karst conduits) and of years (through the fractured rock mass as a whole) respectively [12].

## 2. EXPERIMENTAL DESIGN

The research field site in the unsaturated zone of fractured and karstified rock presents a 340 m long artificial tunnel, 5 to 25 meters below the surface (Fig. 1 and 2). The tunnel direction is nearly constant running southwest– northeast ( $\text{N}66^\circ\text{E}$ ). The surface is covered with grassland and small beech forests which usually cover outcrops. The unsaturated fractured and karstified limestone has a negligible matrix porosity and very high fracture density with some larger conduits [15].

An agrometeorological station (Fig. 3) has been installed on the surface, where precipitation, evaporation, air temperature, air moisture, wind speed and direction (both at two levels) are continuously measured. It is located near the tunnel entrance at a height of 825 m.

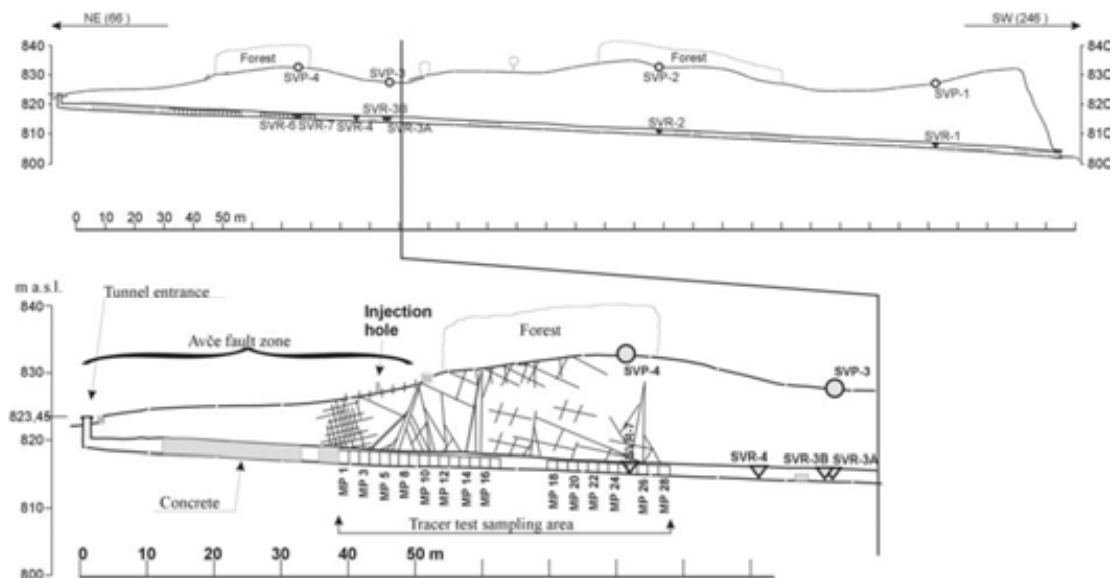


FIG. 2. Longitudinal cross-section of the tunnel [16]. Sampling points SVP-1 to SVP-4 and SVR-1 to SVR-7 were used for hydrogeochemical characterisation of the research site. Sampling points MPI-1 to MPI-28 were used for the fertiliser and multi-tracer experiments.



FIG. 3. Surface installations at the RS Sinji Vrh — agrometeorological station, injection borehole for multi-tracer tests and area where fertiliser was applied.

A long term time series study was undertaken to characterise the hydrogeochemical environment at the research site. This included analyses of physical and chemical parameters, isotope composition of oxygen and deuterium in precipitation, water in the unsaturated zone and aquifer discharge (the karst spring Hubelj). Eight sampling points (SVR-1 to SVR-7; Fig. 2) were constructed in the research tunnel in such a way to enable measuring of discharge and so the collected water is prevented from contact with the air (Fig. 4). Precipitation was collected for  $\delta^{18}\text{O}$  analyses near the entrance of the tunnel in a specially adapted rain gauge [5]. Isotopic composition of sampled waters was analysed in Joanneum research, Institute of Water Resources Management, Graz. Standard analytical error for oxygen is  $\pm 0.05\text{‰}$  and for deuterium  $\pm 0.5\text{‰}$ .

On the grassland, an area of  $150\text{ m}^2$  was used for a fertiliser application experiment (Fig. 5). For this purpose suction cups were installed at two levels (depth of 15 and 45 cm) in the karstic soil above the tunnel. For these experiments a special water collecting structure was made and installed in the tunnel. Each sampling segment consists of metal girders across which a plastic sheet is tightened. Special funnels were made to collect water in narrow sampling containers (Fig. 5). The water seeping from the ceiling of the tunnel is gathered in 1.5 m long segments with a total collecting surface of  $2.2\text{ m}^2$ . A total of 28 segments (MP1 to MP28; Fig. 2) have combined length of 49 meters. This length provides contiguous collection points apart from a 7 meter interruption between samplers MP17 and MP18 where the rock is too dry [4].

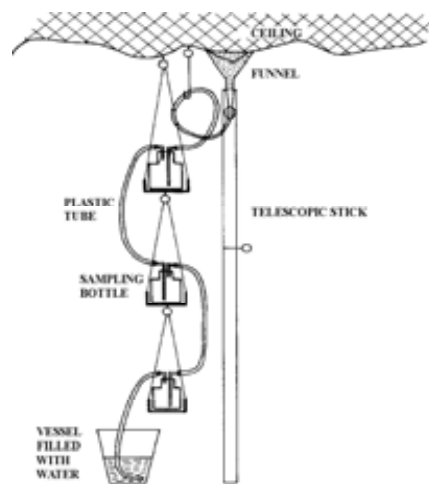


FIG. 4. Schematic of the water sampling system used in the tunnel for isotope analysis [17].



FIG. 5. Construction for collecting water samples in the tunnel with automatic device for flow rate and fluorometer for the multitracer experiment.

### 3. CHARACTERISATION OF THE TEST SITE

An automatic meteorological station was installed at RFS Sinji Vrh in 1999. The station measures temperature, evaporation, humidity, precipitation, wind speed and wind direction. All data are stored in a local database. In 1998 only measurements of daily precipitation, temperature and evaporation were carried out. Fig. 6 depicts an example of precipitation, evaporation and temperature distribution. The grassland close to the tunnel entrance is cut twice a year and used for livestock food; there are no other crop and irrigation practices. In the summer months goats are kept at the edge of the plateau (Fig. 2).

Standard soil parameters were determined. The consolidated unsaturated rock was investigated with geophysical methods. The 0.2–1 m thick soil is a typical karstic pocket soil (calcaric brown soil), very similar to a rendzina but with characteristic deeper pockets extended along weak zones like fractures in the underlying rock (Fig. 7). In a 0.7 m deep soil profile the Ah-horizon has a thickness of 0.15 m, and the B-horizon a depth of 0.55 m. In the latter a horizon with more roots and higher organic content (Brz1) can be distinguished (Tab. 1). The soil has a middle value of cationic exchange, since the soil particles bound only 25–35 meq/100 g of soil. On the sorptive part of the soil particles 15–25 meq bases/100 g of soil are bound. The V-ratio is higher than 50%; therefore the soil is eutric and saturated with bases.

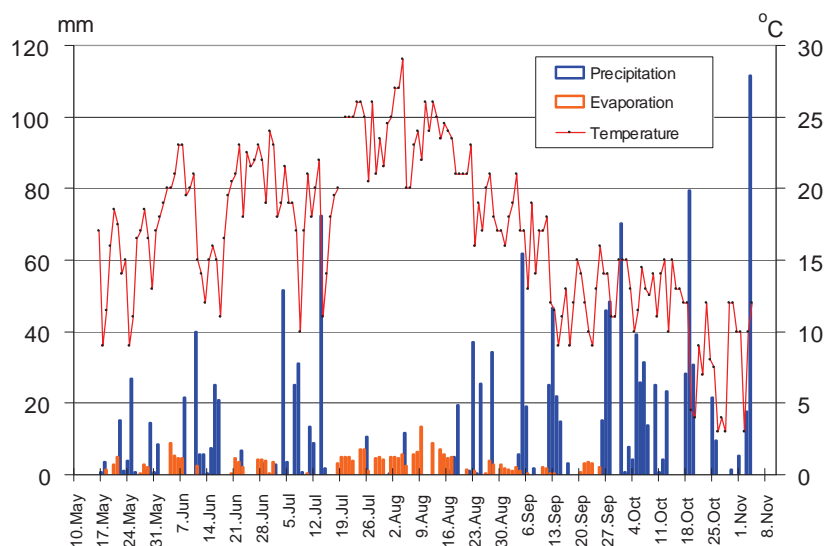


FIG. 6. Precipitation, evaporation and air temperature data from May to November.



FIG. 7. Soil profile at the RFS Sinji Vrh..

Before the first fertiliser application experiment, soil samples were taken from two different depths and analysed for nitrate and ammonium nitrogen contents. At a depth of 10–20 cm there was 6.5 mg N–NO<sub>3</sub><sup>-</sup>/kg soil and 9.6 mg N–NH<sub>3</sub>/kg soil, whereas in depth of 30–40 cm there was 7.8 mg N–NO<sub>3</sub><sup>-</sup>/kg soil and 5.1 mg N–NH<sub>3</sub>/kg soil.

The soil samples were taken for determination of the hydraulic functions of the soil (pF curves). A pF curve represents the ability of a porous media to retain water. Fig. 8 presents the pF curves for the soil depth of 30 cm and 60 cm. The curves are very similar and differ only for some mass % at low-tension conditions. The data demonstrates that the water retention capacity of the soil at the study site is relatively low.

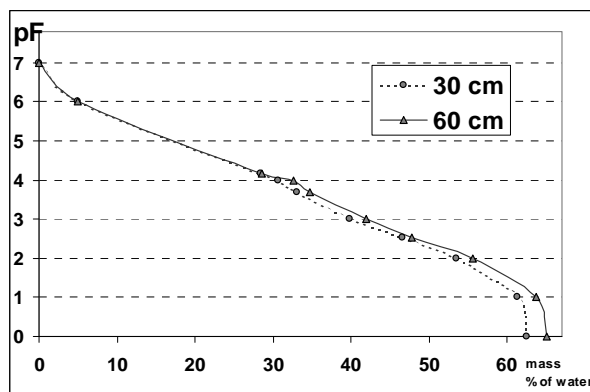


FIG. 8. pF curves for the soil depths of 30 and 60 cm. Note logarithmic pF scale.

Soil samples were also taken for determination of hydraulic conductivity. The hydraulic conductivity of these soil samples varies from 9E–4 to 1.25 cm/min; the average value is 0.4 cm/min.

Detailed structural mapping and geophysical measurements were performed in order to define the structure of the fractured rock. The results of the ground penetrating radar (GPR) investigations of subsection B (see Fig. 2) indicated four key hydrogeological features: the depth of pronounced rock desaturation; near surface fast vertical flow; drainage areas; and the areas of retained water [18]. It is assumed that the limestone is mainly dry to 3 m below the surface (Fig. 9), except in areas of karst channels where the dry zone is deeper. Below 3–5 m a relatively saturated area was detected, which represents storage in the unsaturated zone (fractured zone). Geoelectrical tomography indicates 1.5 m zone of subsurface clay and very fractured (crushed) limestone at the Avče fault area (Fig. 2 and 9). On the hill a compact limestone zone with surface clay-filled fractures is detected [19].

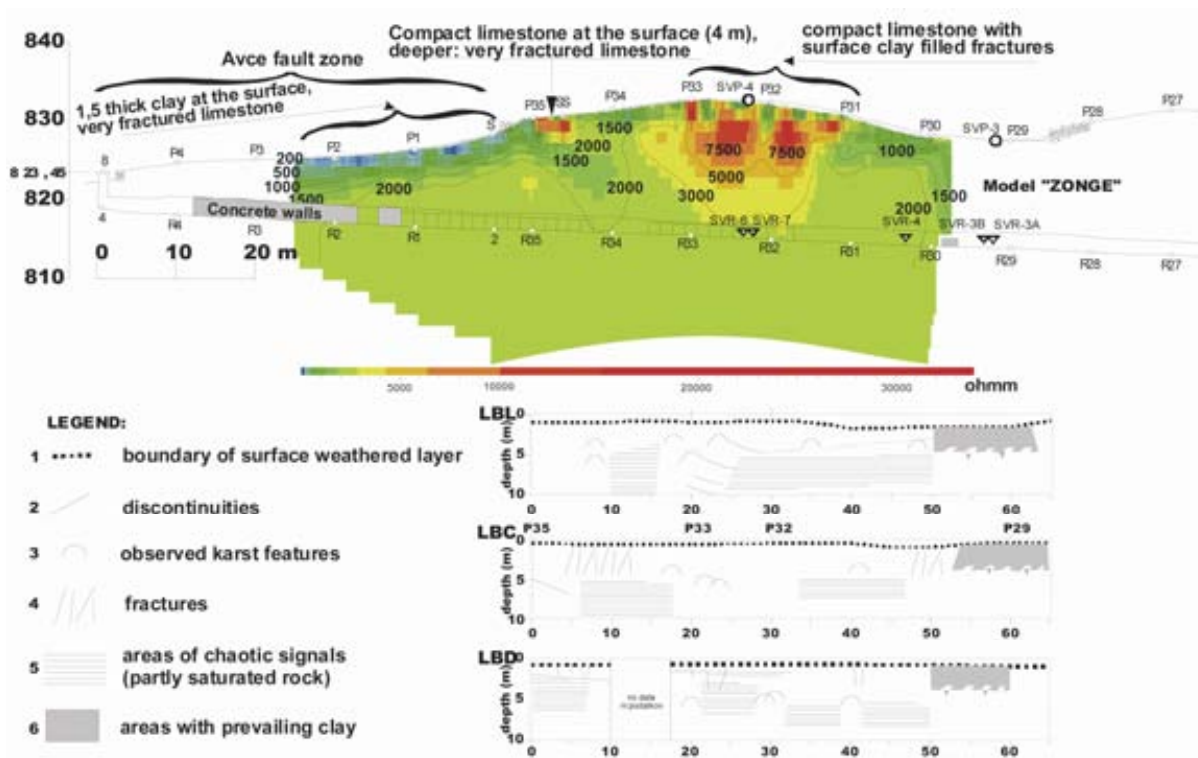
## 4. RESULTS OF ISOTOPE STUDIES

### 4.1. Long term $\delta^{18}\text{O}$ and $\delta^2\text{H}$ isotope study

The isotope time series study was based on the long-term observations: a two and a half year period of monthly monitoring from 1999–2001 [20] and from 2001–2004 seasonal (quarterly) monitoring. Oxygen isotopic composition in sampled waters of the last (quarterly) sampling period is presented in Fig. 10. Precipitation has the largest range of values: from –4,64‰ to –9‰. The mean value of oxygen isotopic composition in precipitation is –6.7‰. Mean values of  $\delta^{18}\text{O}$  composition of sampled water (unsaturated zone and aquifer) are lower than the mean precipitation value. The  $\delta^{18}\text{O}$  composition of sampling point SVR–1 ranges between –7.18 and –8.31‰, its mean value is –7.99‰. The mean value of sampling point SVR–3A is –8.07‰, with a range of –7.7 to –8.84‰. Similar values are found in waters from the sampling point SVR–3B and Hubelj spring. Isotopic composition of these waters ranges between –7.89 to –8.41‰, and –7.8 to –8.57‰ respectively. The mean value in SVR–3B is –8.09‰, whereas the mean value of Hubelj at base flow is –8,18‰. The  $\delta^{18}\text{O}$  composition of water from sampling point SVR–7 deviates from other sampling points: its mean value is –7.34‰ and ranges from –6.84 to –8.14‰ [21].

TABLE 1. RESULTS OF STANDARD SOIL PROFILE ANALYSIS.

Parameter	Unit	A horizon 0–15 cm	Brz1 15–33 cm	Brz 33–70 cm
pH in 0,1M KCl	–	5.6	7.1	7.6
P <sub>2</sub> O <sub>5</sub>	mg P <sub>2</sub> O <sub>5</sub> /100 g soil	4.5	1.8	1.1
K <sub>2</sub> O	mg K <sub>2</sub> O/100 g soil	10.7	10.4	8.4
N – total	%	0.42	0.15	0.08
Humus	%	7.04	2.51	1.19
H <sup>+</sup>	meq/100 g soil	17.81	7.5	2.81
K <sup>+</sup>	meq/100 g soil	0.26	0.25	0.20
Ca <sup>++</sup>	meq/100 g soil	12.68	24.32	22.38
Mg <sup>++</sup>	meq/100 g soil	3.41	1.46	0.98
S	meq/100 g soil	16.39	26.07	23.59
T	meq/100 g soil	34.2	33.57	26.40
V	%	47.9	77.7	89.4
sand	%	17.1	12	25.2
silt	%	34.3	16.6	14.7
clay	%	48.6	71.4	60.1
texture class	–	MG–G	G	G



meq = miliequivalent; S = total sum of bases, T = sorption capacity, V=S/T

FIG. 9. Geoelectrical tomography longitudinal profile above the tunnel axis and interpreted GPR longitudinal profiles (LBL: 5 m to the south, LBC: above the tunnel axis and LBD: 5 m to the nord) (see Fig. 2) [16].

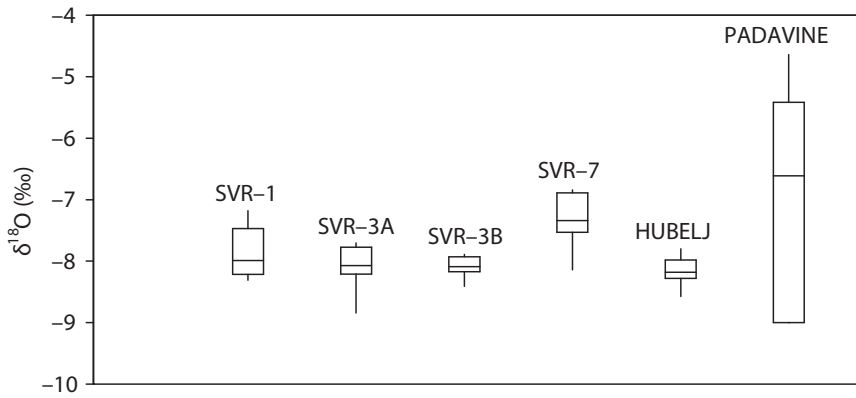


FIG. 10. The  $\delta^{18}\text{O}$  composition of sampled waters (precipitation, unsaturated zone (SVR-*i*) and Hubelj spring).

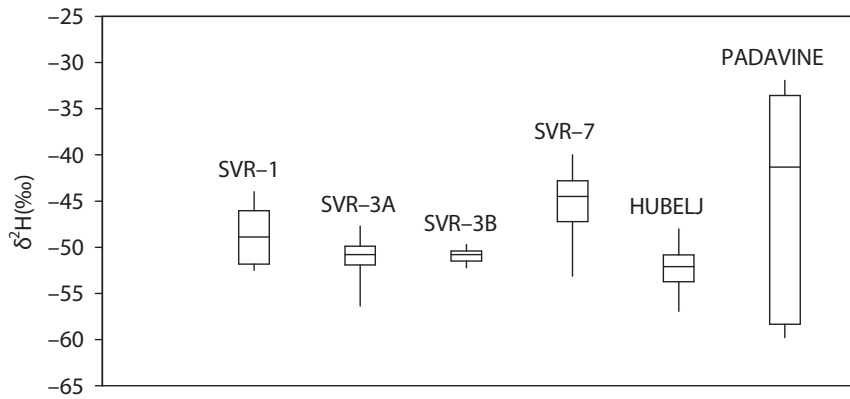


FIG. 11. The  $\delta^2\text{H}$  composition of sampled waters (precipitation, unsaturated zone (SVR-*i*) and Hubelj spring).

Hydrogen isotopic composition in sampled waters of the last (seasonal) sampling period is presented in Fig. 11 and behaves in a similar manner to the oxygen isotopes. Isotopic composition of  $\delta^{18}\text{O}$  and  $\delta^2\text{H}$  follow the same mixing linear trend, therefore only  $\delta^{18}\text{O}$  results are described.

Time series data of  $\delta^{18}\text{O}$  isotope composition for the last sampling period are depicted in Fig. 12. In spite of the sparse dataset, differences among particular sampling points can be observed. Since all sampling points recharge from the same altitude, above all the sampling points in the research tunnel, it can be assumed that these differences are the result of variations in residence times of sampled waters. The variation of the groundwater  $\delta^{18}\text{O}$  isotope composition decreases with increasing residence time. The variation becomes practically negligible after the groundwater average residence time exceeds 5 years [22]. The variation of the  $\delta^{18}\text{O}$  isotope composition (Figs 10 and 12) confirms residence times which have been determined based on the high frequency monthly sampling [20]. For SVR-7 this residence time is in the order of months; for the Hubelj spring base flow residence time is two to three years; about five years for SVR-3A and SVR-3B; and at least ten years for SVR-1.

Table 2 presents a comparison of the mean values of the  $\delta^{18}\text{O}$  isotopic composition of high frequency (monthly) [20] and the last period (quarterly) [21] sampling. The mean value of the  $\delta^{18}\text{O}$  composition in sampling point SVR-1 remains the same, whereas the mean values of SVR-7 and Hubelj spring differ slightly from the previous investigation period. The largest change of the mean values appears in sampling points SVR-3A and SVR-3B and precipitation. In the last sampling period the  $\delta^{18}\text{O}$  composition become slightly enriched.

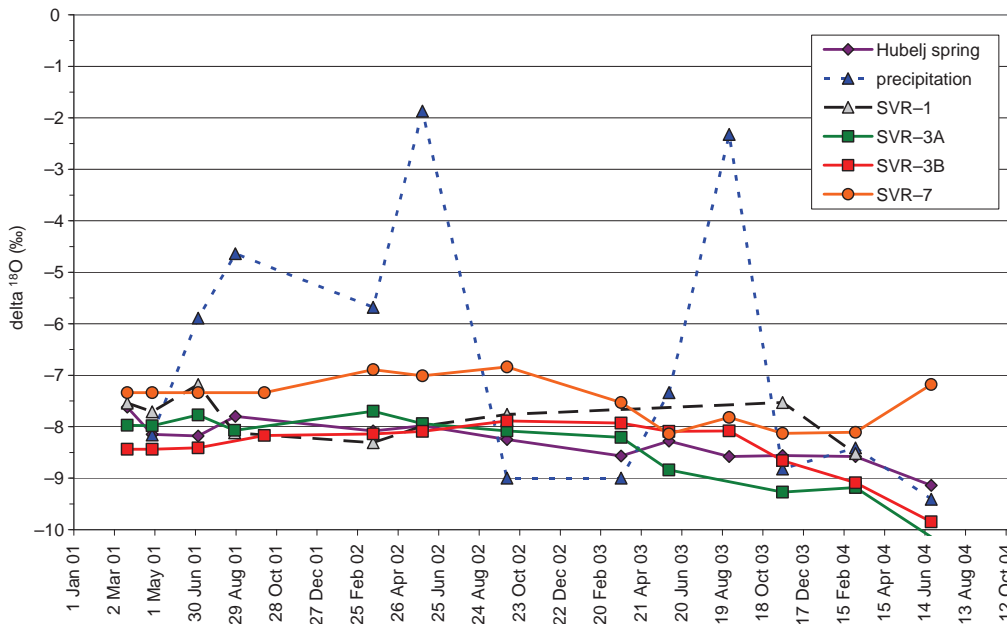


FIG. 12. Time series of the  $\delta^{18}\text{O}$  isotope composition in precipitation, unsaturated zone water (SVR-1, SVR-3A, SVR-3B and SVR-7) and in the Hubelj spring.

TABLE 2. MEAN  $\delta^{18}\text{O}$  COMPOSITION AND LMWL FOR SAMPLING POINTS IN THE PAST (BASED ON MONTHLY SAMPLING) AND LAST (QUARTERLY) SAMPLING PERIOD

sampling period	SVR-1	SVR-3A	SVR-3B	SVR-7	Hubelj Spring	Precipitation
$\delta^{18}\text{O}$ (‰)						
1999–2000	-7.9	-9.1	-8.9	-7.2	-8.5	-7.5
2001–2004	-7.9	-8.4	-8.4	-7.5	-8.3	-6.7
LMWL						
1999–2000	$\delta^2\text{H} = 7.7 \times \delta^{18}\text{O} + 12.3$				$\delta^2\text{H} = 7.5 \times \delta^{18}\text{O} + 11$	$\delta^2\text{H} = 8.1 \times \delta^{18}\text{O} + 13.6$
2001–2004	$\delta^2\text{H} = 7.0 \times \delta^{18}\text{O} + 5.5$				$\delta^2\text{H} = 8.2 \times \delta^{18}\text{O} + 14.4$	–

The relationship between  $\delta^{18}\text{O}$  and  $\delta^2\text{H}$  for the precipitation data for the last (quarterly) sampling period was not determined due to the paucity of data. From high frequency monitoring precipitation data a local meteoric water line (LMWL) was calculated [20] (Eq. 1) and shows a shift from the GMWL towards the Mediterranean meteoric water line. The mean  $\delta^{18}\text{O}$  isotope composition was 7.5 ‰ (Tab. 2).

$$\delta^2\text{H} = 8.1 \times \delta^{18}\text{O} + 13.64 \quad (1)$$

From high frequency monitoring the relationship between  $\delta^{18}\text{O}$  and  $\delta^2\text{H}$  in the unsaturated zone water was determined (Eq. 2, Tab. 2) [20].

$$\delta^2\text{H} = 7.7 \times \delta^{18}\text{O} + 12.3 \quad (2)$$

The relationship between  $\delta^{18}\text{O}$  and  $\delta^2\text{H}$  in the unsaturated zone water for the last (quarterly) sampling period is

$$\delta^2\text{H} = 7.0 \times \delta^{18}\text{O} + 5.5 \quad (3)$$

It should be pointed out, that this calculation is made on a limited dataset from SVR1, 3A, 3B and 7 quarterly sampling, whereas Eq. 2 is based on the high frequency sampling and two additional sampling points (SVR 2 and 4).

#### 4.2. Tracing experiment with deuterium

In the frame of Association of Tracer Hydrology<sup>1</sup> project a multitracer experiment was performed at the RFS Sinji Vrh in autumn 2003. Deuterium (90%), potassium bromide, lithium chloride, zinc sulphate, sulfonic acid, pyranine, naphthionate, uranine, Sulforhodamine B, micro spheres and bacteriophages P22H5 were used as tracers. The aim of this tracer experiment was to quantify channel flow and fractured zone flow and to determine different behaviour of conservative tracers, which was observed in previous tracer experiments.

For this tracer experiment a new borehole was drilled through the soil cover on top of the research field with a depth of 0.9 m, protected by a PVC pipe, enabling direct injection into the fractured karstified carbonate rock (Fig. 2 and 3). The injection team (Fig. 13) prepared the tracer 'cocktail' stepwise (according to the Tab. 3) in a 25 L container, mixed thoroughly until complete dissolution was reached. The tracer container was slowly poured out into the open borehole. Tracer cocktail was flushed with 25 L water. The injection was performed on a rainy day when the temperature was 11°C, on the next few days were sunny and dry.

For this tracer experiment sampling points MP1 to MP10 in the tunnel (Fig. 2) were selected due to the injection position. Two automatic devices for flow rate and conductivity (Fig. 4) were installed in the sampling points MP4 (10.10.2003) and MP5 (3.10.2003). For all other sampling points the amount of water was measured by each sampling campaign. Isotopic analysis of the sampled waters was performed in GSF, Institute of Hydrology, Munich.



FIG. 13. Injection of the tracer 'cocktail'..

---

<sup>1</sup> Association of Tracer Hydrology is a group of tracer hydrology experts. Until now the project was not funded and the researchers perform their work in the frame of their own project. Analyses were done in laboratories of cooperating institutes, which are listed in Table 2.

TABLE 3. TRACER COCKTAIL FOR THE SINJI VRH MULTITRACER EXPERIMENT

Tracer	Amount	Preparation	Laboratory for analysing
lithium chloride	300 g	3.0 L	Joanneum Research – IWRM, Graz
zinc sulphate	250 g		
sulfonic acid	10 mg		University of Karlsruhe, AGK – Angewandte Geologie Karlsruhe
pyranine	10 g		
naphthionate	20 g		
micro spheres	10 mL		
uranine	1.5 g		University of Bonn, Geological Institute
Sulforhodamine B	5 g		
potassium bromide	300 g	1.0 L	Joanneum Research, IWRM
deuterium (90 %)		~ 0.2 L	GSF – Inst. for Hydrology, Munich
bacteriophages P22H5	~ 10 <sup>14</sup> p.f.u	4.0 L	National Inst. for Biology, LJ
rinsing water for the several tracer bottles		2.2 L	
	Σ	10.4 L	

Tracers appeared immediately after the first significant precipitation event, respectively four days after the injection. The most pronounced breakthrough appeared for uranine, deuterium and chlorine ions. The  $\delta^2\text{H}$  composition for all sampling points MP1–MP10 is presented in Fig. 14. This tracer experiment again confirmed the presence of fast flow through a channel above the sampling points MP4 and MP5 (see Fig. 2 and Fig. 14), where the response is rapid and the detected concentrations are high. The peak  $\delta^2\text{H}$  composition in MP5 was 2455‰ and it appeared in the first sample after the injection (four days after the injection and immediately after the first rain event). The highest deuterium value in MP4 appeared after 21 days (18 days after the first rain event) with a composition of 306‰. It should be pointed out, that deuterium was injected at a high enough concentration in order to get significant concentration in fracture system, but this caused a high concentration in the fast pathways such as MP4 and MP5. In other sampling points, where the hydraulic conductivity is significantly lower, then the  $\delta^2\text{H}$  composition reached up to –15 ‰ (MP6). The smallest maximum appeared in MP10 and it was –38 ‰. In the fractured system (MP1–MP3, MP6–MP10: Fig. 14) the breakthrough was not obvious as it was close to the background variation (–30 to –60 ‰) in unsaturated zone water.

In addition to deuterium,  $\delta^{18}\text{O}$  was measured in water samples. The relationship between  $\delta^{18}\text{O}$  and  $\delta^2\text{H}$  in the unsaturated zone water was determined based on high frequency monitoring (see Eq. 2). In Fig. 15 and Fig. 16 d-excess according to this formula is depicted for MP1–MP5 and MP6–MP10 in a smaller scale. Significant reactions to precipitation occurred in sampling points MP6, MP8 and MP9. MP6 is connected to the fast channel, whereas MP8 and MP9 represent the broken zone of a fault. MP9 is connected to the fractured zone, which represent a storage zone, where flow is slow with higher dispersion of the tracer, since the maximum concentration appeared 182 days after the injection. In other sampling points (MP1–MP3, MP7 and MP10) the maximum d-excess values were around 20 but it is not clear whether the isotope composition change depicts tracer breakthrough or only variations in background. The appearance of deuterium in different sampling points and the appearances of maximum concentrations are summarized in Tab. 4.

The new injection borehole for the multi-tracer experiment obviously intercepted the main fracture, therefore the tracer was flushed after the first precipitation event. It is suggested, that tracer dispersed into the smaller surrounding fractures below the borehole (soil – unsaturated rock zone) and was flushed by subsequent larger precipitation events.

### 4.3. Fertilizer application experiments

Two fertiliser application experiments were performed; for both experiments the synthetic fertilizer KAN (calcium ammonium nitrate) was used in accordance with the appropriate agricultural practice. For the meadow with two mowings an application rate of 40 kg N/ha was used, therefore for 150 m<sup>2</sup> of test area (Fig. 3) 0.6 kg N was required. Regarding 28% N portion in KAN, 2.25 kg of that fertilizer was used. Electrical conductivity, temperature and pH were measured in situ in water samples during the experiment (Fig. 4). The water samples were also examined in the laboratory for nitrate ion and nitrite ion concentrations and nitrogen isotope <sup>15</sup>N.

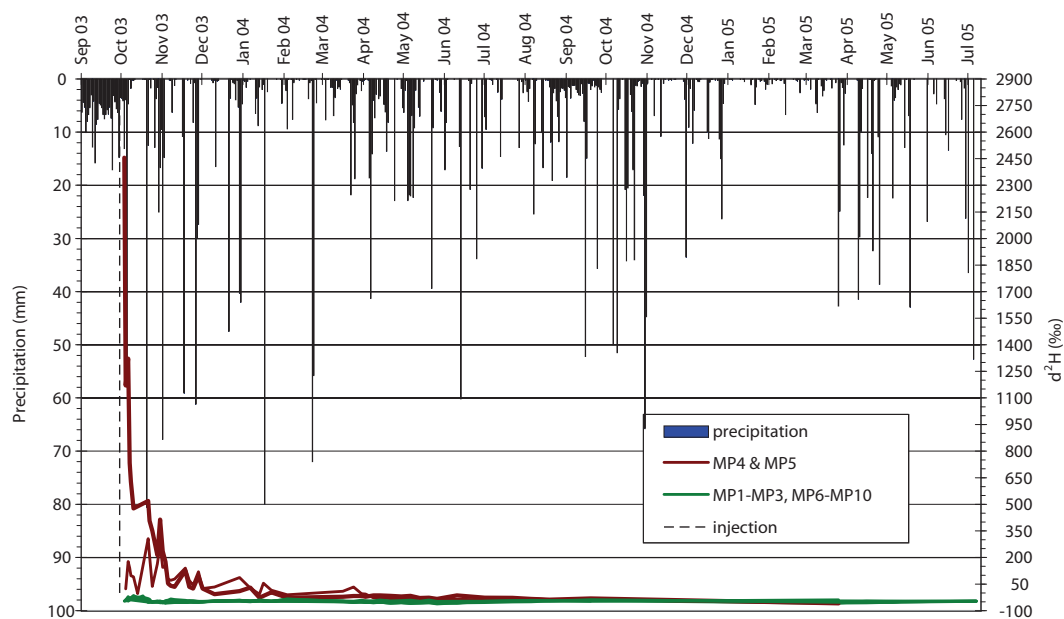


FIG. 14. Deuterium isotope composition of water in sampling points MP1–MP10.

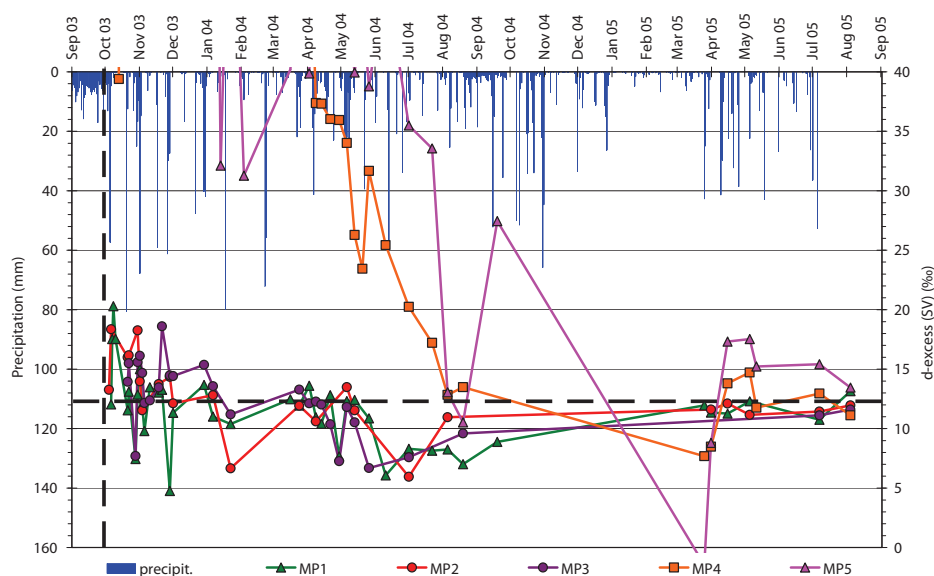


FIG. 15. Deuterium excess in sampling points MP1–MP5 (vertical dashed line: injection, horizontal dashed line: d-excess for Sinji Vrh unsaturated zone).

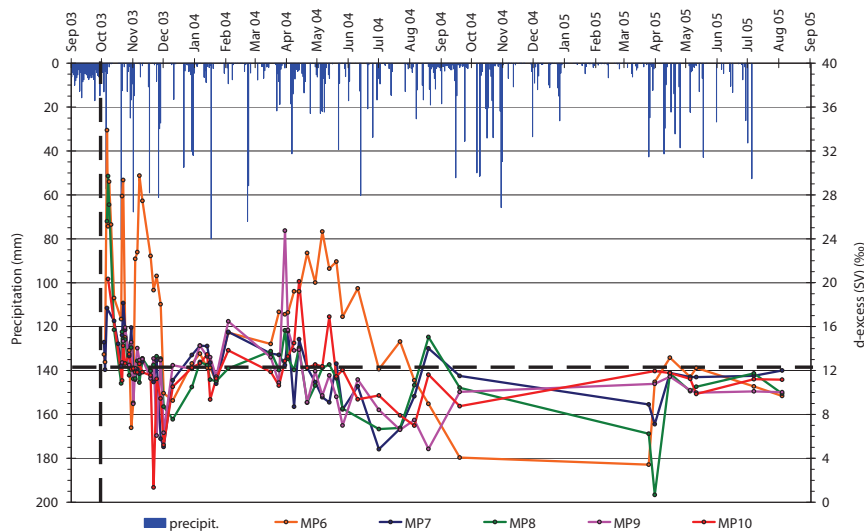


FIG. 16. Deuterium excess in sampling points MP1–MP10 (vertical dashed line: injection, horizontal dashed line: d-excess for Sinji Vrh unsaturated zone).

TABLE 4. THE FIRST APPEARANCE OF DEUTERIUM IN DIFFERENT SAMPLING POINTS AND THE APPEARANCE OF MAXIMUM  $\delta^2\text{H}$  COMPOSITION

	Appearance of tracer (days)	Max. $\delta^2\text{H}$ composition (%)	Max. value of d-excess (UNZ SV)	Appearance of Max. value (days)
MP1	7.4	-18.5	20.3	8.4
MP2	4.4	-28.4	18.4	6.4
MP3	21.4	-34.6	18.6	52.4
MP4	4.4	305.6	372.0	21.4
MP5	3.4	2454.9	2522.5	3.4
MP6	3.4	-14.9	33.9	6.4
MP7	3.4	-16.6	18.2	22.4
MP8	6.4	-23.1	29.7	7.4
MP9	21.4	-33.65	24.7	182.4
MP10	7.4	-38.3	20.3	7.4

In the first fertiliser application experiment (experiment G1) nitrate appeared in water samples of almost all sampling points after approximately 30–35 days (Fig. 17), which was five days after the heavy rain (4 July; 51.7 mm), followed by more or less constant rain [23]. The first precipitation event (Fig. 17) caused dissolution of the fertiliser and transported it into the soil zone. The highest nitrate concentration (15.1 mg/L) appeared at the measuring point MP5 (Fig. 17). Previous tracer experiments and structural mapping identified this sampling point as a fast channel with the potential to permit large contaminant fluxes (see Fig. 2: tracer test sampling area). Natural background unsaturated zone concentrations measured in springtime, which are dominated by mineralization processes in the soil, were higher than the observed unsaturated zone nitrate concentrations following fertiliser application. The second fertiliser application experiment (G2) was performed in order to obtain further information on nitrate percolation through the soil cover. For this reason, suction cups were installed in the soil and isotope analysis was carried out on water obtained from multiple sampling points (MP2, MP5, MP10 and MP21 in Fig. 18). The nitrate appeared one week after one very large precipitation event (68.8 mm; 21 Sept.), about 22 days after fertiliser was applied. Since the isotope composition of the synthetic fertilizer KAN is about 0‰, the isotope data  $\delta^{15}\text{N}$  (Fig. 18) confirmed that the nitrate source was the fertiliser applied on the meadow in experiment G2 [23]. The nitrate transport along the fast channel at measuring point MP5 was showed the first breakthrough of nitrate after 8 days. In some measuring points another flush of the nitrate was detected (MP21 and MP10). After another very large precipitation event in the following spring (1 March; 85.1 mm) the nitrate was flushed again, which released nitrate previously retained in microfractures of the unsaturated zone (MP2 in Fig. 18).

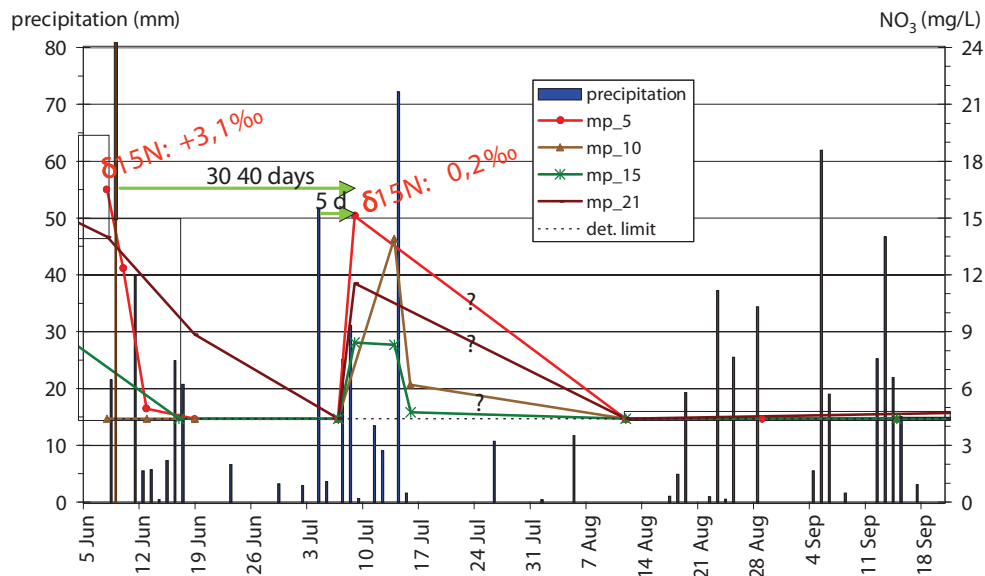


FIG. 17. Precipitation events and nitrate concentrations (detection limit: 4.4 mg/L) in sampling points MP5 for experiment G1 with  $\delta^{15}N$  data for MP5.

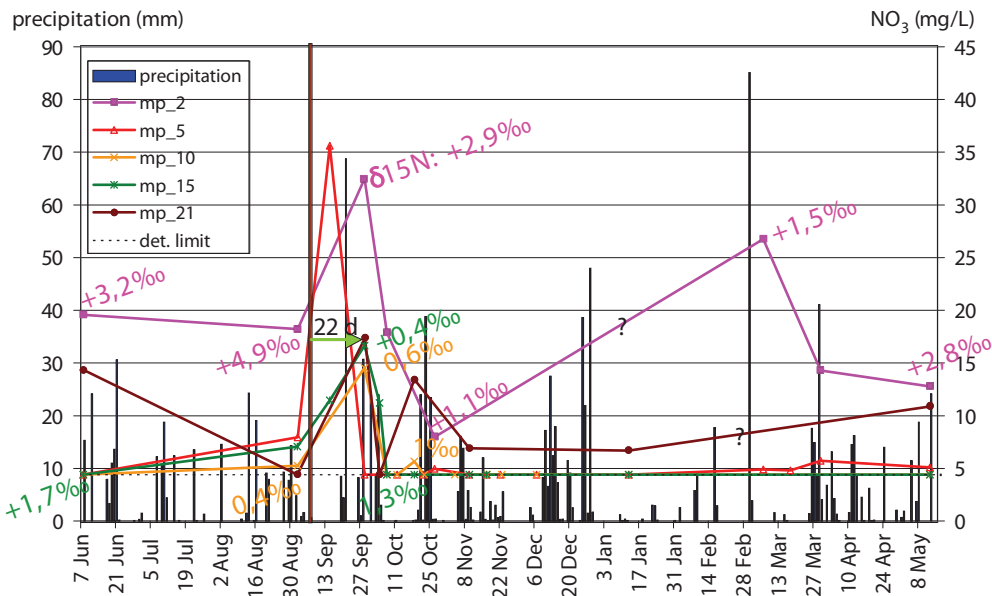


FIG. 18. Precipitation events and nitrate concentrations (dashed horizontal line: detection limit at 4.4 mg/L) in sampling points MP2, MP5, MP10, MP15 and MP21 for experiment G2 with  $\delta^{15}N$  data.

## 5. CONCLUSIONS

Fractured and karstified rocks are highly heterogeneous and complex, therefore knowledge of the rock structure is of paramount significance for predicting flow and transport. The transport of pollutants depends on i) saturation rate of the soil and unsaturated zone, ii) on precipitation events and iii) on the presence of channels and interconnected fracture networks. Pollution remains in the fractures of the upper part of the unsaturated zone and is flushed by subsequent large precipitation events which can occur several months or years afterwards. The degree of flushing is highly dependent on the antecedent moisture conditions within the unsaturated zone.

If there has been no precipitation prior to the application of a tracer then the first observed point of breakthrough will be the maximum concentration measured. Modeling such breakthrough curves can be problematic.

The results of isotopic investigations gave additional information about the transport processes in the unsaturated zone. Results of  $\delta^{18}\text{O}$  and  $\delta^2\text{H}$  isotope composition provided a better understanding of the research area and provides guidelines for further long-term and short-term monitoring strategies.

The tracer experiment has shown different flow velocities. Karst conduits or large fractures/faults show no storage capacity, the most rapid flow, and very limited dispersion. Broken and fractured zones have some storage capacity, which leads to retardation and the slower flow. The fractured and karstified rock could be seen as discrete conduits within highly fractured rock. The latter could be considered as a permeable matrix, since the rock (limestone) matrix porosity (intracrystalline) is negligible and the system could be best modelled with a hybrid model (comprising discrete conduits and a continuum of dense fractured system) rather than a dual porosity model (where there would be a continuum of conduits and a continuum of dense fractured rock). This is a subject for future research.

Results of the fertiliser application experiments have shown that a thin autochthonous soil cover on karstic rock is insufficient to retain nitrate and prevent pollution of groundwater. However, the maximum nitrate concentrations (up to 16 mg/L in G1 and up to 36 mg/L in G2) were lower than natural background values and the drinking water limit. Therefore the usage of fertilisers should be in accordance with strictly defined standards. Further detailed studies on this aspect are needed within the frame of the research into karstic aquifer vulnerability. Additional experiments with an emphasis on biogeochemical transformations (e.g. measurement of nitrogen gas,  $\text{N}_2\text{O}$ , soil nitrogen compounds, dissolved nitrogen compounds including isotopes, and microbiological processes) is planned in order to better understand the behaviour of nitrate in soil and the unsaturated zone.

#### ACKNOWLEDGEMENTS

We acknowledge the financial support from the Ministry of Science and Technology of the Republic of Slovenia for research projects under the research grants No. J1-7172-94 and J1-0462-98, for doctoral scholarship for Barbara Čenčur Curk (S21-210-005/15249/97) and Branka Trček (S21-215-007/13034/97) and for joint projects with Ministry for Physical Planning of the Republic of Slovenia, under the research grant No. V2-8575-96. This work was supported also by the International Atomic Energy Agency under the research grant No11519. We express our sincere thanks to Dr W. Stichler (GSF, Germany) for analyses of  $\delta^{18}\text{O}$  and  $\delta^2\text{H}$  and his valuable advice.

#### REFERENCES

- [1] ČENČUR CURK, B., Terenski eksperimentalni poligoni kot osnova pri študiju prenosa snovi v nezasičeni kraško-razpoklinski kamnini (Experimental field sites as a basis for the study of solute transport in the vadose zone of karstified rock), *Acta hydrotech.* **15/20** (1997) 111.
- [2] VESELIČ, M., Study of Mass Transport in Fractured and Karstified Rocks, Project Proposal for 1995–1997 Research Grant of the Ministry of Science and Technology of the Republic of Slovenia, Ljubljana (1995) 12.
- [3] JANEŽ, J., “Underground connections in dependency to hydrogeological conditions”, *Karst Hydrogeological Investigations in South-Western Slovenia, Acta Carsologica* **26/1**, Ljubljana, (1997) 329–332.
- [4] VESELIČ, M., ČENČUR CURK, B., “Test studies of flow and solute transport in the unsaturated fractured and karstified rock on the experimental field site Sinji Vrh, Slovenia”, *New approaches characterizing groundwater flow (K.P., SEILER, WOHNLICH, S., Eds.) (Proc. XXXI International Association of Hydrogeologists Congress, Munich, Germany, 10–14 September 2001)*, Lisse, Balkema, (2001) 211–214.
- [5] TRČEK, B., Mass transport monitoring in the unsaturated zone of the karst aquifer by natural tracers, Doctor thesis, University of Ljubljana, Ljubljana (2001) 125.

- [6] BEHRENS, H., BENISCHKE, R., BRICELJ, M., HARUM, T., KÄSS, W., KOSI, G., LEDITZKY, H.P., LEIBUNDGUT, CH., MALOSZEWSKI, P., MAURIN, V., RAJNER, V., RANK, D., REICHERT, B., STADLER, H., STICHLER, W., TRIMBORN, P., ZOJER, H., ZUPAN, M., Investigations with Natural and Artificial Tracers in the Karst Aquifer of the Lurbach System (Peggau-Tanneben-Semriach, Austria), *ATH – Transport Phenomena in Different Aquifer*, Graz, (1992) 9–158.
- [7] ČAR, J., Geological description, in *Karst Hydrogeological Investigations in South-Western Slovenia*, *Acta Carsologica* **26/1** (1997) 68–73.
- [8] JANEŽ, J., “Geological structure and hydrogeological position of the Hubelj spring”, *Karst Hydrogeological Investigations in South-Western Slovenia*, *Acta Carsologica* **26/1**, Ljubljana (1997) 82–86.
- [9] PETRIČ, M., Trnovsko-Banjška Planota Plateau and Surroundings, *Acta Carsologica* **26/1**, Supplementum , 7th Int.Symp.on Water Tracing, Field Guide of Karst in Slovenia (1997) 36–55.
- [10] MATIČIČ, B., “Agricultural threats to pollution of water of Trnovsko-Banjška Planota”, Kranjc, A.(editor). *Karst hydrogeological investigations in south-western Slovenia*, *Acta Carsologica* **26/1**, Ljubljana (1997) 102–113.
- [11] URBANC, J., Characteristics of oxygen and hydrogen isotope composition in waters from the carbonate rocks, Doctor thesis, University of Ljubljana, Ljubljana (1993) 144.
- [12] STICHLER, W., TRIMBORN, P., MALOSZEWSKI, P., RANK, D., PAPESCH, W., REICHERT, B., “Environmental isotope investigations”, *Karst hydrogeological investigations in south-western Slovenia*, *Acta Carsologica* **26/1**, Ljubljana (1997) 213–236.
- [13] PEZDIČ, J., LOJEN, S., BARBINA, V., QUARIN, L., URBANC, J., “Isotopic research on groundwater in the basin of Natisone river (NE Italy)”, *Isotopes in water resources management: Proceedings of a symposium on isotopes in water resources management*, Vol. 1 (Proc. series). Vienna, IAEA (1996) 209–214.
- [14] PEZDIČ, J., “Isotope effects in the karst infiltration matrix”, *Isotope Workshop*, Krakow 1st to 6th of July, Poland (2000) 134–136.
- [15] ČENČUR CURK, B., VESELIČ, M., Laboratory and Experimental Study of Contaminant Transport in Fractured and Karstified Rock, *RMZ – Materials and geoenvironment* **46/3**, Ljubljana, (1999) 425–442.
- [16] VESELIČ, M., ČENČUR CURK, B., TRČEK, B., “Experimental field site Sinji Vrh”, *Tracers in the unsaturated zone (Markierungsstoffe in der ungesättigten Zone)*, *Steir. Beitr. Hydrogeol.* **52** (2001) 45–60.
- [17] TRČEK, B., VESELIČ, M., URBANC, J., The suitability of carbon isotope composition as natural tracer in karst aquifer investigations, *Acta Carsologica* **29/1**, Ljubljana (2000) 153–161.
- [18] TRČEK, B., CAR. M., VESELIČ, M., The use of isotopic, hydrogeochemical and ground-penetrating radar investigations in the study of the unsaturated zone of the karstic aquifer – *Uporaba izotopskih, hidrogeokemijskih in georadarskih raziskav pri študiju nezasičene cone kraškega vodonosnika*, *RMZ – Materials and geoenvironmen* **47/3-4**, , Ljubljana (2000) 335–344.
- [19] ČENČUR CURK, B., Flow and solute transport in fractured and karstified rocks, Doctor thesis, University of Ljubljana, Ljubljana (2001).
- [20] TRČEK, B., Epikarst zone and the karst aquifer behaviour: a case study of the Hubelj catchment, Slovenia, Ljubljana, *Geološki zavod Slovenije* (2003)100.
- [21] TRČEK, B., Transport processes in the unsaturated zone of the karst aquifer, Phase report on isotope research, Geological survey, Ljubljana (2003) 7.
- [22] CLARK, I.D., FRITZ, P. *Environmental Isotopes in Hydrogeology*, New York, Lewis Publishers, (1997) 173–174.
- [23] ČENČUR CURK, B., PINTAR, M., KARAHODŽIČ, M., VESELIČ, M., “Nitrate transport through karstic soil and unsaturated karstic rock”, Present state and future trends of Karst studies : proceedings of the 6th international symposium and field seminar Marmaris Turkey, 17–26 September 2000, Vol. 1 (GÜNAY, G., Ed.), *International hydrological programme*, No. 49, Vol. 1, Paris, UNESCO (2001) 191–195.

# BEHAVIOUR OF NITROGEN IN THE UNSATURATED ZONE IN SOUTHERN AFRICA

A.S. TALMA  
Quaternary Dating Research Unit,  
CSIR, Pretoria, South Africa

G. TREDoux, J.F.P. ENGELBRECHT  
Groundwater Science Research Group,  
NRE/CSIR, Stellenbosch, South Africa

## ABSTRACT

Large areas in southern Africa have high levels of nitrate (>50 mg N/L) in groundwater caused either by natural nitrogen fixation or by pollution. Certain environmental conditions such as episodic groundwater recharge enhance such high levels and increase its variability. Soil samples were taken from two entirely different sites to identify sources and transport of nitrate through the soil. In arid Botswana, occasional high nitrate pulses with distinct pollution  $^{15}\text{N}$  signatures are observed in groundwater following extreme rainfall events. These are thought to result from a combination of regular recharge along preferential flow paths and rapid recharge through unleached soils during episodic recharge in this area. Soil samples down to 3 metres in different environments showed the usual vertical decrease of nitrate in both polluted and natural environments. One profile collecting outwash from a large polluted area showed an increase of nitrate and chloride with depth and represents a situation where episodes of rapid flushing of pollutant nitrate towards the water table may be expected. In humid sandy soils near Cape Town, South Africa, a comparison was made between soils from a reference area covered by leguminous vegetation and from an adjacent agricultural land previously fertilised with sewage sludge. The soil in the reference area was drier due to deeper moisture withdrawal by trees. In the agricultural land constant ammonia levels occur throughout the depth profile while nitrate levels decrease with depth.  $^{15}\text{N}$  levels in ammonia increase towards the water table, while  $^{15}\text{N}$  levels in nitrate remains practically constant with depth. These profiles show the recovery effect of the vadose zone after sludge deposition on the surface was discontinued. Considering both profiles, the results show the different responses that are possible under widely varying conditions of recharge and pollution load and link up with the chemical and isotope content of groundwater.

## 1. INTRODUCTION

Nitrogen in the form of nitrate is becoming a significant pollutant in groundwater in many parts of southern Africa, as it is in other parts of the world. Increasing population numbers are leading to a rising water demand, while the available water resources, which in the arid regions of southern Africa mostly consist of groundwater, remain very limited. Consequently, improved land-use management and protection of groundwater quality are required.

Extremely high nitrate values (from both natural and anthropogenic sources) are observed in the water from many southern African boreholes [1]. The present authors are involved in a project entitled: *Developing Control Measures for the Increasing Nitrate Hazard in Groundwater in Rural Areas in Botswana, Namibia and South Africa*. The aim of the project is to investigate aspects of groundwater nitrate sources in the region. This project is carried out in collaboration with the water authorities of Namibia, Botswana and South Africa. The regional project sponsored by the Department of Science and Technology (DST) in South Africa entails the collation of all groundwater nitrate data from the three countries into a common database (Fig. 1), field investigation of selected groundwater nitrate occurrences and the development of source identification, and where possible, remediation criteria [1]. The contribution that the South African partners could add to the IAEA CRP project was to investigate aspects of nitrogen transformation in soils in more detail. The approach was to investigate the production and transport of nitrate in the soil and unsaturated zone originating both from pollution sources and from natural soil nitrogen during its passage to groundwater. Both nitrate sources are significant in the context of regional nitrate occurrences. Nitrogen isotope ratios are known to be useful source indicators in the saturated zone and are considered as an important tool for work in the unsaturated zone.

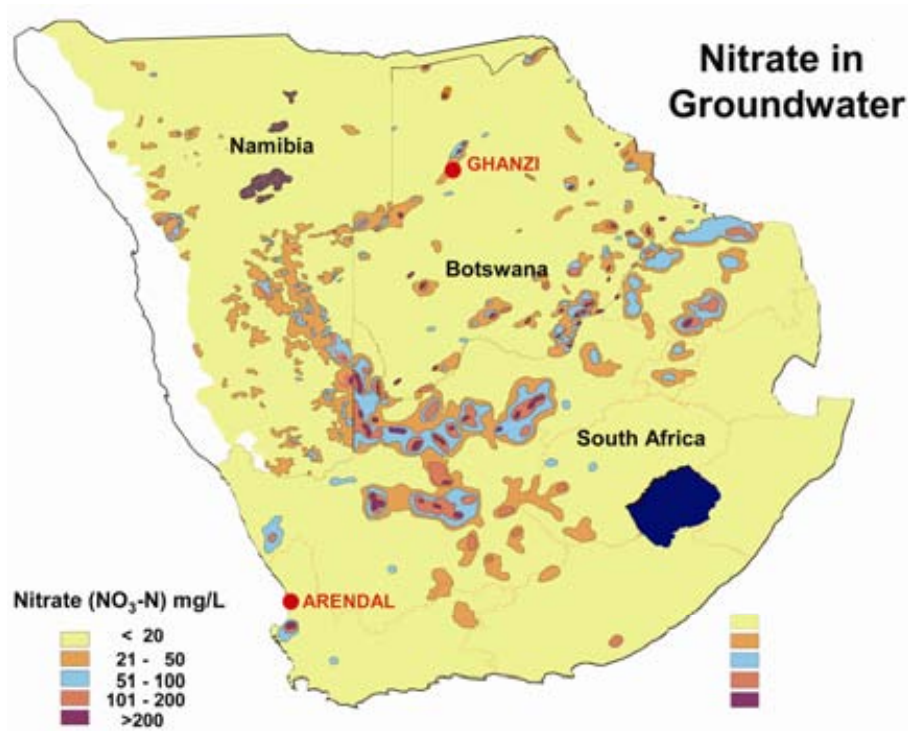


FIG. 1. Map depicting nitrate concentrations in groundwater in Botswana, Namibia and South Africa. The information is based on databases maintained by water authorities in the three countries.

Two sites were studied within the scope of the present project. The first site was at a remote location near Ghanzi, in western Botswana. In this area nitrate levels in groundwater have, at times, exceeded 500 mg N/L<sup>1</sup> in response to high-recharge events [2]. Within the same region one also finds boreholes with nitrate levels in the range up to 50 mg N/L, but where the nitrate level remains constant over some years. The other study site is on the farm Arendal, near Cape Town, South Africa. This agricultural site was regularly fertilised with municipal sludge over a period of five years to provide soil moisture retention for growing fodder crops [3]. In 1995 groundwater chemistry showed that there was obvious transformation of organic N of the sludge to nitrate at this site and therefore soil profiles were taken in the context of the present project for investigating the process. In both cases the objective was to explore the potential of <sup>15</sup>N as a tool for interpreting the processes involved in nitrification in the unsaturated zone.

## 2. THE GHANZI STUDY

### 2.1. Site background

The town of Ghanzi, in western Botswana south of the Okavango Delta, is located in the Kalahari, an arid savanna region. At this location, the Ghanzi Ridge forms a prominent topographic feature while the sand cover is thinner and groundwater levels are, according to Kalahari standards, quite shallow (Appendix I). The land around Ghanzi is utilised for cattle ranching where the cattle are living off grass amongst *Acacia* trees [4]. Nitrate levels in groundwater in this area are generally high (up to 50 mg N/L) but cattle can easily tolerate such levels under normal circumstances.

<sup>1</sup> In the present report, the South African practice, to express nitrate, nitrite, and ammonium concentrations in water as mg N/L is followed. 1 mg N/L = 4.4 mg NO<sub>3</sub>/L = 1.3 mg NH<sub>4</sub>/L.

Heavy rainfalls occurred during the summer of 1999/2000 reaching its peak in February 2000 with extensive flooding in the area: the rainfall during that season exceeded those encountered during any of the previous 20 years (Fig. 2). In September 2000, cattle (especially pregnant cows) started dying within minutes after drinking borehole water. On at least four farms several hundred heads of cattle died within weeks. The livestock losses were diagnosed by veterinarians to be due to excessive nitrate levels in the drinking water. Chemical analysis of the water showed that nitrate levels in the affected boreholes reached up to 700 mg N/L [2, 5]. It is assumed that the increase in the nitrate concentration in groundwater must have occurred rapidly, since there was insufficient time for the animals' digestive systems to adapt to the increasing nitrate levels.

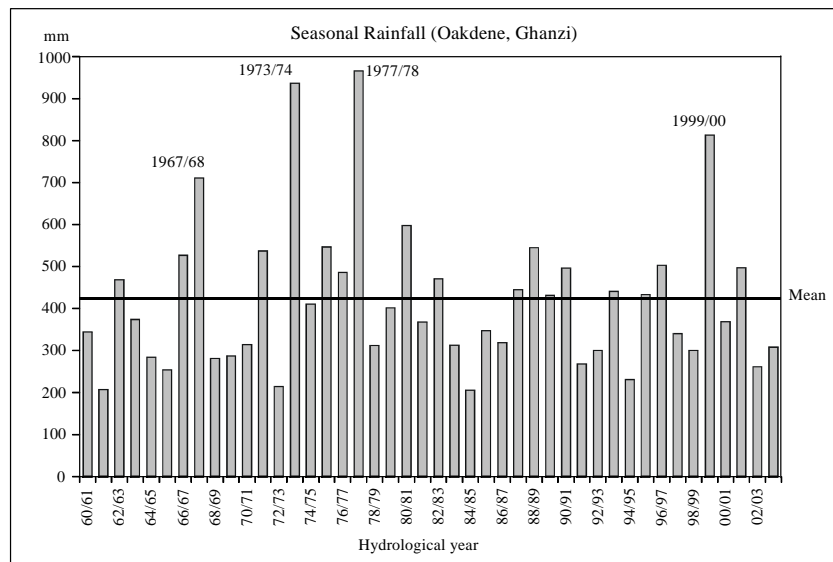


FIG. 2. Rainfall record at the farm Oakdene, near Ghanzi [12] area.

Investigation over a few years has shown that the groundwater nitrate in boreholes in this area has both a natural soil nitrogen and a pollution-derived component [2, 5]. Groundwater shows a baseline concentration of natural nitrate of about 50 mg N/L, which has remained constant during the past few years (Fig. 3 and [5]). Superimposed on the natural background, there is an excess quantity of nitrate forming and accumulating in the vadose zone which is mainly derived from animal pollution during the drier years. <sup>15</sup>N values confirm that the additional nitrate is mainly derived from pollution (Fig. 4). This nitrate component accumulates during dry seasons and is transferred to the groundwater table only during seasons with a very high rainfall (as was the case in 2000, Fig. 2). Such abnormally high and rapid recharge causes the nitrate to be flushed into the phreatic aquifer from where it was used for stock watering (Fig. 5). The high nitrate water, which overlies a large reserve of good quality water is gradually removed by abstraction or other processes with the result that the quality of the abstracted groundwater improves with time (Fig. 3). There are clear indications [2] that the regular (possibly annual) low salinity groundwater recharge takes place through dissolution structures ('sinkholes') in areas where surface calcrete occurs. Observations indicated that the high intensity recharge events take place during flooding over a much larger area in all depressions amongst the sand dunes and reaches the groundwater table through openings in the calcrete layer located in most instances below ground level (Fig. 6).

## 2.2. Soil Profile Sampling and Analysis

Field studies of the unsaturated zone were made on three farms in the Ghanzi area to obtain information of the soil conditions for testing the hypothesis that two distinct sources of nitrogen contribute to the groundwater nitrate load. The objective was to compare the effects of different land use on the nitrogen composition in soils. Profiles were obtained in March 2001 and in February 2003 (Table 1). Profiles were sampled in the following environments:

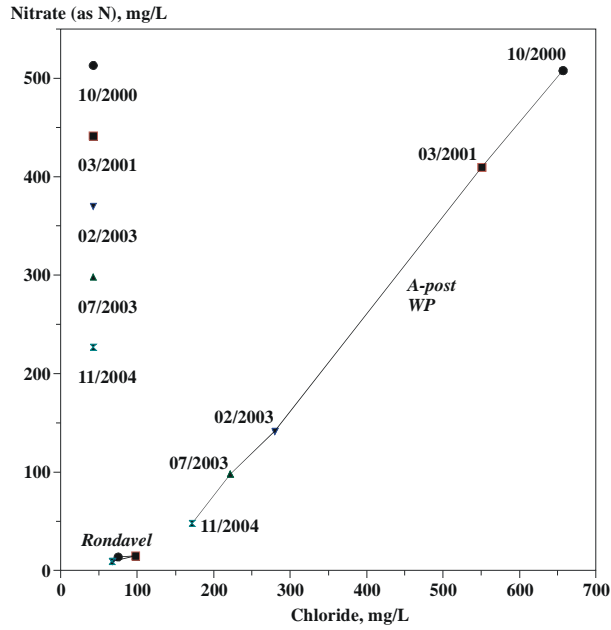


FIG. 3. Nitrate vs. chloride graph for two boreholes typifying low and high nitrate occurrences in the Ghanzi area. The month and year of sampling is indicated at each point. At 'Rondavel' the low nitrate level remained constant. At 'A-post WP' the nitrate and chloride levels decreased substantially from the high level in 2000 until 2004.

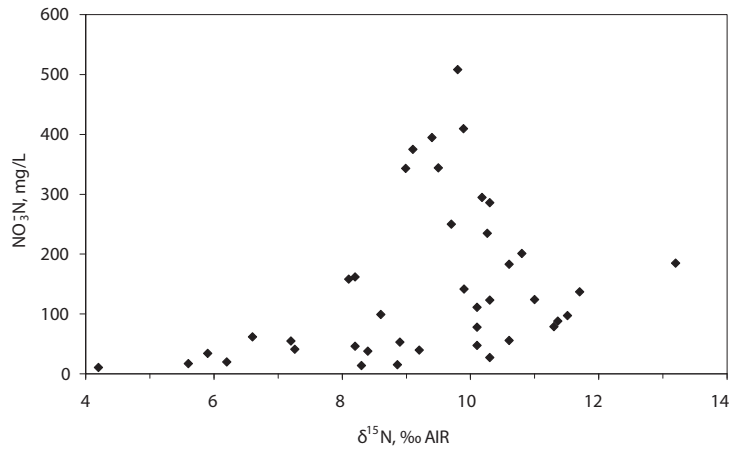


FIG. 4. Relation between  $^{15}\text{N}$  and nitrate concentration for groundwater samples collected in the Ghanzi area between 2000 and 2004. Based on the criteria initially proposed by Kreitler [11], samples with  $\delta^{15}\text{N} < +8\text{‰}$  are classified as natural nitrate and those with  $\delta^{15}\text{N} > +9$  as derived from faecal pollution.

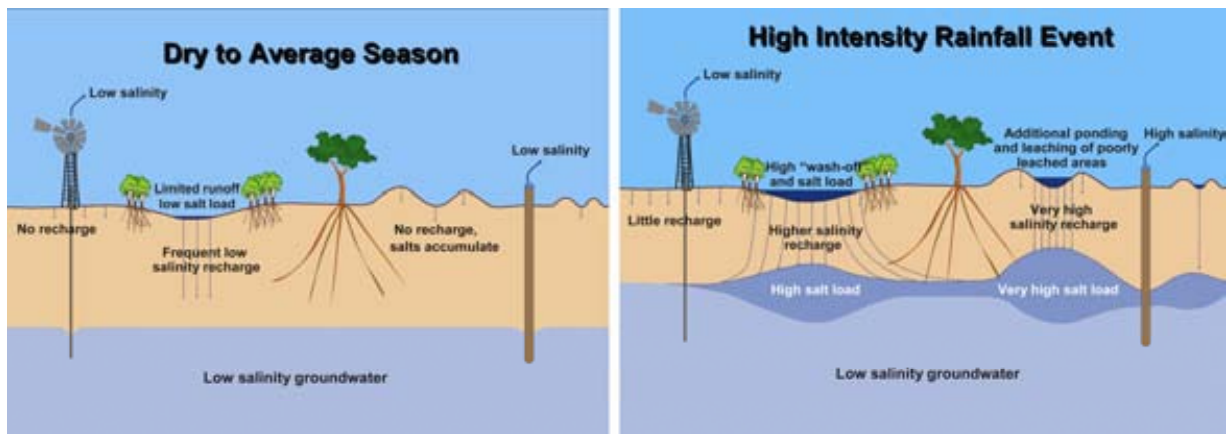


FIG. 5. Presentation of hypothesis for explaining the recharge mechanisms for low nitrate (dry season) and high nitrate (high intensity rain) on the Ghanzi Ridge. The ‘limited runoff’ situation illustrated on the left in the top diagram represents the regular, low-salinity groundwater recharge that occurs annually in limited areas along well-leached preferential flow paths. The situation depicted on the right represents the setting where no recharge occurs during the dry periods (top diagram) but where flooding produces recharge with high salt loads only during exceptionally wet seasons (bottom diagram). In such seasons run-off is generated over larger, non-leached areas and a higher salt load is also contributed along the regular recharge flow path (refer left side of bottom diagram).



FIG. 6. Example of opportunistic recharge shows local flooding which may be responsible for episodic recharge (February 2003).

- An undisturbed grazing area with very low cattle density (profile 5: ‘veld’) consisting of grass, shrubs and a few acacia trees. This location was selected to represent the situation of natural nitrate formation.
- Sandy areas that have moderate cattle traffic (profiles 1, 9 and 13: ‘cattle’). In terms of pollution potential these sites represent situations between ‘veld’ and ‘kraal’ (see below).
- Enclosures populated daily by cattle in which high loads of manure are present (profile 3). This profile is identified by the local name ‘kraal’, denoting an area where cattle may stay overnight, usually provided with a stock watering point.

- One site (silty profile 4: ‘pan’) is a local low position that drains an area of about one to two hundred square metres. The catchment of this site carries moderate cattle traffic but also partly drains a ‘kraal’.
- One site (sandy profile 2: ‘outwash’) is in a slight depression that drains an area of about two hundred square metres, including a ‘kraal’. The site is located near a large tree (Fig. 7).
- Two sites (profiles 8 and 14) that were situated near farm houses and that could be influenced by discharge from septic tanks discharging household sewage.

Hand augering was used to obtain soil samples from depths down to a maximum of 3 metres (Table 1). Soil samples were immediately transferred to double polyethylene bags and stored cool. Except for the one ‘pan’ sample (profile 4), the soils all consist of sandy material with less than 5% silt and clay. The maximum depth of sampling was limited by a calcrete (caliche) layer occurring widely in this area at depths ranging between surface and 3 metres. At the depth of the calcrete, the hand auger could not penetrate any further.

Soil analyses were carried out by Bemlabs (Somerset-West, South Africa) using appropriate standard methods. Although special care was taken, it is possible that moisture may have been lost during transport of the samples and the moisture values shown may be under-estimations. The nitrogen quantities available in these profiles were however too small to carry out any nitrogen isotope analyses. The discussion is, therefore, confined to interpreting the soil chemistry data.

### 2.3. Results

The soil chemical depth profile data (Table 2) show diverse trends of which a selection has been presented in Fig. 8. Profile 4, from a small pan probably ten metres in diameter, shows high siltation and also contains some small stones. Profiles 8 and 14 were taken at locations that may have been influenced by nearby septic tanks (French drains). Profile 8 was taken close to a *Tylosema esculentum* (Marama bean) shrub. This is a plant that is known to be a very productive nitrogen fixer and forms edible tubers underground that can be as large as 60 kg. The bacterial counts on profile 14 are higher than the others which could confirm a septic tank influence or bacteria introduced by the animal faeces in the kraal.



FIG. 7. Area where outwash from a kraal collects and location of soil profile 2 (March 2001).

TABLE 1. SOIL SAMPLING DETAILS OF GHANZI SAMPLES

	Depth range (m)	Remarks
<b>Profile 1</b>	0–0.10	
March 2001	0.65–0.75	
De Graaf, old farm 21°37' 51"S 21°58' 11"E	1.10–1.20	
Near gate	1.45–1.55	
Moderate cattle traffic	1.95–2.05	
	2.80–2.90	Calcrete
<b>Profile 2</b>	0–0.15	
March 2001	0.40–0.50	
De Graaf, old farm 21°37' 51"S 21°58' 11"E	0.70–0.80	
Near large tree	1.35–1.45	
Slight depression	1.80–1.90	
Collects significant outwash from kraal	1.95–2.05	
	2.80–2.90	
	3.35–3.45	Calcrete
<b>Profile 3</b>	0–0.10	High organic carbon
March 2001	0.10–0.20	
De Graaf farm at generator 21°34' 55"S 21°57' 54"E	0.20–0.40	
In kraal; High cattle density	0.40–0.50	Calcrete
<b>Profile 4</b>	0–0.15	
March 2001	0.15–0.25	
De Graaf farm, SE of generator 21°34' 55"S 21°57' 54"E	0.30–0.40	
Pan in depression; moderate cattle traffic	0.50–0.60	Calcrete
<b>Profile 5</b>	0–0.20	
March 2001	0.20–0.40	
De Graaf farm, north of homestead	0.40–0.50	
21°34' 54"S 21°57' 54"E	0.50–0.60	
In pasture with very low cattle density	0.65–0.80	
	0.80–0.95	
	0.95–1.05	Calcrete
<b>Profile 8</b>	0.95–1.05	
February 2003 P Brown farm, north of De Graaf	1.95–2.05	
21°34' 49"S 21°57' 56"E Near house and septic tank, close to <i>Tylosema esculentum</i> plant; No cattle	2.95–3.05	Calcrete
<b>Profile 9</b>	0.45–0.55	
February 2003	0.95–1.05	
Lewis farm, furthest post 21°40' 53"S 21°55' 57"E	1.45–1.55	
At engine pump; next to kraal	2.40–2.50	Calcrete
<b>Profile 13</b>	0.45–0.55	
February 2003	0.95–1.05	
De Graaf, old farm 21°37' 51"S 21°58' 11"E	1.45–1.55	
Near trees	1.95–2.05	
	2.45–2.55	
	2.95–3.05	Calcrete
<b>Profile 14</b>	0.25–0.35	
February 2003	0.45–0.55	
De Graaff, old farm 21°37' 51"S 21°58' 11"E	0.95–1.05	
Near home and septic tank	1.45–1.55	

TABLE 2. ANALYTICAL RESULTS FROM THE GHANZI SOIL SAMPLES (ANALYSES BY BEMLAB, SOMERSET WEST).

Depth m	Stone %	Clay %	Silt %	Sand	pH	Na	K	Ca	Mg	EC mS/m	C	N	NH <sub>4</sub> -N	NO <sub>3</sub> -N mg/kg	Cl	S	Moist %	Sat	HTC/100mL	
																			22° C	37° C
0.10	0.2				6.6	42	310	181	67	312	0.698	0.049	2.16	38.4	69	32	2.0	31		
0.75	0				6.5	2.9	173	45	13.2	408	0.078	0.031	1.88	10.4	41	4	1.9	29		
1.20	0				6.7	4.1	171	36	15.1	275	0.029	0.027	3.84	8.0	17	5	1.3	31		
1.55	0				6.5	4.2	109	19	5.6	340	0.039	0.03	3.76	6.0	51	5	1.5	33		
2.05	0.2				6.5	20	252	22	5.7	233	0.019	0.028	4.72	6.8	10	5	2.1	28		
2.90	14.5				7.3	22	208	26	3.8	456	0.048	0.03	5.04	5.4	34	7	3.4	32		
0.15	0				7.2	405	2490	99	49	711	2.424	0.109	4.84	60.0	651	260	9.3	51		
0.50	0				7.5	114	849	145	36	332	0.262	0.048	6.2	18.0	103	51	5.9	37		
0.80	0				7.3	127	844	51	14	445	0.068	0.04	2.68	37.6	206	75	4.7	34		
1.45	0				6.9	154	488	56	14	185	0.087	0.038	5	39.2	240	88	4.5	41		
1.90	0.5				6.3	296	131	164	36	192	0.039	0.037	3.68	36.6	308	85	4.8	39		
2.05	0.3				7.3	431	42	402	72	318	0.039	0.039	4.24	57.0	617	108	6.9	42		
2.90	1				7.3	182	54	725	106	360	0.029	0.034	3.92	39.4	959	69	7.6	43		
3.45	0.6				7.4	94	86	472	215	309	0.019	0.039	3.92	67.2	685	58	6.6	40		
0.10	0.4				7.7	254	1474	72	31	415	6.652	0.499	4.6	49.6	1096	153	4.4	82		
0.20	1.5				7.4	71	666	139	45	233	0.572	0.1	3.76	31.7	51	31	1.2	39		
0.40	1.7				7.3	72	553	96	30	180	0.281	0.057	5.05	12.6	34	23	2.7	37		
0.50	3.4				7.2	92	619	111	35	217	0.184	0.058	4.24	11.6	103	26	4.2	39		
0.15	25.9				7.7	472	65	99	24	207	0.048	0.044	3.84	54.6	51	35	14.9	102		
0.25	34.3				8	519	35	23	6.2	182	0.019	0.039	4.12	43.2	86	68	12.2	103		
0.40	29.8				8.2	555	32	18	4.2	174	0.019	0.027	5.88	27.1	51	80	13.6	101		
0.60	42				8.3	613	28	29	4.8	211	0.029	0.031	4.68	29.6	62	116	9.9	102		
0.20	0.3				7.1	15.2	36	168	27	138	0.126	0.035	4.52	14.0	10.3	3	1.8	36		
0.40	0.3				6.5	8.9	41	155	27	183	0.029	0.035	5	15.2	17.1	2	1.5	35		
0.50	0.1				6.6	8.5	36	187	28	160	0.068	0.048	5.12	11.6	6.9	1	2.2	37		
0.65	0.1				6.5	9.1	38	225	33	117	0.068	0.044	4.44	7.6	3.4	2	2.6	39		
0.80	0.1				6.3	8.2	21	127	17	233	0.107	0.048	6.56	7.6	6.9	2	3.1	43		
0.95	0.4				6.4	12.1	21	237	26	163	0.068	0.032	4.6	9.6	3.5	3	3.1	38		
1.05	6.6				7.1	6.7	9.1	179	13	79	0.126	0.036	5.92	10.0	1.7	1	3.3	39		

TABLE 2 (cont.). ANALYTICAL RESULTS FROM THE GHANZI SOIL SAMPLES (ANALYSES BY BEMLAB, SOMERSET WEST).

Depth m	Stone	Clay	Silt	Sand	pH	Na	K	Ca	Mg	EC	C	N	NH <sub>4</sub> -N	NO <sub>3</sub> -N	Cl	S	Moist	Sat	HTC/100mL	
							cmol/kg			ms/m	%	%		mg/kg			%		22° C	37° C
1.00	0	0.8	2.7	97	6.9					16.1	0.234	12.8	12.8	2.94	2.1		1.7		21300	13800
PROFILE 8	0	3.2	0.7	96	6.2					7.8	0.326	5.03	5.03	1.40	1.1		1.7		2890	3140
KRAAL	2.1	4.6	2.7	93	5.7					14.6	0.277	5.9	5.9	1.61	2.0		4.3		15000	14200
0.50	0	2	2.1	96	6.8					66.7	0.42	3.57	3.57	25.4	6.8		2.0		45600	50400
PROFILE 9	0	2	2.7	95	6.6					15.2	0.298	3.97	3.97	5.28	1.5		2.3		9550	5980
KRAAL	0.6	4.8	0.3	95	6.4					18.2	0.313	4.05	4.05	2.27	3.0		2.4		15500	11700
2.50	3.8	4.8	0.9	94	7.7					22.8	0.266	2.92	2.92	2.30	3.1		2.9		5030	5020
0.50	0	5	0.5	95	7.8					45.3	0.462	2.25	2.25	12.1	5.1		4.2		40500	46500
1.00	0	6.6	0.9	93	7					27.3	0.376	6.18	6.18	6.1	1.4		3.5		58000	44400
PROFILE 13	0	5.6	1.7	93	6.5					20.5	0.311	3.75	3.75	2.6	2.4		3.2		10400	8520
KRAAL	0.6	5	2.3	93	7.9					36.1	0.264	2.14	2.14	1.9	3.3		3.9		5120	4970
2.50	0	2.6	0.9	96	8.2					39.5	0.296	3.97	3.97	2.1	3.2		4.4		6650	5320
3.00	0.4	2.6	1.5	96	8.1					28.3	0.364	4.1	4.1	2.2	2.9		4.1		23800	16200
0.30	0	0	1.7	98	6.6					18.6	0.439	5.98	5.98	6.9	1.3		7.3		1016001	100000
0.50	0	3.2	0.3	97	5.8					21.5	0.374	6.23	6.23	7.4	2.5		8.0		83209	56000
PROFILE 14	0	0.6	2.5	97	5.3					31.6	0.335	6.43	6.43	4.1	3.2		2.1		80400	31800
KRAAL	0	0	2.1	98	5.1					8.9	0.343	8.71	8.71	2.8	0.9		1.5		2770	2253

The comparison should be made between profile 5 representing natural veld conditions on the one hand and increasing levels of pollution in the following situations: profiles 1, 9 and 13 with moderate cattle traffic, the polluted conditions within the 'kraal', the depression ('pan') in profile 4 draining an area with moderate cattle traffic as well as a part of the 'kraal', and the sandy depression receiving outwash from a 'kraal' (profile 2) (Fig. 7). The selection of the depressions for soil sampling is directly related to the observations that rainwater runoff collects in such areas facilitating groundwater recharge in sandy regions (Fig. 7). During high intensity rainfall events, large areas may be flooded only with very local surface runoff due to the flatness of the overall topography and the absence of any significant drainage systems. The only slight undulations in the landscape are related to the occurrence of low dunes. This mechanism is considered as the key to groundwater recharge in the arid areas with extensive sand cover and this is seen to be confirmed in the data collected during the study at Ghanzi.

#### 2.4. Discussion of Ghanzi data

Overall, there seems to be a pattern of slightly increasing soil moisture with depth (Fig. 8). The soil infiltration pattern in this arid area is one of infiltration during a few rainfall events in summer and beyond that, continuous evaporation from the soil [5]. The pan area (profile 4 with high clay and silt content) retained moisture longer than the sandy soils found elsewhere. Overall the first group of profiles (#1–5 sampled in March 2001) have higher moisture contents than those sampled two years later (#8–14 sampled in Feb 2003) (Table 2). Seasonal moisture differences in Kalahari soils have also been observed by Selaolo [6] to vary on time scales of months in response to rainfall. It is hardly likely that all the soil moisture down to 3 metres depth is available to recharge groundwater at water table depths of 5 to 7 metres and deeper. The calcrete layer probably impedes vertical moisture transport to some extent and *Acacia* tree roots are known to penetrate at least that deep [7]. The exact thickness and permeability of the calcrete layer in this area is not known in detail but from observations at outcrops and from boreholes it can be estimated to be in the order of 0.5 m to over one metre thick. Dissolution features or 'sinkholes' can be observed in the calcrete outcrops and probably also exist below the sand surface.

Profile 2 shows a different moisture pattern than the others apart from the 'pan' (profile 4), perhaps due to the fact that it was located in a slight depression subject to much outwash from the kraal and this is considered to represent an example of direct recharge to beyond the calcrete horizon (Fig. 7). This is typical of the rapid recharge mechanism that is postulated for the area and responsible for the high nitrate, high  $^{15}\text{N}$  pollution in local groundwater. At profile 3 the high organic (manure) content of the soil in the upper layer easily retains the moisture expected to originate from the frequenting of the cattle but it does not seem to penetrate deeply, at least not during the dry conditions. This is clearly demonstrated by the very high chloride only in the upper layer (Table 2, Fig. 8).

The organic N concentration is very high at the surface in those profiles (2 and 3) where manure is present on the surface. Limited variability is evident up to a depth of one metre but beyond that the concentration remains between 300 and 400 mg N/kg regardless of the surface input values (Fig. 8). Surface soils samples collected from a similar natural veld area near Maun (200 km north-east) also had organic N contents of 300–400 mg/kg [8]. This would imply that at least at these points in the Ghanzi area, considerable quantities of nitrogen are available in the form of organic compounds in the soil profile. It would also mean that the organic nitrogen at the surface is mainly present in the form of particles that do not penetrate the soil to great depth.

The nitrate concentrations in the soil profiles are at least an order of magnitude lower than organic N (Fig. 8). Only in the most polluted circumstances, (for example in profile 2, receiving the outwash from the 'kraal' area) does nitrate persist throughout the profile as was also seen in Serowe (eastern Botswana) [9]. In all the other profiles, the nitrate level drops to less than 10 mg N/kg below 1 metre depth. Therefore, it can be concluded that nitrate is highly mobile and is moving rapidly through the soil column and easily reaches the groundwater, probably due to its high solubility. The fact that nitrate derived from pollution sources, as identified by  $^{15}\text{N}$ , is present in the groundwater (Fig. 4) confirms the high mobility. The ammonium levels near the surface are another order of magnitude smaller than nitrate (Fig. 8). In contrast to nitrate, ammonium levels remain relatively constant throughout the profile regardless of the pollution levels at the surface. The variation is exaggerated in Fig. 8 due to the large scale.

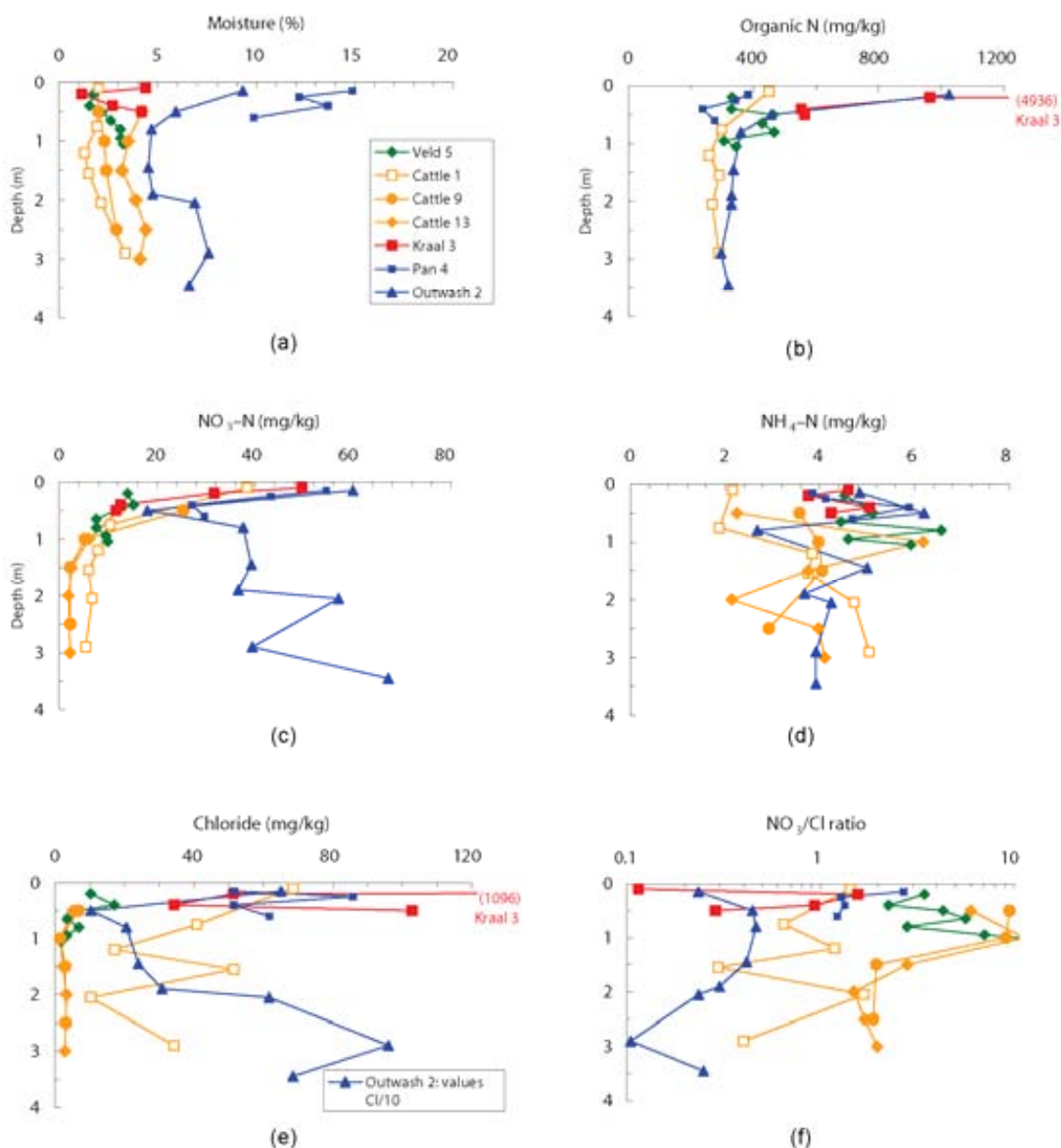


FIG. 8. Soil profile analytical results for the Ghanzi test site; a) moisture content, b) organic matter, c) nitrate, d) ammonia, e) chloride and f) Nitrate/chloride molar ratio

The graphs showing the various forms of nitrogen in Fig. 8 indicate that the main store of nitrogen in the soil column is in the form of organic nitrogen. Both  $\text{NO}_3$  and  $\text{NH}_4$  levels are much lower (typically 2 to 20 mg N/kg) compared to the organic nitrogen level (in the order of hundreds of mg/kg). If there is a direct input of nitrate, then it is rapidly removed. If nitrate is formed in situ, then it has hardly any effect on the vertical distribution of organic N in the soil. The local groundwater does not contain ammonium, probably due to retention of ammonium on the clay component in the soils. Any ammonium that forms in the cattle manure on the surface is expected to volatilize and in the subsurface it would seem that conditions are sufficiently oxidizing that ammonia does not form and neither is there significant nitrate production.

The chloride concentrations in the soil column below 1 metre depth, are low: less than 20 mg/kg (Fig. 8). In polluted situations (profiles 1, 2, 3, 4), the chloride concentrations are much higher, in some cases also deeper into the profile. In the case of profile 2, which is associated with outwash from a 'kraal', the chloride concentration is exceptionally high (note the scale reduction of Cl for this

profile in Fig. 8). Therefore, this profile represents a total anomaly compared to all other profiles. The nitrate concentration in this profile is also anomalous, indicating that other factors must be playing a role here. In nitrate polluted groundwater of the area the nitrate and chloride concentrations correlate (e.g. Fig. 3). It is, therefore, postulated that profile 2 which is located close to a borehole where stock losses occurred, in fact shows the presence of the salts that can be leached into the groundwater during extreme high rainfall events, such as that of February 2000. During such events large quantities of rain water collect in topographic depressions in areas where groundwater recharge does not occur regularly (Fig. 6). This is illustrated in the ‘very high salt load’ water body in the lower sketch, called ‘high intensity rainfall event’, in Fig. 5). It will be essential to follow up on this postulation in order to confirm the mechanism. However, the fact that this profile provided evidence of the presence of high salinity water in the soil column means that it does exist at least in isolated places, which may explain why the very high nitrates and salinities were only observed at some, but not all, boreholes in this area [5].

The  $\text{NO}_3^-/\text{Cl}^-$  ionic ratio seems to be very useful for identifying polluted areas (Fig. 8). The higher ratios are typical for unpolluted profiles while low ratios between 0.1 and 1 are typical for polluted profiles.

### 3. THE ARENDAL STUDY

#### 3.1. Site background

This site is a small land holding of 20 ha size that is operated as an agricultural interest by a family with an alternative primary income. The farm is located in the Western Cape Province, 60 km north of Cape Town. Details of the site are given in Appendix II. The test site is surrounded by similar small-holdings housing a stud farm to the east and a poultry farm to the west. A limited number of pigs and cattle are reared on the site and fodder crops are grown on a 8 ha portion of the land (Fig. 9). The site is underlain by a shallow unconfined sandy aquifer with water depths at approximately 3 metres. The groundwater is, therefore, relatively vulnerable to pollution. No irrigation is applied to this land: the only water input is the 450 mm mean annual rainfall. Cattle fodder is harvested each year. The rest of the land on the up-gradient side to the north is uncultivated and covered with invasive alien vegetation *Acacia saligna* (‘Port Jackson’). These bushes are subjected to an eradication programme using rust fungus. This is only partly successful, with the result that much deadwood is laying amongst some still living trees.



FIG. 9. Google Earth image of the Arendal test site with profile localities. The area has a southward slope with AD3 is located at 165 m and AD1 at 142 m amsl.

TABLE 3. PROPERTIES OF SLUDGE CAKE USED AT ARENDAL (BULK MEAN VALUES FROM COLVIN [3])

	Cl	Total Kjeldahl N	NH <sub>4</sub> -N	NO <sub>x</sub> -N	Dissolved Organic Carbon
Sludge composition (mg/kg dry mass)		3.5	2	15	–
Leachate composition: 1:5 extract (mg/L)	80	1200	400	>0.2	500

TABLE 4. <sup>15</sup>N ANALYSES OF WATER AND SLUDGE SAMPLES AT ARENDAL (FROM COLVIN [3])

	NH <sub>4</sub> -N mg/kg	δ <sup>15</sup> N (NH <sub>4</sub> ) ‰AIR	NO <sub>x</sub> -N	δ <sup>15</sup> N (NO <sub>3</sub> ) ‰AIR	Cl mg/L
Groundwater in cultivated area (borehole A1)	–	–	17 mg/L	+21.9	50–140
Groundwater in un-cultivated area (borehole A3)	–	–	10 mg/L	+4.8	10
Extract from sludge sample 1	9120	+27.9	101 mg/kg	+15.7	–
Extract from sludge sample 2	250	+23.0	770 mg/kg	+43.1	–

In 1996/7 Colvin [3] carried out a study at this site to establish the effect of municipal sludge coverage on this type of soil. Between 1991 and 1996, dried sewage sludge cake (Table 4) from a waste water treatment plant was used as a soil conditioner and fertilizer. The medium grained sandy soil has very poor water retention capacity and sludge application enabled the soil to remain wet for up to a few weeks after a rain event. Sludge was applied at the rate of 100 ton/ha during April (just before the rainy and planting season) and ploughed in. In 1996, well points were jetted down to the water table in both the cultivated and the northern forested areas (Fig. 7). Groundwater samples were taken three-monthly during a year's sampling (Table 4). Soil samples were also taken and analyzed. The effect of the sewage sludge manifested itself as increased nitrogen levels in the cultivated soil that ultimately found their way to the water table [3]. <sup>15</sup>N analyses of groundwater nitrate in 1997 indicated that considerable isotope enrichment occurred during the mineralisation of organic N to nitrate in the soil or sludge medium while the uncultivated land under the leguminous *Acacia* cover showed the normal δ<sup>15</sup>N of vegetation (Table 4). These data suggested that a useful isotopic study should be possible at this site. The aim of the study at this site was to compare the soil responses between the cultivated and forested land.

### 3.2. Soil Profile Sampling and Analysis

Groundwater samples were collected from two existing boreholes in the cultivated area (Borehole 1 and 2) that are 24 metres apart and from one borehole in the forested area (Borehole 3). The chemical data of the groundwater samples are shown in Table 5. Two soil profiles (AD1 and AD2, both 10 m north of boreholes 1 and 2 respectively) were taken from the cultivated land in April 2005 (Fig. 9). Soil samples were collected by hand auger down to depths well below the water table (3.0–3.7 m). A comparison profile (AD3) was taken within the forested area. Augering could not be used in profile AD3 due to the low moisture content of the soil at the time of sampling and samples were, therefore, taken by hand down to 1 metre depth only (Table 6).

TABLE 5. CHEMICAL COMPOSITION OF GROUNDWATER SAMPLES COLLECTED IN APRIL 2005 FROM BOREHOLES IN THE ARENDAL TEST SITE

Borehole ID:	Bh 1	Bh 2	Bh 3
Potassium as K mg/L	3.2	1.9	0.6
Sodium as Na mg/L	34	51	22
Calcium as Ca mg/L	12	8	2.6
Magnesium as Mg mg/L	12	16	5.6
Ammonia as N mg/L	0.4	1.0	1.2
Sulphate as SO <sub>4</sub> mg/L	17	18	9.4
Chloride as Cl mg/L	53	78	29
Alkalinity as CaCO <sub>3</sub> mg/L	11	3.0	13
Nitrate plus nitrite as N mg/L	16	18	4.5
Dissolved Organic Carbon mg/L	2.2	1.1	2
Conductivity mS/m (25°C)	38	45	19
pH (Lab) (25°C)	6.0	5.4	6.6
NO <sub>3</sub> <sup>-</sup> /Cl (ionic ratio)	0.74	0.67	0.38

TABLE 6. ANALYTICAL RESULTS FROM THE ARENDAL SOIL SAMPLES (SOIL ANALYSES BY BEMLAB, SOMERSET WEST, ISOTOPE ANALYSES BY THE UNIVERSITY OF NEBRASKA, USA)

	Depth m	C %	N %	NH <sub>4</sub> -N mg/kg	$\delta^{15}\text{N}$	NO <sub>3</sub> <sup>-</sup> -N mg/kg	$\delta^{15}\text{N}$	Cl mg/kg	Moist %	Clay %	Silt %	Sand %
Profile	0.30	0.20	0.007	15.4	-	5.9	+5.8	12.4	2.6	2.8	0.4	97
AD 1	0.60	0.41	0.013	11.3	+16.7	2.5	+3.0	17.9	2.9	2.0	0.8	97
	1.00	0.51	0.004	11.9	-	2.8	-	11.0	3.1	0.2	1.8	98
	1.30	0.35	0.013	10.5	-	2.0	+1.3	4.1	3.7	0.0	1.8	98
	1.70	0.20	0.007	10.6	-	2.0	-	2.8	3.1	0.0	2.6	97
	2.10	0.17	0.014	10.4	-	2.4	-	5.5	5.1	0.0	0.6	99
	2.60	0.28	0.012	38.2	-	2.8	-	12.4	15.3	0.0	2.2	98
	3.00	0.21	0.012	10.7	-	4.1	-	31.8	14.3	7.8	1.0	91
	3.50	0.41	0.013	12.2	-	4.2	+9.9	26.2	14.3	9.6	0.6	90
	4.00	0.15	0.009	12.3	-	3.4	-	11.0	15.2	6.6	2.0	91
	4.50	0.51	0.008	10.8	+12.3	2.4	+10.3	9.7	15.9	3.8	0.4	96
	Depth m	C %	N %	NH <sub>4</sub> -N mg/kg	$\delta^{15}\text{N}$	NO <sub>3</sub> <sup>-</sup> -N mg/kg	$\delta^{15}\text{N}$	Cl mg/kg	Moist %	Clay %	Silt %	Sand %
Profile	0.10	0.21	0.031	12.4	+12.8	5.0	+4.2	1.1	0.32	0.6	0.0	99
AD 2	0.30	0.27	0.010	13.6	-	5.6	-	4.1	1.9	0.0	1.8	98
	0.50	0.48	0.016	11.9	+13.4	3.3	+4.4	12.4	3.2	0.0	1.6	98
	0.90	0.39	0.009	12.2	+16.0	2.8	+4.3	4.1	2.9	0.0	2.0	98
	1.20	0.43	0.009	11.5	-	1.9	-	11.1	3.5	0.0	0.6	99
	1.50	0.21	0.012	12.5	-	2.3	-	9.7	4.5	0.0	0.4	100
	2.00	0.24	0.012	11.0	+21.3	1.9	+2.4	5.5	3.5	0.0	0.6	99
	2.50	0.47	0.012	11.7	+22.0	2.1	+1.5	16.6	3.2	2.6	0.4	97
	3.00	0.15	0.012	11.0	-	2.6	-	6.9	9.7	2.4	0.2	97
	3.50	0.18	0.013	11.5	-	2.6	-	17.8	15.5	1.0	3.0	96
Profile	0.10	0.30	0.018	12.1	+6.5	1.7	+3.3	24.9	0.2	0.0	2.4	98
AD 3	0.30	0.32	0.014	13.1	+12.5	1.6	+2.5	19.3	0.5	0.0	2.2	98
	0.60	0.64	0.010	11.7	+19.8	1.3	+1.8	20.7	0.5	0.4	0.6	99
	1.00	0.22	0.014	12.2	-	2.0	-2.0	59.4	0.5	1.2	0.4	98

Soil samples were transferred to sealed plastic bags and kept at 5°C. Standard soil analyses were done at the laboratories of Bemlab (Somerset–West) on the soil samples and their extracts (Table 6). Subsequently, 2N KCl (1:5) extracts were made from some of the soil samples and analysed for <sup>15</sup>N in both the ammonia and nitrate fractions at the University of Nebraska, USA. Budget and sample sizes limited the number of analyses that could usefully be made and all the results that were obtained are shown in Table 6.

### 3.3. Results

The two soil profiles (AD1 and AD2) in the cultivated area are very similar in most respects (Fig. 10) and can be considered virtually the same as far as the nitrogen species are concerned. Moisture levels in the soil close to the surface were low, since the sampling was done at the end of the dry season (April) before the onset of winter rains. The prominent difference in the moisture content between the two cultivated sites is probably the result of local clay lenses that influence the hydraulic properties of the vadose zone on a small scale. There is an occurrence of high clay content at the water table at 3 to 4 metres depth. A brown colouration of the soil by iron was observed at the water table for both AD1 and AD2. During the previous study ferricrete was observed at the groundwater table in other parts of the site [3]. The chloride profile is variable and there is no region of constant chloride concentration with depth to indicate a depth range not influenced by plants: even though the plant influence is probably limited to the upper 10-20 cm. It is likely that the chloride variation is a reflection of the variable rainfall patterns of the past few years, coupled with variable chloride input from such rains. In the forested area there is likely enhanced moisture withdrawal at greater depth by the bushes growing there, which then cause the chloride to concentrate more than is the case in the cultivated site.

Ammonia levels in all of the three soil profiles are relatively high for such sandy soils and generally constant throughout the profiles at approximately 12 mg/kg. The nitrate content near the surface is half the level of ammonia and decreases rapidly with a sharp increase again at the water table in both profiles (3.0 and 3.7 m). The NO<sub>3</sub>/Cl (atom/atom) ratios are distinctly different between the two sites. Those of the deeper soils at the cultivated sites are at 0.3 to 1.0 consistent with 0.74 and 0.57 found in nearby groundwater (Table 5). The <sup>15</sup>N contents of both nitrate and ammonia vary considerably with depth (Fig. 10). <sup>15</sup>N of nitrate decreases in all profiles, down to approximately the water table (moisture content > 14%). At the water table, <sup>15</sup>N of nitrate is +10‰ AIR which is lower than the +23‰ that was found in the groundwater of borehole A1 in 1996 (Table 5). The <sup>15</sup>N pattern of the ammonia is the mirror image of that of nitrate within the available samples (Fig. 10).

The forested site showed lower moisture levels towards the depth sampled (1.0 m) and higher Cl levels (Table 6). NH<sub>4</sub> and NO<sub>3</sub> levels are more or less similar. The NO<sub>3</sub>/Cl ratio of soil is 0.09 at 1 m compared to 0.38 in the groundwater (borehole A3 in Fig. 9): so some changes may be taking place deeper than 1 m, which are not evident in the present sampling run.

### 3.4. Discussion of Arendal data

The differences between the forested (AD 3) and the agricultural sites (AD 1 & 2) are profound (Fig. 10), even though the forested site was sampled only over the top one metre depth. The higher water withdrawal in the forested site, presumably at all levels, results in lower moisture contents and higher Cl levels (Table 6). Nitrate and ammonia levels were also generally lower on a mg/kg basis though higher when expressed in mg/L of interstitial water.

For all profiles the high ammonia content in the soil and its small variation with depth is striking, since ammonia is usually considered to be a less stable compound in nature, yet there appears to be little variation with depth. The organic nitrogen contents in the soils are low (in the order of 100 mg N/kg, Table 6). One is therefore likely dealing with ammonia that was developed during the time that sludge was deposited on the land (1991 to 1996). The cation ammonia, is readily adsorbed on clay materials and therefore less mobile than the nitrate ions. Yet, in spite of the variable clay content in each of the profiles, ammonia levels are constant throughout all three profiles. The high <sup>15</sup>N content of the ammonia is in accordance with the expected result of a nitrogen source from which ammonia was removed in gaseous form thereby causing isotope enrichment of the un-reacted material.

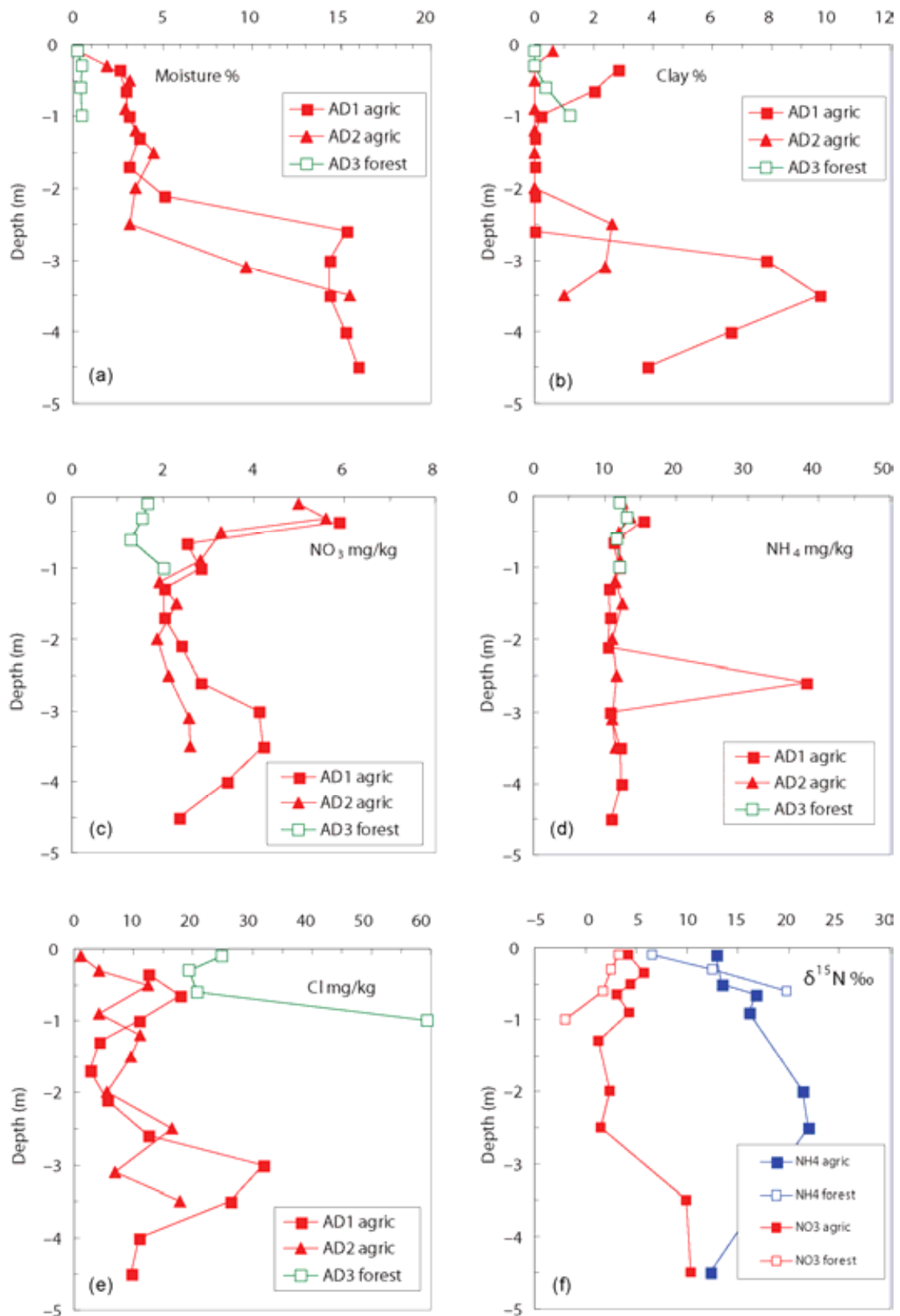


FIG. 10. Soil profile analytical results for the Arendal test site; a) moisture content, b) clay content, c) nitrate, d) ammonia, e) chloride and f)  $\delta^{15}\text{N}$  contents.

Nitrate, on the other hand, is more mobile and its pattern in the soil profiles conforms to the normal pattern of rapid decrease as it is being absorbed by plants in the upper half a metre of soil. Thereafter there seems to be little change in the isotope ratio since nitrate behaves in a conservative fashion in the absence of plants and in aerobic conditions. Some  $^{15}\text{N}$  decrease is apparent down to 2 metres depth. It is possible that there is some nitrification of ammonia (to nitrate) which would decrease the  $^{15}\text{N}$  content of nitrate towards lower values (given an approximate  $-20\text{‰}$  separation from  $\text{NH}_4$  to  $\text{NO}_3^-$  in the soil column [10]).

Near the water table (at 3 metres depth) the situation changes (Fig. 10). The  $^{15}\text{N}$  values of both ammonia and nitrate approach the average of  $+10\text{‰}$ , which is close to  $+6$  to  $+8\text{‰}$  usually considered appropriate for unpolluted water [2, 11] and distinctly lower than the  $+23\text{‰}$  that was found in nitrate in this groundwater in 1997 (Table 4). It seems therefore that the aquifer is now returning to its 'normal' state after the sludge deposition period of 1991 to 1996. It should be illuminating to monitor this site for the next 5 years to follow the change from polluted to unpolluted state.

In the forested area, there is basically a similar pattern for  $\delta^{15}\text{N}$  in both ammonia and nitrate vertically, except that the surface  $\delta^{15}\text{N}$  is lower and the isotopic change within the first metre depth is greater (Fig. 10). Deeper sampling should show whether a  $^{15}\text{N}$  reversal is also present in this area.

Both reversed vertical isotope patterns are therefore postulated to be the result of gasification of the ammonium in soil, nitrification of ammonia and denitrification at the water table. Future investigation should look at the relation between organic  $^{15}\text{N}$  and those of the  $\text{NO}_3^-$  and  $\text{NH}_4$  species and follow the change with time.

#### 4. CONCLUSIONS FROM BOTH SITES

The nitrate concentration in groundwater is closely related to the processes controlling groundwater recharge. This is due to the fact that nitrate is generated in the soil zone either by natural nitrogen fixation or nitrification of nitrogen species in pollutants such as manure and sludge. In the arid climate of the Ghanzi site, groundwater recharge is limited to high rainfall events and the collection of sufficient runoff in topographic depressions. From the profiles it would seem that recharge is highly variable from point to point. The nitrate content of the groundwater depends on the conditions at the soil surface and the frequency of leaching of each particular area. The results identified at least one area where a considerable quantity of salts generated by pollution is held in the unsaturated zone which could be flushed to the groundwater table at a subsequent high rainfall event.

Data from both study sites showed varying degrees of nitrogen input to groundwater. In the Ghanzi case, the input is much more diverse, both in terms of the likely concentrations of organic carbon, organic nitrogen and chloride on the surface and the degree to which these could be mineralised and transported. At Arendal the spatial distribution of nitrogen on the surface is more regular even if the input may be variable from season to season. Levels of ammonia in the profiles of both sites are higher than nitrate and vertically uniform. This suggests that the ammonia oxidation is a slow step and likely to be limited by microbiological and/or moisture related factors.

In the cooler, more humid, climate at Arendal, ammonium levels in the soil profile are much higher while the nitrate-N concentration in the soil is much lower compared to the hotter and more arid climate at Ghanzi. It is concluded that nitrification is enhanced in the case of Ghanzi and that higher nitrate levels may be reached. Furthermore, the overall lower moisture availability in the arid Botswana region is certainly the main factor causing the high nitrate levels in groundwater as there is much less water into which the nitrate can be dissolved.

Particularly in the case of Ghanzi the lower  $\text{NO}_3^-/\text{Cl}$  ratios in the polluted areas complement the  $^{15}\text{N}$  isotope determination of groundwater to identify the source of the nitrate.

In both cases further research is required. At Ghanzi repeated sampling is needed in the same area over time with probes installed to measure soil moisture, water levels, etc. The present study has had great

value in providing excellent indications how a more extensive project should be designed to cover the nitrate generation processes in that area. Increased efforts need to be made to obtain sufficient samples for  $^{15}\text{N}$  analysis of ammonia and nitrate. At Arendal the situation is somewhat less diverse due to less variation in the soil conditions and a less extreme climate. However, repeated sampling over several years are needed for full justification of the conclusions and following changes after cessation of sludge deposition on this site.

### ACKNOWLEDGEMENTS

We thank the land owners in Ghanzi and Arendal on whose property we were able to work. We acknowledge the help of the Botswana Geological Survey Department for their cooperation and logistical support when sampling in the Ghanzi area. We appreciate the advice of Martin Schwiede with practical soil sampling matters and the help of Christine Colvin to simplify the Arendal sampling. The financial support of the IAEA through funding from the CRP, *Application of Isotopes to the Assessment of Pollutant Behaviour in the Unsaturated Zone for Groundwater Protection*, and the interest of K M Kulkarni is highly appreciated. The funding from the Department of Science and Technology of South Africa enabled the conception of the project and this is gratefully acknowledged.

### REFERENCES

- [1] TREDoux, G., ENGELBRECHT, J.F.P., TALMA, A.S., "Nitrate in groundwater in Southern Africa", *New Approaches Characterizing Groundwater Flow*, Vol 1, (SEILER, K.-P., WOHNLICH, S., Eds), Balkema, Rotterdam, (2001) 663–666.
- [2] TREDoux, G. AND TALMA, A.S., "Nitrate pollution of groundwater in Southern Africa", *Groundwater pollution in Africa*, (XU, Y, USHER, B., Eds), Taylor & Francis/Balkema, Leiden, ISBN 10: 0-415-41167-X (2006) 15–36.
- [3] COLVIN, C. "Sludge application to agricultural land", A study of the effect of agricultural practices on ground water quality. (CONRAD, J.E., et al.), WRC report 641/1/99, Pretoria (1999).
- [4] THOMAS, D., SHAW, P., *The Kalahari Environment*, Cambridge University Press, Cambridge (1991).
- [5] TREDoux, G., ENGELBRECHT, J.F.P., TALMA, A.S., "Nitrate in groundwater in arid and semi-arid parts of southern Africa", *Environmental Geology in Semi-Arid Environments* (VOGEL, H., CHILUME, C., Eds), DGS, Lobatse, Botswana (2005).
- [6] SELAULO, E.T., *Tracer Studies and Groundwater Recharge Assessment in the Eastern Fringe of the Botswana Kalahari*, PhD thesis, Free University, Amsterdam (1998) 229.
- [7] SCOTT, D.F., LE MAITRE, D.C., *The interaction between vegetation and groundwater*, WRC report 730/1/98, Pretoria (1999).
- [8] ARANIBAR, J.N., et al., Nitrogen-cycling in the soil-plant system along a precipitation gradient in the Kalahari sands, *Glob. Change Biology* **10** (2003) 359–373.
- [9] SCHWIEDE, M., DUIJNISVELD, W., BÖTTCHER, J., "Investigation of processes leading to nitrate enrichment in soils in the Kalahari region, Botswana" (VOGEL, H., CHILUME, C., Eds), *Environmental Geology in Semi-Arid Environments*, DGS, Lobatse, Botswana (2004).
- [10] HÖGBERG, P., Tansley review no 95:  $^{15}\text{N}$  natural abundance in soil-plant systems, *New Phytol.* **137** (1997) 179–203.
- [11] KREITLER, C.W., Nitrogen-isotope ratio studies of soils and groundwater nitrate from alluvial fan aquifers in Texas, *J Hydrol.* **42** (1979) 147–170.
- [12] EATON, R.C., Rainfall records from 1960 to 2002 of the farm Oakdene (Ghanzi district, Botswana), personal communication, 22 October 2002.

## APPENDIX I

### GHANZI SITE DETAILS

#### Location

Farm: Nogono / Dakota, 40 km east of Ghanzi town, western Botswana.  
Latitude: 21° 34'–41' S  
Longitude: 21° 56'–59' E

#### Climate

Mean temperature:  
Minimum monthly: June: 4.5°C  
December: 19.3°C  
Maximum monthly: June: 24.0°C  
November: 33.8°C  
Mean annual (July to June) rainfall (1960 to 2000):  
Minimum: 206 mm  
Maximum: 966 mm  
Mean: 426 mm  
Mean monthly rainfall (1960 to 2000):  
Maximum: January 103 mm, Range: 20 to 366 mm  
Minimum: July 0.3 mm, Range: 0 to 10 mm  
Mean potential evaporation: >2000mm/year.

#### Physiographic unit

The study area is situated in the so-called Hardveld in Botswana. It is being described as a structural surface developed mostly on Precambrian rocks.

#### Geology

The Ghanzi Group is of Neoproterozoic age and consists mainly of siliciclastic sedimentary rocks and subordinate carbonates. The local soil cover consists of Kalahari sand and calcrete.

#### Soil type

The whole of Botswana is classified as having aridic soil moisture regimes all year round, except for parts in the northwest, north and the east. In these areas the soil may remain moist for up to four months from November, unless a dry spell occurs for a period longer than three weeks. The Ghanzi Ridge is on the southern edge of the area where the soil moisture regime could be described as ustic.

#### Vegetation

Local vegetation is classified as tree savannah. This consists of grass, low shrubs and Acacia trees.

#### Ground water table depth

In October 2000, the water levels varied from approximately 3 m to 7 m. The shallower water table occurred at a borehole with very little nitrate and the deeper water table at a high nitrate borehole.

## APPENDIX II

### ARENDAL SITE DETAILS

#### Location

Farm: Arendal, Atlantis district, 70 km north of Cape Town.  
Latitude: 33° 34' 30" S  
Longitude: 18° 33' 54" E  
Altitude: 150–143 m amsl

#### Climate (data from GNIP database)

##### Mean temperature:

June: 12 °C

November: 19 °C

##### Mean annual rainfall (1960 to 1987):

Minimum: 396 mm

Maximum: 652 mm

Mean: 513 mm

##### Mean monthly rainfall (1960 to 1987):

Monthly maximum: January 14 mm

Monthly minimum: July 77 mm

Mean potential evaporation: 1500 mm/year.

Mean recharge in vegetated areas: 10% (= 50 mm/year)

#### Physiographic unit

Coastal sands.

#### Geology

Quaternary Springfontein sands underlain at 20–30 metre depth by basement rocks of the Cape Granites.

#### Soil type

Medium to fine grained, well-sorted silica sands. Average properties:  $d_{10}$  0.16;  $d_{60}$  0.24;  $d_{90}$  0.30;  $K_{bulk}$  (Hazen's formula) 21–24 m/day [3].

#### Vegetation

Originally Cape fynbos. For at least the last 50 years, the land at the study site has been used for cattle fodder production. Locally patches of Port Jackson trees (*Acacia saligna*) occur.

#### Ground water table depth

2–4 metres: varying by 1 metre annually due to seasonal rainfall influence and 1 metre across the study area following the topography.

# CHEMICAL AND ISOTOPIC STUDY OF POLLUTANT TRANSPORT THROUGH UNSATURATED ZONE IN DAMASCUS OASIS (SYRIAN ARAB REPUBLIC).

B. ABOU ZAKHEM, R. HAFEZ  
Syrian Atomic Energy Commission (SAEC),  
Damascus, Syrian Arab Republic

## ABSTRACT

The primary objectives of this study were to determine the hydrochemical and isotopic characteristics of groundwater and to study vertical transport processes for trace elements through the unsaturated zone, from the surface water into the groundwater system. A third objective was to identify the importance of the unsaturated zone in protecting groundwater from contamination. Distribution of trace elements, including Cu, Pb, Cr, Cd, Zn and As in the soil with depth were measured. Mineralogy was investigated using X ray diffraction techniques and grain size distribution in three drilled soil profiles (KA, KB and KS) in Damascus Oasis, which indicated that the soil consists mainly of calcite, a mineral that has the ability to bind some of the trace elements. Measurement of nitrate concentrations in groundwater permitted an investigation of the urban, industrial and agricultural pollution in the Oasis, in particular, in the eastern part of Damascus city and in the north of the Oasis where the irrigation by treated wastewater is applied. Depending on the chemical characteristics of the studied trace elements and soil conditions, these elements can have high concentrations in the upper part of the soil (20–30 cm depth), due to absorption by clay minerals and organic matter. The high concentrations represent pollution by leather industries (tannery) in the area. The trace element concentrations decrease towards the east in parallel with river flow direction. The lower part of profiles show low trace element concentrations below the international permitted limit. The low concentrations of trace elements in groundwater are also below the international limit, indicating significant concentrations of contaminants are not presently entering the water table. The isotopic composition of shallow groundwater indicates the underground recharge, originated from the Anti-Lebanon Mountain, is more significant than the direct recharge through unsaturated zone. It is concluded the unsaturated zone and the decrease of groundwater levels have played an important role in groundwater protection from heavy metals pollution.

## 1. INTRODUCTION

As a result of rapid increases in population and industrial development, high pollution level are observed in the surface water, groundwater, and soil in the area of Damascus Oasis. A large number of wells and extensive pumping have caused a decrease in the piezometric water head, and has led to soil and water salinity problems, especially in the eastern part of the Oasis [1]. Many hydrological and hydrochemical studies have been conducted in order to determine the extent of surface and groundwater pollution [2–7]. These studies distinguished between chemical and biological pollution in Damascus Oasis. Contamination of soil and groundwater by heavy metals in industrial sites and urban regions is a worldwide pollution problem. Several studies [8–14] were conducted. Groundwater and soil pollution by trace elements is one of the main problems in Damascus Oasis. This pollution is due to discharge of industrial wastes from food, leather, textile, cement and asbestos industries as carbonate, sulphate, chloride, heavy metals, acids, metal paintings and phenols into the Barada River [4]. In addition, irrigation with sewage water in agricultural zones has increased nitrate concentrations in groundwater.

This study was done under the framework of CRP project No SYR.11517/R0 in cooperation with International Atomic Energy Agency (IAEA) entitled “Application of isotopes to the assessment of pollutant behaviour in the unsaturated zone for groundwater protection”.

## 2. ENVIRONMENTAL BACKGROUND

Damascus Oasis plays an important economical role for Damascus city through agricultural, industrial and urban activities. It has an area about 1200 km<sup>2</sup> and the mean elevation of the Oasis is about 650 m (a.s.l.). It is located in the southern part of the Syrian Arab Republic (Fig.1). The climate is Mediterranean type, which is characterized by rainy and cold winters and hot dry summers [15]. The mean annual rainfall is between 221 mm/y as measured at the Mazzeh meteoric station and 136 mm/y as measured at Damascus airport meteoric station [16].

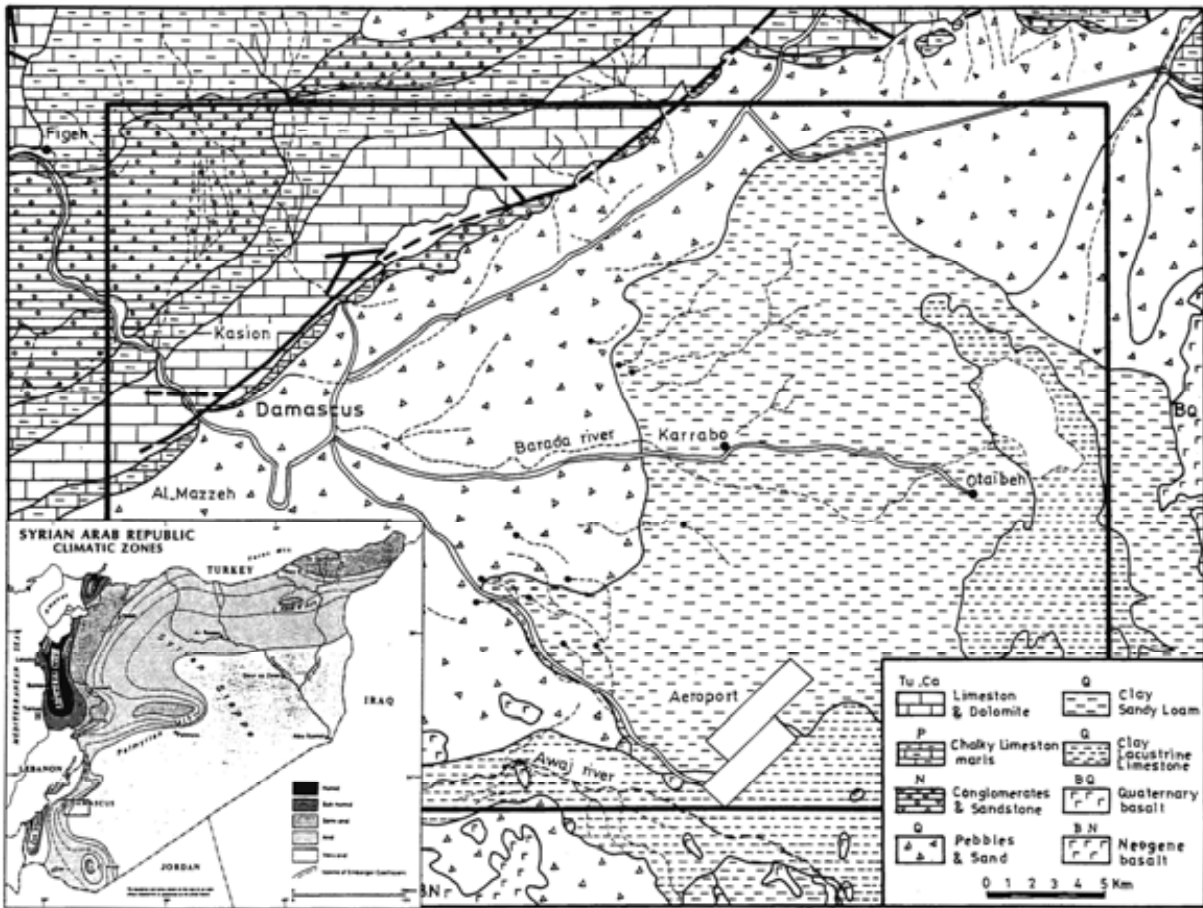


FIG. 1. Geological map of study area [17].

The Damascus basin has a convex structure that is bounded by faults with a NE-SW orientation. Quaternary sediments of the Damascus depression near the Rabweh area grades, from pebble, gravel and conglomerates, fine sand and silty soil in the centre of the Oasis to more recent Quaternary sediments consisting of loamy and clayey lacustrine deposits near Oteibeh Lake. In the south and southeastern part of the Oasis there are basaltic lava flows of Neogene and Quaternary age (Fig.1) [17].

The Barada and Awaj are the main rivers in the hydrographic network in Damascus Oasis. The Barada River originates in the Anti-Lebanon Mountain with an elevation of 1500 m (a.s.l.) and terminates in Oteibeh Lake (597 m) during the flood period only. Since the 1970s, Oteibeh Lake has been dried and the Barada River does not reach the Lake. The Barada River is fed by the Barada spring, which has an average discharge of 3.12 m<sup>3</sup>/s and by the Cretaceous karstic Figeih spring, which has an average discharge 7.7 m<sup>3</sup>/s. The Awaj River originates from many springs in the eastern part of Haramoun mountain, (elevation 2814 m (a.s.l.)) and terminates in Hyjaneh Lake, again only during flood period.

In Damascus Oasis, the main aquifer is a Quaternary formation 400 m thick. This aquifer consists of several sub-aquifers (multi layers) that differ in lithological characteristics. Sediments consist of gravel, conglomerates and sand. In some places the aquifer becomes semi-confined by clay lenses. The water type is typically calcium bicarbonate or magnesium bicarbonate [18, 2]. The piezometric levels in the Oasis change according to the alternation of flood and dry periods. Recently, distinctive changes in piezometric levels have been occurred. These changes are caused by extreme dry years (1999 to 2001). In the north of Oasis, the water table has risen as a result of return flow by irrigation water supplied by treated sewage water. Groundwater recharge sources in Damascus basin are from the surface water (Barada and Awaj rivers), irrigation channels and the direct infiltration from precipitation. Several wells were drilled in Damascus Oasis, approximately more than 20 000 wells,

which are used for agricultural purposes. Over exploitation beyond the natural replenishment had caused a continual drop in piezometric levels and formation of deep hydrological depression associated with increasing in salinity especially in the eastern part of the Oasis (Oteibeh and H.Awamid). At the beginning of the 90 s, groundwater depth in the Oasis was between 6–10 m depth in the western part and 20–50 m depth in the eastern part. Recently, the groundwater depth decreases to 20–30 m depth in the western part and 60–80 m depth in the eastern part of the Oasis. Groundwater flow direction is from west to east in paralleled with the flow direction of Barada River.

In January 2001, heavy metal concentrations in the Barada River were measured by the Ministry of irrigation and found to be below the permitted concentrations limit, which indicates there is no pollution in surface water, even though the concentrations increased from upstream to the downstream.

Falouh [1] studied heavy metal concentrations in the Barada River stream sediments, where it was concluded that the surface water is highly vulnerable to direct pollution, in particular, in industrial areas. While groundwater pollution by heavy metals is less than that in surface water and in stream sediments, high concentrations of Cd and Pb were found in stream sediments in the industrial areas nonetheless.

Comparing results of Falouh [1] as described earlier with the results of this study, it is found that the trace elements in groundwater, show low concentrations and are below the permitted limit for drinking water, however, concentrations were higher in some samples compared to the Falouh study. It is speculated that after three extremely dry years between 1999 and 2001, during which time the groundwater levels have decreased by about 20 m, the risk of groundwater pollution by heavy metals is less because the unsaturated zone, which plays a protective role, has become thicker.

### 3. METHODOLOGY

Twenty six drinking wells were selected in the Oasis for sampling (Fig.2). Water samples were collected from these wells during November and October, 2001. The wells are located on the both sides of the Barada River, between Damascus city and Oteibeh Lake. Physical parameters, including pH, temperature, electrical conductivity (EC), total alkalinity (ALK) and dissolved oxygen (DO) were measured in-situ. Sample location (latitude and longitude) was determined using a portable GPS instrument (Table 1). Major element analyses were performed, using Chromatograph (Dionex 120) and stable isotopes ( $^{18}\text{O}$ ,  $^2\text{H}$ ) of water samples were measured using mass spectrometer (delta plus) in the laboratory of Geology department (SAEC) (Table 2). Trace element concentrations in groundwater were measured using the anodic stripping voltametric method [19] with a 693 VA processor, Metrohm (Table 3). Three soil profiles (KA, KB and KS) in Kabbas area was drilled to a depth of 550, 375 and 220 cm using a hand-auger. The water table was located at 20 m depth. A total of sixty seven soil samples were taken at 10 cm intervals. The location of the soil profiles is near one of the most polluted areas in Damascus Oasis where the leather industries (tannery) are located (Fig. 2).

Water content measurements, defined as the ratio of the mass of water to the total mass (solid and liquid) after heating the soil sample to 105°C [20], grain size distribution [21] and mineralogical analysis using X ray diffraction were performed on each soil sample. Soil samples digested prior to analyses Cd, Cr and As using Atomic Absorption with three different methods; furnace with a detection limit were analyzed of 10 ppb, flame with detection limit of 5 ppm, and hydrolyte methods with detection limit of 10 ppb. Pb, Zn and Cu were analyzed using Energy Dispersive X ray Florescence (EDXRF) (Chemistry Dept. Syrian Atomic Energy Commission (SAEC). The detection limits were 14 ppm, 33 ppm for Pb and Cu, respectively [22]. Total Organic Carbon (TOC) content in the soil was analyzed using “Apollo 9000” instrument and stable isotope in the soil was analyzed using Gas Chromatograph Mass Spectrometer (GC–IRMS) were performed in Environmental Engineering Research Centre in Belfast, UK.



TABLE 1. GROUNDWATER SAMPLE IDENTIFICATION, LOCATION AND FIELD MEASUREMENTS

Location	Sample ID	Coordinates N 33° E 36°	Elev. m(asl)	Date	Well Depth (m)	Water Depth (m)	T (°C)	pH	EC ( $\mu$ S/cm)	DO (mg/L)	Total Alk. (mg/L)
Teshreen	DT	30'-58"	711	9/12/2001	80	40	18.5	7.4	623	-	180
Mazraa	MD	31'-43"	718	9/12/2001	60	31	18.9	7.3	786	12.8	259.9
Jobar	DJ	31'-13"	704	9/12/2001	80	-	18.4	7.1	850	12.6	320.3
Hamoriah	DH	31'-46"	704	9/12/2001	84	-	17.8	7.0	1207	12.4	481.9
Otaya	DO	31'-28"	653	9/12/2001	-	-	18.3	7.5	1073	12.2	300
Shifoneih	DSH	33'-21"	649	9/12/2001	75	20	19	7.2	1268	-	350
Tal-Swan	DTS	35'-35"	623	9/12/2001	-	-	19.9	7.3	1665	-	392
Medaa	DMI	33'-51"	625	9/13/2001	125	75	21.5	7.6	1340	-	301.6
Baharieh	DB	31'-48"	630	9/13/2001	150	80	23.8	7.6	585	-	219.5
Oteibeh	DOT	28'-56"	627	9/13/2001	350	85	27.7	7.7	2850	10.9	94.6
H.Awamid	DHR	26'-44"	622	9/13/2001	300	90	25.5	7.3	1299	-	277.6
D.Salman	DDS	28'-22"	634	9/13/2001	130	70	20.9	7.5	634	-	246.3
Babila	KBA	28'-17"	799	9/17/2001	80	30	19.6	7.0	979	8.5	433.1
Shabaa	DSHA	27'-05"	800	9/17/2001	60	60	18.2	7.0	1230	8.8	440
H.Terkman	DHT	26'-18"	800	9/17/2001	247	75	24.4	7.7	822	7.5	75.6
Gezlanieh	DGH	26'-47"	697	9/17/2001	200	100	25	7.8	931	8.0	209
Jaramana	DGR	29'-09"	740	9/17/2001	60	40	19	7.4	935	9.6	390
Harasta.Q	DHQ	29'-27"	630	9/18/2001	100	40	19.6	7.1	921	8.8	356.7
Nola	DNO	28'-06"	671	9/18/2001	125	85	20.4	7.5	625	8.5	263.4
Zebdin	DZB	23'-58"	671	9/18/2001	100	30	17.5	7.1	1027	8.8	450
D.Assafir	DDA	28'-04"	671	9/18/2001	70	32	18	7.2	1075	8.9	449.7
H.Blass	DMHB	36'-40"	704	10/10/2001	121	-	21.5	6.9	1744	10.8	305
S.Qadam	DMQS	28'-03"	704	10/10/2001	-	-	20.7	7.9	690	10.1	210
I-Assaker	DMIA	30'-16"	691	10/10/2001	70	-	19.3	7.5	692	9.6	293
E.Terna	DMT	30'-59"	694	10/10/2001	125	42	19.1	7.4	941	9.3	320
Kabass	DMKB	33'-29"	687	10/10/2001	55	20	18.7	7.2	1253	8.9	370
Fiqeh Spr.	F10	-	860	9/12/2001	-	-	14	8.3	302	-	108

TABLE 2. CHEMICAL AND ISOTOPIC COMPOSITION OF GROUNDWATER SAMPLES

Location	Code	Date	Na <sup>+</sup> mg/L	K <sup>+</sup> mg/L	Mg <sup>++</sup> mg/L	Ca <sup>++</sup> mg/L	Cl <sup>-</sup> mg/L	NO <sub>3</sub> <sup>-</sup> mg/L	SO <sub>4</sub> <sup>-2</sup> mg/L	Calcite SI*	rCa/rMg **	δ <sup>18</sup> O ‰	δ <sup>2</sup> H ‰
Teshreen	DT	12/09/01	17.2	0.5	6.6	57.2	19.8	20.7	26.6	0.2	8.62	-8.11	-45.38
Mazraa	MD	12/09/01	35.2	1.7	22.1	80.3	34.7	60	35.2	0.17	3.63	-8.49	-47.69
Jobar	DJ	12/09/01	16.3	1.4	21.2	110.3	29.4	59.1	16.9	0.37	5.2	-8.12	-45.59
Hamoriah	DH	12/09/01	25.2	1.7	35.6	124.6	71.1	82.3	16	0.17	3.5	-7.85	-44.32
Otaya	DO	12/09/01	23.7	1.3	28.7	105.9	87.1	69.9	24.6	0.38	3.69	-7.83	-44.21
Shifonieh	DSH	12/09/01	24	1.3	33.5	137.2	96.8	110.8	25.6	0.18	4.09	-7.54	-42.36
T.Sawan	DTS	12/09/01	75.4	3.4	71.4	96.0	117.4	52.8	205.8	-0.24	1.34	-7.2	-41.66
Medaa	DMI	13/09/01	107.1	2.6	46.1	67.6	168.6	2.6	88.7	0.22	1.46	-8.72	-51.97
B.Balad	DB	13/09/01	26	1.9	22.5	49.8	40.3	7.2	37.8	0.16	0.17	-9.11	-54.06
Oteibeh	DOT	13/09/01	323.2	10.0	73.8	199.2	214.2	0.1	994.7	0.55	2.69	-9.21	-56.75
H.Awamid	DHR	13/09/01	71.6	2.9	47.9	88.6	90.9	0.1	212.6	0.12	1.85	-8.75	-51.68
D.Salman	DDS	13/09/01	20.3	1.6	18.8	64.1	37.8	9.5	27.2	0.07	3.41	-8.55	-50.39
Babila	KBA	17/09/01	34.9	3	21.9	115	45.7	58.7	25.1	0.34	5.24	-8.28	-46.53
Shabaa	DSHA	17/09/01	33.4	1.4	29.0	129.3	70.7	61.8	27.1	0.5	3.69	-7.76	-45.55
H.Terkman	DHT	17/09/01	39.4	2.1	16.2	43.3	120	11.3	27.1	0.32	2.6	-7.65	-50.55
Gezlanieh	DGH	17/09/01	103.8	2	21.2	46.9	132.3	10.5	84.7	0.23	2.21	-7.83	-49.42
Jaramana	DGR	17/09/01	25.3	6.6	18.8	116.9	46.2	54.1	25.5	0.33	6.25	-8.07	-44.99
H.Quantara	DHQ	18/09/01	21.7	1.4	20.0	108	61.7	36.1	20.3	0.25	5.39	-8.09	-46.53
Nola	DNO	18/09/01	14.7	0.8	17.5	75.4	41.5	18.4	17.9	0.32	4.3	-8.19	-47.12

TABLE 3. TRACE ELEMENT CONCENTRATIONS OF GROUNDWATER SAMPLES

Location	Code	Date	Pb (ppb)	Cd (ppb)	Zn (ppb)	Cu (ppb)
Teshreen	DT	10/10/01	2.7±0.1	<0.25	79.4±0.6	1.4±0.2
Mazraa	MD	12/09/01	<1	<0.25	7.2±0.2	1.3±0.1
Jobar	DJ	12/09/01	<1	<0.25	7.9±0.3	1.2±0.2
Hamoriah	DH	12/09/01	1	0.4	5.8±0.1	2.4±0.2
Otaya	DO	12/09/01	<1	<0.25	5±0.2	4.5±0.2
Shifonieh	DSH	12/09/01	<1	<0.25	6.4±0.2	2.2±0.1
T.Sawan	DTS	12/09/01	<1	<0.25	5.7±0.1	1±0.1
Medaa	DMI	12/09/01	4.8±0.1	<0.25	84.1±0.8	18.9±0.2
B.Balad	DB	13/09/01	<1	<0.25	62.8±1.7	5.4±1.1
Oteibeh	DOT	13/09/01	<1	0.4	15.6±0.8	1.6±0.2
H.Awamid	DHR	13/09/01	<1	<0.25	33.7±0.3	4.5±0.2
D.Salman	DDS	13/09/01	<1	<0.25	14.8±0.5	<0.1
Babila	KBA	13/09/01	1.2±0.2	<0.25	5.1±0.2	4.7±0.6
Shabaa	DSHA	17/09/01	1.9±0.4	<0.25	18.6±0.6	6.6±0.7
H.Terkman	DHT	17/09/01	<1	<0.25	71.1±1.7	1.7±0.1
Gezlanieh	DGH	17/09/01	1.2±0.2	<0.25	44.4±0.8	1.8±0.2
Jaramana	DGR	17/09/01	1.3±0.07	<0.25	12.7±0.5	15.3±0.1
H.Quantara	DHQ	17/09/01	2.5±0.2	<0.25	93±2.6	7.1±0.6
Nola	DNO	18/09/01	1.4±0.1	<0.25	219.6±5.7	2.5±0.2
Zebdin	DZB	18/09/01	1	0.3	8.6±0.3	1.77±0.2
D.Assafir	DDA	18/09/01	<1	<0.25	5.3±0.2	2.3±0.05
H.Blass	DMHB	18/09/01	2.3±0.2	<0.25	11.9±0.6	6.5±0.6
S.Kadam	DMQS	10/10/01	1.9±0.06	<0.25	11.7±0.2	<0.1
I.Assaker	DMIA	10/10/01	2.7±0.2	0.4	12.6±0.2	2.8±0.2
E.Terma	DMT	10/10/01	1.5±0.3	<0.25	14.4±0.3	10.3±0.3
Kabbass	DMKB	10/10/01	<1	<0.25	9.2±0.3	<0.1
Figeh Spr.	F10	12/09/01	2±0.3	<0.25	24.6±1	2.5±0.1
Concentration limit (WHO standard)*			0.01 ppm	0.003 ppm	5 ppm	1 ppm
Concentration Limit (Syrian standard)**			0.01 ppm	0.005 ppm	3 ppm	1 ppm

\*WHO: World Health Organization. \*\* Syrian standard.

The particle size distribution profile shows the soil is homogeneous with depth. Approximately 35% consists of clay, 40% of loam, and 25% of sand (Fig. 4).

Generally, the mineralogical analysis shows that the main mineral composition is calcite (70%), followed by quartz (20%) dolomite (5%) and clay (5%) (Fig. 5). This result reflects the carbonate nature of the bedrock, outcrops in the surrounding areas.

From the soil surface to 1.2 m depth, copper has high concentration; this is a common characteristic of soil due to bioaccumulation in the upper part, and atmospheric input of the metal. Copper forms several minerals, which are easily soluble during the weathering process, especially in acidic environments. Therefore, Cu is considered among the more mobile of the heavy metals in hypergenic processes. However, it has the ability to chemically interact with minerals, clay and organic components of the soil. Thus, Cu is a rather immobile element in soils. Soil minerals are capable of absorbing Cu ions from solution and these properties depend on the surface charge that is strongly controlled by pH [23]. The highest copper concentration in this profile is 237 ppm at 25 cm depth. The concentrations gradually decrease to 75 ppm at 1.2 m depth. Between 1.2 and 5.5 m depth, the

concentrations range between 75 and 85 ppm, with an average value of 79 ppm (Fig. 6). The high concentration of Cu in the upper part of the soil is due to availability of organic matter, which can absorb copper in the soil. X ray results of the KA profile indicate that the main component is calcite, representing 80 % of the soil minerals. Carbonates also have a great affinity to bind the Cu to the soil in a non-diffusible form. The international concentration limit for Cu in soil is 60 ppm [23]. Our results indicate a high pollution level of Cu in the upper part of the soil, which is likely the result of industrial wastes from a nearby leather industry.

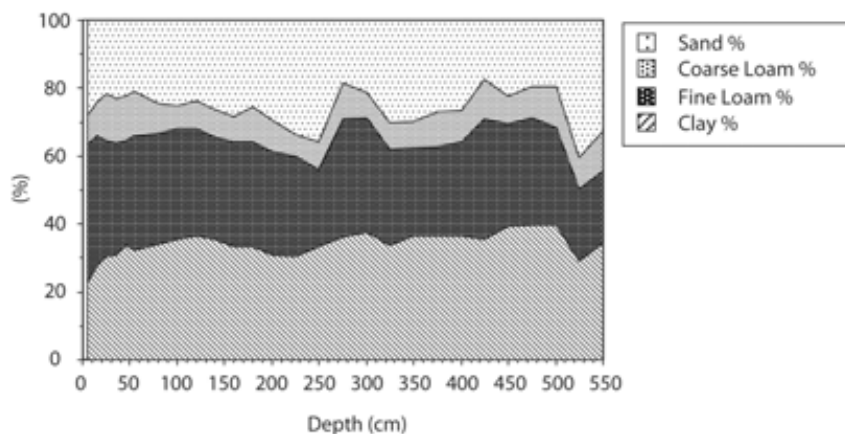


FIG. 4. Particle size distribution, (profile KA).

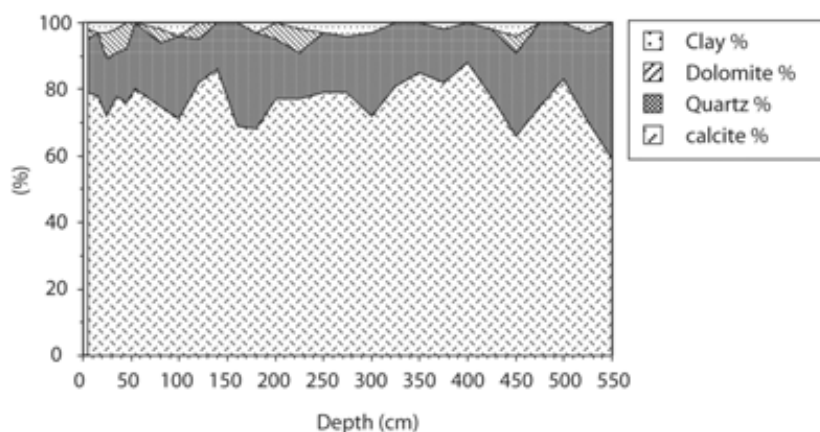


FIG. 5. Mineral analyses “X-R.D”, (profile KA).

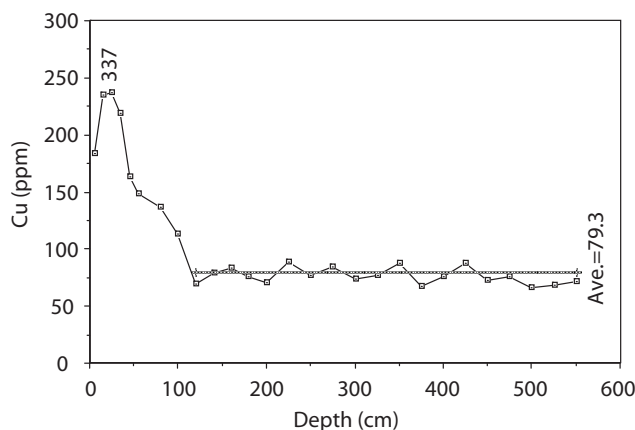


FIG. 6. Variation of Cu with depth, (profile KA).

The geochemical characteristic of  $Pb^{+2}$  resembles the divalent alkaline earth group of metal. Thus Pb has the ability to replace K, Ba, Sr and Ca in minerals and on sorption sites. Pb is the least mobile element among other heavy metals, and organic matter is considered as an important sink of Pb in polluted soils. Gilani [24] found that Pb bound in organic matter is between 46 to 65% of the total Pb in the soil.

Lead concentration in soil varies with depth as shown in Fig. 7. Concentrations reach 209 ppm at 15 cm depth, which is the highest value obtained, then decrease to 76.5 ppm at 1.2 m depth. From 1.2 to 5.5 m depth the Pb concentration is rather stable at 65 ppm. It is clear that Pb is retained in the top soil horizon. The high concentration of Pb may be related to an organically rich top horizon (root zone) of these uncultivated soils, in addition to Pb precipitated from the air derived from car exhaust. The international limit for Pb in the soil is 189 ppm [23]. The high Pb concentration indicates high pollution level in the top horizon of the KA profile. Pb has the tendency to be concentrated in calcium carbonate particles which is the main chemical constituent in the soil profile.

Chromium compounds are known to naturally occur with valences of +3 (Chromic) and +6 (Chromate). Cr behaviour with depth in the profile (KA) is shown in Fig. 8. High concentrations of Cr are found in the top surface of soil (0–45 cm) where the highest value is 146 ppm. Concentrations decrease to about 14 ppm and stabilize to an average value of 23 ppm with depth. The international Cr concentration in soil is 70 ppm. The high accumulation of Cr in the top soil indicates that pollution from leather manufacturing waste is predominant. However, the concentration between 50 and 550 cm is under the maximum allowable value, which that indicates there is no downward migration of Cr in the soil. The soil profile contains a high percentage of  $CaCO_3$ , which can play a role in fixing Cr to that mineral within the upper part of the soil. Organic matter also plays important role in Cr binding.

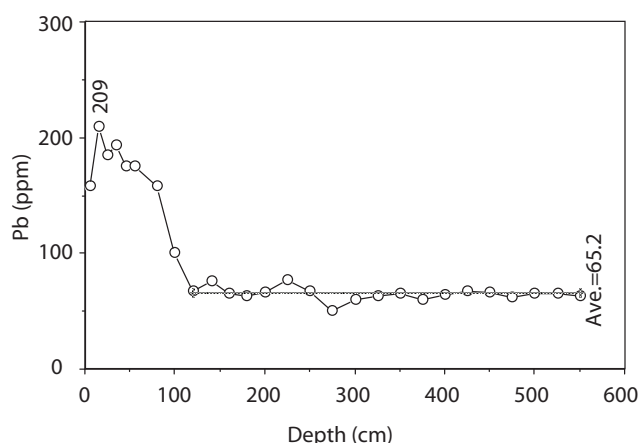


FIG. 7. Variation of Pb with depth, (profile KA).

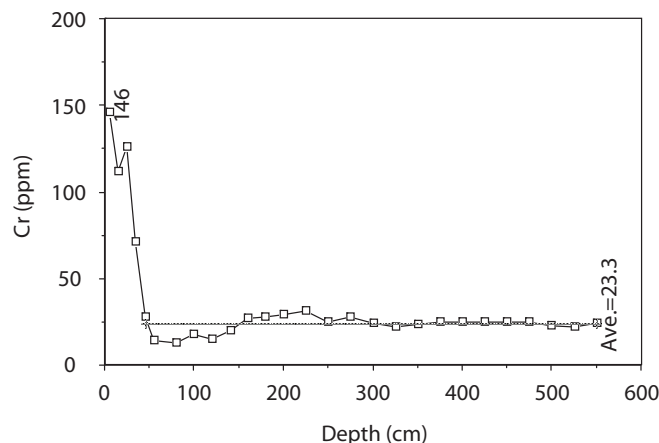


FIG. 8. Variation of Cr with depth, (profile KA).

Zinc as  $Zn^{+2}$  is mobile in oxidizing environments, but it is easily absorbed by minerals and organic components. Thus in most soil types, clays and soil organic matter are capable of retaining Zn strongly. Zn is most readily mobile and available in acidic light mineral soils. Solubility and availability of Zn is negatively correlated with Ca saturation and P compounds in soils. It has been found that an excess of copper can induce Zn deficiency. The main pollution source of Zn is the non-ferrous metal industries [23].

It was found that Zn has the same behaviour as Cu, Pb and Cr in the soil. The highest concentrations are found (557 ppm) near the soil surface (05 cm) (Fig.9). Concentrations decrease gradually to about 107 ppm at 1.2 m depth and stabilized to an average value of 112 ppm with depth. This behaviour is due to retention of Zn by organic matter in the upper layer of the soil.

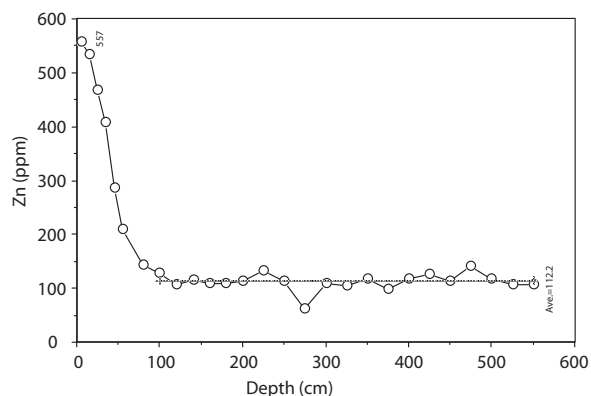


FIG. 9. Variation of Zn with depth, (profile KA).

The international limit for Zn concentration in soil is 125 ppm, and the upper part of the profile exceeds this limit. The most important valence state of Cd in natural soil is +2 and its movement is controlled by pH. In acidic soil, Cd is most mobile in the pH range of 4.5 to 5.5. It is found in various forms as exchangeable bases, adsorbed to clay surfaces and organic matter, and fixed within the crystalline lattice of mineral particles. Sewage sludge and phosphate fertilizers are the main source of Cd [23].

Cd has a tendency to increase slightly with depth as shown in Fig.10; this average rate of increase is calculated as 20 ppb per 1m depth. This could be as an indication of Cd mobility with water leached through unsaturated zone. From the soil surface to a depth of 0.15 m concentration of Cd are high and peak at 566 ppb. Concentrations decrease to 309 ppb at 0.5 m depth and increase to 500 ppb at 5 m depth. The average value of Cd is 480 ppb along the profile, but this value increases at 5.25 m to 960 ppb. It is not possible to follow the evolution of the peak because the sampling procedure was stopped at 5.5 m depth. The international limit for Cd in soil is 5 ppm, which indicates that there is no Cd pollution. The high concentrations at depth could be due to downward movement of Cd with infiltrated water. An aggregation of Cd with Magnesium oxides could occur, which may explain the high Cd concentration in the soil [19].

The studied area is characterized by alluvial carbonate sediments resulting from the outcrop of Cretaceous carbonate and Paleogene formations through erosion and weathering [17]. The river bed is characterized by very fine fluvial and rich in organic matter soil that is related to the river flow and the biomass activities, especially in the root zone. In profile KA, Total Organic Matter (TOC) varied from 75 000 ppm to 22 000 ppm between 0–80 cm depth (Fig. 11), which represents the agricultural. Between 1 and 2.3 m depth, TOC reaches 55 000 ppm, then it decreases to 35 000 ppm at 2.5m depth in a very fine sandy soil. Beneath this layer is a rich organic matter soil where TOC increases to about 72 000 ppm at 2.75 m depth. From 3.25 m depth to the bottom of the profile TOC has an average value of 50 000 ppm. It is observed that TOC is related to the soil structure and its organic matter that plays an important role in the retention of trace elements.

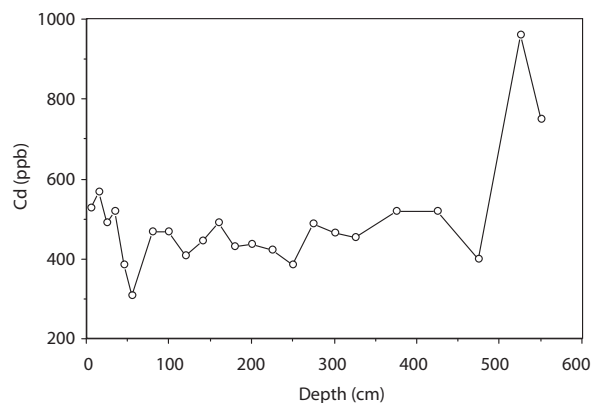


FIG. 10. Variation of Cd with depth, (profile KA).

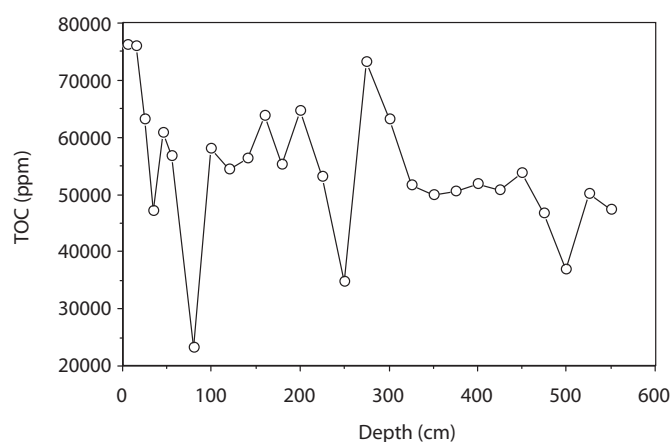


FIG. 11. Variation of Total Organic Carbon (TOC) with depth, (profile KA).

Oxygen-18 in pore water in KA (Fig.12) was analyzed directly by equilibration of CO<sub>2</sub> with the soil samples. It is observed that there is enrichment in  $\delta^{18}\text{O}$  at the top soil of the profile (+0.5‰) as a consequence of evaporation near the soil surface. Then it decreases to  $-1.5\text{‰}$  at 0.6 m depth, followed by several evaporation fronts at 0.8 m, 2.25 m and 3.75 m depth. Generally,  $\delta^{18}\text{O}$  values tend to decrease to  $-2.5\text{‰}$  at the bottom of the profile. The observed secondary evaporation peaks in the profile could be explained by the alternation of periods with dry and enriched  $\delta^{18}\text{O}$  contents with wet period with depleted  $\delta^{18}\text{O}$  content [25–27].

The Carbon-13 content in the soil is varied between  $-9$  to  $-9.5\text{‰}$  at the top soil surface to 0.25 m depth (Fig. 13). It increases gradually to  $-2\text{‰}$  at 3.5 m depth and decreases to  $-5\text{‰}$  at 5.5 m depth. Carbon-13 content variation is related to the structure, composition of the soil and its enrichment of organic matters. In the profile the upper part is richer in organic matter due to the extensive root zone, whereas, concentrations drop towards the bottom of the profile. Generally, this soil is a carbonate type under arid and semi-arid climate that affect the carbon-13 content in the soil [28].

Nitrogen-15 content in the upper part of the soil (to 0.8 m depth) averages 10‰. It increases to 30‰ at 1 m depth, possibly due to denitrification process [28] (Fig. 14). It decreases to  $-9.5\text{‰}$  at 1.2 m depth and increases to 18‰ at 2.5 m depth and varies between 0–10‰ between 3–5.5 m depth with an average content 5‰. The upper part of the profile may be enriched in  $\delta^{15}\text{N}$  because of the intensive organic matter from plant and animal residual sources. From 3 m depth downwards the profile,  $\delta^{15}\text{N}$  content is relatively stable and represents soil content under arid and arid climate.

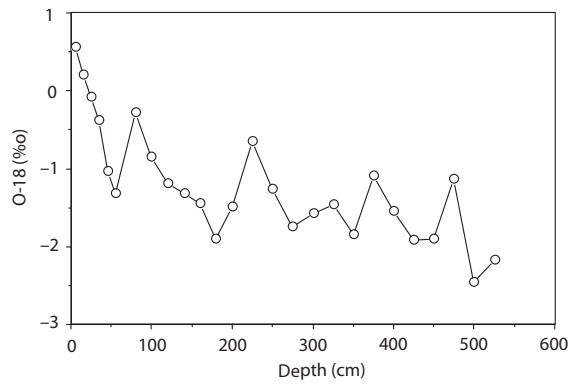


FIG. 12. Variation of  $\delta^{18}\text{O}$  with depth, (profile KA).

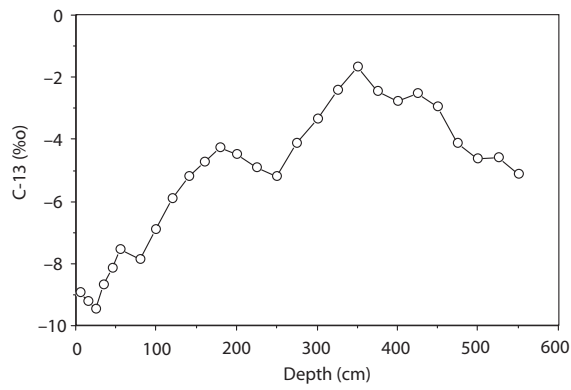


FIG. 13. Variation of  $\delta^{13}\text{C}$  with depth, (profile KA).

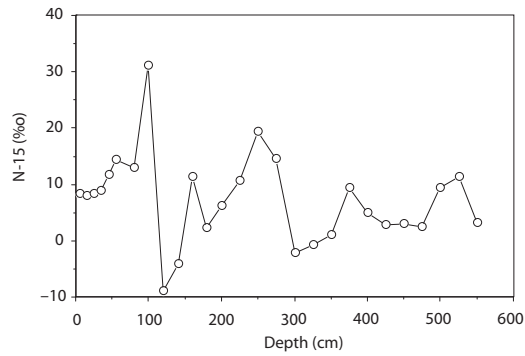


FIG. 14. Variation of  $\delta^{15}\text{N}$  with depth, (profile KA).

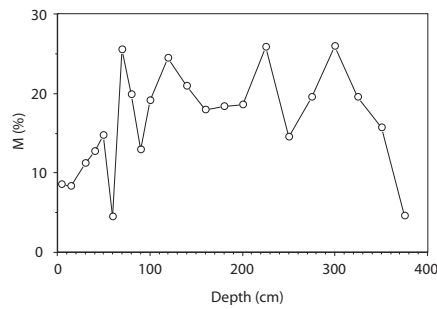


FIG. 15. Moisture content and depth (profile KS).

#### 4.1.2. Profile KS

This profile is located east of leather industries (Kabbas area), and 2 km to the east of KA profile. The depth is 375 cm with depth interval of 10 cm at surface to 25 cm in the lower part of profile. The variations of moisture content with depth are shown in Fig. 15. From soil surface the moisture is about 9%, and then it increases gradually to 20% at 1m depth. From 1 m depth, it changes around this value till 3.3 m depth. The moisture content decreases to 5% when there is sandy layers, e.g. at 1 m, 2.3 and 3.7 m depth. The moisture content increases to 26% where there is clay layers, e.g. at 70 cm, 120 cm, 220 cm and 300 cm depth.

The mineralogy analyses show that the main part of profile is calcite 80%, quartz 10% and 5% of clay and dolomite (Fig. 16). Particle size distribution with depth (Fig. 17) shows that it consists of 20% clay, 40% loam and 40% sand averagely. The upper part, from 0–80 cm, the loam and clay constitute 75% of the soil, and decrease to 25% at about 80–130 cm depth. Then they increase to 70% from 130–210 cm depth and 75% at 260–360 cm.

In the upper part of the profile from the soil surface to about 70 cm depth, Cu concentrations are high with a peak of 73.8 ppm at 40 cm depth. From 70 cm to the bottom of the profile the Cu contents vary between 10–33.2 ppm with an average value of 16.5 ppm (Fig. 18).

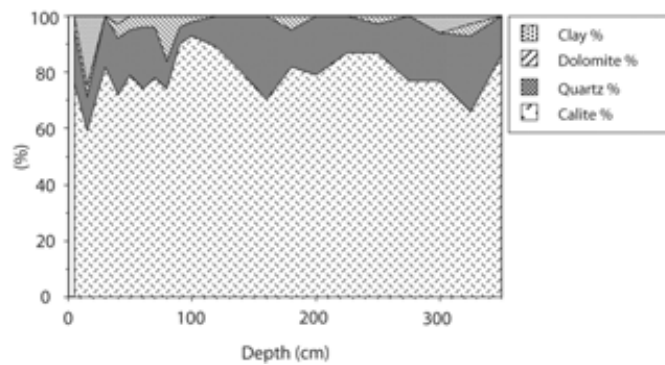


FIG. 16. Mineral analyses “X-R.D”, (profile KS).

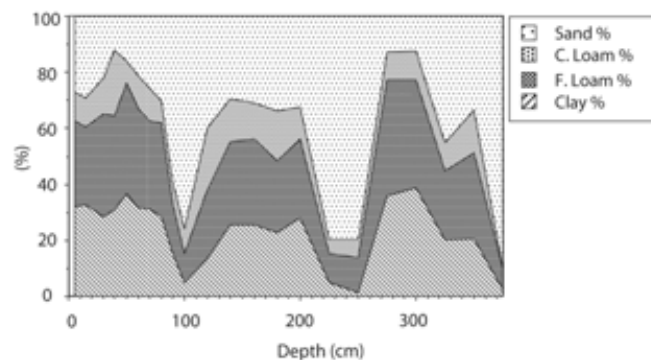


FIG. 17. Particle size distribution, (profile KS).

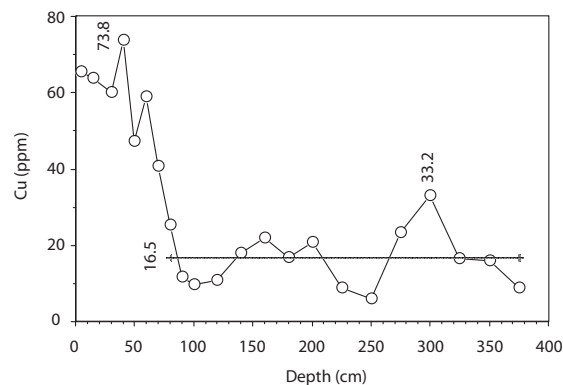


FIG. 18. Variation of Cu with depth, (profile KS).

The high Cu concentrations in the upper part of the profile are due to organic matter and fine soil particles that absorb Cu.

There is a correlation between the particle size and Cu, and when the clay and loam ratio are high, at about 40 cm and between 160–200 cm and at 300 cm depth, the Cu content is high. This indicates retention by fine particles that inhibit Cu migration downwards with percolated water.

Comparing the Cu distribution with depth in both profiles KA & KS, it is observed that Cu content in KS decreases compared to that in KA. This is due to the location of KS, which is 2 km to the east of Kabbas area. The average value in KA profile is 79.2 ppm, whereas it is 16.5 ppm in KS profile.

Zinc is known to be more mobile in the acid soil, but it is easily retained by organic matter and clay. Generally, Zn shows the same behaviour of Cu along the profile.

In the upper part of the profile from the soil surface to about 30 cm depth, Zn is high with a peak concentration of 219 ppm. From 70 cm till the end of the profile the Zn contents vary between 20–110 ppm with an average value of 59.5 ppm (Fig. 19). The increase in Zn concentrations in the upper part of the profile is due to absorption by organic matter of Zn brought in by contamination.

As noted above for Cu, a correlation exists between Zn concentration and particle size in the soil.

Comparing the Zn distribution with depth in both profiles KA & KS, it is generally observed that Zn in KS decreases compared to KA due to the location of KS. The highest content 550 ppm is found at 15 cm depth in profile KA, while it is 219 ppm at 30 cm depth in KS profile. The average value in KA profile is 112.2 ppm, whereas it is 59.5 ppm in KS profile.

The Pb profile that the highest concentration of 143 ppm at 40 cm depth then decreases sharply to about 5.3 ppm at 90 cm depth and changes around this varying around this value through the profile (Fig. 20).

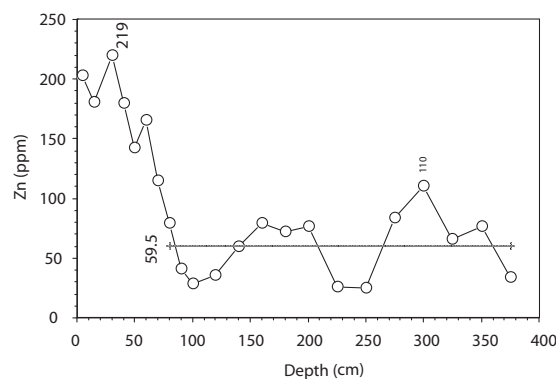


FIG. 19. Variation of Zn with depth, (profile KS).

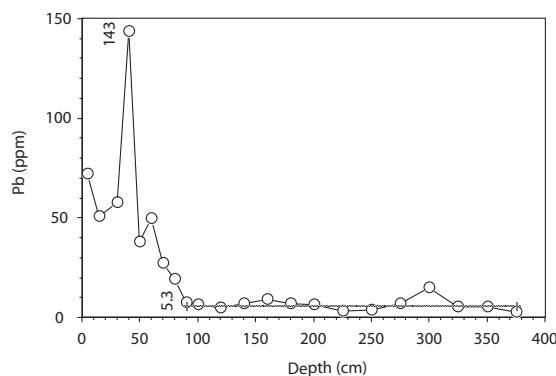


FIG. 20. Variation of Pb with depth, (profile KS).

Comparing the Pb contents in both profiles KS and KA, it is seen that the lead has higher in KA than in KS because of the location of KS farther from industrial and traffic zones.

Total Organic Carbon content is varies from 50 000 ppm at the surface to 65 000 ppm at 30 cm depth (Fig. 21). This zone is impacted by previous agricultural use. Between 0.8–1.5 m depth, TOC increases to 70 000 ppm then it decreases to 55 000 ppm at 1.6 and 2 m depth in the sandy layers. From 2.5 m depth to the end pf profile, TOC is relatively constant at about 58 000 ppm. TOC is related to the structure of the soil and the existence of this organic matter plays a important role in prevention of downward infiltration by the trace elements.

Carbon-13 content in the top soil is between  $-9\text{‰}$  and  $-9.5\text{‰}$  (Fig. 22). It increases gradually to  $-6\text{‰}$  at 2 m depth and decreases to  $-8.5\text{‰}$  between 2.25 and 2.5 m depth, possibly due to the effect organic matter. It increases to  $-4.5\text{‰}$  at 3.75 m depth. Carbon-13 content variation is related to the structure of the soil. In the profile the upper part richer in organic matter the isotopic ratio is lighter. It becomes poorer towards the bottom of the profile. The soil is carbonate type under arid and semi arid climate that affect the Carbon-13 content in the soil [28].

Nitrogen-15 content in the top soil is about  $10\text{‰}$  at 0.6 m depth (Fig. 23). It decreases gradually to  $-22\text{‰}$  at 0.7 m depth. It changes between  $0\text{‰}$ – $20\text{‰}$  and it is in average  $10\text{‰}$  between 0.8 to 3.75 m depth. This is an indication of enriched  $^{15}\text{N}$  in some organic matter layers. The increase in  $^{15}\text{N}$  at 3 m depth to  $50\text{‰}$  may be due to denitrification process.

#### 4.1.3. Profile KB

This profile is located to the south of leather industries, 0.8 km from KA profile. The depth is 220 cm, with depth interval of 10 cm at surface to 25 cm in the lower part of profile.

The variation of moisture content with depth is shown in Fig. 24. The moisture content increases from 2% at the soil surface to 13% at 80 cm depth. There is a strong relation between the moisture content and particle size. It is observed that the moisture content increases to 13% at 80 cm and 140 cm depth when there is clay loam layer, while it decreases to 4% at 1 m and 1.8 m depth.

Particle size distribution with depth (Fig. 25) shows that from soil surface to 80 cm depth, the core consists of 20% clay, 40% loam and 40% sand. Between 100 and 120 cm depth, the clay decreases to 10%, loam to 30% and increases of sand to 60%, while between 180 and 220 cm depth the clay decreases to 2%, loam to 3%, sand to 30% and the gravel about 65%.

The mineralogy of KS and KB is relatively similar with 80% calcite, 10% quartz and 5% of clay and dolomite.

In the upper part of the profile from the soil surface till about 80 cm depth, Cu shows a peak of 60 ppm at 20 cm depth. From 80 cm till the end of the profile the Cu contents vary between 28 and 40.5 ppm with an average value of 34.5 ppm (Fig.26).

It is observed there are two secondary peaks at 160 and 200 cm depth indicates there is a good correlation between the grain size distribution of soil and the Cu content.

Comparing the Cu distribution with depth in both profiles KA & KB, it is generally observed that Cu in KB is less than in KA, due to the location of KB about 0.8 km to the south of Kabbas area. The average value in KA profile is 79.2 ppm, whereas it is 34.5 ppm in KB profile.

In the upper part of the profile from the soil surface till about 20 cm depth, Zn shows a peak of 162.8 ppm. From 70 cm till the end of the profile the Zn contents vary slightly around an average value of 51.2 ppm (Fig. 27). The variation of Zn contents with depth is similar to that of Cu in this profile.

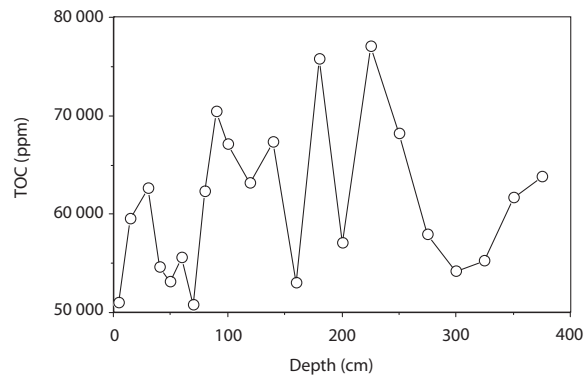


FIG. 21. Variation of Total Organic Carbon (TOC) with depth, (profile KS).

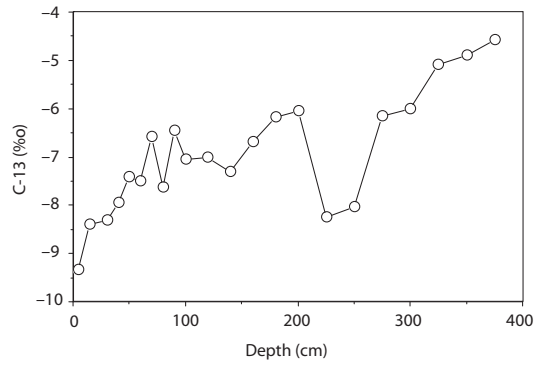


FIG. 22. Variation of  $\delta^{13}C$  with depth, (profile KS).

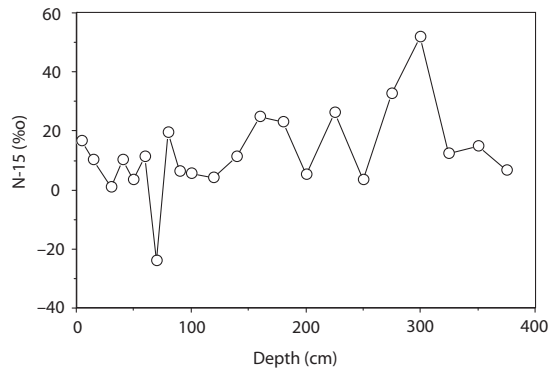


FIG. 23. Variation of  $\delta^{15}N$  with depth, (profile KS).

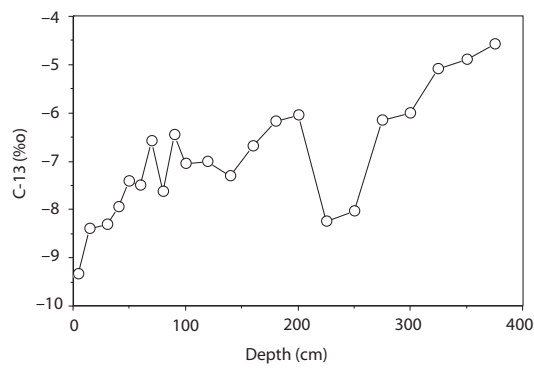


FIG. 24. Moisture content and depth (profile KB).

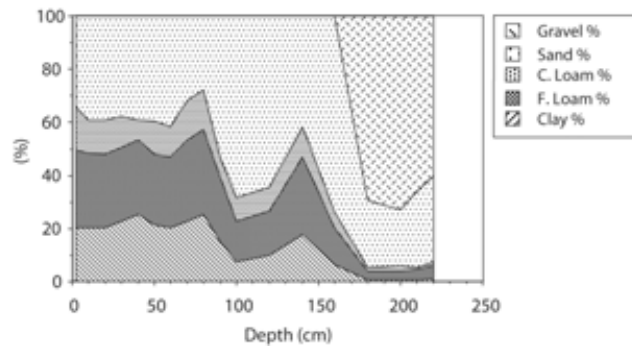


FIG. 25. Particle size distribution, (profile KB).

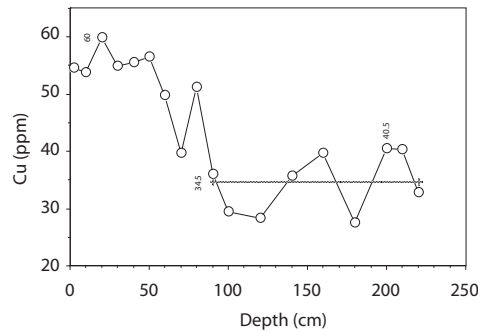


FIG. 26. Variation of Cu with depth, (profile KB).

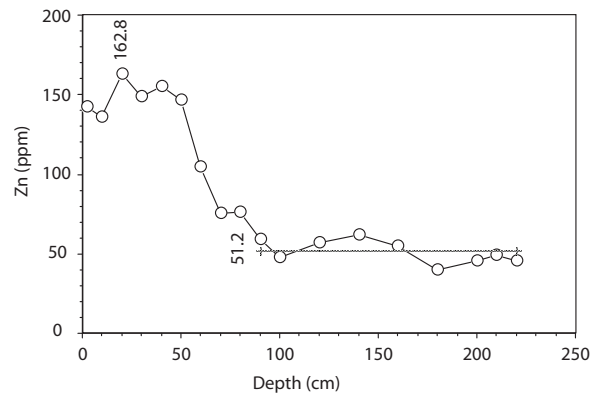


FIG. 27. Variation of Zn with depth, (profile KB).

Comparing the Zn distribution with depth in both profiles KA & KB, the content decreases from 162.8 ppm at 20 cm depth in KB profile to 51.2 ppm in average in the lower part of profile, while in KA profile the content decreases from 557 ppm at 15 cm depth to 112.2 ppm in the lower part of profile.

### ***Cu spatial distribution***

Tanneries (leather industries) are located in the eastern suburb of Damascus city on the borders of Barada River, whose water is used for cleaning purpose with industrial wastes released to the river either directly or through the estuaries, which results in surface water and soil pollution.

Profiles (KA, KB, KS) indicate the maximum Cu concentration in the soil column is located at a depth of 20–30 cm depth, and it is 247 ppm in the nearest profile (KA), and decrease towards the east in to 73.8 ppm (KS) and to the south 60 ppm to the south (KB) (Fig. 28).

The main source of pollution is in tannery area where the industrial wastes are released to the river. The pollution front extends in the same direction of the river and the Cu concentration decreases to 100 ppm at 1.8 km east and 0.8 km south. The river bed sediments are considered polluted by Cu in an

area approximately 2 km long and 1 km width. The Cu concentration decreases in paralleled with the river flow direction, but is impacted during periods of low flow rate by lack of dilution may cause an enlargement in the pollution area.

**Zn spatial distribution**

Zn concentration in the tannery area is high at 20–30 cm depth. It reaches 550 ppm in KA profile and decreases towards the east to 219 ppm in KS profile and to the south to 162.8 in KB profile (Fig. 29).

The Zn concentration, like the Cu concentration, decreases parallel to the river flow direction. The concentration decreases to the east in the direction of surface water flow and south in the direction of the estuaries. Low flow rates in the river can cause high Zn pollution rate. The area is polluted with concentrations of 200 ppm in an area 2 km long and 0.8 km width. The pollution rate depends on the river bed sediments, the river surface water flow, and flow from its estuaries.

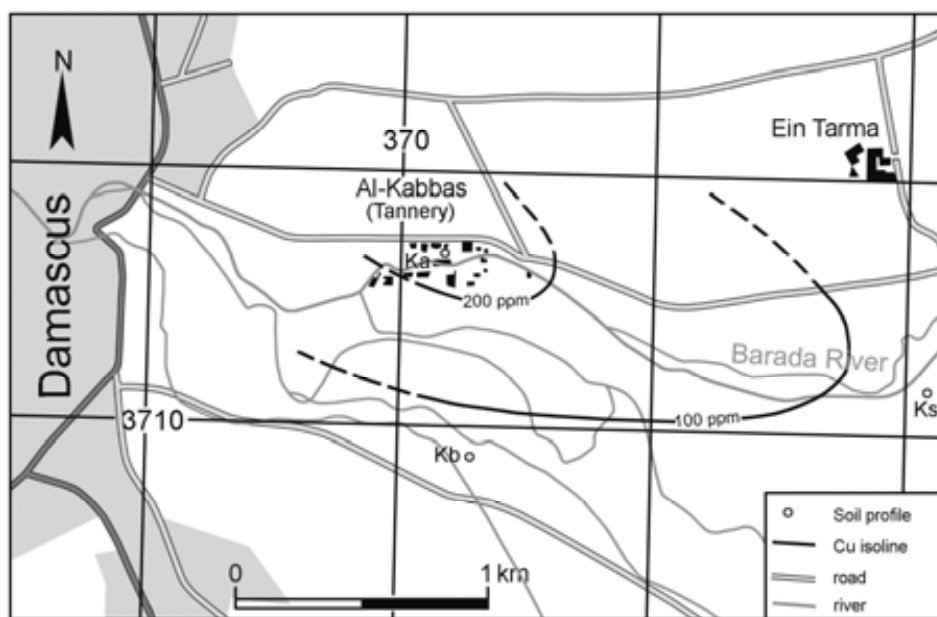


FIG. 28. Cu concentration isoline in the soil, Damascus Oasis, (Syrian Arab Republic).

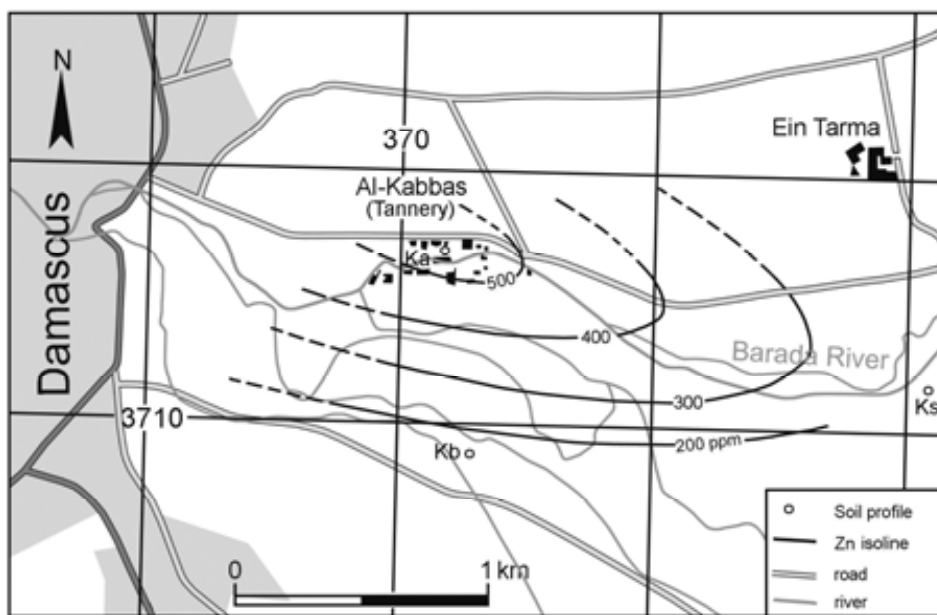


FIG. 29. Zn concentration isoline in the soil, Damascus Oasis, (Syrian Arab Republic).

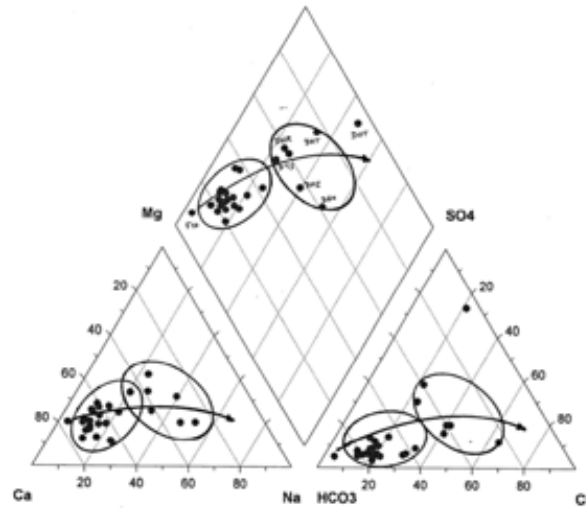


FIG. 30. Piper diagram showing relative concentration of major ions in groundwater (meq/L) — salinity increases.

## 4.2. Water analysis results

### 4.2.1. Chemical analysis

Major ion concentrations were plotted on a piper diagram, as shown in Fig. 30 for groundwater sampled in the area using Hydrowin program. There are three groups of samples:

- The first group is represented by Figh spring (F10) (reference fresh water sample) and samples from the western part of the Oasis (Teshreen area DT). This group has a calcium bicarbonate composition. The EC ranges from 302  $\mu\text{S}/\text{cm}$  in (F10) to 623  $\mu\text{S}/\text{cm}$  in (DT).
- The second group is represented by DT, KBA, DJ, DNO and DZB situated in the centre of Oasis, water is a magnesium bicarbonate type and becomes a sodium chloride type towards the east. Maximum EC is about 1027  $\mu\text{S}/\text{cm}$  in (DZB).
- The third group includes Oteibeh sample DOT and the surrounding areas DHR, DTS, DMI, DGH, DHT. The water has the highest concentrations of sodium, chloride and sulphate. In DOT the EC is 2850  $\mu\text{S}/\text{cm}$  and the concentrations of  $\text{SO}_4$  is 994.6 mg/L. Generally, the salinity increases along the groundwater flow direction from the west to east of Oasis, as it is indicated by arrows on piper diagram in Fig.31. Therefore, the main source of salinity is dissolution of minerals in the host rock.

The saturation index of Calcite (Cal. SI) in groundwater indicates the water is in equilibrium to slightly over saturated with respect to calcite.

The ratio  $r_{\text{Ca}}/r_{\text{Mg}}$  ( $r = \text{meq}/\text{L}$ ) is high near Figh spring as recharge zone (between 6 and 9) and decreases to (1–4) in areas near Oteibeh lake. The Mg concentration increases towards the east of Oasis (Oteibeh Lake) in paralleled with groundwater flow.

### 4.2.2. Chloride variations in the Oasis

Distribution of Cl concentrations in groundwater in the study area is shown in Fig. 31. Cl increases from 19.76 mg/L in Teshreen (DT) towards both the northeast in T. Sawan (DTS) to a value of 117.38 mg/L, and towards the southeast in Gezlanieh (DGH) to a value of 132.29 mg/L. These variations are mainly due to dissolution of mineral from the host rock in the eastern part of Damascus Oasis (Oteibeh Lake). It should be mentioned that a relatively high value of chloride was observed in H.Blass (DMHB), which is located in an industrial area.



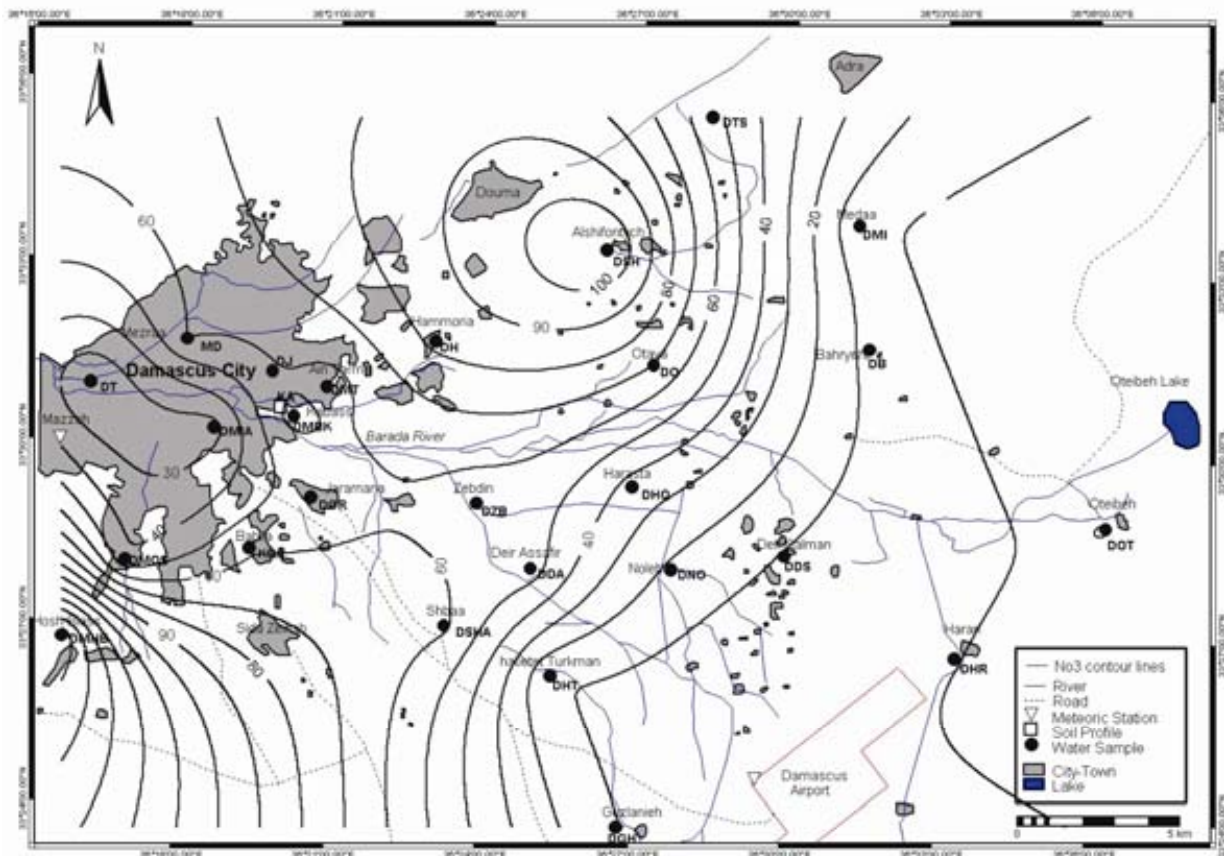


FIG. 32. Map of  $\text{NO}_3^-$  distribution in the study area.

#### 4.2.5. Trace element concentrations in groundwater

Most of the trace elements analyzed in this study, especially heavy metals, do not exist in soluble forms for a long time in waters. They occur mainly as suspended colloids or are fixed by organic and mineral substances. Water pollution by trace elements is an important factor in both geochemical cycling of these elements and in environmental health. It was observed that the trace element concentrations of Pb, Cd, Zn and Cu at all sampling sites were within the permitted international and Syrian concentrations limits for heavy metals in groundwater [30, 31] (Table 3).

A sampling survey was performed in the area by the Ministry of irrigation in order to detect the temporal variations of trace elements in groundwater. There was no contamination of groundwater samples; however, the heavy metals had relatively higher concentrations in 2000 than the more recent measurements.

#### 4.2.6. Isotopic analyses ( $^{18}\text{O}$ and $^2\text{H}$ )

##### 4.2.6.1. Isotope contents in groundwater

The frequency distribution of  $\delta^{18}\text{O}$  content in groundwater (Table 2), shows that  $^{18}\text{O}$  varies between  $-6.5\text{‰}$  and  $-9.5\text{‰}$  with average value of  $-8.25\text{‰}$ . In Fiegh spring the  $\delta^{18}\text{O}$  is more depleted where it is ranged between  $-8.5$  and  $-9.5\text{‰}$ , which presents the recharge origin. The groundwater is more enriched in stable isotopes towards the eastern part of Damascus Oasis (Oteibeh lake).

It is shown from Fig. 33 that the recharge zone of shallow groundwater in Damascus Oasis is from the area of Fiegh Spring.

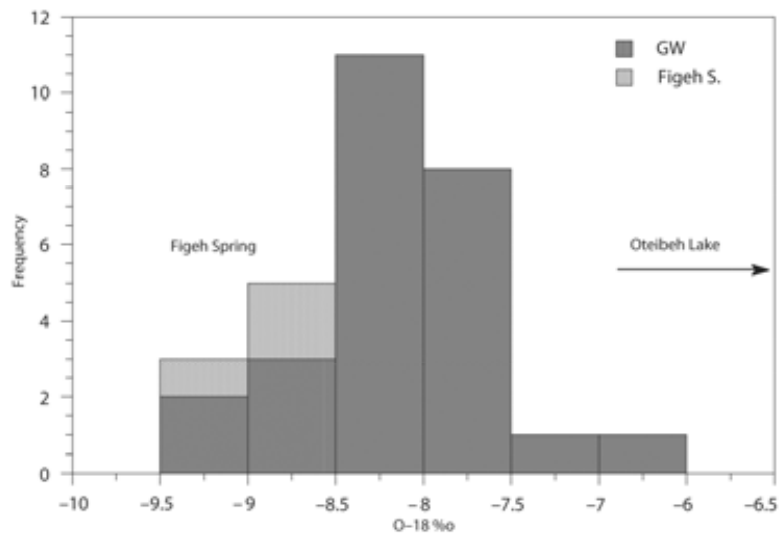


FIG. 33. Frequency distribution of  $\delta^{18}\text{O}$  content in groundwater, Damascus Oasis (Syrian Arab Republic).

#### 4.2.6.2. Deuterium and $^{18}\text{O}$ relationship in groundwater

All the water samples are distributed between the Global Meteoric Water Line with d-excess = +10‰ [32] and the Mediterranean Meteoric Water Line with d-excess = +22‰ [33]. This indicated the groundwater recharge is mainly from precipitation of continental origin. The main recharge zone is located in the Eastern Anti-Lebanon Mountain and has a d-excess between 15 and 22‰ [34–36]. These values are similar to that in some of the Mediterranean areas [28, 37]. The intercept between the groundwater sample line with Mediterranean Meteoric water line present the precipitation that recharge the hydrological zone before any evaporation process. This point is  $\delta^{18}\text{O} = -9$  and  $\delta^2\text{H} = -51$ ‰. The correlation between Deuterium and  $^{18}\text{O}$  fits the sample points with the relation (Fig. 34):

$$\delta^2\text{D} = 3.2 + 6.2 \times \delta^{18}\text{O}, R^2 = 0.744$$

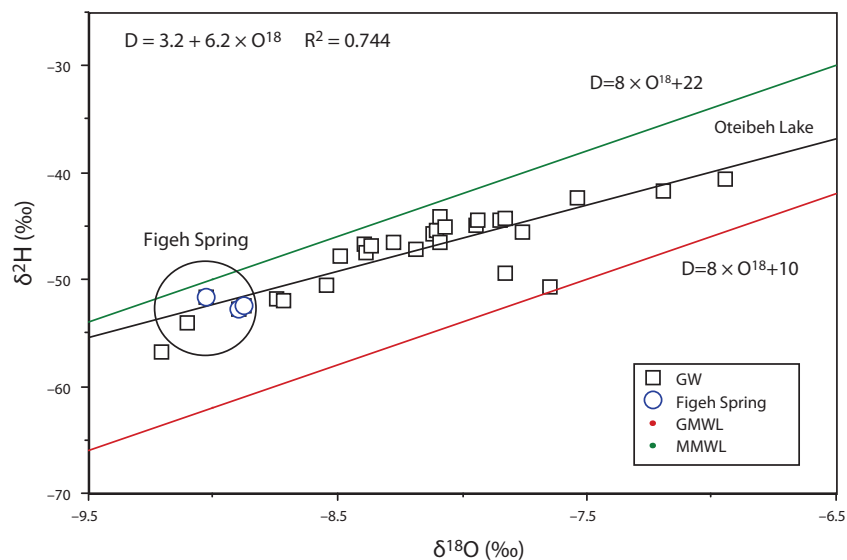


FIG. 34. Deuterium and oxygen-18 relationship in groundwater, Damascus Oasis (Syrian Arab Republic).

The slope of this line indicates that samples of groundwater have prone to evaporation from west of Damascus city till Oteibeh lake in the east, where the groundwater is more enriched with stable isotopes. It is shown from Fig. 35 that the groundwater is more related to the Mediterranean meteoric water line (MMWL), which is due to the location of the area east of Mediterranean sea. The recharge zones are close to the recharge area of Figh spring, which is believed to be located in the Anti-Lebanon mountain chain.

## 5. CONCLUSIONS

The chemical composition of groundwater is classified into three groups of samples:

- Figh spring sample has Ca-HCO<sub>3</sub> type with low salinity. It is considered as a reference sample of fresh water.
- The second group presents the water samples taken from Teshreen pumping station to the centre of the Oasis. This group is characterized by Ca-Mg-HCO<sub>3</sub> type. The salinity increases towards the east.
- The third group is represented by Oteibeh water sample and the samples from the surrounding area. This group has Na-Cl and Na-SO<sub>4</sub> type with relatively high salinity due to dissolution processes.

Nitrate distribution indicates that at Teshreen and west of Oasis water samples are not polluted by nitrate and are below the permitted limit of NO<sub>3</sub> in drinking water. Nitrate pollution increases from the eastern part of Damascus city in a north-south zone starting from H.Blass to Kabass and Zebdeen to Shifonieh in the north, where a high nitrate concentration was measured. The pollution level decreases towards the east. It can be concluded from these results that high nitrate concentration in groundwater is due to the urban, industrial pollution in H.Blass and agricultural pollution from irrigation that uses sewage water near Shifonieh.

Soil profiles shows the distribution of trace elements (Cu, Pb, Cr, Zn, Cd and As) with depth have high concentration at the surface horizon between 0–1 m depth. Below the upper zone, the concentrations varied slightly around an average value to the bottom of the profile. The high concentrations in the upper part of the unsaturated zone indicate the high level of pollution likely, from leather industries in the area, and the concentrations are above the permitted limit of these elements in the soil. In contrast, concentrations of these trace elements in the lower part of the profiles are below the permitted limits. The high pollution level in the upper part can be explained by absorption of these elements by the organic matters and clay minerals.

All the trace element profiles indicted that there is no migration from the surface through unsaturated zone. Thus, the unsaturated zone is considered as a filter that concentrates the trace elements in the upper part.

Cu and Zn spatial distribution maps indicated the pollution front has the same direction of the river and the pollution concentration decreases towards 2 km east and 1 km southern of Kabbas area (20–40%). The Cu and Zn concentrations decrease in paralleled with the river flow direction. However, low flow rate causes decrease in dilution process that causes enlargement in pollution area.

The results of trace elements analysis in groundwater showed all the samples are under the international and Syrian permitted limits. Previous studies of surface water pollution indicted relatively high pollution levels in the areas close to the industrial zone.

The isotopic composition of shallow groundwater indicates the recharge zones are related to that of Figh spring and are more enriched by stable isotopes towards Oteibeh Lake. The groundwater samples are distributed around evaporation line with a slope of 6.3, which is related to the eastern Mediterranean precipitation. Thus, the recharge of this aquifer and Figh Spring is derived from the Anti-Lebanon Mountain.

## ACKNOWLEDGEMENTS

The authors would like to gratefully acknowledge Prof. Dr. I. Othman, Director General of Atomic Energy Commission of Syria (AECS), for his guidance and support. Special thanks to Dr. K. M. Kulkarni Chief Scientific of the CRP (IAEA). Thanks are due to Prof. Dr. R. Kalin and his teamwork, Queen University in Belfast, for his comments and doing some of the sample analyses. Thanks to Dr. R. Nasser, head of Geology Department in SAEC, to Dr. A. Khuder, researcher in chemistry Department of AECS, Dr. R. Rajab, a researcher in the Hydrology Department of Arab Center for the Studies of Arid Zones and Dry Lands (ACSAD). Finally, thanks to M. Kudmani and B. Rumeeh in the Ministry of Irrigation and B. Katta and M. Wannous, I. Abou Madi in Geology department, S.A. Baker, S. Ibrahim, H. Issa and O. Shayiah in the AECS for doing part of the laboratory analysis.

## REFERENCES

- [1] FALOUH, J., Water resources in Barada and Awaj River basins in the Syrian Arab republic, Workshop on the assessment the soil and groundwater ability to pollution, 7–10 Feb., 2000, Beirut, Lebanon (1999) 145–170.
- [2] AL-AMMARIN, A., Hydro-geophysical study of well fields for drinking water supply of the city of Damascus, M.Sc. research thesis, Damascus University (2000) 316.
- [3] DEEB A., Pollution of groundwater and surface water in Damascus basin (Syrian Arab Republic), scientific report, Ministry of Irrigation, Syrian Arab Republic (2000).
- [4] JABI, M., et al., Pollution of Barada River and its estuaries, Ministry of Irrigation, Pollution Dept., Syrian Arab Republic (1990) 290.
- [5] KHUDER, A., KALIFEH, K., ABBAS, M., Distribution of some chemical elements in Barada River soils, Sci. report, Syrian Atomic Energy Commission (SAEC), Syrian Arab Republic (1996) 73.
- [6] AL-MASRI, M.S., ABA, A, KHALIL, H., AL-HARES, Z., Sedimentation rates and pollution history of a dried Lake: Al-Oteibeh Lake, Sci. Total Environ. **293** (2002) 177–189.
- [7] ABOU ZAKHEM, B., HAFEZ, R., Study of recharge and evaporation process in the unsaturated zone of Damascus basin (Syrian Arab Republic), IAEA-TECDOC-890, IAEA, Vienna (1996) 33–59.
- [8] STERCKMAN, T., DOUAY, F., PROIX, N., FOURRIER, H., Vertical distribution of Cd, Pb and Zn in soils near smelters in the North of France, Environ. Pollut. **107** (2000) 377–389.
- [9] HELENA, B., PARADO, R., VECA, M., BARRADO, E., FERNANDEZ, J.M., FERNANDEZ, L., Temporal evolution of groundwater composition in an aquifer (Pisuerga River, Spain) by principal component analysis, Wat. Res. **34** 3 (2000) 807–816.
- [10] CHEN T.B., WONG, J.W.C., ZHOU, H.Y., WONG, M.H., Assessment of trace metal distribution and contamination in surface soils of Hong Kong, Environ. Pollut. **96** 1 (1997) 61–68.
- [11] MIRELES, A., SOLIS, C., ANDRADE, E., LAGUNAS-SOLAR, M., PINA, C., FLOCCHINI, R.G., Heavy metal accumulation in plants and soil irrigated with wastewater from Mexico city, Nucl. Instrum. Methods Phys. Res. Sect. B **219–220** (2004) 187–190.
- [12] SAETHER, O. M., STORROE, G., SEGAR, D., KROG, R., Contamination of soil and groundwater at a former industrial site in Trondheim, Norway, Appl. Geochem. **12** (1997) 327–332.
- [13] EDMUNDS, W.M., KINNIBURGH, D.G., MOSS, P.D., Trace metals in interstitial waters from sandstones: acidic inputs to shallow groundwater, Environ. Pollut. **77** (1992) 129–141.
- [14] YOUNAS, M., SHASAD, F., AFZAL, SH., KHAN, M.I., ALI, K., Assessment of CD, Ni, Cu and Pb pollution in Lahore, Pakistan, Environ. Int. **24** 7 (1998) 761–766.
- [15] SOUMI, G., CHAYEB, R., Water need and plant irrigation techniques, Rep. UNDP, FAO, SYR/86/015, Agriculture Ministry (1989) 33.
- [16] HOMSI, M., BOUNI, M., KURDI, A., Damascus basin climate and its role in economical plans and the climatic changes, Nat. Meteorol. Rep. (1989) 35.
- [17] PONIKAROV, V.P., Explanatory notes on the geological map of Syria, scale 1/200 000, sheet VII (Damascus) , Techno-export (1966).

- [18] SELKHOZPROMEXPORT, Water resources use in Barada and Auvage basins for irrigation of crops, volume II, Book 2, USSR, Moscow (1986) 484.
- [19] KHANDEKAR, R.N., TRIPATHI, R.M., RAHNNATH, R., MISHRA, V.C., Simultaneous determination of Pb, Cd, Zn, Cu in surface soil using differential pulse anodic stripping voltametry, *Indian J. Environ. Health* **30** (1988) 98–103.
- [20] ARANYOSSY, J.F., “Study of water movement in the unsaturated zone using natural and artificial isotopes”, Regional seminar on application of isotope and nuclear techniques in hydrology in arid and semi arid lands, Ankara, Turkey (1985) 29.
- [21] DAY, P.R., Particle fractionation and particle-size analysis (1969) 21.
- [22] AL-MEREY, R., KARAJO, J., ISSA, H., Evaluation of quantitative analysis methods in XRF technique using certified reference materials, Syrian Atomic Energy Commission SAEC, Syria (2000) 24.
- [23] KABATA-PENDIAS, A., PENDIAS, H., Trace elements in soils and plants, Warsaw, Poland (1984) 315.
- [24] GILANI, A., Soil pollution in some Arab countries as result of sewage treated water and sludge application, Beirut, Lebanon (2000) 41–48.
- [25] BARNES, C.J., ALLISON, G.B., The distribution of deuterium and oxygen-18 in dry soil (I Theory). *J. Hydrol.* **60** (1983) 141–156.
- [26] ALLISON, G.B., HUGHS, M.V., The use of natural tracers as indicators of soil-water movement in temperate semi-arid region. *J. Hydrol.* **60** (1983) 157–173.
- [27] ALLISON, G.B., BARNES, C.J., HUGES, M.V., The distribution of deuterium and oxygen-18 in dry soil (II. Experimental), *J. Hydrol.* **65** (1983) 377–397.
- [28] CLARK, I., FRITZ, P., *Environmental Isotopes in Hydrogeology*, Lewis publishers, USA (1997) 311.
- [29] ABOU ZAKHEM, B., HAFEZ, R., General hydro-isotopic study of direct infiltration and evaporation process through the unsaturated zone in Damascus Oasis, Syrian Arab Republic, IAEA-TECDOC-273, IAEA (2001) 131–170.
- [30] AL-OU DAT, M., Pollution and protection of environment, *Al Ahali journal*, Damascus, Syrian Arab Republic (1998) 244.
- [31] AL-OU DAT, M., KEJEIJAN, B., Heavy elements in the environment and their impact on the human health, *Sci. Report. SAEC*, Damascus, Syrian Arab Republic (2001) 55.
- [32] CRAIG, H., Isotopic variations in meteoric water, *Science* **133** (1961) 1702.
- [33] NIR, “Development of isotope methods applied to groundwater hydrology”, *Proc. of a symposium on isotope technique in hydrological cycle*, *Am. Geophys. Union Monogr Series*, No 11 (1967).
- [34] KATTAN, Z., Effects of sulphate reduction and geogenic CO<sub>2</sub> incorporation on the determination of <sup>14</sup>C groundwater ages — a case study of the Palaeogene groundwater system in north-eastern Syrian Arab Republic, *Hydrogeol. J.* **10** (2002) 495–508.
- [35] GEYH M.A., BENDER, H., RAJAB, R., WAGNER, W., “Application of <sup>14</sup>C groundwater dating to non-steady systems”, *Proc. of a symposium on application of tracers in arid zone hydrology*, IAHS publ. no. 232 (1995) 225–234.
- [36] WAGNER, W., GEYH, M.A., *Application of Environmental Isotope Methods for Groundwater Studies in the ESCWA Region*, United Nations (1999) 129.
- [37] GAT, J.R., CARMI, I., Evolution of the isotopic composition of atmospheric water in Mediterranean Sea Area, *J. Geophys. Res.* (1970) 3039–3048.



# CONTAMINANT ATTENUATION THROUGH GLACIAL DRIFT OVERLYING THE CHALK AQUIFER IN SOUTHERN EAST ANGLIA, UK

D.C. GODDY, W.G. DARLING  
British Geological Survey,  
Wallingford, Oxfordshire, UK

## ABSTRACT

The Chalk is the major aquifer in the UK. Parts of the Chalk are covered in places by glacial drift deposits, which can have a significant influence on recharge and contaminant movement, particularly where dominated by low-permeability lithologies such as the boulder clay (Till) sheet of East Anglia. Fracturing in Till has been widely observed and its potential for providing a route for rapid contaminant movement identified. A groundwater sampling programme has been undertaken and two cored boreholes drilled to investigate the degree of attenuation effected by the Till cover. Results from CFC and nitrate sampling show the Chalk groundwater beneath the interfluvial is old and has negligible nitrate concentrations. Groundwaters beneath the valley and Till edge have a component of modern water and generally high nitrate concentrations. Evidence for denitrification is also found. Data from gas samplers shows modern air deep in the unsaturated zone suggesting a by-pass route for recharge. The Till layer attenuates nitrate concentrations in groundwater by restricting the downward movement of recharging rainwater and promoting denitrification both in terms of redox conditions and by increasing the time of exposure to these conditions.

## 1. INTRODUCTION

The Chalk is the major aquifer in the UK, providing 15% of the water supply nationally and up to 35% regionally in the south and east. It is a soft microporous and fractured calcium carbonate aquifer with high intergranular porosity (25–45%) but low intergranular hydraulic conductivity as a result of small pore-neck size. The fracture component has low porosity (0.1–1%) but can increase the hydraulic conductivity by up to three orders of magnitude [1]. In the unsaturated zone of the Chalk of Southern England, recharge has an apparent downward velocity of  $\sim 1$  m/a [2], probably achieved rather discontinuously by relatively immobile pore water flooding into fractures when tensions permit [3]. However, faster ‘preferential’ flow through fractures may be important especially for transport of trace contaminants such as pesticides [4].

The Chalk aquifer is a highly complex natural system [5, 6] and consequently is very difficult to measure or sample in a systematic manner in either the saturated or unsaturated zones. Recharge can be localized due to the highly inhomogeneous nature of the shallow weathered Chalk [7]. Major aquifers in the UK are partially covered by Drift, which can have a significant influence on contaminant movement, particularly where dominated by low-permeability lithologies such as clay. The extensive Till (boulder clay) sheet of East Anglia, characterised by a thick sequence of low-permeability deposits overlying the important Chalk aquifer, is one such example and the focus of this study. The complexity of drift cover in Britain, coupled with a wide variety of depositional environments, means that a large number of hydrogeological settings or ‘domains’ exist. Clearly these need to be characterised and their influence on recharge assessed.

The predominant route taken by contaminants in low-permeability drift-covered areas remains far from well-established. In Till for example it could be more or less direct, via intergranular movement (Scenario 1, Fig.1a). Oxidised Till is likely to have a higher permeability than unoxidised Till. Previously it had generally been considered that Till is unlikely to possess significant fracture permeability. However, in recent years, fracturing in Till has been widely observed and its potential for providing a route for rapid contaminant movement recognized [7,8] (Scenario 2, Fig. 1b). Other routes for contaminant movement to aquifers overlain by Drift are possible and include permeable lenses within the Till (Scenario 3, Fig. 1c) or direct entry at the edge of the Till (Scenario 4, Fig. 1d). It is also possible that no significant contaminant movement or attenuation occurs.

Earlier investigation of the East Anglian Till [9] left unexplored several aspects of the effect of Drift cover. The biggest questions left unresolved were: (i) the residence times of the various groundwater components, (ii) the degree of importance of fracture-related bypass flow and (iii) the mechanism of attenuation of dissolved nitrate. Through measuring CFCs in groundwaters and in the gaseous phase as an indicator of residence time, and determination of nitrate and the products of denitrification, this study attempts to address some of these questions.

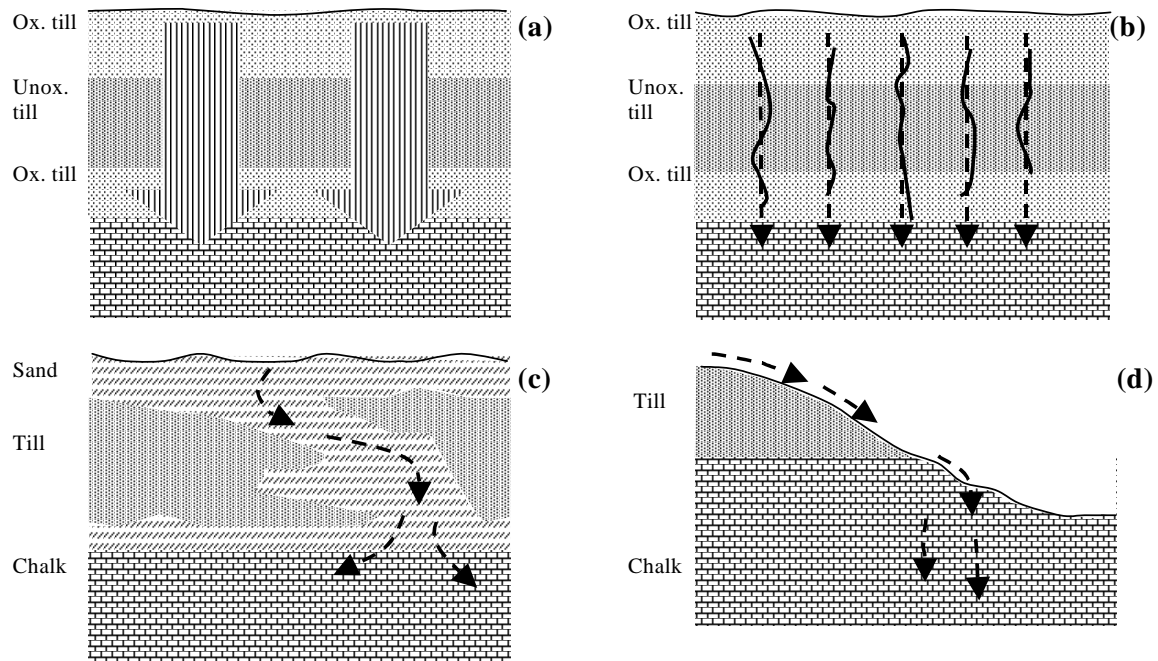


FIG. 1. Scenarios for contaminant movement to Chalk through till. (a) Scenario 1: dispersed contaminant movement occurs through till pores, (b) Scenario 2: contaminant movement occurs through till fractures, (c) Scenario 3: contaminant movement occurs through permeable lenses in the till, (d) Scenario 4: contaminant movement occurs at the edge of the till outcrop.

The overall objective of this paper is to understand the effects of the extensive Drift (superficial deposits) cover overlying the Chalk aquifer on contaminant attenuation, specifically nitrate. This requires an identification of the key Chalk hydrogeological environments, an understanding of water movement and measurement of nitrate and likely products of denitrification. Although the drift cover may not have particularly significant resource implications, it is an important consideration when attempting to model or predict the movement of water and contaminants through the Chalk.

## 2. GEOLOGY, HYDROGEOLOGY AND SITE DESCRIPTIONS

### 2.1. Geology

The Lowestoft Till (Quaternary) is sometimes referred to as the Chalky Boulder Clay. This Till covers much of the N Essex—S Suffolk district in a plateau-forming sheet commonly between 30 and 50 m in thickness [10], which locally varies with the elevation of the ground. The Drift/Chalk interface is largely a planar feature with a regional dip to the south-east. The valley of the River Stour, the most significant watercourse in the district, is considered part of a glacial buried valley, which has cut down into the planar surface of the Chalk.

The Lowestoft Till is characteristically an unstratified bluish-grey silty sandy clay with pebbles where it is unoxidised [11]. A weathered, oxidised zone of brown and orange-brown in colour between 0.2 and 2 m thick is commonly developed beneath the soil and an oxidised zone is often present at the base of the sequence. Fractures with oxidised surfaces are occasionally found in the Till. The pebble

erratics are usually some 50–75 mm in diameter and consist largely of well-rounded Chalk clasts, but also include sub-angular flints. The Till was deposited during the Middle Pleistocene glaciation, which was also the source of much of the other drift cover in the general area.

The thick Till domain is probably the most important for contaminant attenuation. Consequently this domain was used for the field study, looking at two distinct sub-domains: the centre and edge of the Till sheet respectively. The required site characteristics included a homogeneous Till sequence between roughly 15 and 30 metres thick overlying Chalk. Two sites were identified: Cowlinge, on an interfluvium several km from any exposed Chalk, and Clare on the edge of the Stour Valley approximately 100 m from the exposed Chalk (Fig. 2).

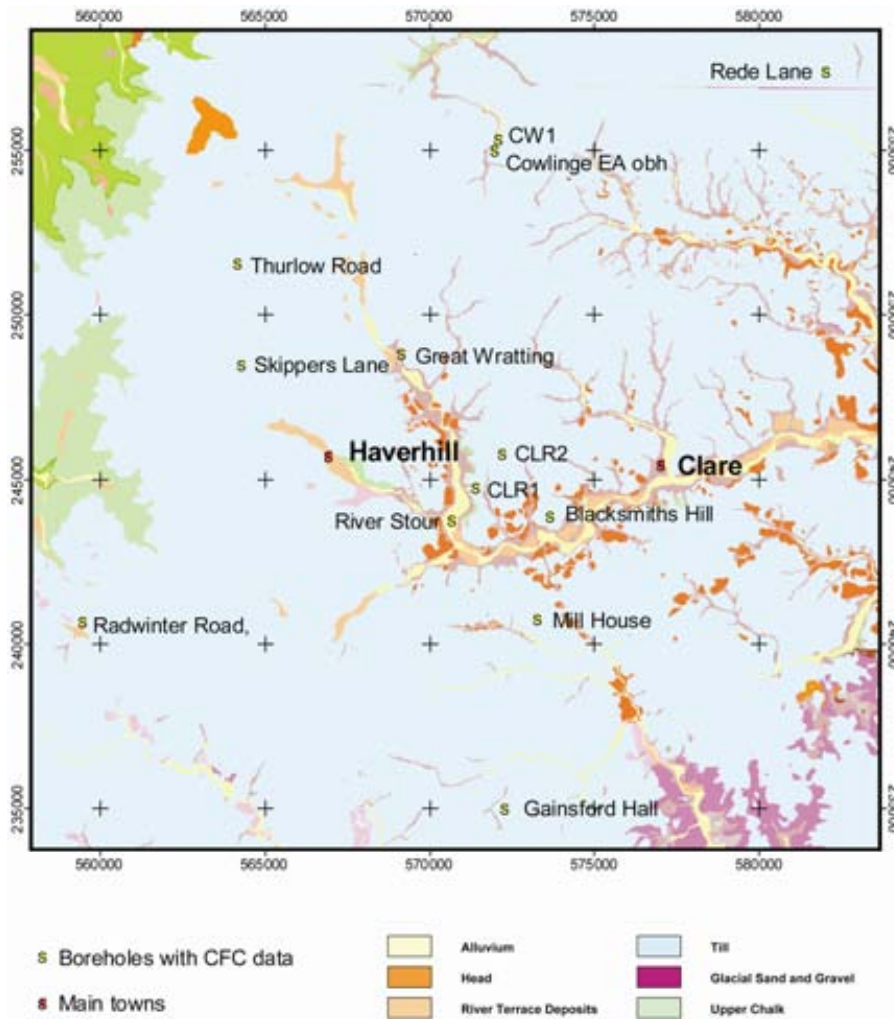


FIG. 2. Location of sampling sites.

## 2.2. Hydrogeology

The principal aquifer in the region is the Chalk which is extensively developed for water supplies [10]. As can be seen from the schematic cross-section (Fig. 3), hydraulic conditions at the two sites differ. In the centre of the Till sheet the groundwater is confined, with a piezometric surface within the Till. Towards the edge, the water level falls to the extent that there is unsaturated Chalk beneath the Till. The regional hydraulic gradient is towards the south-east. The River Stour is likely to be in hydraulic continuity with groundwater. Contours on the potentiometric surface [10] show highs of over 70 mAOD beneath the Till plateau, indicating some recharge to the Chalk through the thick Till sequence (Fig. 3). Annual fluctuation of the potentiometric surface where the Chalk is confined by the

Till is about 2 m in a hydrograph to the east (NGR TL 846 410) of the drill site, which compares with about 9 m in a hydrograph from the exposed Chalk to the north-west (NGR TL 594 591). The end of the recession and recovery periods on the confined hydrograph[10] coincides closely with the times on the exposed Chalk hydrograph. This suggests that there is little if any time lag in the recovery beneath Drift compared to the exposed Chalk environment.

The Chalk is a dual-porosity aquifer that relies on fractures and jointing for much of its transmissivity. The upper 10-20 m of the Chalk, particularly where it is exposed, may be poorly-jointed putty-chalk, and have a reduced permeability. Storage of water takes place mostly in the intergranular matrix of the Chalk, which has high porosity but low hydraulic conductivity. Beneath the Till the Chalk groundwater carbonate hardness rises to 260–350 mg/L and non-carbonate hardness to 300–400 mg/L [10]. This compares to a non-carbonate hardness of 50 100 mg/L in exposed Chalk. The chloride ion concentration increases to over 100 mg/L (Fig. 3) and sulphate also shows high concentrations where the Till cover is thickest. This compares to a concentration of 15–50 mg/L Cl in the exposed Chalk. Whilst these highs might generally reflect reduced recharge they also coincide with highs in the groundwater surface which are indicative of recharge through the Till. These highs in the groundwater surface may partly relate to low transmissivity in the Chalk in these areas.

The boulder clay itself has a low intergranular permeability. However, fractures and sand lenses in the clay may enhance the overall permeability, although the extent and properties of these is not well known. The boulder clay in this area probably reduces recharge to the Chalk and also reduces the vulnerability of the Chalk aquifer to contamination. Furthermore, clay minerals (especially smectitic clays) within the boulder clay have the ability to attenuate contaminants by sorption and cation exchange [12].

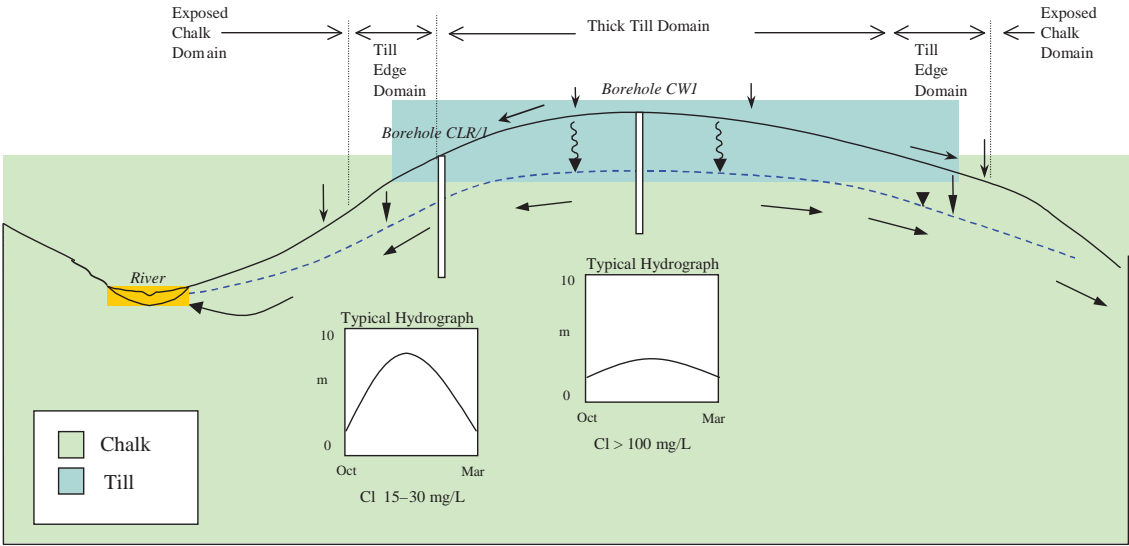


FIG. 3. Schematic cross-section.

Beds of sand and gravel within the Till can be unsaturated, but most are partially or fully saturated. These perched water tables typically have limited storage indicative of their isolated nature. Groundwater derived from sands and gravels within the Till and beneath the Till, where they overly low-permeability bedrock, is characterised by high non-carbonate hardness (calcium sulphate and magnesium sulphate). Total dissolved solids (TDS) concentrations often exceed 700 mg/L and chloride ion concentrations are mostly between 60 and 110 mg/L[10].

### 2.3. Sampling sites

At Boyton End, near the town of Clare, Suffolk, a borehole number CLR1 was drilled to a total depth of 31 m, through 21.4 m of Till and into the unsaturated and saturated Chalk (NGR 7142 4477) in the Till edge domain (Fig. 3). The borehole was constructed with a groundwater piezometer and six gas piezometers.

Near the village of Cowlinge (also Suffolk), a second borehole CW1 was drilled to a total depth of 80 m, through 35.8 m of Till into the saturated Chalk. A further 9 sites were identified in the area for groundwater sampling and are shown in Fig. 2. Table 1 shows the depth of the drift cover at each of these sites.

TABLE 1. TILL DEPTH AT EACH OF THE GROUNDWATER SAMPLING LOCATIONS.

	Till Depth (m)
CLR1	21
Blacksmith Hill	20
Mill House	31
Great Wrattling	2.4
Gainsford Hall	40
Rede Lane	50
Radwinter Road	32
Skippers Lane	29
Thurlow Road	10
CW1	36
Cowlinge EA obh	29

## 3. SAMPLING AND ANALYSIS

### 3.1. Chlorofluorocarbons (CFCs)

Pumped groundwaters were sampled by the bottle-in-can method [13]. Unsaturated zone gases were sampled using evacuated glass bulbs. Analysis was carried out using a purge-and-trap system (cooling to  $-50^{\circ}\text{C}$  and desorbing at  $100^{\circ}\text{C}$ ) coupled to a GC with electron capture detection. For dissolved CFCs detection limits of roughly 0.02 pmol/L and 0.13 pmol/L were possible using 35 mL of water for CFC-11 and CFC-12 respectively. This is equivalent to 0.3 and 4 % of modern water respectively. Calibration was carried out by using an air standard prepared at the University College Galway Atmospheric Research Station in Mace Head, Ireland.

### 3.2. Nitrate

Filtered, unacidified aliquots of groundwater were collected in Nalgene bottles. Nitrate-nitrogen ( $\text{NO}_3\text{-N}$ ) was determined using standard colorimetric methods.

### 3.3. Nitrous oxide

Pumped groundwater samples were collected in evacuated glass bulbs with known headspace volumes. Nitrous oxide ( $\text{N}_2\text{O}$ ) was analysed using a Porapak-Q column with nitrogen carrier gas and an electron capture detector. A certified gas standard was run with the samples to calibrate the results.

### 3.4. Nitrogen/argon ratio

Samples for N<sub>2</sub>/Ar measurement were prepared by gas-pipetting an aliquot of headspace gas (see N<sub>2</sub>O above) into a 'finger'-type vessel containing approximately 0.5 g of copper flakes. Atmospheric air was sampled in the same way to produce 'air spikes' against which to calibrate the results. The sealed fingers were then heated at 450°C for 15 min in order that all O<sub>2</sub> could be removed by the copper. After cooling, the fingers were attached to a VG Optima Mass Spectrometer and analysed by ratio measurement of the mass 28 (N<sub>2</sub>) and 40 (Ar) peaks[14]. This allows analysis on a dynamic (i.e. constant flow) mass spectrometer, which is an improvement on static mass spectrometry because of the absence of 'cracking' effects in the ion source. A higher precision is therefore possible. Ratios of N<sub>2</sub>/Ar were calculated by reference to the results obtained for air samples. Precision is ±0.2%.

## 4. RESULTS AND DISCUSSION

### 4.1. Regional concentrations

A summary of the percentage of modern water as determined by the CFC data is given in Table 2. The percentage of modern water in the groundwater samples varies from 5–97 % based on the CFC-11 measurement and from 6–97% based on the CFC-12 measurement. In the majority of cases the percentage of modern water determined by CFC-12 is greater than that determined by CFC-11. Where the percentage of modern water determined by CFC-12 is less than CFC-11 then the values are generally low (i.e. both CFCs indicate a small fraction of modern water) or the two values are very close (note the relative fractions of modern water determined by the two CFCs in the River Stour). At one Till-edge site (Great Wrattling) there was evidence of CFC pollution, possibly associated with leakage from cold storage facilities at the adjacent pork-processing plant.

Nitrate, nitrous oxide and the N<sub>2</sub>/Ar ratio for the sampled groundwaters are given in Table 3. The majority of the sites sampled contain nitrate-N concentrations below the 0.2 mg/L limit of detection. In general terms nitrate concentrations are highest where the Till layer is thinnest, with the one exception of the Thurlow Road Site.

TABLE 2. SUMMARY OF % OF MODERN WATER PRESENT IN SAMPLES AS DETERMINED BY CFC-11 AND CFC-12.

	CFC-11 % modern	Stdev	CV (%)	CFC-12 % modern	Stdev	CV (%)	(F12-F11)/F12
CLR1	79	7	9	97	15	16	0.19
Blacksmith Hill	77	10	13	82	15	19	0.06
Mill House	35	30	85	82	28	34	0.57
Great Wrattling	>modern			>modern			
River Stour	97			94			-0.03
Gainsford Hall	5			15			0.67
Rede Lane	10			58			0.83
Radwinter Road	10			9			-0.08
Skippers Lane	6			66			0.90
Thurlow Road	12			8			-0.52
CW1	24			33			0.28
Cowlinge EA obh	11			6			-0.71

TABLE 3. SUMMARY OF NITRATE (AS NITROGEN) NITROUS OXIDE CONCENTRATIONS IN SELECTED GROUNDWATERS TOGETHER WITH THE N<sub>2</sub>/AR RATIO.

	NO <sub>3</sub> -N mg/L	N <sub>2</sub> O µg/L	N <sub>2</sub> /Ar Mean	Stdev	CV (%)
CLR1	39.6		46.2	3.5	7.6
Blacksmith Hill	8.3	26	44.5	2.2	4.8
Mill House	<0.2	1100	42.0	1.7	4.1
Great Wrattling	4.5	34	44.6		
River Stour	8.7				
Gainsford Hall	<0.2		39.2		
Rede Lane	<0.2		39.9		
Radwinter Road	<0.2				
Skippers Lane	<0.2		38.8		
Thurlow Road	<0.2		44.5		
CW1	<0.2		49.4		
Cowlinge EA obh	<0.2		46.1		

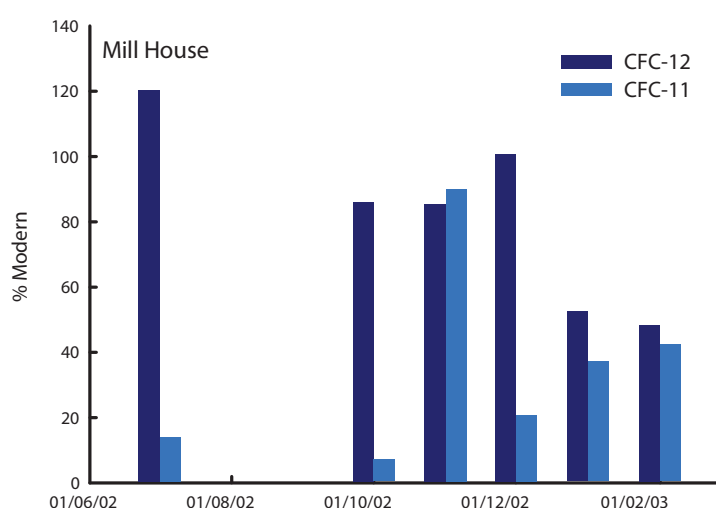


FIG. 4. Concentrations of CFC-11 and CFC-12 at the Mill House site sampled over 7 months from July 2002.

Where significantly lower fractions of CFC-11 relative to CFC-12 are present it is probable that environmental conditions are more reducing (as the CFC-11 is degraded under reducing conditions) which might coincide with denitrification. Site CW1 contains relatively more CFC-12 than CFC-11 and has N<sub>2</sub>/Ar ratios significantly above the background value of ~40, based on equilibration at 10°C plus minor excess air. Both suggest that some denitrification is taking place. At the Mill House site, there is considerable variation in the fraction of modern water as indicated by CFC-11 and CFC-12 (Fig. 4), with the suggestion that CFC-11 has been degraded under reducing conditions. Data from the N<sub>2</sub>/Ar measurement however shows little N<sub>2</sub> enhancement although the concentration of N<sub>2</sub>O in the water is very high. It is suggested therefore that denitrification is occurring at this site but that conditions are not suitable for the formation of nitrogen gas (i.e., a suitable microbial population is not present). A similar observation has previously been made for a site underlying a cattle slurry storage lagoon [15].

With the exception of the River Stour, Great Wrating and CLR1, groundwater is composed of between 6 and 80% modern water. Where the Till depth is greater than 5 metres this suggests that some preferential water movement is taking place.

#### 4.2. Modelling Gas Movement at CLR1

The variation with depth in CFC-12 concentration in the gas samplers positioned in borehole CLR1 are given in Fig. 5. The dotted line also shows the time lag for CFC-12 passing through a 26.8-metre unsaturated zone, calculated with the model of Cook and Solomon [16]. Gas- and liquid-filled porosities of 0.05 and 0.3 were used respectively, along with gas- and liquid phase tortuosities of 0.05 and 0.5. A liquid phase velocity of 0.3 m/a was used in the simulation. Other parameters for the properties of CFC-12 are given elsewhere [16]. The dashed line shows the time lag for CFC-12 passing through a three layer version of the Cook and Solomon model so as to simulate the unsaturated zone geology at this site. Layer one uses gas- and liquid filled porosities of 0.04 and 0.2; layer two 0.05 and 0.03; and layer three 0.3 and 0.05 respectively. Layer one uses gas- and liquid-phase tortuosities of 0.03 and 0.03; 0.1 and 0.2 in layer 2; and 0.05 and 0.5 in layer 3. The liquid phase velocity used was 0.1 m/a.

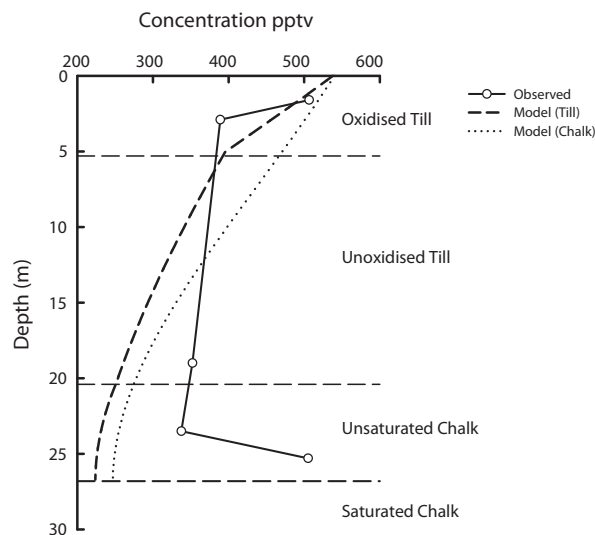


FIG. 5. Variation in CFC-12 in gas samplers positioned in borehole CLR1 and two simulated profiles using the model of Cook and Solomon [16].

The small reduction in gaseous phase concentration in the unoxidised Till combined with the large step in concentration in the oxidized Till proved too difficult to model with this 1-D model. Highest concentrations, of the order of 100% modern, are seen at the top of the profile in the oxidised Till as would be expected. Lowest concentrations are found towards the bottom of the unoxidised Till. It could be argued that this should in reality be zero (i.e. pre-CFC usage) and that the presence of a proportion of modern air is an artefact of the installation process, even though great care was taken to evacuate any modern air from the system following sampler installation. The high moisture content and relatively high liquid phase velocity common in the Chalk mean advection in the liquid phase is much greater than diffusion in the gas phase and as such, time lags are all approximately equal to the water residence times. The gas concentration at 20 metres indicates atmospheric penetration of the Till layer to this depth takes some 20 years. This is in sharp contrast to the <1 year for penetration of a Chalk unsaturated zone of similar thickness suggested by gas tracer tests [17]. These results infer that fracturing in the unsaturated zone of the Chalk has an important influence on gas concentrations. The higher than predicted CFC-12 concentrations in the unoxidised Till and rise in CFC-12 values in the unsaturated Chalk beneath the Till likely reflect the existence of groundwater recharge round the Till edge bringing more modern water (and air) into the system together with fluctuations in the water table. At 20 metres, the observed data contains roughly 15% modern air when compared with the model.

### 4.3. Conceptual Model Development

The groundwaters show considerable variability both in water type and in apparent residence time. However, a pattern can be discerned (Fig. 6) which suggests that two groundwaters of different origins are present. The first type includes the Chalk groundwaters from the interfluvial at distances greater than 1 km from the edge of the till sheet. These have low nitrate (<0.2 mg/l N) and appear to be relatively old waters (proportion of modern water <15% as indicated by CFC measurements).

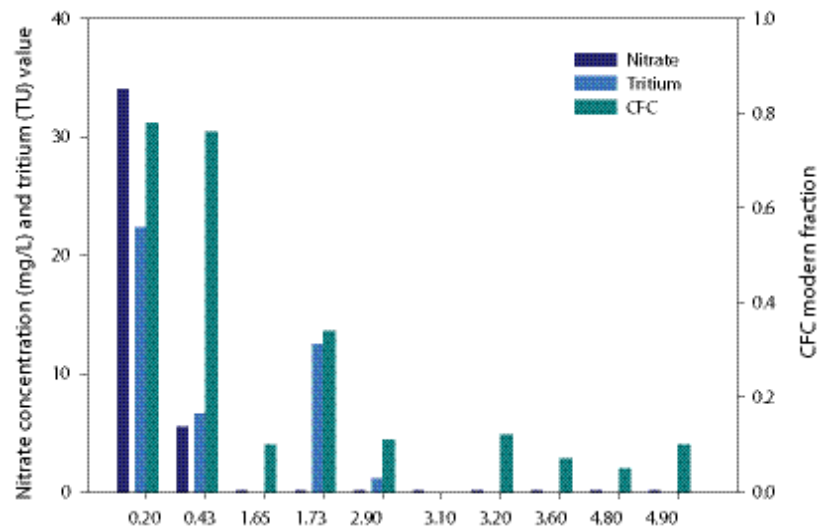


FIG. 6. Concentrations of several groundwater tracers along the cross-section as shown in Fig. 3

The second water type occurs within the main river valleys and beneath the edge of the till sheet. These groundwaters, which have high nitrate concentrations, are of modern origin (proportion of modern water >70% according to CFCs) and are largely derived from rainfall of the last few decades.

It is postulated that there are also two distinct groundwater flow systems in the Chalk aquifer and more than one recharge mechanisms (Fig. 7). One groundwater system is represented by the relatively old groundwaters present beneath the interfluvial. Here, the aquifer is confined (or semi-confined) and recharge occurs mainly as slow leakage through the till. Discharge from this aquifer system is limited by the low transmissivity of the Chalk and occurs as lateral flow into the more transmissive Chalk of the river valleys. Rapid infiltration to the Chalk occurs at the margins of the till sheet because fracturing in the till is better developed. The bulk of recharge beneath the interfluvial occurs as slow 'piston flow', allowing time for diffusional exchange to occur between infiltration and till porewaters.

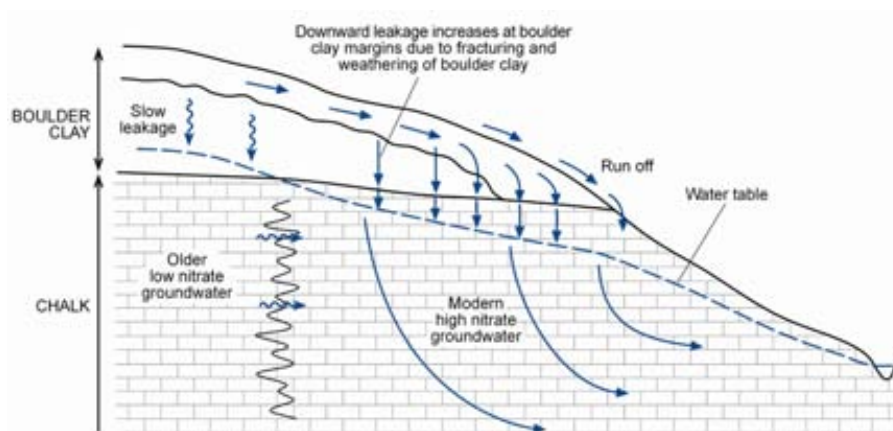


FIG. 7. Conceptual model showing enhanced recharge to the Chalk occurs where fracturing and weathering develops at the edge of the till sheet.

## 5. CONCLUSIONS

The conceptual model of the Chalk-till system developed as a result of this study indicates that the till has a major impact on recharge. The Chalk groundwaters beneath the valley and till edge are very different; they have a large component of modern water and generally high nitrate concentrations. The groundwaters beneath the interfluvium do have a small modern component; CFC concentrations in these groundwaters suggest that this could be up to 15%. Data from the gas samplers when compared with a 1-D transport model seem to support this. These results show that the Till layer attenuates nitrate concentrations in groundwater by restricting the downward movement of recharging rainwater and promoting denitrification both in terms of redox conditions and time of exposure to them. Some water movement clearly occurs via preferential 'by-pass' flow paths.

## REFERENCES

- [1] PRICE, M., MORRIS, B.L., ROBERTSON, A.S., A study of intergranular and fissure permeability in Chalk and Permian aquifers, using double-packer injection testing, *J. Hydrol.* **54** (1982) 401–423.
- [2] DARLING, W.G., BATH, A.H., A stable isotope study of recharge processes in the English Chalk, *J. Hydrol.* **101** (1988) 31–46.
- [3] PRICE, M., LOW, R.G., MCCANN, C., Mechanisms of water storage and flow in the unsaturated zone of the Chalk aquifer, *J. Hydrol.* **233** (2000) 54–71.
- [4] GOODDY, D.C., BLOOMFIELD, J.P., CHILTON, P.J., JOHNSON, A.C., WILLIAMS, R.J., Assessing herbicide concentrations in the saturated and unsaturated zone of a Chalk aquifer in Southern England, *Ground Water* **39** (2001) 262–271.
- [5] FOSTER, S.S.D., MILTON, V.A., The permeability and storage of an unconfined Chalk aquifer, *Hydrol. Sci. Bull.* **19** (1974) 485–500.
- [6] PRICE, M., DOWNING, R.A., EDMUNDS, W.M., „The Chalk as an aquifer”, *The hydrogeology of the Chalk of north-west Europe* (DOWNING, R.A., PRICE, M., JONES, G.P., Eds ), Clarendon Press, Oxford (1993) 35–58.
- [7] LLOYD, J.W., HARKER, D., BAXENDALE, R.A., Recharge mechanisms and groundwater flow in the Chalk and Drift deposits of southern East Anglia, *Q. J. Eng. Geol.* **14** (1981) 87–96.
- [8] GERBER, R.E., BOYCE, J.I., HOWARD, K.W.F., Evaluation of heterogeneity and field-scale groundwater flow regime in a leaky till aquitard, *Hydrogeol. J.* **9** (2001) 60–78.
- [9] KLINCK, B.A., BARKER, J.A., NOY, D.J. WEALTHALL, G.P., Mechanisms and rates of recharge through glacial till: Experimental and modelling studies from a Norfolk site, *British Geological Survey Technical Report WE/96/1* (1996).
- [10] MOSELEY, R., PARKER, J.M., BRUCE, B.A., CHURCH, F.M., *Hydrogeological map of southern East Anglia*, Institute of Geological Sciences (1981).
- [11] MARKS, R.J., The sand and gravel resources of the country around Clare, Suffolk: description of 1:25 000 resources sheet TL74, *Mineralogical Assessment Report Institute of Geological Sciences*, No. 97 (1981).
- [12] KLINCK, B.A., HOPSON, P.M., LEWIS, M.A., MACDONALD, D.M.J., INGLETHORPE, S.D.J., ENTWISTLE, D.C., HARRINGTON, J.F., WILLIAMS, L., *The hydrogeological behaviour of the Clay with Flints of southern England*, *British Geological Survey Technical Report*, WE/97/5 (1997).
- [13] OSTER, H., SONNTAG, C., MUNNICH, K.O., Groundwater age dating with chlorofluorocarbons, *Water Resour. Res.* **37** (1996) 2989–3001.
- [14] MARTIN, G.E., SNOW, D.D., KIM, E., SPALDING, R.F., Simultaneous determination of argon and nitrogen, *Ground Water* **33** (1995) 781–785.
- [15] GOODDY, D.C., CLAY, J.W., BOTTRELL, S.H., Redox-driven changes in pore-water chemistry of the Chalk unsaturated zone beneath unlined cattle slurry lagoons, *Appl. Geochem.* **17** (2002) 903–921.
- [16] COOK, P.G., SOLOMON, D.K., Transport of trace gases to the water table: Implications for groundwater dating with chlorofluorocarbons and krypton 85, *Water Resour. Res.* **31** (1995) 263–270.
- [17] DARLING, W.G., KINNIBURGH, D.G., GOODDY, D.C., “Gas composition and processes in the unsaturated zone of the Chalk and Triassic Sandstone aquifers, England”, *Isotope Techniques In The Study Of Environmental Change*, IAEA, Vienna, Austria (1997) 265–274.

# USE OF ISOTOPES FOR THE STUDY OF POLLUTANT BEHAVIOUR IN THE UNSATURATED ZONE AT THREE SEMI-ARID SITES IN THE USA

R.L. MICHEL, J.A. IZBICKI, P.B. MCMAHON, D.A. STONESTROM  
US Geological Survey,  
Reston, Virginia, USA

## ABSTRACT

As part of the International Atomic Energy Agency CRP on movement of pollutants through the unsaturated zone, three areas were examined in the United States. The three areas were: 1. A radioactive waste disposal site near Beatty Nevada. 2. The Upper Mojave Desert in Southern California. 3. The High Plains Aquifer (HPA) in the mid-continental area of the country. All sites were in arid to semi-arid locations with deep (>30 meters) unsaturated zones. Tritium results from all three sites indicate that recharge is focused and not an areal phenomena. Typically, in arid sites, ephemeral streams seem to be locations of focused recharge. It is also evident that lateral movement is an important part of movement of liquid, solutes, and gasses through the unsaturated zone. Models should be at least two dimensional to correctly represent this movement. The use of CFCs in the unsaturated zone can help in constructing these models. The studies in the HPA have shown that the onset of irrigation has mobilized naturally-occurring salts and moved them toward the water table. Due to the depth to the water table in the HPA, these salts have not yet entered the groundwater in most locations. At present, large quantities of both natural and agricultural chemicals are stored in the unsaturated zone and the potential exists for increased contamination from these chemicals in future years if this movement continues. In the case of the HPA, the switch from flood to sprinkler irrigation has slowed the movement of these contaminants. There is very little evidence of mitigation of agricultural contaminants below the root zone. Some reactions may occur at the saturated/unsaturated zone interface but it does not seem to have a major impact on chemical concentrations.

## 1. INTRODUCTION

Recharge of the world's aquifers mostly occurs through the unsaturated zone (UZ) [1]. For proper management of aquifer resources it is important to know the location and rate of recharge. This Coordinated Research Program wanted to investigate the application of isotopes to meet several objectives in UZ research:

1. Determine the best strategies for determining the location of recharge and outline methods of determining the recharge rate through the UZ.
2. Determine the transport processes that are important for movement of pollutants in the unsaturated zone. This included the determination of potential reactions in the depths between the root zone and the water table and how they alter the concentrations of solutes. Of particular interest were changes in the concentrations of common contaminants such as nitrate, heavy metals and organic pesticides/herbicides. Determine whether reactions in the unsaturated zone only occurred in the root zone and the Saturated/Unsaturated Interface Region (SUIR) which lies at the top of the water table, or can occur at other depths under proper circumstances. In the SUIR conditions exist that allow reactions to modify the unsaturated zone chemistry, i.e. the presence of water and oxygen. However, the question of whether the SUIR is the only active region for chemical reactions in the UZ has yet to be determined.
3. Study the transport of gasses through the unsaturated zone. Occasionally contaminants can move as gasses through the UZ although this is probably not a common method of aquifer contamination. A more important issue is that many gasses are used for age-dating of waters beneath the UZ. One of the major issues that have caused problems for hydrologists is the initial-value problem which is crucial in determining what groundwater dates mean in terms of real years. This is particularly true for carbon-14 but is also an issue for chlorofluorocarbons (CFCs) and other transient age-dating techniques. Another issue related to gas movement is the release of certain gasses ( $N_2O$ ) which are probably formed in the UZ. Some of these gasses, which are greenhouse gasses, could have climatic impacts. It is important to know what the rates of formation are for these gasses in the UZ and how rapidly they can exit the UZ to the atmosphere.

## 2. SITES

During the CRP, the United States group has been involved with three sites where unsaturated zone processes have been studied. They are: 1. The Amargosa Desert Research Site (ADRS) near Beatty, Nevada. 2. The Upper Mojave Desert, near Victorville, California. 3. The High Plains Aquifer with sites in Texas, Kansas, Nebraska, and Colorado. All three sites can be considered arid or semi-arid.

### 2.1. Amargosa Desert Research Site

The ADRS (Fig. 1) is located next to a low-level nuclear waste depository in an arid region with a deep unsaturated zone (<http://nevada.usgs.gov/adrs>). Basic hydrologic studies started in the late 1970s and more recently were expanded to include contaminant transport. In the late 1980's, intensive sampling of isotopic concentrations began. Information on contaminant migration comes from an array of shallow gas-sampling tubes (less than two meters deep), two vertical arrays of deeper tubes in grouted boreholes (up to 109 m deep), core samples, ground-water sampling wells, and plant-water studies. An instrumented site approximately 3 km away from the disposal area serves as an uncontaminated control. Studies at the ADRS have been primarily focused on lateral transport of contaminants from the waste site into the adjacent UZ and to the water table. Gas samples from the shallow UZ and plant-water samples were analyzed for tritium, hydrogen, and volatile organic compounds (VOCs). Gasses from the deep UZ were analyzed for tritium,  $^{14}\text{C}$ , and VOC's. Core samples from the deep UZ (to 110 m) were analyzed for tritium, stable isotopes of water, and salts.

### 2.2 Upper Mojave Desert

Ten unsaturated zone cores were collected at the Upper Mojave Desert site (Fig. 2). Five sites were in the channel of the Oro Grande Wash, a beheaded ephemeral stream that has a constrained channel. Flow only occurs after rain storms or following snow melt and usually halts within one to two days. Sites were selected at the upper, middle and lower (3 cores) part of the wash. A control site was selected a few meters outside of the channel at the lower site and another control site was located above the head of the stream. Three additional sites were selected in Sheep Creek Wash, a stream which tends to meander more, especially at the lower part of the wash.

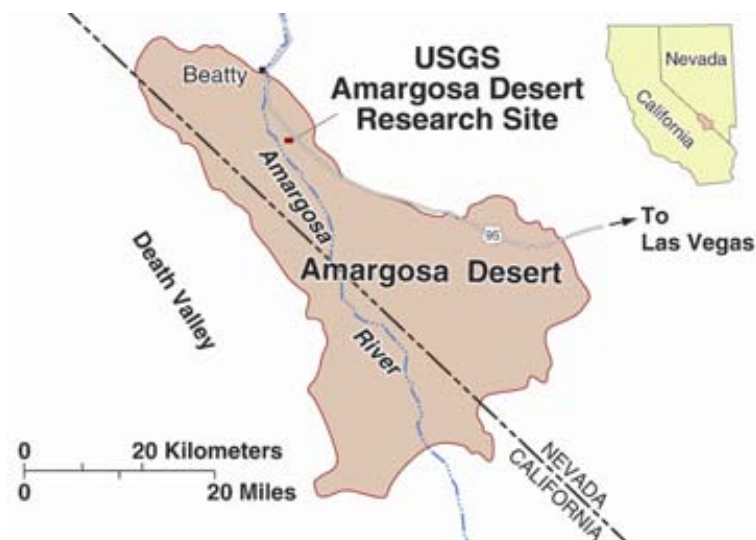


FIG. 1. ADRS site near Beatty, Nevada. Site is adjacent to a low-level radioactive waste disposal site.

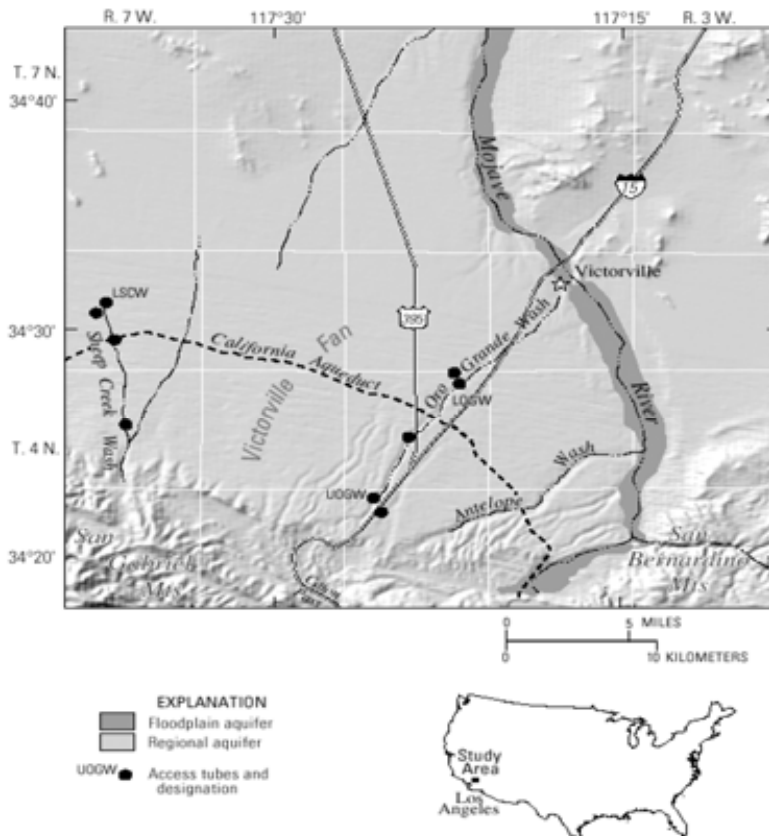


FIG. 2. Location of sampling sites for Upper Mojave Desert sampling program. Three soil cores were collected within Oro Grande Wash and Sheep Creek Wash. Two control sites on the fan were also cored.

A control site outside of the wash was also collected at the lower part of this wash. The water table is 100–200 meters deep at these locations. This program focused on looking at preferential recharge in arid areas for two reasons: 1. Determine the water balance of the groundwater table under the upper Mojave Desert. 2. Determine an appropriate site to use for artificial recharge. Stable isotopes of water, tritium and salts were analyzed in the soil water in the unsaturated zone. Physical properties of the unsaturated zone minerals were also analyzed. CFCs and CO<sub>2</sub> were analyzed in unsaturated zone gasses at most sites.

### 2.3 High Plains Aquifer

Nine cores were collected in the High Plains aquifer system in the Great Plains of the United States (Fig. 3). A control site and two sites under or close to irrigated fields were chosen in the Southern High Plains (Texas), the Central High Plains (Kansas) and the Northern High Plains (Colorado and Nebraska). The control sites were located on rangeland which had never been used for agriculture. The cropland sites had originally been dry-land farmed, but flood irrigation was started in the 1950s. Sprinkler irrigation had replaced flood irrigation at all sites by the 1990s. There have been significant declines in the water table depth at all irrigated sites during the past 40 years. There has been very little change in water table levels under the rangeland sites.

Cores were analyzed for nitrate and other salts, pesticides and herbicides, tritium, stable isotopes of water and nitrate, and physical properties of the minerals. Groundwaters were analyzed for chemicals and isotopes at all sites as well. Gas ports were installed at selected depths at all sites and pore gasses were analyzed for CFCs, N<sub>2</sub>O, and CO<sub>2</sub> at all sites and <sup>14</sup>C at two sites in the Northern High Plains.



FIG. 3. High Plains Aquifer study area. Three cores, one from a rangeland site and two from irrigated sites, were collected in the Northern, Central, and Southern sites.

### 3. METHODS

Boreholes at all sites were installed using an air hammer drilling method [2, 3]. This avoided the use of drilling fluids and prevented contamination of the cores with extraneous water. Thus, water samples could be collected from the cores for analysis of pore fluids for isotopic concentrations. Core liners were used and the cores were divided in the field into sections between 0.2–0.5 meters long while still in the core liner using a method developed by the Yucca Mountain Project [4]. The section of liner was then capped at both ends and sealed in a aluminum pouch by an iron to avoid any exchange of moisture before analyses. The sealed samples were then returned to the various laboratories for analyses.

Water for tritium was extracted using a vacuum distillation procedure. The soil samples (about 500–1000 gms) were placed in a vacuum oven and extracted at a temperature of about 80°C into a trap of dry ice and propanol. The amount of liquid extracted depended on the moisture content of the core, but generally ranged from a few mL to 200 ml of water. If sufficient water was available (>25 ml), the samples were then electrolyzed to enrich the tritium concentrations [5] and the residual water was then counted by liquid scintillation counting. Samples that were too small to enrich were counted directly to obtain tritium concentrations. The precision of the measurement was dependent on the amount of water extracted from the core. Stable isotopes of water were measured in the same core from which tritium samples were extracted. A separate sample of about 200 gms of core was deposited in a boiling flask and covered with xylene. The flask was hooked up to a reflux condenser and an azeotropic distillation was carried out [6]. The distillation continued until all the water was removed (typically ~2 hours). The water, which is denser than xylene, was collected in a side flask during the distillation, and then drained off into a holding flask. Paraffin was used to remove the last of the xylene from the water prior to analyses for stable isotopes. Deuterium concentrations were measured using the zinc reduction method and  $^{18}\text{O}$  concentrations were measured using the carbon dioxide equilibration method.

## 4. WATER MOVEMENT

Normally, there is expected to be very limited movement of water through the UZ in arid and semi-arid areas. Recharge by this process has been thought to be minimal in most arid regions. However, work in the last decade [7–10] has indicated that recharge is frequently focused in selected areas in these types of terrain. Thus, studies of recharge in these sites require an understanding of the topography to determine the most likely sites where recharge occurs.

### 4.1. *Armagosa Desert Research Site*

The locations studied at the ADRS were all areas where there was expected to be no recharge. The site had been originally selected as a low-level waste site in the early 1950s on the assumption that no movement occurred toward the water table and the contaminants would be well contained. No evidence of recharge was found at any of the boreholes although recharge occurs beneath near an ephemeral channel 2.5 km away [11, 12].

### 4.2 *Upper Mojave Desert*

The work in the upper Mojave Desert was directly focused on the extent of recharge at the ephemeral streams within the basin. It was thought that there was very little recharge in the upper Mojave Desert under the current climatic conditions except for the occurrence of bank recharge adjacent to the Upper Mojave River. However, carbon-14 measurements of groundwater and flow models indicated that there must be another source of recharge somewhere within the upper desert. It was suspected that certain ephemeral streams in which water only flows immediately after large storms would be the most logical locations for recharge. Unsaturated zone cores were collected in two ephemeral streams to determine if recharge was occurring in these sites. Wells were drilled at three locations near the streams as control sites. Tritium measurements showed that almost no recharge occurred at the control sites. Measurements of salt showed that for the two sites in the desert a large chloride peak was located just below the root zone indicating several thousand years of salt build up (Fig. 4). In such situations, it has been found that chloride accumulation is a better indicator of recharge than tritium or  $^{36}\text{Cl}$  [13]. Using the chloride method, it was determined that recharge was not occurring at these two control sites. All sites located within the ephemeral streambeds showed that tritium migrated into the UZ to a deeper depth than that found at the control sites. Typical penetration depth for tritium at the control sites was about 5 meters, similar to the depth of the chloride peak, which is the presumed depth of the root zone influence. The tritium penetration in the streambed varied from site to site but was deeper than the control sites at all locations. Deepest penetration was found at the Middle Oro Grande site where tritium was present at over 30 meters depth giving a recharge rate of about 4 cm/yr (Fig. 4). Recharge rates were much lower at the Sheep Creek sites than in Oro Grande Wash, probably due to the fact that the stream tends to meander. Total recharge throughout the breadth of this wash may be similar to that of Oro Grande Wash, but it is spread out over a wider channel.

Chloride concentrations generally reflected the fact that recharge was occurring in these stream beds. There was no chloride peak close to the size of those found at the control sites. In the case of Upper and Middle Oro Grande Wash, chloride concentrations were low throughout the depth profile, indicating little accumulation. The Lower Oro Grande Wash displayed a complex pattern for both tritium and salt, indicating a complex recharge process at this location (Fig. 4). A salinity maximum was found at about 25 meters, which is below the depth where chloride accumulation would be expected to occur due to evaporation. Tritium was found in pore waters both above and beneath this chloride maximum, but not found in the pore water within the maximum [9]. This is an indication that water can move laterally and circumvent some aquitard layers if they are not laterally extensive. Temperature probes were installed at all sites to compare changes in temperature with the tracer data. These probes indicate changes in temperature which are due to colder water flowing past them during recharge events [14]. The control sites showed the highest average temperature and no changes in temperature during winter, indicating no recharge. All sites where tritium had penetrated beneath about 5 meters also showed temperature variations during the winter. This change was related to recharge of colder winter precipitation through these sites. Thus, temperature probes of this nature are a valuable asset in determining where recharge is occurring. Using this information, the determination for placement of sites for UZ cores and more extensive studies can be made.

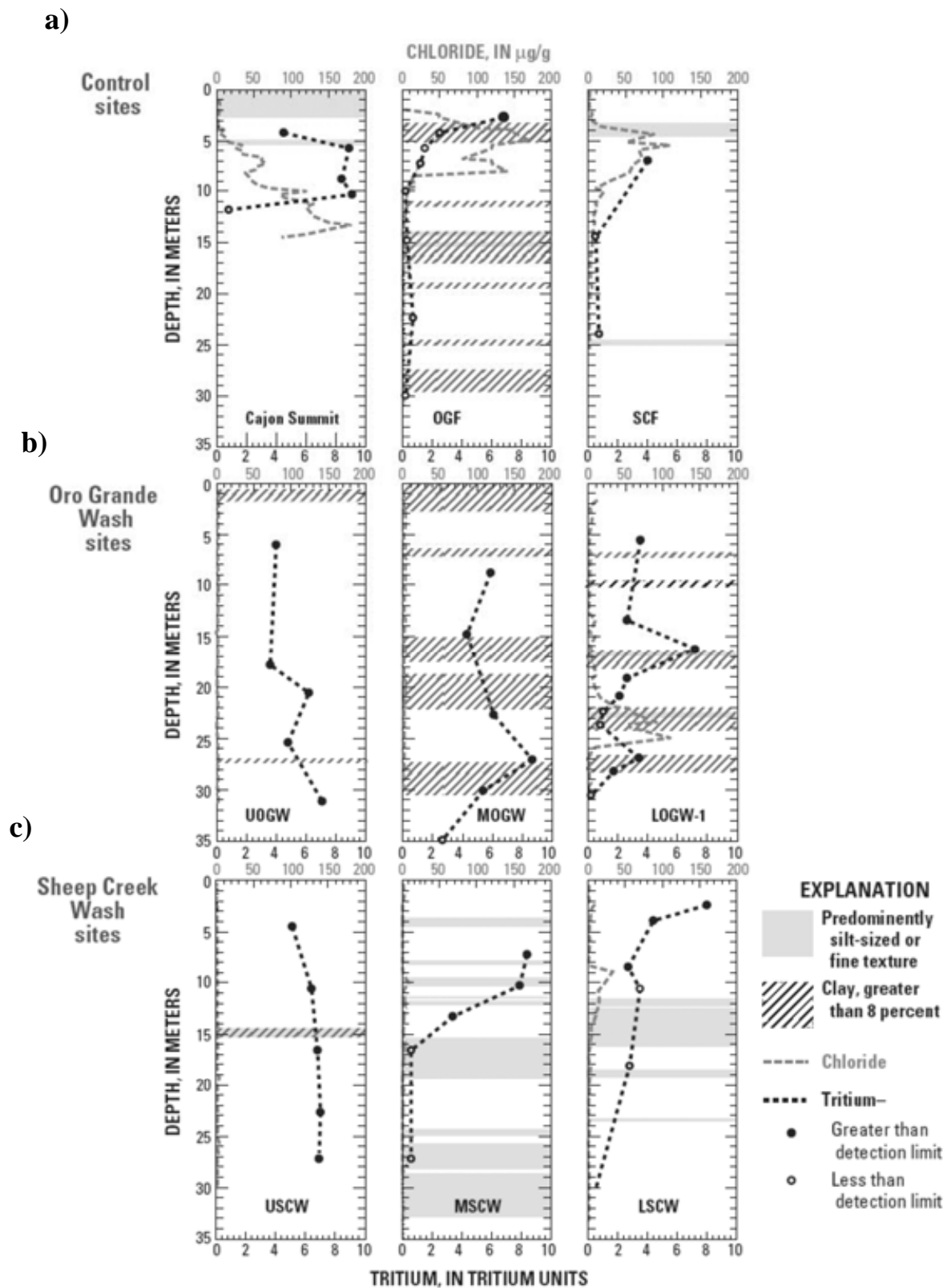


FIG. 4. Tritium and chloride concentrations from soil cores collected during the Upper Mojave Desert study. At the control sites (a), tritium does not penetrate below a large chloride peak present at about 5 meters. Tritium penetration is greater at sites within the Oro Grande Wash (b) and Sheep Creek Wash (c). The tritium and chloride pattern at LOGW shows a complex pattern with tritium occurring beneath a salinity peak with no tritium. This indicates that lateral movement is a significant factor at this site and probably others.

Stable isotopes were measured in all cores. The results from the Oro Grande Wash showed an evaporative effect for samples near the surface. Water at lower depths showed some variation, probably due to local processes. The one major change was at Middle Oro Grande Wash where at 100 m, a major shift in isotopic concentration occurred which was originally interpreted as due to a climate change. As indicated in the section on gas processes, this was later concluded to be incorrect. Data from the control site showed a strong evaporative signal at the surface. At lower depths, it appears that no recent precipitation is present reinforcing the view that no recharge is currently occurring. The samples from Sheep Creek were too low in water content to give reliable stable isotopes results in many cases.

### 4.3 High Plains Aquifer

Part of the rationale behind the work on the High Plains Aquifer was to observe the difference in recharge and solute movement when prairie land is converted to agricultural use. A control site and two sites where irrigation was practiced were selected at each of the three locations to study these differences. The only control site where significant recharge was taking place at occurred in the Northern High Plains (Fig. 5). Here a significant tritium maximum, presumably due to tritium bomb peak waters from the 1960s, was found at about 12 meters. At the two control sites in the Central and Southern High Plains, very little if any recharge occurs under the current climatic conditions. Flood irrigation was started at the irrigated sites in the 1950s at most sites, followed by a switch to sprinkler irrigation in the late 1980s and 1990s. It is clear from tritium data that post-bomb water has moved into the deep unsaturated zone at all irrigated locations. Recharge rates are difficult to access since the profiles do not exhibit a simple pattern. This is possibly due to the interspersing of precipitation tagged with post-bomb tritium and irrigation water which initially had no tritium. At one location on a core from Kansas, a highly evaporated  $^{18}\text{O}$  signal is contained in a section of the core that is tritium-free. This is likely water from flood irrigation that was evaporated but went into the unsaturated zone prior to gaining significant tritium via exchange. The tritium interface method was used to estimate recharge in irrigated sites at all locations. In the Southern and Central High Plains sites, it was also possible to use the presence of a chloride peak in the sub-surface to estimate recharge. It was assumed that this chloride peak had originally been near the surface prior to irrigation and was displaced downward during irrigation. The fact that the chloride peak still existed in the unsaturated zone indicated that recharge water from the irrigation period had not yet reached the water table. This verified the fact that the tritium interface had also not yet reached the water table. Both the chloride and tritium interface method gave similar recharge rates and indicated that irrigation water had not yet reached the water table at most sites.

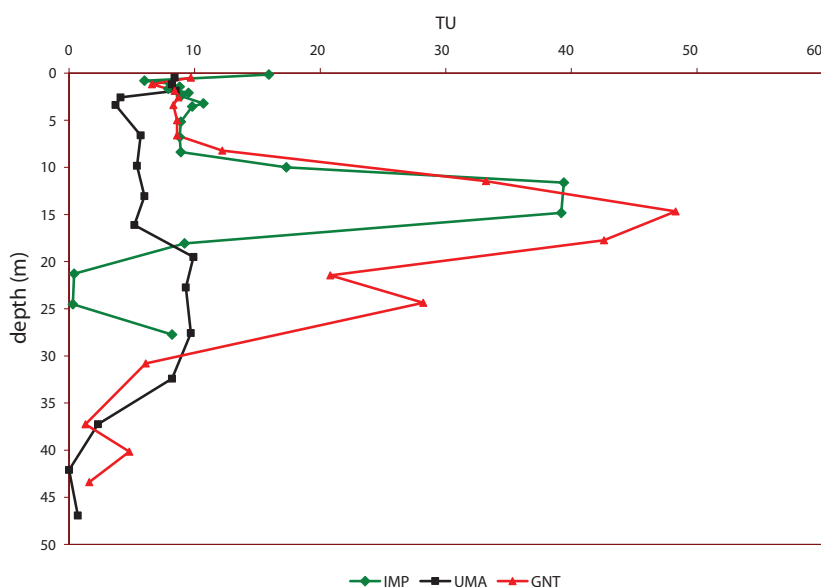


FIG. 5. Tritium concentrations from a control site (IMP) and two irrigated sites in the Northern High Plains Aquifer.

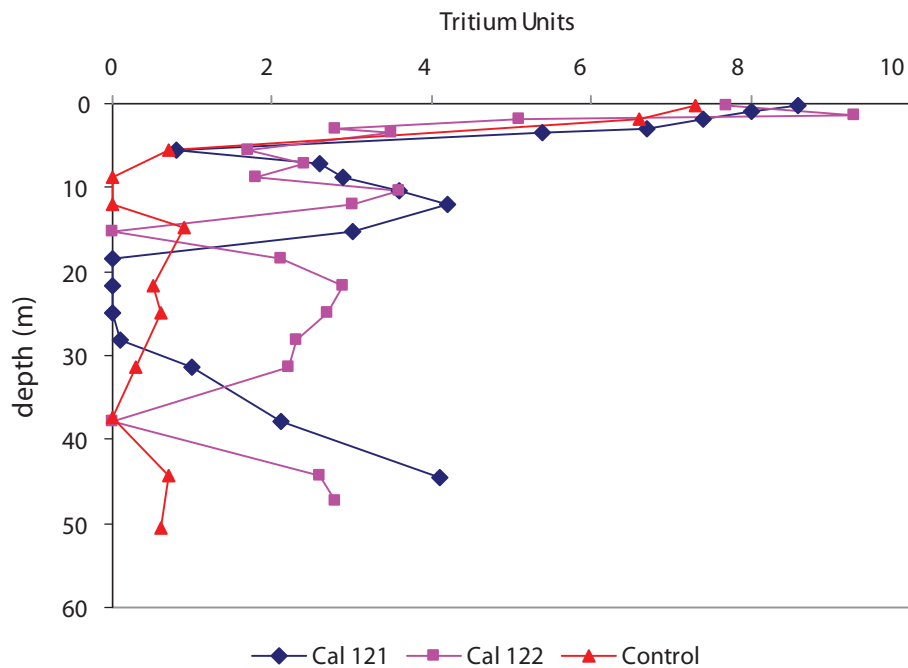


FIG. 6. Tritium concentrations in three cores from the unsaturated zone for the Central High Plains Aquifer in Kansas. The two irrigated sites show significant tritium concentrations near the water table. This is likely due to the residual water left from groundwater as the water table drops. The groundwater has been increasing in tritium concentration with time so the tritium concentrations increase with depth.

Many groundwaters under the irrigated sites contain tritium indicating that some recent recharge is occurring somewhere in the vicinity. No irrigation site seemed to show tritium concentrations throughout the core, indicating that recharge is not occurring at these locations. There are undoubtedly locations within the area where preferential recharge occurs [15]. Unlike the work in the Mojave Desert, the sites in this study were not chosen to look for preferential recharge here. There are also indications of tritium being present in the UZ above the water table below the bomb-tritium interface. This is particularly clear at the Central High Plains sites where tritium is found to be present below zones of no tritium (Fig. 6). In these cases the tritium is present at depths that were below the original water table. This suggests that the tritium is the result of retreating groundwater that had already been tagged with bomb tritium. As can be seen in Fig. 6, tritium concentrations increase with depth in some cases, indicating an increase in the tritium concentrations with time in the groundwater that is recorded in the pore waters above the retreating water table.

## 5. POLLUTANT MOVEMENT

Two of the projects were undertaken to study pollutant movement in the unsaturated zone: 1. The ADRS site in Beatty Nevada studied transport of radionuclides away from the containment area through the unsaturated zone. 2. The work on the High Plains Aquifer was studied movement of agricultural contaminants through the unsaturated zone. These studies were to determine how the contaminants were able to move through the unsaturated zone and whether chemical reactions within the unsaturated zone could impact concentrations. It had been postulated [16] that no reactions occurred at any location in the unsaturated zone except the root zone and the Saturated-Unsaturated Interface Region (SUIR).

### 5.1 Armagosa Desert Research Site

The work at ADRS has shown that tritium and carbon-14 can migrate laterally away from the waste site on decadal timescales (Fig. 7). Most unsaturated zone studies concern themselves exclusively with

vertical migration, but the work at Beatty shows that lateral transport can be dominant where a point source, such as the waste depository, exists. Other pollutants transmitted from the site include various volatile organic compounds. There is no evidence of the migration of non-volatile substances away from the waste site. Thus, it is likely that the transport of tritium and carbon-14 are primarily gas/vapor processes. These transport processes seem to prefer to move along geological strata, with the greatest movement found in coarse gravel layers at about 1.5, 24 and 48 meters below land surface. These layers provide preferential pathways for gasses leaving the waste containment site. While modeling of gas flow has been able to explain the transport of carbon-14 away from the site, tritium cannot be moved by vapor processes in the concentrations and distances seen [17]. It is possible that some other mechanism is involved which moves tritium primarily in a gaseous form but a potential mechanism has not been identified as yet.

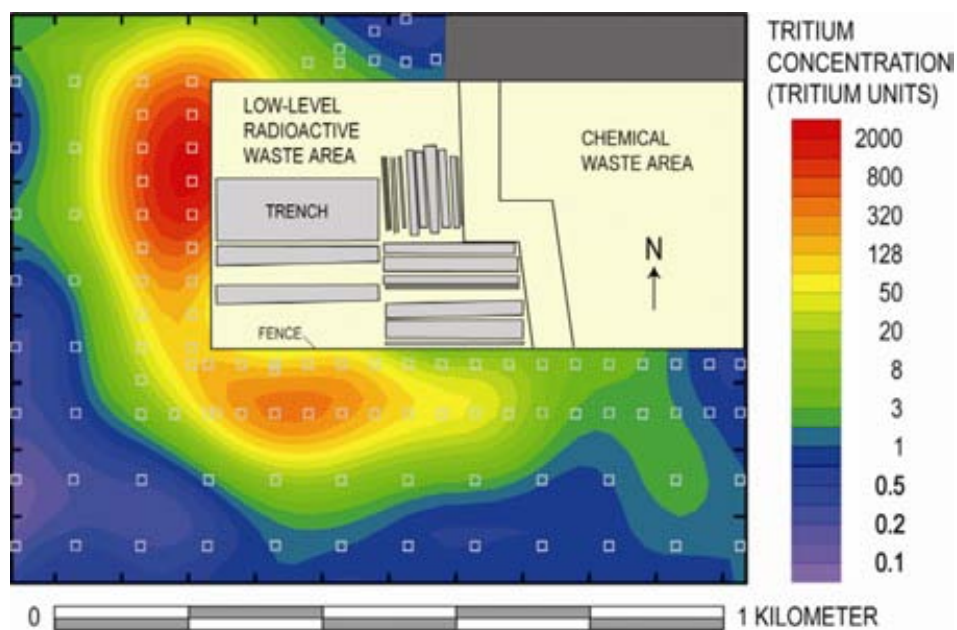


FIG. 7. Lateral spreading of tritium at the ADRS [19].

## 5.2 High Plains Aquifer Sites

The work in the High Plains Aquifer has focused on the movement of herbicides, pesticides and salts through the unsaturated zone. In particular, the differences in rate of migration between irrigated and non-irrigated (control) sites were studied. It was also of interest to see if any reactions changed nutrient concentrations in the unsaturated zone. All three control sites showed no herbicides or pesticides in the unsaturated zone nor were they found in the aquifer under the site. Very high nitrate was found near the surface at the central control site in Kansas ( $>200 \mu\text{g-N/g}$ ). It is known that nitrate can accrue in near surface layers in arid soils and presumably this peak was derived by these types of processes [18]. Below the peak the nitrate concentrations in pore water dropped to close to  $0 \mu\text{g-N/g}$ . The other two control sites had concentrations near 0 throughout the unsaturated zone column and there was no near surface nitrate peak present. As recharge is occurring at the control site in the Northern High Plains (Fig. 5) it is probable that the nitrate has not been able to accumulate prior to its movement out of the surface zone at this location. Nitrate concentrations in groundwater at the control sites were low ( $0.9\text{--}2.4 \text{ mg-N/L}$ ) with concentrations increasing south to north. Chloride peaks did appear at the control sites for the Southern and Central High Plains indicating some accumulation and very low recharge rates.

At the irrigated sites, nitrate concentrations were found in the range of several  $\mu\text{g-N/g}$  throughout the soil columns. This is a clear indication that some of the nitrate applied to the field has been transmitted

through the soil layer to lower depths in the unsaturated zone. Also, no peaks of nitrate or chloride were found near the surface at the cropland sites. In some cases the chloride peak appears to exist further down in the subsurface and this lower peak has been used to estimate recharge rates. The recharge estimate is based on the assumption that the chloride peak was close to the surface prior to irrigation, and moved downward with the irrigation front. The depth that it is presently located, coupled with the amount of water present above the peak and the time since the onset of irrigation, can be used to estimate recharge [15]. Recharge rates very similar to those found by the tritium interface method were obtained.

In one Kansas core, a nitrate peak was also observed in the subsurface. N-15 measurements on this peak indicate that the nitrate in the peak originated from soil nitrification processes and not from fertilizer. This peak is likely the nitrate that was present in the shallow sub-surface in natural conditions. The onset of irrigation has resulted in a large quantity of nitrate and other chemicals being moved from the near surface layer into the unsaturated zone above the water table. The nitrates in the unsaturated zone can have either a natural source or an agricultural source, and isotopes can occasionally be used to differentiate the sources. At the present time, it appears that the nitrate and chloride that accumulated naturally here has not yet been transmitted to the water table at the irrigated sites. Thus, these are non-agricultural chemicals that have been mobilized by irrigation. They are potential contaminants that could make their way into the groundwater within the next few decades depending on irrigation practices.

Pesticides and herbicides have also been measured in the soils and groundwaters at these sites. The control sites have very little or no measurable organic contaminants, as no application of these chemicals at these locations was ever carried out there. There is also very little organic contamination between the root zone and the water table at any site. Most organic contaminants found at irrigated sites are in the upper two meters of the core, i.e. within the soil zone. They are strongly absorbed here and probably tend to be degraded before they can make their way into the UZ. Thus, there appears to be very little transmission of these contaminants through the UZ. However, some of these organics are found at the water table, indicating that another more direct pathway must exist for their movement into groundwater. These contaminants must enter the water table in areas where preferential recharge is occurring and not at the sites studied in this program.

## **6. UNSATURATED ZONE GASSES**

The CRP was asked to study the movement of gasses through the unsaturated zone, and possible production of gasses within the UZ and at the SUIR. Of particular interest is how the gas concentrations just above the water table relate to concentrations in water at the water table surface, occasionally referred to as the initial value problem for gas tracers such as  $^{14}\text{C}$ . Unfortunately, funds were not available to measure the carbon-14 concentrations in the unsaturated zone at most sites. Thus, for carbon-14, we were unable to answer this question. However, at all sites, measurements were carried out for CFCs and at the High Plains Aquifer sites measurements of  $\text{N}_2\text{O}$  were obtained.

### ***6.1 Armagosa Desert Research Site***

This site had high concentrations of several CFCs used for decontamination in the nuclear industry and co-disposed with radioactive waste. The main radionuclide contaminants found in unsaturated zone gasses at the site are carbon-14 and tritium. As noted above, it is clear that lateral transport is the dominant mechanism for pollutant migration at this site (Fig. 7). Lateral movement of gasses is often ignored on the assumption that only vertical transport is significant, and most studies focus on vertical profiling. This has generally been based on the assumption that the source function was horizontally constant. However, lateral migration can be rapid and this process furnishes a mechanism for gasses to bypass impervious lenses through which little or no vertical transmission would be expected. This has important implications for the work in the Upper Mojave Desert described below.

## 6.2 Upper Mojave Desert

CFCs were measured at all sites in the Mojave Desert study. In general, there was very little difference in concentrations between control sites and recharge sites. As the recharge is limited even in the recharge sites, it can be expected that concentrations should be similar with depth if soil properties and tortuosities are similar [20]. Using a one dimensional model developed by Weeks et al. [21], we were able to successfully model most of the gas distributions in the Upper Mojave Desert using reasonable porosities and tortuosities. The only exceptions were gas concentrations at 150 meters at Middle Oro Grande where essentially no CFCs were present (Fig. 8). This contrasted with concentrations at Middle Sheep Creek where CFCs were present at 150 meters depth in concentrations expected for the anticipated tortuosities. It was postulated that a layer exists where tortosity is so high that gasses can not migrate below it on a timescale of a few decades. A check of the physical properties of the core indicated that no layer existed which was significantly different than layers higher in the core or in other cores. However, as noted in the section on water transport, a shift is noticed in stable isotopes below 100 meters that had originally been attributed to climatic shifts (Fig. 9). It is now suspected that a layer at below 100 meters is impermeable to both gas and liquid movement. Layers physically similar to this layer in the core occur at other depths and apparently do not inhibit gas movement. It has been postulated that the lateral extent of this layer is much greater and thus, unlike in the other locations, the gasses cannot simply flow around it in a reasonable timescale. Thus, the ability of gasses to move laterally helps to mask small layers that would normally be impervious to gas transport.

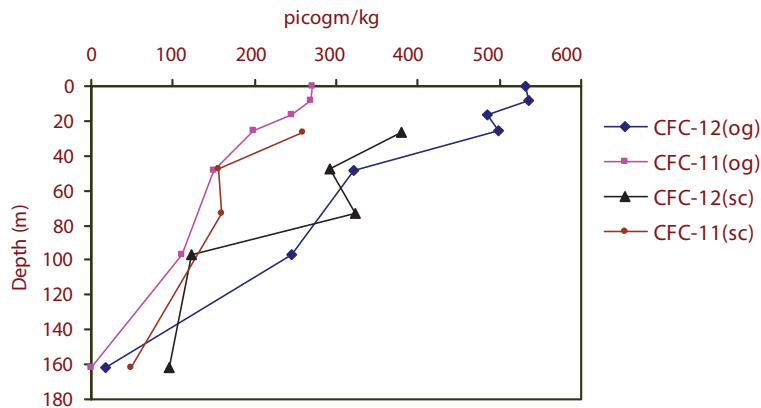


FIG. 8. Comparison of CFC concentrations in pore gas from Middle Oro Grande Wash and Middle Sheep Creek Wash.

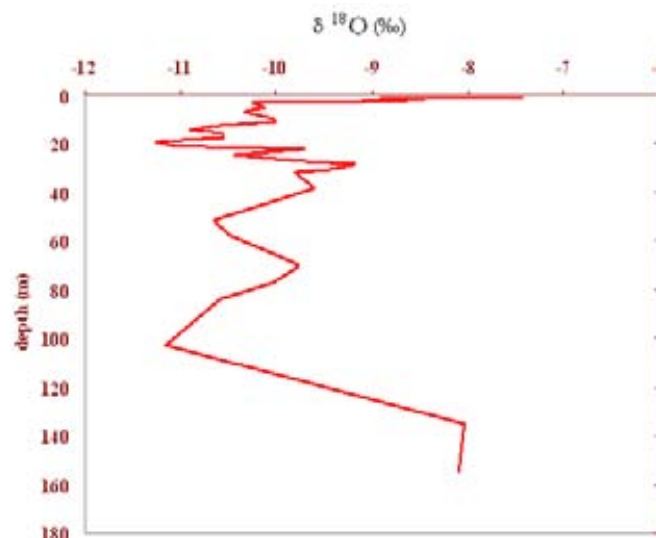


FIG 9. Oxygen-18 data from Middle Oro Grande Wash. Note the major shift in concentrations below 100 meters coincident with the sharp drop in CFCs seen in Figure 8.

As one of the goals of this program was to find locations for banking of imported water (i.e. storing of water for future use in groundwater), it is clear that this site would not be suitable for such a function. This could not have been noticed from tritium measurements as that isotope had not penetrated to this depth. Tritium concentrations at shallower depths indicated recharge was occurring in the upper layer of the site. Only stable isotopes, which were subject to different interpretations without the gas data, indicated a significant shift below 100 meters. Thus, CFCs should be considered an important component in studies of the UZ.

### **6.3 High Plains Aquifer System**

Measurements of CFCs and N<sub>2</sub>O were conducted at all sites during this study. Several collections were undertaken and it appears that about a year is required for the gas concentrations to return to normal after drilling. N<sub>2</sub>O concentrations showed that in most cases the major production of this gas (which can be indicative of nitrate reduction) is at the SUIR. However, in one case, where a very wet layer was present in the UZ, it was clear that N<sub>2</sub>O production was occurring. Thus, it is possible for nitrate concentrations to be mitigated above the SUIR in proper conditions.

CFC concentrations at all control sites could be reasonably simulated by a one-dimensional model using expected soil parameters. However, in the irrigated sites, concentrations were much greater than expected at most locations. This is attributed to a draw down of the water table which causes an advective transport of the gasses into the unsaturated zone.

## **7. CONCLUSIONS**

Several conclusions can be drawn from our work.

- Recharge in arid and semi-arid areas is focused at a few locations and these need to be identified if recharge estimates for the area are desired.
- Other physical information such as that provided by temperature probes is helpful in identifying potential recharge sites.
- Irrigation modifies recharge in all settings studied, and the extent depends on the type of irrigation.
- Irrigation has mobilized natural salts in some semi-arid areas and resulted in their moving toward the water table.
- Nitrogen isotopes can be used to determine the sources of nitrate (natural or agricultural) in the unsaturated zone when mobilization of natural salts may occur.
- Measurement of gasses is an important adjunct in UZ studies and can help distinguish where large lateral extends of impermeability are present.
- Lateral movement of gasses is an important and over looked factor in many approaches and models.
- Drilling impacts gas concentrations in the UZ and approximately a year is required for concentrations to return to normal.
- It is possible for some reactions to occur to mitigate nitrate concentrations above the SUIR, although this process was much smaller than processes going on in the SUIR at our sites. This may impact other chemicals as well.
- Large burdens of nutrients may be stored in unsaturated zones in many locations and continued irrigation may ultimately result in these chemicals reaching the water table.

## REFERENCES

- [1] NIMMO, J. R., HEALY, R.W., STONESTROM, D.A., "Aquifer recharge", Encyclopedia of Hydrological Sciences: Part 13: Groundwater, (ANDERSON, M.G., BEAR, J., Eds), Chichester UK, John Wiley & Sons (2005) 2229–2246.
- [2] DRISCOLL, F. G., Groundwater and Wells. 2nd Ed., Johnson Filtrations Systems, Saint Paul, Minnesota (1986).
- [3] J.A. IZBICKI, RADYK, J., MICHEL, R.L., Water movement through a thick unsaturated zone underlying an intermittent stream in the western Mojave Desert, southern California, USA, *J. Hydrol.* **238** (2000) 194–217.
- [4] HAMMERMEISTER, D.P., BLOUNT, D.O., MCDANIEL, J.C., "Drilling and coring methods that minimize the disturbance of cuttings, core, and rock formations in the unsaturated zone, Yucca Mountain, Nevada", Proc. the NWWA Conference on Characterization and Monitoring of the Vadose (Unsaturated) Zone, National Well Water Association, Worthington, Ohio (1986) 507–541.
- [5] OSTLUND, H.G., WERNER, E., The electrolytic enrichment of tritium and deuterium for natural tritium measurements, *Tritium in the Physical and Biological Sciences*, Vol 1 (1962) 95–104.
- [6] REVESZ, K., WOODS, P.H., A method to extract soil water for stable isotope analysis, *J. Hydrol.* **115** (1990) 397–406.
- [7] WOOD, W.W., SANFORD, W.E., Chemical and isotopic methods for quantifying ground-water recharge in a regional, semi-arid environment, *Groundwater* **33** (1995) 458–468.
- [8] SCANLON, B.R., LANGFORD, R.P., GOLDSMITH, R.S., Relationship between geomorphic settings and unsaturated zone flow in an arid setting, *Water Resour. Res.* **35** (1999) 983–999.
- [9] IZBICKI, J.A., CLARK, D.A., PIMENTEL, I., LAND, M., RADYK, J., MICHEL, R.L., Data from a thick unsaturated zone underlying Oro Grande and Sheep Creek Washes in the western part of the Mojave Desert, near Victorville, San Bernardino County, California, 1994-1999, US Geological Survey Open File Report 00-262 (2000).
- [10] HOGAN, J.F., PHILLIPS, F.M., SCANLON, B.R. (Eds), Groundwater recharge in a desert environment, The southwestern United States, American Geophysical Union Water Science and Applications Series, Vol. 9, American Geophysical Union, Washington, D.C. (2004) 294.
- [11] STONESTROM, D.A., PRUDIC, D.E., STRIEGL, R.G., "Isotopic composition of water in a deep unsaturated zone beside a radioactive-waste disposal area near Beatty, Nevada", U.S. Geological Survey Toxic Substances Hydrology Program (MORGANWALP, D.W., BUXTON, H.T., Eds), Proc. of the Technical Meeting, Charleston, South Carolina, March 8–12, 1999, Vol. 3, Subsurface Contamination from Point Sources, U.S. Geological Survey Water Resources Investigations Report 99–4018C (1999) 467–473.
- [12] STONESTROM, D.A., PRUDIC, D.E., LACZNIAK, R.J., AKSTIN, K.C., "Tectonic, climatic, and land-use controls on ground-water recharge in an arid alluvial basin, Amargosa Desert, U.S.A.", Groundwater Recharge in a Desert Environment: The Southwestern United States (HOGAN, J.F., PHILLIPS, F.M., SCANLON, B.R., Eds), Water Science and Applications Series, Vol. 9, American Geophysical Union, (2004) 29–47.
- [13] COOK, P.G., WALKER, G., "Evaluation of the use of  $^3\text{H}$  and  $^{36}\text{Cl}$  to estimate groundwater recharge in arid and semi-arid environments", *Isotopes in Water Resources Management*, International Atomic Energy Agency, Vienna, Austria (1996) 397–403.
- [14] STONESTROM, D.A., CONSTANTZ, J., (Eds), Heat as a tool for studying the movement of ground water near streams, U.S. Geological Survey Circular 1260 (2003) 96.
- [15] MCMAHON, P.B., DENNEHY, K.F., BRUCE, B.W., BOHLKE, J.K., MICHEL, R.L., GURDAK, J.J., HURLBUT, D.B., Storage and transit time of chemicals in thick unsaturated zones under rangeland and irrigated cropland, High Plains USA, *Water Resour. Res.* **42** 3 (2005).
- [16] RONEN, D., MAGARITZ, M., ALMON, E., AMIEL, H., Anthropogenic anoxification (eutrofication) of the water table region of a deep phreatic aquifer, *Water Resour. Res.* **23** (1987) 1554–1560.

- [17] MAYERS, C.J., ANDRASKI, B.J., COOPER, C.A., WHEATCRAFT, S.W., STONESTROM, D.A., MICHEL, R.L., Modeling tritium transport through a deep unsaturated zone in an arid environment. *Vadose Zone Journal* **4** (2005) 967–976.
- [18] BOYCE, J. S., MUIR, J., EDWARDS, A.P., OLSON, R.A., Geologic nitrogen in Pleistocene loess of Nebraska, *J. Environ. Qual.* **5** (1976) 93–96.
- [19] ANDRASKI, B.J., STONESTROM, D.A., MICHEL, R.L., HALFORD, K.J., RADYK, J.C., Plant based plume-scale mapping of tritium contamination in desert soils, *Vadose Zone J.* **4** (2005) 819–827.
- [20] MILLINGTON, R.J., Gas diffusion in porous media, *Science* **130** (1959) 100–102.
- [21] WEEKS, E.P., EARP, D.E., THOMPSON, G.M., Use of atmospheric fluorocarbons F-11 and F-12 to determine the diffusion parameters of the unsaturated zone in the Southern High Plains of Texas, *Water Resour. Res.* **18** (1982) 1365–1378.

## LIST OF PARTICIPANTS

- AUSTRIA**  
Albrecht, Leis  
Institut fuer Wasser Ressourcen Management  
Joanneum Research Forschungsgesellschaft m.b.H.  
Elisabethstrasse 16/II  
A-8010 Graz,
- CHINA**  
Guo, Yonghai  
China National Nuclear Corp. (CNNC)  
10, Xiao-guan-dong-li  
Anwai, Chaoyang  
P.O.Box 9818  
Beijing 100029
- GERMANY**  
Stichler, Willibald  
Institut fuer Grundwasseroekologie  
Helmholtz Zentrum Muenchen Deutsches  
Forschungszentrum fuer Gesundheit  
und Umwelt GmbH  
Ingolstaedter Landstrasse 1
- INDIA**  
Kulkarni, Umesh Prabhakar  
Isotope Applications Division (IAD)  
Bhabha Atomic Research Centre (BARC)  
Department of Atomic Energy (DAE)  
Trombay  
Mumbai, Maharashtra 400 085
- PAKISTAN**  
Azam, Tasneem  
Pakistan Institute of Nuclear Science and  
Technology (PINSTECH)  
Pakistan Atomic Energy Commission (PAEC)  
Lehtrar Road  
P.O.Box 1482, Nilore  
Islamabad 45650
- SLOVENIA**  
Čencur Čurk, Barbara  
Department for Water Resources  
and Technical Hydrogeology Institute for Mining,  
Geotechnology and Environment  
93 Slovenceva  
1000 Ljubljana
- SOUTH AFRICA**  
Talma, Aritius Sybrandus Siep  
Quaternary Dating Research Unit  
Council for Scientific and Industrial Research (CSIR)  
P.O. Box 395  
0001 Pretoria

**SYRIAN ARAB REPUBLIC**

Abou Zakhem, Boulos  
Department of Geology and Nuclear Ores  
Atomic Energy Commission of Syria (AECS)  
P.O. Box 6091  
Damascus

**UNITED KINGDOM**

Darling, W. George  
Keyworth Groundwater Systems and  
Water Quality Programme  
British Geological Survey (BGS)  
Crowmarsh Gifford  
Wallingford, Oxfordshire OX10 8B

**UNITED STATES  
OF AMERICA**

Michel, Robert  
Water Resources Division  
US Geological Survey (USGS)  
402 National Center  
12201 Sunrise Valley Drive, MS 431  
Reston VA 20192